Composite Pavement Systems, Volume 1: HMA/PCC Composite Pavements

DETAILS

135 pages | 8.5 x 11 | PAPERBACK
ISBN 978-0-309-12945-9 | DOI 10.17226/22685

AUTHORS

Rao, Shreenath; Darter, Michael; Tompkins, Derek; Vancura, Mary; Khazanovich, Lev; Signore, Jim; Coleri, Erdem; Wu, Rongzong; Harvey, John; and Vandenbossche, Julie

The Second
STRATEGIC HIGHWAY RESEARCH PROGRAM

SHRP 2 REPORT S2-R21-RR-2

Composite Pavement Systems

Volume 1: HMA/PCC Composite Pavements

Shreenath Rao
Applied Research Associates, Inc.
Littleton, Colorado

Michael Darter
Applied Research Associates, Inc.
Tucson, Arizona

Derek Tompkins, Mary Vancura, and Lev Khazanovich
University of Minnesota
Minneapolis

Jim Signore
University of California
Berkeley

Erdem Coleri, Rongzong Wu, and John Harvey
University of California
Davis

Julie Vandenbossche
University of Pittsburgh
Pennsylvania

TRANSPORTATION RESEARCH BOARD

WASHINGTON, D.C.
2013
www.TRB.org

Subscriber Categories

Construction
Design
Highways
Pavements

The Second Strategic Highway Research Program

America's highway system is critical to meeting the mobility and economic needs of local communities, regions, and the nation. Developments in research and technology—such as advanced materials, communications technology, new data collection technologies, and human factors science—offer a new opportunity to improve the safety and reliability of this important national resource. Breakthrough resolution of significant transportation problems, however, requires concentrated resources over a short time frame. Reflecting this need, the second Strategic Highway Research Program (SHRP 2) has an intense, large-scale focus, integrates multiple fields of research and technology, and is fundamentally different from the broad, mission-oriented, discipline-based research programs that have been the mainstay of the highway research industry for half a century.

The need for SHRP 2 was identified in *TRB Special Report 260: Strategic Highway Research: Saving Lives, Reducing Congestion, Improving Quality of Life,* published in 2001 and based on a study sponsored by Congress through the Transportation Equity Act for the 21st Century (TEA-21). SHRP 2, modeled after the first Strategic Highway Research Program, is a focused, time-constrained, management-driven program designed to complement existing highway research programs. SHRP 2 focuses on applied research in four areas: Safety, to prevent or reduce the severity of highway crashes by understanding driver behavior; Renewal, to address the aging infrastructure through rapid design and construction methods that cause minimal disruptions and produce lasting facilities; Reliability, to reduce congestion through incident reduction, management, response, and mitigation; and Capacity, to integrate mobility, economic, environmental, and community needs in the planning and designing of new transportation capacity.

SHRP 2 was authorized in August 2005 as part of the Safe, Accountable, Flexible, Efficient Transportation Equity Act: A Legacy for Users (SAFETEA-LU). The program is managed by the Transportation Research Board (TRB) on behalf of the National Research Council (NRC). SHRP 2 is conducted under a memorandum of understanding among the American Association of State Highway and Transportation Officials (AASHTO), the Federal Highway Administration (FHWA), and the National Academy of Sciences, parent organization of TRB and NRC. The program provides for competitive, merit-based selection of research contractors; independent research project oversight; and dissemination of research results.

SHRP 2 Report S2-R21-RR-2

ISBN: 978-0-309-12945-9

Library of Congress Control Number: 2013936446

Copyright Information

Note: SHRP 2 report numbers convey the program, focus area, project number, and publication format. Report numbers ending in "w" are published as web documents only.

Notice

The project that is the subject of this report was a part of the second Strategic Highway Research Program, conducted by the Transportation Research Board with the approval of the Governing Board of the National Research Council.

The members of the technical committee selected to monitor this project and review this report were chosen for their special competencies and with regard for appropriate balance. The report was reviewed by the technical committee and accepted for publication according to procedures established and overseen by the Transportation Research Board and approved by the Governing Board of the National Research Council.

The opinions and conclusions expressed or implied in this report are those of the researchers who performed the research and are not necessarily those of the Transportation Research Board, the National Research Council, or the program sponsors.

The Transportation Research Board of the National Academies, the National Research Council, and the sponsors of the second Strategic Highway Research Program do not endorse products or manufacturers. Trade or manufacturers' names appear herein solely because they are considered essential to the object of the report.

SHRP 2 Reports

Available by subscription and through the TRB online bookstore:

www.TRB.org/bookstore

Contact the TRB Business Office:
202-334-3213

More information about SHRP 2:

www.TRB.org/SHRP2

THE NATIONAL ACADEMIES

Advisers to the Nation on Science, Engineering, and Medicine

The **National Academy of Sciences** is a private, nonprofit, self-perpetuating society of distinguished scholars engaged in scientific and engineering research, dedicated to the furtherance of science and technology and to their use for the general welfare. On the authority of the charter granted to it by Congress in 1863, the Academy has a mandate that requires it to advise the federal government on scientific and technical matters. Dr. Ralph J. Cicerone is president of the National Academy of Sciences.

The **National Academy of Engineering** was established in 1964, under the charter of the National Academy of Sciences, as a parallel organization of outstanding engineers. It is autonomous in its administration and in the selection of its members, sharing with the National Academy of Sciences the responsibility for advising the federal government. The National Academy of Engineering also sponsors engineering programs aimed at meeting national needs, encourages education and research, and recognizes the superior achievements of engineers. Dr. Charles M. Vest is president of the National Academy of Engineering.

The **Institute of Medicine** was established in 1970 by the National Academy of Sciences to secure the services of eminent members of appropriate professions in the examination of policy matters pertaining to the health of the public. The Institute acts under the responsibility given to the National Academy of Sciences by its congressional charter to be an adviser to the federal government and, on its own initiative, to identify issues of medical care, research, and education. Dr. Harvey V. Fineberg is president of the Institute of Medicine.

The **National Research Council** was organized by the National Academy of Sciences in 1916 to associate the broad community of science and technology with the Academy's purposes of furthering knowledge and advising the federal government. Functioning in accordance with general policies determined by the Academy, the Council has become the principal operating agency of both the National Academy of Sciences and the National Academy of Engineering in providing services to the government, the public, and the scientific and engineering communities. The Council is administered jointly by both Academies and the Institute of Medicine. Dr. Ralph J. Cicerone and Dr. Charles M. Vest are chair and vice chair, respectively, of the National Research Council.

The **Transportation Research Board** is one of six major divisions of the National Research Council. The mission of the Transportation Research Board is to provide leadership in transportation innovation and progress through research and information exchange, conducted within a setting that is objective, interdisciplinary, and multimodal. The Board's varied activities annually engage about 7,000 engineers, scientists, and other transportation researchers and practitioners from the public and private sectors and academia, all of whom contribute their expertise in the public interest. The program is supported by state transportation departments, federal agencies including the component administrations of the U.S. Department of Transportation, and other organizations and individuals interested in the development of transportation. **www.TRB.org**

www.national-academies.org

SHRP 2 STAFF

Ann M. Brach, *Director*
Stephen J. Andrle, *Deputy Director*
Neil J. Pedersen, *Deputy Director, Implementation and Communications*
James Bryant, *Senior Program Officer, Renewal*
Kenneth Campbell, *Chief Program Officer, Safety*
JoAnn Coleman, *Senior Program Assistant, Capacity and Reliability*
Eduardo Cusicanqui, *Financial Officer*
Walter Diewald, *Senior Program Officer, Safety*
Jerry DiMaggio, *Implementation Coordinator*
Shantia Douglas, *Senior Financial Assistant*
Charles Fay, *Senior Program Officer, Safety*
Carol Ford, *Senior Program Assistant, Renewal and Safety*
Elizabeth Forney, *Assistant Editor*
Jo Allen Gause, *Senior Program Officer, Capacity*
Rosalind Gomes, *Accounting/Financial Assistant*
Abdelmename Hedhli, *Visiting Professional*
James Hedlund, *Special Consultant, Safety Coordination*
Alyssa Hernandez, *Reports Coordinator*
Ralph Hessian, *Special Consultant, Capacity and Reliability*
Andy Horosko, *Special Consultant, Safety Field Data Collection*
William Hyman, *Senior Program Officer, Reliability*
Michael Marazzi, *Senior Editorial Assistant*
Linda Mason, *Communications Officer*
Reena Mathews, *Senior Program Officer, Capacity and Reliability*
Matthew Miller, *Program Officer, Capacity and Reliability*
Michael Miller, *Senior Program Assistant, Capacity and Reliability*
David Plazak, *Senior Program Officer, Capacity*
Onno Tool, *Visiting Professional*
Dean Trackman, *Managing Editor*
Connie Woldu, *Administrative Coordinator*
Patrick Zelinski, *Communications/Media Associate*

ACKNOWLEDGMENTS

This work was sponsored by the Federal Highway Administration in cooperation with the American Association of State Highway and Transportation Officials. It was conducted in the second Strategic Highway Research Program (SHRP 2), which is administered by the Transportation Research Board of the National Academies. The project was managed by James Bryant, Senior Program Officer for SHRP 2 Renewal.

The R21 research team thanks the SHRP 2 Renewal project panel for directing the team through this research and helping us focus our research activities. We especially thank Dr. James Bryant for his encouragement and guidance throughout 4 years of this project.

We are grateful to the staff at Minnesota Department of Transportation for their role in developing, constructing, instrumenting, and testing the field sections constructed at MnROAD. We would specifically like to mention Ben Worel, Tim Clyne, Mark Watson, Maureen Jensen, and Len Palek. We also acknowledge Stewart Krummen and others at C. S. McCrossan for their flexibility in dealing with several issues that arose during the design and construction phases.

We are especially grateful to FHWA and to the Mobile Concrete Laboratory for collecting extensive field data during MnROAD construction. In particular, we acknowledge Jagan Gudimettla and Gary Crawford for providing this opportunity and working closely with the team.

We thank the Illinois State Tollway Highway Authority and particularly Steve Gillen and Ross Bentsen for their roles in the construction of test sections at the Illinois Tollway.

We also thank the State Highway Agencies in the United States and the Ministries of Transportations in Canada for responding to surveys; providing us with access to field sections; and providing traffic, materials, and performance information for these field sections.

We acknowledge Walter Fleischer with HEILIT+WOERNER Construction of Munich, Germany, Dr. John Bolander from the University of California at Davis, Dr. Mihai Marasteanu from the University of Minnesota, Minneapolis, and Dr. Susanne Aref of Aref Consulting Group, LLC for their contributions.

We also acknowledge Harold Von Quintus, Dr. William Vavrik, Jag Mallela, Dr. Alex Gotlif, Dr. Suri Sadasivam, Biplab Bhattacharya, Gregg Larson, Dr. Frank Fang, Leslie Titus-Glover, Paul Littleton, and Carmine Dwyer from Applied Research Associates, Inc., for their contributions to various parts of this research, and Robin Jones for editorial review.

Our sincere thanks to several graduate students at the University of Minnesota, the University of California at Davis, and the University of Pittsburgh who helped through various phases of field data collection and analysis. They include Kyle Hoegh, Priyam Saxena, and Luke Johanneck from the University of Minnesota and Matthew Geary, Miguel Luis, Thomas Adams, Manik Barman, Zichang Li, Feng Mu, and Somayeh Nassiri at the University of Pittsburgh.

FOREWORD

James W. Bryant, Jr., PhD, PE, *SHRP 2 Senior Program Officer, Renewal*

Volumes 1 and 2 of the R21 project present the state of the practice and guidelines for designing and constructing new composite pavements. Volume 1 provides the tools needed to design and construct new hot-mix asphalt (HMA) concrete over a portland cement concrete (PCC) composite pavement that takes full advantage of using differing materials. Volume 2 provides guidance on the design and construction of two-layer, wet-on-wet PCC pavements where the upper layer is a thin high-quality layer (hard nonpolishing aggregate, higher cement content, higher quality binder) and excellent surface characteristics with the lower layer containing a higher percentage of local aggregates and recycled materials. Both volumes detail performance data on existing composite pavement systems and provide step-by-step guidance on the design of composite pavements using mechanistic-empirical design methods for both types of new composite pavements.

Composite pavements have proved in Europe and the United States to have long service life with excellent surface characteristics, structural capacity, and rapid renewal when needed. Based on statistics compiled in 2000, approximately 30% of the urban interstate system and just over 20% of the rural interstate system is classified as "composite" pavement. In most cases the composite pavements are the result of maintenance and rehabilitation activities and not intentionally designed new composite pavement systems.

This project developed the guidance needed to design and construct new composite pavement systems. The research determined the behavior, properties, and performance for both HMA/PCC and the PCC/PCC composite pavements under many climate and traffic conditions. Experimental composite pavements were constructed at MnROAD in Minnesota and the University of California Pavement Research Center at Davis, where the pavements were instrumented and monitored under climate and heavy traffic loadings. A composite pavement consisting of HMA over jointed plain concrete also was constructed in the field by the Illinois Tollway north of Chicago. At the Tollway, extensive field surveys were performed on 64 sections of the two types of composite pavements.

This project also evaluated, improved, and further validated applicable structural, climatic, material, and performance prediction models, and design algorithms that are included in the AASHTO *MEPDG* and DARWin-ME, CalME, NCHRP 1-41 reflection cracking, NCHRP 9-30A rutting, and the Lattice bonding model. The current DARWin-ME overlay design procedure for HMA/PCC and a special R21 version of the *Mechanistic-Empirical Pavement Design Guide* (*MEPDG* [v. 1.3000:R21]) can be used for new PCC/PCC composite pavements.

The key to the sustainable features of new composite pavements is the ability to use higher levels of recycled materials in the lower concrete layer. Additionally, the thickness of the lower concrete layer can be reduced when considering the insulating effect of the top pavement surface. Intentionally designed and constructed composite pavements will help highway agencies meet the goal of building economical, sustainable pavement structures that use higher levels of recycled materials and locally available materials.

CONTENTS

Executive Summary

Types of Composite Pavement Systems

Two composite pavement design strategies were determined to provide both excellent surface characteristics (low noise; very smooth, nonpolishing aggregates; and durability) that can be rapidly renewed and long-lasting structural capacity for any level of truck traffic. These two composite pavement design strategies reflect the Strategic Highway Research Program 2 (SHRP 2) Renewal philosophy of "get in, get out, stay out."

- High-quality, relatively thin, hot-mix asphalt (HMA) surfacing—such as dense HMA, stone matrix asphalt (SMA), porous HMA, asphalt rubber friction course (ARFC), or Novachip gap-graded asphalt rubber hot mix—over a new portland cement concrete (PCC) structural layer—such as jointed plain concrete (JPC), continuously reinforced concrete (CRC), joined roller compacted concrete (RCC), or a lean concrete base/cement-treated base (LCB/CTB).
- High-quality relatively thin PCC surfacing atop a thicker, structural PCC layer.

Both types of composite pavements have strong technical, economical, and sustainable merit in fulfilling the key goals of the SHRP 2 program, including long-lived pavements, rapid renewal, and sustainable pavements. A survey of U.S. and international highway agencies conducted under the SHRP 2 R21 project revealed considerable interest in both HMA/PCC and PCC/PCC composite pavements.

Research Objectives

The objectives of this research were to investigate the design and construction of new composite pavement systems. The previous technology for the design and construction of new composite pavements was limited. The structural and functional performances of these composite pavements were not well understood or documented. There were no existing mechanistic-empirical (M-E) performance models of these pavement systems, and they need to be developed or improved for use in design, pavement management, and life-cycle cost analysis (LCCA). In addition, the current construction techniques, guidelines, and specifications were insufficient to construct composite pavements properly.

These types of composite pavements give significant flexibility to the designer to optimize the pavement design in terms of life-cycle costs, reduction in future lane closures, and improved sustainability. They essentially exhibit the advantages of conventional HMA and PCC pavements

while minimizing their disadvantages. The research in this study, which was conducted from 2007 to 2011, had the following key goals.

- Objective 1. Determine the behavior, material properties, design factors, and performance parameters for each type of composite pavement.
- Objective 2. Develop and validate mechanistic-empirical (M-E) based performance prediction models and design procedures that are consistent with the *Mechanistic-Empirical Pavement Design Guide* (*MEPDG*).
- Objective 3. Develop recommendations for construction specifications, techniques, and quality management procedures for adoption by the transportation community.

Constructed and Field Survey Sections

Experimental composite pavements were constructed at two major research sites (MnROAD, Minnesota, and the University of California Pavement Research Center [UCPRC] at Davis, California) and were instrumented and monitored under actual climate and heavy traffic loadings. An HMA/JPC composite pavement also was constructed by the Illinois Tollway north of Chicago. Extensive field surveys were performed in the United States, Canada, and Europe of 64 sections of the two types of composite pavements and used in the analysis and validation.

MnROAD/Minnesota Department of Transportation

One of the major research sites was set up by MnROAD in Minnesota.

- **Design and materials:** Three sections were constructed. The top layer PCC mix contained increased cement content and a high-quality, very durable aggregate (granite). The aggregate in the top lift was gap-graded and had a maximum size of 0.5 in (12.7 mm). All basic components of the lower-layer PCC were selected to reduce costs, investigate methods of sustainability, and investigate the reuse of materials into structural components. Higher traffic in the outside lane and lower traffic in the inside lane provided two levels of traffic. JPC was the basic type of pavement with transverse joints at 15 ft and dowels at all PCC/JPC joints and in the travel lane only for HMA/JPC joints.
  - **Cell 70:** This section consisted of 3 in. HMA over 6 in. of JPC (50% recycled concrete aggregate [RCA]; 40% fly ash replacement) over an unbound aggregate base course. The inner lane transverse joints included no dowels, but the outer lane included dowels. Transverse joints across both lanes were sawed and sealed for reflection crack control.
  - **Cell 71:** This section consisted of a 3-in. high-quality PCC layer over a 6-in. low-cost PCC layer (50% RCA; 40% fly ash replacement).
  - **Cell 72:** This section consisted of a 3-in. high-quality PCC layer over a 6-in. PCC layer with 60% fly ash replacement and inexpensive coarse aggregates.
  - **Texturing of Cells 71 and 72:** (1) Exposed aggregate concrete (EAC) achieved by brushing the surface, (2) conventional diamond grinding, and (3) ultradiamond grinding.
- **Specification development:** Full specifications for bidding were developed for each type of composite pavement.
- **Instrumentation and data acquisition:** Instrumentation installed in the pavements included thermocouples for measuring temperature throughout the pavement structure and humidity sensors to measure concrete moisture (relative humidity) levels within the slab. Static strain for static loads generated was measured with vibrating wire (VW) strain gauges to provide several critical pieces of information related to the performance of the pavement layers, responses to temperature and moisture changes, slab curvature, and in-place drying shrinkage. Dynamic strain sensors to measure the slab response to loads applied by truck traffic and the falling weight deflectometer (FWD) were also installed. All data were stored at the MnROAD facility.

- **Construction:** An initial 200-ft test section for PCC/PCC was built and the EAC surfaced prepared. The lessons learned were invaluable for building the main line, which was constructed in May 2010. Construction went well with no serious problems.
- **Loading and monitoring:** Pavements were opened to I-94 traffic in July 2010 and have been loaded ever since except for short closures for monitoring. A full year of heavy traffic has been achieved and the findings included in this report.

University of California at Davis Pavement Research Center

The other major research site was set up by the Pavement Research Center at the University of California at Davis.

- **Design:** The composite HMA/JPC pavement has four 12-ft-wide lanes to accommodate two HMA mixtures, with two HMA thicknesses, two PCC thicknesses, and PCC with and without dowels for load transfer. Each lane has three sections, each consisting of three slabs of 15-ft length. Each pass of the Heavy Vehicle Simulator (HVS) covered two transverse joints and one 15-ft slab in each section.
- **Specification development:** California State specifications were used for construction with some additional requirements.
- **Instrumentation:** Joint deflection measurement devices were installed to measure absolute vertical movement of PCC slab joints, from which the relative movement of the two slabs on each side of the joint can also be measured. Horizontal joint deflection measurement devices were used to measure relative horizontal joint movement caused by the opening and closing of PCC slab joints. Thermocouples and moisture sensors were installed to measure PCC and HMA temperature and relative humidity at various depths. Dynamic strain gauges were placed at slab corners and centers and between HMA lifts in the thicker HMA layers to measure strains occurring under the moving HVS wheel. Static strain gauges were installed to measure slowly changing PCC strains at the top and bottom of the slab caused by creep, shrinkage, warping, and curling.
- **Construction:** PCC was placed in August 2009, and the HMA was placed shortly thereafter. The PCC and two types of HMA both met their respective California Department of Transportation (Caltrans) paving specifications. An anionic SS-1h emulsion tack coat was applied. On Lanes A and B, the mix placed was a ¾-in. (19-mm) maximum aggregate size, dense graded mix with polymer modified PG 64-28 binder (PG64-28PM). On Lanes C and D, the mix placed was a ½-in. (12.5-mm) maximum aggregate size mix with gap-graded aggregate and an asphalt rubber binder produced using the "wet process" (RHMA-G).
- **Loading and monitoring:** The HVS was used to load and evaluate the pavement for HMA rutting, joint reflection cracking, and PCC slab fatigue cracking. The slab cracking loadings required 200,000 and 320,000 heavy wheel repetitions to be applied on two 5-in.-thick non-doweled slabs with thin and thick HMA, respectively. Additional cracking tests may be performed after the R21 project using other funding.

Illinois Tollway

There was also a research site set up in Illinois.

- HMA/JPC composite sections were constructed near Gurnee, Illinois, on the ramps from I-94 to Milwaukee Avenue (off-ramp in the eastbound direction and on-ramp in the westbound direction). The ramps were constructed in October and November 2010 to emulate best practices of constructing HMA/JPC composite pavements using recycled aggregate in the PCC slab.
- The project consisted of using stockpiled recycled asphalt pavement (RAP) coarse aggregate in the PCC mix with a warm-mix asphalt (WMA) surface layer. The relatively thin (2-in.

[50-mm]), high-quality dense-graded WMA layer was placed and bonded to the newly placed 9-in. (225-mm), low-cost PCC lower lift after the PCC had hardened sufficiently.
- The PCC slab included a partial replacement of cement with fly ash (~20% to 25%). The use of RAP and fly ash offers environmental advantages by diverting the material from the waste stream, reducing the energy investment in processing virgin materials, conserving virgin materials, and minimizing pollution.
- For WMA, the mix was heated to a lower temperature than for conventional HMA (~60°F to 90°F reduction). Lower temperatures mean less fuel consumption, lower stack emissions, and less fume and odor generation at the plant and job site.
- Coarse aggregate fractionated from the RAP comprised 30% of the total coarse aggregate in the PCC mix. Aggregate fines less than 4.75 mm (No. 4) used in the PCC mix were specified to come from virgin aggregate sources. RAP was fractionated, cleaned, and washed. As much as 15% of the total recycled coarse aggregate could consist of agglomerated sand/asphalt particles.
- The PCC surface was cured and textured after placement to ensure adequate bond with the HMA layer. A tack coat was sprayed on to ensure bond. The transverse joints were sawed and sealed in the HMA layer over the joints in the JPC.

Field Surveys of In-Place Composite Pavement Sections

Data were gathered from field surveys of in-place composite pavement sections. A variety of HMA/PCC composite pavement structures were identified:

- Thin asphaltic surfaces, including dense HMA, porous HMA, SMA, ARFC, Novachip, and WMA; and
- Concrete lower layers, including JPC, CRC, jointed RCC, jointed LCB, and jointed CTB.

A variety of PCC/PCC composite pavement structures were also identified:

- High-quality thin concrete surfaces, including EAC, higher strength PCC, and diamond-ground PCC; and
- Concrete lower layers, including JPC (some with recycled concrete, regular concrete, and lower cost concrete) and CRC.

European countries have been constructing HMA/PCC and PCC/PCC composite pavements for several decades and have substantial experience. HMA/PCC composite pavement was evaluated in the Netherlands using porous 2- to 3-in. HMA/CRC on more than a dozen major heavily trafficked projects, all of which exhibit low noise levels, no rutting, and no reflection cracking. Germany has built SMA surfaces on JPC and recently over CRC. One SMA/JPC section was 15 years old under heavy traffic with sawed and sealed joints that had performed very well. Austria, Germany, and the Netherlands have all constructed many projects with 2- to 3-in. EAC PCC/JPC since the late 1980s. The entire 200 miles of the A1 freeway across Austria is of this design, with the lower layer PCC containing recycled concrete and about 10% RAP. This highway lies in the harsh climate of the Alps with lots of snow and ice. None of these sections exhibited significant problems and have performed very well over 20 years.

In reviewing these case studies and discussing the composite pavements with the host engineers and practitioners, a number of benefits to importing and implementing European techniques were identified. Dutch, German, and Austrian researchers claim that composite pavements provide similar structural performance as an equivalently thick single layer at the same price in Europe, yet the road surface has higher quality and longer life friction and noise reduction because of the high-quality top layer. Furthermore, composite pavements allow for the optimization of costs and materials throughout the pavement cross section:

- High-quality materials can be used in lesser quantities in the upper layer, where they will be of the most benefit to the system; and

- Less expensive materials can be used in greater quantities in the lower layer, where they will contribute structurally without detracting from the quality and performance of the overall pavement.

Studies in Spain provided valuable information on reflection cracking for HMA/RCC and HMA/CTB and the forming of joints in the RCC and CTB. Since 1991, Spain has used the wet-forming process to form joints. Long-term results show the effectiveness of wet-formed joints every 8 to 13 ft in terms of a reduction in joint deflections and high values of joint load transfer efficiency. The studies also show that short joint spacing led to fewer reflection cracks, tighter cracks, and improved performance.

Composite Pavement Design

The design procedures in DARWin-ME for HMA overlay of jointed plain concrete pavement (JPCP) and continuously reinforced concrete pavement (CRCP) and in the *MEPDG* for bonded PCC overlay of JPCP and CRCP were found to be the most comprehensive and applicable for design of new composite pavements. Through use of appropriate inputs, the overlay procedure could be used for new composite pavement construction. Extensive testing and evaluations were performed, and many bugs related to composite pavements, as well as significant improvements, were identified and fixed in the *MEPDG*. A new version of the *MEPDG* (v. 1.3000:R21) was developed to use the Bonded-PCC-over-JPCP project to simulate newly constructed PCC/PCC and address limitations of the existing structural and environmental models for PCC/PCC.

CalME

UCPRC has been developing an M-E pavement design method for Caltrans. The associated software is called CalME. CalME rutting and reflection cracking models were evaluated for the SHRP 2 R21 project. The rutting models were calibrated using the results of the HVS and MnROAD test sections, while the reflection cracking model was tested using the results of some of the HVS test sections. Although the number of test cells used in the calibration was small, the results showed that the CalME models can predict measured performance effectively using average calibration coefficient values. A sensitivity analysis was performed to evaluate the effects of climate, traffic, HMA mix type, aggregate base stiffness, crack spacing, and HMA thickness. The sensitivity analysis showed that HMA mix type is the primary factor that affects both rutting and reflection cracking.

NCHRP Report 669 Reflection Cracking

In National Cooperative Highway Research Program (NCHRP) Report 669, a reflection cracking model was developed specifically to be implemented in the *MEPDG* and DARWin-ME. The procedure was reviewed, tested, and recommended for implementation in DARWin-ME. It appears that this approach and model will reasonably predict transverse joint reflection cracking for HMA/JPC composite pavements. The existing empirical reflection cracking model was intended as a placeholder and does not predict well.

NCHRP 9-30A Permanent Deformation of HMA Surface

The objective of NCHRP Project 9-30A was to recommend revisions to the HMA rut depth transfer function in the *MEPDG* software developed under NCHRP Project 1-37A. The recommended revisions were based on the calibration and validation of multiple rut depth transfer functions, with measured material properties and performance data from roadways and other full-scale pavement sections that incorporate modified or other specialty mixtures, as well as

unmodified asphalt binders. The NCHRP 9-30A rutting models for HMA/PCC composite pavements were evaluated and recommendations made for additional research. In summary, all three transfer functions did a fair job of predicting the measured rutting values using mixture properties and other pavement layer properties extracted from project files. Thus, the three rut depth transfer functions described and included in NCHRP 9-30A are believed to be reasonable for composite pavements.

Lattice Model for PCC/PCC Bonding

Extensive work was performed to fully develop and use lattice models for composite slab simulations for debonding of the top PCC layer from the bottom PCC layer. Completed models coupled the lattice models with finite element models to provide a comprehensive model of the PCC/PCC interface bonding. For model simulations of realistic paving conditions in which newly constructed PCC/PCC pavements are placed in a reasonable time frame, debonding of the layers did not occur. Furthermore, additional simulations of layer behavior took into account unrealistic extreme thermal gradients and highly reduced shear strengths at the interface, and these simulations found failure at the interface in only the most extreme of cases, which would not be encountered in the field. This conclusion is supported by observations from the European PCC/PCC experience, as consultants to the R21 project were unable to cite an instance of PCC/PCC debonding. Based on these observations and model simulations, it was the assessment of the research team that debonding is only a concern in PCC overlays of existing PCC pavements, which was out of the scope of the SHRP 2 R21 project.

Recommendations for Composite Pavement Design

Based in part on these models and improvements made to the *MEPDG*/DARWin-ME software, the following can now be used in the design of new composite pavements:

- New HMA/JPC, HMA/RCC or LCB, and HMA/CRC can be designed using the overlay design feature in DARWin-ME.
- PCC/JPC and PCC/CRC can be designed using *MEPDG* (v. 1.3000:R21), which includes modifications to the allowable PCC layer thicknesses, representative PCC layer properties, slab and base interaction properties (full versus zero friction), PCC/PCC subgrade response modeling, and the distribution of the temperature nodes representing a thermal gradient through the composite pavement system.

Research Products

The products from this research can be classified into five broad categories: (1) design, (2) construction and materials, (3) training, (4) informational, and (5) other.

Design Products

MEPDG (v. 1.3000:R21) developed under this study includes modifications to the allowable PCC layer thicknesses, representative PCC layer properties, slab and base interaction properties (full versus zero friction), PCC/PCC subgrade response modeling, and the distribution of temperature nodes through the composite pavement system. Many of these revisions specifically targeted the Enhanced Integrated Climatic Model (EICM) used by the *MEPDG.* This new program will be submitted to the American Association of State Highway and Transportation Officials (AASHTO) for consideration to incorporate the improvements into the DARWin-ME software. In addition, bug fixes and improvements related to both types of composite pavements were made to the *MEPDG* software throughout the R21 contract (e.g., crack opening

error in HMA/CRC), and all of these modifications have been incorporated into the DARWin-ME software.

The structural fatigue damage and cracking models for both types of composite pavement were validated using all available data: MnROAD test sections, UCPRC test sections, and the existing 64 sections located in the United States, Canada, the Netherlands, Germany, and Austria. The existing global calibration factors were determined to be adequate. However, this does not mean that slab thickness will be the same for conventional or two-layer composite pavements.

- Various other structural and performance models for key distresses (rutting, joint faulting, smoothness) in new composite pavements were validated.
- Several detailed *MEPDG* design examples for composite pavements were prepared for guidance purposes. Comparisons of several examples with conventional JPCP or CRCP indicated a 1- to 3-in. reduction in required thickness for composite pavement. This reduction for HMA/JPC or HMA/CRC was attributable to a reduction in temperature gradients.
- Detailed recommended revisions were made to incorporate composite pavements into the *MEPDG*/DARWin-ME *Manual of Practice*.
- LCCA guidelines and examples were prepared. The life-cycle costs for composite pavement can be lower than those for conventional HMA or PCC pavements:
  - Use of the *MEPDG* (v. 1.3000:R21) and DARWin-ME to design HMA/JPC (including jointed RCC or LCB) or HMA/CRC. The HMA surface insulates the PCC slab from both temperature and moisture gradients. This has major implications regarding the reduction of stresses at the top and bottom of the slab and the resulting reduced fatigue damage, especially at the top of the slab. Comparative designs show a significant reduction in composite slab thickness.
  - In urban areas with high congestion and high costs of lane closures, rapid renewal is paramount. HMA/PCC can be designed for the PCC to structurally last to have a long life (if durable materials are used). The thin HMA can be milled and replaced rapidly with minimal disruption to traffic. PCC/PCC has a longer surface life but, when needed, the surface can be diamond ground to rapidly restore smoothness and friction and reduce pavement/tire noise.
  - In situations where high-quality aggregates for PCC are not available (or are expensive because of long haul distances), local PCC aggregates may be susceptible to polishing and other durability-related distresses. In these situations, HMA or PCC surfaces can protect the structural integrity of the PCC and can be milled and diamond ground and rapidly renewed as needed.
  - Many urban areas and some rural areas exist with old PCC pavements that can be removed and processed and recycled directly back into lower layer PCC. This provides excellent improved sustainability opportunities for composite pavements.
  - In areas where low pavement noise is required, such as urban areas with large populations in close proximity to the pavements, porous HMA surfacing of PCC provides the lowest level of noise measured. An alternative was discovered at the MnROAD site, where the next generation diamond grinding was performed on the EAC surfacing, and measurements showed the lowest noise concrete surface measured. These surfaces can be renewed rapidly into the future as needed.
  - Arizona has built many miles of major freeways with porous rubberized asphalt surface over new JPC and CRC to minimize noise. Arizona has had success with this type of pavement, but performance data on this type of pavement in other parts of the country are limited. Low noise is a major reason porous HMA/PCC and EAC PCC/PCC composite pavements are constructed in European countries.
  - Where conventional HMA pavements exhibit transverse cracks and deterioration of transverse cracks is a problem, HMA/CRC is a good alternative to eliminate reflection of transverse

cracks. No low-temperature transverse cracks were observed in HMA/JPC or HMA/CRC, and no longitudinal wheelpath cracks have been observed in HMA/PCC pavements.
- Composite pavements can be an economical choice when widening existing PCC or HMA/PCC pavement such that the widened section is compatible structurally with the existing pavement. Both the new and the existing lanes typically are covered with one or more lifts of HMA.

Construction and Materials Products

Construction specifications and guidelines were developed as part of construction at MnROAD and UCPRC for use by agencies considering constructing new HMA/PCC and PCC/PCC composite pavements. These include two-lift wet-on-wet construction of PCC/PCC pavements, timing and sequencing of operations, texturing procedures and related guidelines, guidelines for paving the stiffer lower lift PCC and the thin upper lift, saw cutting of joints, and the challenging exposed aggregate brushing technique. The MnROAD construction also involved the use of ultrasonic tomography to assess PCC/PCC layer thicknesses and bond quality at the PCC/PCC and slab/base interfaces. The PCC upper layer was diamond ground using a next generation grind that produces a smoother and quieter surface.

Material specifications include those for recycled aggregate, cementitious materials such as cement and fly ash, aggregate type and gradation for EAC, and retarding/curing compound. Procedural specifications include those related to wet-on-wet construction, timing of paving operations, texturing, saw cutting, sealing of sawed and sealed joints, tack coat application for HMA/PCC, and so forth.

Concrete freeze–thaw durability is a major concern for pavements in many parts of the United States and Canada. The upper layer PCC mixture will experience the most freeze–thaw cycles, but the lower layer mixtures will experience freeze–thaw cycles as well. The International Union of Testing and Research Laboratories for Materials and Structures (Paris) (RILEM) CIF concrete freeze–thaw standard was adopted based on European PCC/PCC experience, and the equipment was imported from Germany for use in SHRP 2 R21. The CIF test evaluates the capillary suction, surface scaling resistance, and internal damage of concrete samples exposed to a 3% by volume sodium chloride solution and freeze–thaw cycles, whereas AASHTO T161 evaluates the internal freeze–thaw damage of concrete submerged in water, and AASHTO T277 evaluates the freeze–thaw scaling resistance of concrete exposed to a 3% sodium chloride solution. RILEM CIF freeze–thaw testing and evaluations were conducted on all the concrete mixtures used at MnROAD.

All of these concrete mixes adequately resisted surface scaling and internal damage (modulus) caused by frost action. Compared with the decrease in relative modulus of other concrete samples studied with the RILEM CIF procedure, the loss of scaled material and the decrease in relative moduli of all of the samples were relatively small. The lack of scaling and internal damage in both lower PCC mixes after 56 freeze–thaw cycles indicated that these mixtures are suitable for use in long-life concrete pavements despite containing recycled concrete aggregates or having a 60% cement replacement with fly ash, respectively. It was expected that the upper lift PCC samples would experience minimal scaling and internal damage caused by frost action because of: the high cement content and low water-to-cement ratio of the mix, as well as the use of high-quality granite aggregates.

Training Products

Materials were prepared to promote the use and accelerate the adoption of new composite pavements. The training materials include both design and construction materials. Design examples for both major types of composite pavements are included.

Informational Products

Includes the final R21 reports (Volumes 1 and 2) and detailed appendices (including a previously published report on the European Survey of Composite Pavements by Tompkins, Khazanovich, and Darter in 2010). In addition, there is also a database of test sections, including material properties, performance, traffic, structure, and location, which are all inputs required for use with the *MEPDG*/DARWin-ME.

Other Products

Three test sections (two PCC/PCC and one HMA/PCC) were constructed at MnROAD with various surface textures (exposed aggregate, conventional grind, next generation grind, HMA) and design features (doweled/nondoweled and with/without sawed and sealed joints for HMA/PCC) with two different PCC mixes in the lower lift. These are the only instrumented in-service composite pavement test sections in existence. The instrumentation includes static and dynamic gauges, moisture gauges, and temperature gauges, all of which are wired into a data acquisition unit for continuously collecting data. These sections were constructed in April through June 2010 and were opened to traffic in July 2010.

Instrumented UCPRC HVS test sections were constructed in May 2010 and loaded with the HVS equipment. The instrumented test cells can be used for future testing. Data were collected from rutting and reflection cracking tests at UCPRC (including laboratory testing). HMA/JPC full-scale fatigue cracking tests using the HVS were conducted to validate the *MEPDG* transverse cracking models, and the results provided validation. Additional testing may continue with other funding sources.

Overall SHRP 2 R21 Products Use

All of these products are available for use by federal, state, local, and other agencies for design, construction, materials, and management of new HMA/PCC and PCC/PCC composite pavements.

Examples of Composite Pavements

In-service composite pavements have been shown to provide long lives with excellent surface characteristics, long-life structural capacity, and rapid renewal when needed. Composite pavements seem to reflect the current direction of many highway agencies to build more economical yet sustainable pavement structures that use recycled materials and locally available materials. The availability of DARWin-ME and the validation accomplished under R21 have made it possible to design these composite pavements with confidence. Table ES.1 provides examples of HMA/JPC and HMA/CRC composite pavements for a range of heavy truck traffic in their first performance period. The following is a brief summary of the field performance of HMA/PCC type of composite pavements.

- Relatively thin asphaltic surfaces that have performed well included a variety of types and thicknesses under heavy traffic: 1- to 2-in. SMA directly on PCC or HMA on PCC, 2- to 4-in. dense graded HMA over PCC, 1-in. porous HMA over dense HMA/PCC, 1-in. asphalt rubber friction course over PCC projects, and 0.625-in. Novachip over HMA/PCC. There were several successful thin asphaltic surface courses that have performed very well over 10 to 15 years. They did not rut significantly. Transverse joint reflection cracks occurred on all JPC and RCC pavements, with most of low to medium severity. Projects in Spain showed that shorter joint spacings (e.g., 10 ft) result in much less reflection cracking and severity. Dowel bars greatly

Table ES.1. Examples of HMA/PCC Composite Pavements in First Performance Period

Composite Pavement; Age and No. of Trucks	HMA Layer	PCC Layer	Performance and Maintenance	Design, Sustainability, and LCCA
ARFC/JPC I-10, Arizona; 17 years and 20 million trucks	1-in. ARFC	14-in. JPC 15-ft joints Dowels	Excellent performance; reflection of transverse joints; low severity; smooth; ARFC has lasted 20 years; no PCC cracks or repairs	DARWin-ME requires thinner slab design; low life-cycle cost over many years; no lane closures
SMA/JPC A93, Germany; 13 years and 47 million trucks	1.2-in. SMA with sawed and sealed joints	10.3-in. JPC 16-ft joints Dowels	Good performance; transverse joints sawed and sealed; smooth; no PCC cracks; SMA spall repair	DARWin-ME gives same slab design; low life-cycle cost; few lane closures
HMA/CRC I-10, San Antonio, Texas; 25 years and 24 million trucks	4-in. HMA	12-in. CRC HMA base	Excellent performance; no reflection cracks; smooth; no punchouts; no maintenance	DARWin-ME gives thinner slab design; low life-cycle cost over many years; no lane closures
HMA/RCC White Road, Columbus, Ohio; 7 years and 70,000 trucks	3-in. HMA with sealed cracks after cracking	8-in. RCC 45-ft joints No dowels	Excellent performance; reflection cracks sealed just after cracked; smooth; no maintenance	DARWin-ME gives thinner slab design; short joint space; low life-cycle cost; no lane closures
HMA/JPC I-94, Minnesota; 1 year and 600,000 trucks	3-in. HMA with sawed and sealed joints	6-in. JPC 15-ft joints Dowels	Excellent performance; sawed and sealed transverse joints good condition; no PCC cracks, smooth; no maintenance	DARWin-ME gives same design; PCC contains 50% RCA and 60% fly ash

Note: Trucks given for heaviest lane, one direction only.

reduced severity of joint reflection cracks on comparative sections in Minnesota. Sawed and sealed joint projects were all in excellent condition and are highly recommended for thin asphaltic surfaces over jointed PCC.

- The JPC, RCC, and LCB concrete layers had a range of thicknesses, from 5 to 14.5 in., with the thicker sections way overdesigned. The RCC ranged from 6 to 15 in. thick (way overdesigned). The LCB/CTB ranged from 6 to 11 in. None of the JPC, RCC, LCB/CTB, or CRC showed any transverse fatigue cracking, except the 5-in. JPC in Minnesota under heavy traffic.
- The CRC layers showed a range of thicknesses, from 8 to 13 in., with percent reinforcement from 0.55% to 0.70%. The only section with punchouts was a section in Arizona with low steel of 0.55% and 0.5 in. ARFC under very heavy traffic over 16 years.
- Joint spacing for JPC typically ranged from 15 to 30 ft. Joints usually were cut in RCC at 15- to 45-ft intervals. Based on other experimental sections in Spain, the shorter joint spacings (e.g., 10 ft) were greatly beneficial in reducing the severity and amount of transverse reflection/shrinkage cracking through the HMA. Sawing and sealing joints was also greatly beneficial in controlling the severity of the cracks in thin asphaltic surfaces.
- Dowels were used on many heavily trafficked JPC sections, but many other sections had none. No dowels were used with RCC or LCB/CTB. Reflection cracks dramatically showed the benefits of dowel bars in controlling joint load efficiency and thus a reduction in HMA deterioration over the joints.
- Truck traffic ranged from low to very heavy. Typically the following ranges existed in the heaviest travel lane:
  - Interstates and freeways: 1.4 million trucks/year (range: 0.5 to 3.6);
  - Highways: 0.2 million trucks/year (range: 0.1 to 0.3); and
  - Local streets: 0.05 million trucks/year (range: 0.004 to 0.08).
- Total trucks in the design lane ranged to 47 million and the age ranged to 45 years.
- One section had a total life of 45 years, during which the asphaltic surface was replaced three times but the PCC did not require any repair. This and another similar HMA/JPC are expected to carry traffic continually into the future with no fatigue cracking, thus no slab replacements,

and more rapid renewal. In fact, fatigue cracks developed only on the exceptionally thin PCC layers on some experimental sections. None of the typical thickness JPC developed any slab fatigue cracking.

Table ES.2 shows examples of HMA/JPC sections that have been through two and three HMA surface replacement cycles that were done rapidly because none of the underlying JPC slabs were cracked and needed replacement. These and other HMA/PCC composite pavements have performed well over many years with only the rapid replacement of the HMA type surface course required. They have performed as "long-life" pavements.

Table ES.3 provides examples of PCC/JPC composite pavements for freeways with heavy truck traffic. These and other PCC/JPC composite pavements have performed well over many years with only the eventual renewal of the surface course required through diamond grinding.

A brief summary of the field performance of PCC/PCC type of composite pavements follows.

- Relatively thin high-quality concrete surfaces include a variety of types and thicknesses:
  - It was noted that 2- to 3-in. PCC over JPC performed well for more than 18 years under very heavy traffic. No debonding of PCC from lower layer PCC was observed, with the exception of some cracking at the transverse joints of the I-75 Michigan project after 18 years.
  - It was noted that 3-in. higher strength PCC over JPC performed well for more than 30 years in Florida. No debonding of the PCC has occurred.
- The JPC concrete lower layers had a range of thicknesses from 6 to 9 in. None of the JPC showed any transverse fatigue cracking.
  - Joint spacing for JPC ranged from 15 to 20 ft.
  - Dowels were used on all of these sections because most were heavily trafficked. As a result, joint faulting was not significant.
- Truck traffic ranged from medium to very heavy. Typically the following ranges existed in the heaviest travel lane:
  - Interstates and freeways: 3.3 million trucks/year (range: 1.8 to 4); and
  - Highways: 0.3 million trucks/year (range: 0.1 to 0.7).

  Practically none of the PCC/JPC slabs showed any transverse fatigue cracks.

- Total trucks in the design lane ranged to 72 million, and the age ranged to 30 years.

Table ES.2. Examples of Long-Life HMA/PCC Composite Pavements Over Several Performance Periods

Composite Pavement; Age and No. of Trucks	Surface and Rehabilitation	Base Slab Characteristics	Performance and Maintenance	Design, Sustainability, and LCCA
HMA/JPC I-5, Seattle, Washington; 45 years and 35 million trucks	4-in. HMA original; 2-in. at 13 years; 2-in. at 16 years; 2-in. at 11 years; (some milling at times of resurfacing)	6-in. PCC No joints No dowels	Excellent performance; transverse cracks at 70 ft reflected medium severity after 8 years; smooth; replaced HMA at 11- to 16-year intervals; no additional transverse cracks; no PCC repairs	DARWin-ME gives thicker slab design; add doweled transverse joints at 10 to 15 ft; saw and seal would extend life; low life-cycle cost over many years; few lane closures for rehabilitation
HMA/JPC I-294, Chicago, Illinois; 19 years and 30 million trucks	1992: 3.5-in. HMA original; 2001: Milled off and added 3-in. HMA; no additional rehabilitation after 10 more years	12.5-in. JPC; 20-ft joint spacing Dowels	Excellent performance; transverse joints reflected medium severity; smooth; replace HMA at 9- to 10-year intervals; no transverse fatigue cracks in JPC; no PCC repairs	DARWin-ME gives thinner slab design; shorter joint spacing; sawed and sealed joints would extend life; low life-cycle cost over many years

Note: Trucks given for heaviest lane, one direction only.

Table ES.3. Examples of PCC/PCC Composite Pavement Characteristics, Applications, and Performance

Composite Pavement; Age and No. of Trucks	Upper PCC Layer	Lower PCC Layer	Performance and Maintenance	Design, Sustainability, and LCCA
PCC/JPC I-75, Detroit, Michigan; 18 years and 72 million trucks	2.5-in. EAC	7.5-in. JPC 6-in. LCB 15-ft joint space Dowels	Fair performance; no transverse fatigue cracking; no joint faulting; smooth; only distress is joint spalling or debonding	Designed for very heavy traffic; low expected life-cycle cost; few lane closures
PCC/JPC FL-45, Florida; 30 years and 5 million trucks	3-in. PCC	9-in. JPC Lower PCC strength A, B, and C; 15- and 20-ft joint spacing Doweled and nondoweled	Excellent performance; low transverse fatigue cracking; low joint faulting	Pavement somewhat overdesigned; low life-cycle cost; no lane closures over 30 years; savings of cement; good sustainability
PCC/JPC A93, Germany; 13 years and 53 million trucks	2.8-in. EAC	7.5-in. JPC 16.4-ft joint space Dowels Tied PCC shoulders	Excellent performance; no transverse fatigue cracking; no joint faulting; smooth; low noise; pavement should last many more years	Designed for very heavy traffic; low life-cycle cost; no lane closures good sustainability
PCC/JPC A1, Austria; 14 years and 47 million trucks	2-in. EAC	7.9-in. JPC (RCA materials) 18-ft joint space Dowels ATB	Excellent performance; no transverse fatigue cracking; no joint faulting; smooth; low noise pavement should last many more years	Designed for very heavy traffic; low life-cycle cost; no lane closures; good sustainability
PCC/JPC K-96, Kansas; 14 years and 2.1 million trucks	3-in. PCC	7-in. JPC 15-ft joint space Dowels PCC shoulders	Excellent performance (new pavement); no distress; smooth	Pavement overdesigned; low expected life-cycle cost; no lane closures
PCC/JPC N279, the Netherlands; 8 years and 11.9 million trucks	3.5-in. EAC	7-in. JPC 15-ft joint spacing Dowels	Excellent performance; no transverse fatigue cracks; smooth; low noise; no other distress	Well-designed; low expected life-cycle cost; no lane closures
PCC/JPC I-70, Kansas; 4 years and 3 million trucks	1.5-in. PCC 8 different surface textures	11.8-in. PCC 15-ft joint space Dowels PCC shoulders	Excellent performance (new pavement); no distress; smooth; low noise; long life expected	Designed for very heavy traffic; low life-cycle cost expected
PCC/JPC I-94, Minnesota; 1 year and 600,000 trucks	3-in. EAC and diamond grinding	6-in. JPC 15-ft joint spacing Dowels	Excellent performance; no transverse fatigue cracks; smooth; no maintenance	DARWin-ME gave this design a 15-year life, PCC 50% RCA, 60% fly ash, good sustainability

Note: Trucks given for heaviest lane, one direction only.

Implementation Road Map

The road to implementation includes continued monitoring of constructed composite test sections at MnROAD. Additional analysis of the instrumentation data and the performance data will be extremely useful for convincing highway agencies of the validity of the concepts, the design procedures, and the construction guidelines and specifications. The MnROAD test sections can be used to hold national and regional open houses or workshops to disseminate information regarding both types of composite pavements.

The products developed as part of the SHRP 2 R21 project will result in improved design and life-cycle cost procedures for composite pavements. The guidelines, techniques, and specifications developed will greatly advance the state of the practice of constructing composite pavements. Composite pavements are congruent with the SHRP 2 Renewal philosophy because they are designed to be long-lasting pavements that can be renewed rapidly. For highway engineers, designers, and agency decision makers, composite pavements provide a cost-effective alternative

to conventional concrete and asphalt pavements over the life cycle of the pavement. Together, the R21 reports, software, and guidelines provide information for these technologies to become widely adopted by the transportation community.

Based on the comprehensive results achieved from this study, the key characteristics of composite pavements were determined to be as follows:

- There are excellent surface characteristics from the thin, high-quality asphaltic or concrete top layers. These include low noise (especially for permeable mixtures), high friction, very good initial smoothness, minimal rutting, and reasonable durability over a 10- to 15-year period.
- There is an ability to rapidly renew a thin surface course as it wears under traffic and weather (removal and replacement of asphaltic materials, diamond grinding, or retexturing of concrete materials).
- There is long life structural design of the lower PCC layer (designed for minimal fatigue damage over a 40-year period or more).
- There is avoidance of certain distress types that occur regularly in conventional pavements but are rare or nonexistent in composite pavements. For example, HMA/JPC or HMA/CRC rarely show top-down HMA or PCC longitudinal cracking in the wheelpaths (thermal gradients are reduced that lower top-down fatigue damage in PCC); these composites rarely show any low temperature transverse cracking (they are bonded to the PCC); and they show only minimal amounts of rutting. Transverse reflection from JPC joints can be controlled by the saw and seal procedure. Transverse reflection of CRC cracks rarely occurred in the HMA/CRC included in the database. PCC/JPC composite pavement has shown no longitudinal top-down cracking and only small amounts of fatigue transverse cracking. The durability of this surface has led to very little polishing in the wheelpaths.
- There are improved life-cycle costs attributable to both lower construction costs and lower maintenance and rehabilitation costs over time.
- There are improved sustainability practices through structural and materials design of the lower PCC layer in both types of pavements. Increased use of recycled or alternative materials (RCA, RAP), increased use of more local and less expensive aggregates, and higher substitution rates for cementitious materials (higher contents of fly ash or other supplementary cementitious materials).

CHAPTER 1

Introduction and Background

This R21 project, "Composite Pavement Systems," focused on providing strong, durable, safe, smooth, and quiet pavements needing minimal maintenance. Two strategies have shown great promise: (1) surfacing a new portland cement concrete (PCC) layer with a high-quality hot mix asphalt (HMA) layer(s), and (2) placing a relatively thin, high-quality PCC surface atop a thicker PCC layer. However, the structural and functional performances of these two types of composite pavements were not well understood or documented. Models for predicting the performance of these pavement systems needed to be developed and/or confirmed for use in design, pavement management, and life-cycle cost analysis (LCCA). In addition, guidance on the development of specifications, construction techniques, and quality management procedures was needed for these technologies to become widely adopted.

Research Objectives and Overview

The objectives of this research were to investigate the design and construction of new composite pavement systems and specifically not those resulting from the rehabilitation of existing pavements. The goal was to:

1. Determine the behavior of new composite pavement systems and identify critical material and performance parameters.
2. Develop and validate mechanistic-empirical (M-E) based performance prediction models and design procedures that are consistent with the *Mechanistic-Empirical Pavement Design Guide (MEPDG)*.
3. Develop recommendations for construction specifications, techniques, and quality management procedures for adoption by the transportation community.

This project consisted of the following three phases:

- Phase 1 consisted of a literature search, survey of various national and international highway agencies, field survey of composite pavements in three European countries, an evaluation of existing design procedures, development of database for full-scale applications, populating the database with information from available projects, and an initial evaluation of existing data. Phase 1 was completed and the Phase 1 interim report prepared and submitted to SHRP 2 in May 2008.
- Phase 2 consisted of further completion of the databases, analyzing the databases, identifying failure mechanisms and other distresses relevant to new composite pavements, performance modeling, and conducting parametric evaluations of the performance models. Phase 2 also included the development of the detailed research plan for Phase 3. Phase 2 was completed and the Phase 2 interim report prepared and submitted to SHRP 2 in May 2009.
- Phase 3 consisted of implementing the research plan developed in Phase 2. Full-scale roadway and accelerated pavement testing (APT) sections were constructed and tested at MnROAD and the University of California Pavement Research Center (UCPRC), respectively. Field composite pavement sites with long-term performance were surveyed, and detailed information was collected in the United States; Ontario, Canada; and three European countries. The results of these investigations were used to refine and validate the performance models and develop the final design guidelines and procedures. Phase 3 also included the development of construction specifications, design guidelines, and a plan for long-term evaluation and validation of the design models, development of training materials, and delivery of the final report for this research.

Overview of Report

The purpose of this report is to present the work performed throughout the course of the project. Included are the executive summary and two volumes. Volume 1 covers HMA/PCC composite pavements and Volume 2 covers PCC/PCC

composite pavements. Each volume includes six chapters. Chapter 1 presents the introduction and background. Chapter 2 includes details of test sections, and Chapter 3 covers the various aspects of the research relevant to analysis and modeling. Design and construction guidelines are included in Chapters 4 and 5, respectively. Chapter 6 includes product summary, conclusions, and recommendations for future research.

Definitions

HMA/PCC composite pavement systems for the purposes of this research are defined as relatively thin HMA layers over a newly placed, but sufficiently hardened, PCC layer (Figure 1.1). The term "HMA" is used to indicate all types of asphalt-based products, including stone matrix asphalt (SMA), dense and porous HMA (including polymer-modified asphalt [PMA]), asphalt rubber friction course (ARFC), and others. The wearing surface is a relatively thin, high-quality type of HMA that could consist of one or more layers of HMA with or without special layers or materials to retard reflection cracks. The PCC layer can consist of jointed plain concrete (JPC) or continuously reinforced concrete (CRC). The PCC materials of this layer can consist of conventional PCC, roller compacted concrete (RCC), or a lower cost PCC (such as with a softer large-aggregate or recycled PCC material, or what has previously been called lean concrete base [LCB]). The PCC substructure is the primary load-carrying layer and is designed to provide a durable, long-lasting pavement with low fatigue damage and a strong base, whereas the HMA layer is primarily a functional layer with excellent surface characteristics that can be renewed rapidly.

History

HMA/PCC composite pavements are by no means a recent development. They have been constructed since the 1950s using a cementitious base with an HMA wearing surface by various national, state/provincial, and local highway agencies, such as the states of New Jersey and Washington; Ontario; and the cities of Toronto, New York, Washington, D.C., and Columbus, Ohio. Columbus has constructed many composite pavements consisting of HMA over RCC on residential and collector streets in the past 15 or so years. Arizona has constructed many new composite pavements over the past 17 years consisting of an ARFC over a thick JPC or CRC layer. Several European countries, such as the Netherlands, the United Kingdom, Germany, and Italy, have constructed major composite pavement projects with low noise HMA surfacing and either CRC or JPC as the lower layer. HMA/PCC composite pavements also are constructed routinely by many highway agencies when widening existing PCC pavements or existing overlaid HMA/PCC pavements. Appendix A provides a review of the history and background of HMA/PCC composite pavements.

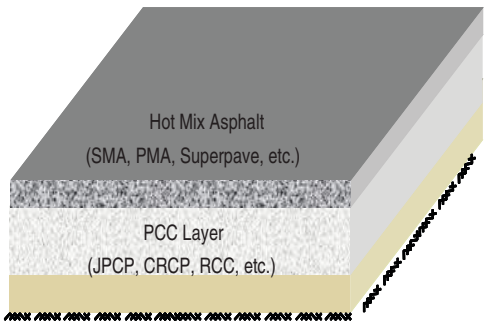

Figure 1.1. Typical cross section for HMA/PCC composite pavements.

Major thrusts toward an engineered composite pavement began in the late 1950s, through the guidance of the Committee on Composite Pavement Design of the Highway Research Board. An important task of this committee was to develop a precise definition of "composite pavement" because by some definitions, any pavement consisting of varied layer materials could be considered a composite structure. The eventual definition decided on by the committee was (Smith 1963):

> A structure comprising multiple, structurally significant, layers of different, sometimes heterogeneous composition. Two layers or more must employ dissimilar, manufactured binding agents.

As part of the movement toward a broader use of composite pavements, numerous design possibilities were suggested for study (Van Breemen 1963), including the HMA/PCC composite pavement detailed in this report. Early full-scale test section research into the construction and evaluation of composite pavements with numerous layering options was conducted in Ontario (Smith 1963, Ryell and Corkill 1973). The focus of the study was multifold, including addressing the following questions:

- Can a smooth-riding pavement be constructed easily by surfacing a concrete base with HMA layers?
- What is the best combination of thicknesses of concrete base and HMA surface for a high-class type of pavement designed to carry heavy traffic with high structural capacity?
- How can reflective cracking be prevented or reduced?

Between the 1950s and the 1970s, several long-term studies on the performance of composite pavements were conducted in the United States and Canada. These studies include the Ontario Highway 401 Study (Smith 1963, Ryell and Corkill 1973); New Jersey Composite Pavement Study (Baker 1973); Federal Highway Administration (FHWA) Zero Maintenance Pavement Study (Darter and Barenberg 1976), which identified HMA/PCC composite pavement as one of the most promising low maintenance pavements; and FHWA Premium Pavements

Study (Von Quintus et al. 1980). Transverse reflective crack deterioration was the major distress type observed on these composite pavements. Rutting was rated as only "minor" to "moderate" even under very heavy traffic (Darter and Barenberg 1976). The thinner HMA over a PCC slab seemed to have a definite effect on minimizing HMA rutting. Ryell and Corkill (1973) concluded that better performance may be achieved if the wide transverse cracks were prevented from occurring, which may be accomplished by the use of "transverse crack inducers" (joints) in the concrete base at approximately 15-ft centers. The authors suggested that the extra cost of this could be offset through use of lower quality concrete in the slab.

In Spain, the technique of forming of joints in RCC and cement treated layers under HMA to control reflective cracking has been used since 1984 (Jofre et al. 1996). The joints were sawed in the beginning, but since 1991 wet-forming methods have been used. Long-term results show the effectiveness of wet-formed joints every 8 to 13 ft in terms of a reduction in deflections and high values of joint load transfer. This study also showed that short joint spacing led to fewer transverse reflection cracks, tighter cracks, and improved performance.

As noted, urban areas have used HMA/PCC composite pavements as their primary pavement design strategy for many years because of the perceived benefits regarding ease of maintenance from the HMA wearing surface and better load carrying capacity of the PCC base. One example is the city of New York, which has been using composite pavements since the 1990s. New York has found that reflective cracking is the primary distress that limits the performance of this design strategy. The city sponsored and built an experimental project that included HMA over jointed PCC (new construction) with various treatments and techniques to retard and prevent the deterioration of reflective cracks in the HMA wearing surface. The reflective cracking treatment that was found to be most economical and has provided consistently good performance was the saw and seal method. This has also worked well for HMA overlays of JPC for many years in many states. For more than 15 years, Arizona has been building a thin ARFC on all JPC pavements constructed in urban areas to provide a low noise surface. Although Arizona has had success with this type of pavement, performance data on this type of pavement in other parts of the country are limited.

Agency Survey

The research team conducted a survey of U.S. and international highway agencies to assess the state of the practice and knowledge regarding composite pavement systems. The goals of this survey included

- Assessing the interest of various highway agencies in designing/building composite pavements within their jurisdiction.

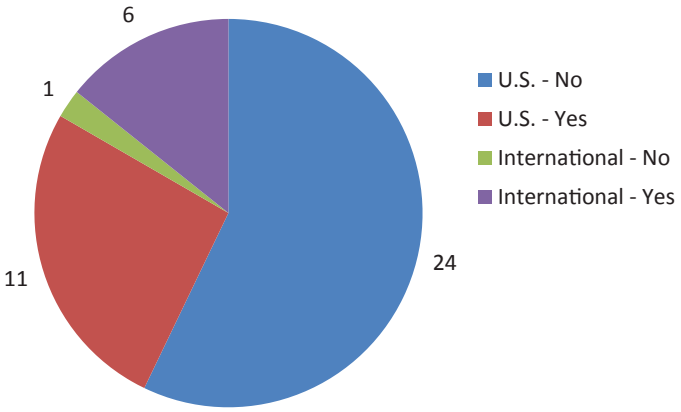

Figure 1.2. Pie chart depicting agency response to the question "Has your agency constructed new HMA/PCC composite pavements in the past 20 years?"

- Identifying agency contacts and projects that can be used in the R21 database for development of the performance models.
- Gathering information on individual agencies' experiences with composite pavements and identifying the appropriate contacts for development of guidelines and construction specifications.

A list of key agencies to be contacted was developed. These agencies included the 50 states of the United States, the District of Columbia, the provinces of Ontario and Quebec in Canada, and Austria, Belgium, Czech Republic, Germany, United Kingdom, the Netherlands, Italy, France, Spain, Sweden, South Africa, and Australia. The initial request consisted of a few questions, and agencies that responded positively were contacted for additional information on specific field sections. Responses were received from 35 of 51 (69%) of the U.S. agencies and 7 of 14 (50%) of the international agencies contacted. The results of the survey are summarized in Figures 1.2, 1.3, and 1.4 and are detailed in Appendix C.

Summary of European Practices

Many European countries have been constructing HMA/PCC composite pavements on major projects for several decades and have substantial experience with the design and construction of composite pavements (Hassan et al. 2008). Members of the SHRP 2 R21 research team conducted a trip to some of these European countries to better understand and document their experiences with the construction of composite pavements. Tompkins, Khazanovich, and Darter (2010) described case study projects visited in the Netherlands, Germany, and Austria.

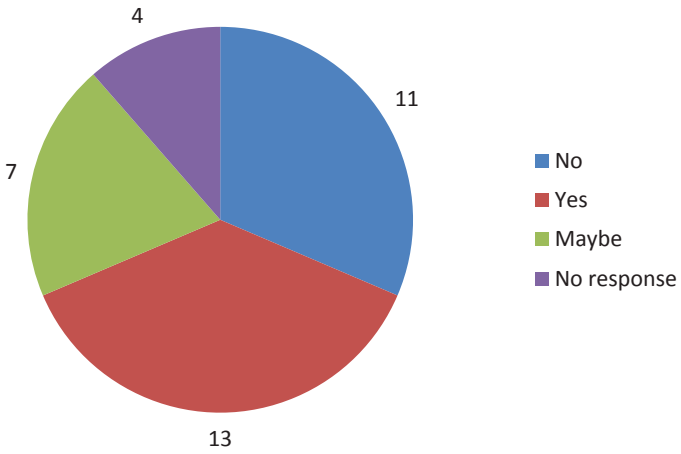

Figure 1.3. Pie chart depicting agency response to the question "Is the design and construction of new HMA/PCC composite pavements of interest to your agency?"

The Netherlands has built porous HMA over recently placed CRC on a number of major projects during the past 13 years. These projects are all performing very well with very low noise levels and no reflection cracking from the CRC despite their relatively thin HMA layer of about 2 to 3 in. Germany has built SMA surfaces on JPC and most recently over CRC. One SMA/JPC section was 15 years old under heavy traffic with sawed and sealed joints that had performed very well. Germany has recently constructed SMA over CRC. The United Kingdom also has constructed major projects and researched thin surface course systems (TSCS) over CRC and found significant technical and functional benefits (Hassan et al. 2008). In reviewing these case studies and discussing the composite pavements with the host engineers and practitioners, a number of benefits to importing and implementing European techniques were identified.

Dutch, German, and Austrian researchers report that composite pavements provide similar structural performance as an equivalently thick single layer at the same price in Europe, with the added benefits of higher quality and longer life friction and noise reduction due to the high-quality top layer. Furthermore, composite pavements allow for the optimization of costs and materials throughout the pavement cross section because

- High-quality materials can be used in lesser quantities in the upper layer, where they will be of the most benefit to the system.
- Lower quality (cheaper) materials can be used in greater quantities and in the lower layer, where they will contribute structurally without detracting from the quality and performance of the overall pavement.

Although there are obstacles to the adoption of composite paving in the United States, it is clear from the European experience that overcoming these obstacles will result in high-quality, durable, and sustainable composite pavements.

Distress Mechanisms

The distress mechanisms for HMA/PCC composite pavements are a combination of those of both HMA and PCC pavements and can be divided into three basic categories: fracture, distortion, and disintegration, as shown in Table 1.1. Details of these distress mechanisms and how they relate to the design of composite pavements are discussed in Appendix D.

Reflection Cracking

Reflection cracking is the most common distress observed in HMA/PCC composite pavements and the most serious in terms of requiring maintenance and rehabilitation. Reflection

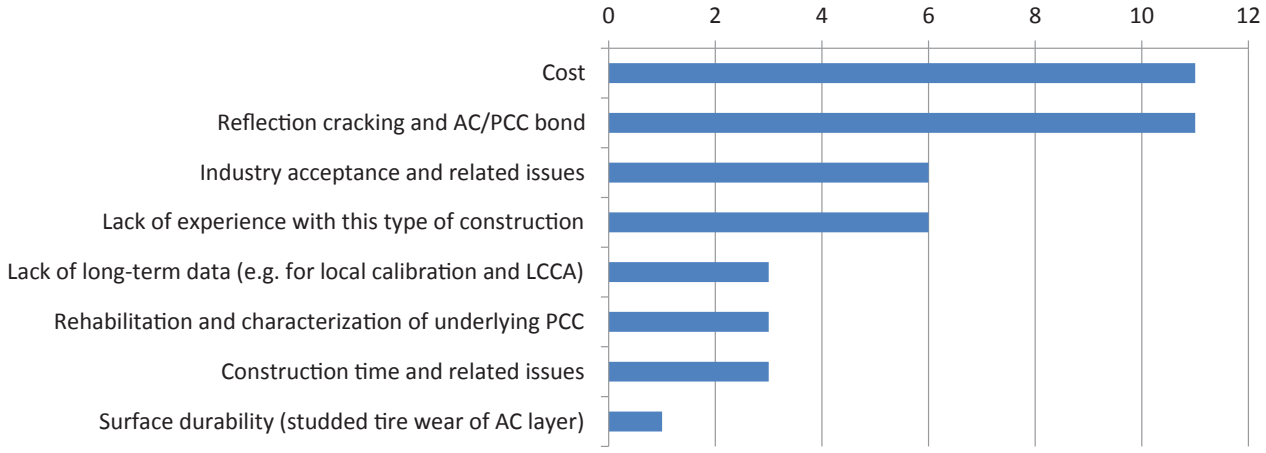

Figure 1.4. Key concerns of agencies regarding construction of HMA/PCC composite pavements in their jurisdictions.

Table 1.1. Pavement Distress Mechanisms for HMA/PCC Composite Pavements

Distress Category		
Fracture	**Distortion**	**Disintegration**
Fatigue cracking of JPC	Rutting	Raveling
Edge punchouts of CRC		Reduced skid resistance
Reflection of transverse cracks and joints		Freeze–thaw degradation
Reflection of longitudinal joints		Spalling at shoulders
		Debonding/loss of friction between HMA/PCC

cracking is caused by horizontal and or differential vertical movements between different layers at a discontinuity in the underlying PCC layer. Thus, the jointing or cracking of the underlying PCC slab is one factor that is critical to reflection cracking, with shorter spaced joints and cracks minimizing the extent and severity of reflection cracking. The load transfer efficiency of these joints and cracks over time is also critical to their occurrence and deterioration. Various systems have been used to retard reflection cracking of HMA layers of new composite structure, including

- *Bond breakers:* Bond breakers (such as stone dust) have been used to isolate the movements of the PCC layer from the HMA layer. However, these are not effective in isolating the movements and the lack of bond between the HMA and PCC layer results in other distresses, such as fatigue cracking, potholes, and slippage cracks.
- *Asphalt-rubber interlayer:* Stress-absorbing membrane interlayer (SAMI) or strain-relieving interlayer and cushion courses (crack relief layer) are used at the underlying joints to reduce the effect of horizontal and vertical movements in the PCC layer. The stress-absorbing membrane and cushion courses are used to minimize the occurrence of reflection cracks and are placed between the HMA and PCC layer. An example of an SAMI type device is the interlayer stress-absorbing composite (ISAC) of three-layer design: low stiffness geotextile (next to PCC layer), viscoelastic membrane, and high stiffness geotextile (next to HMA layer).
- *Fabrics and geotextiles:* Certain paving fabrics and geotextiles that retard reflection cracks have been used with varying degrees of success.
- *Geogrids:* Geogrids and other reinforcing materials have been placed within the HMA to prevent or delay the cracks from propagating to the surface of the HMA.
- *Reflection crack relief interlayer (RCRI):* This can include a cushion course of high-void coarse open-graded HMA mix containing 25% to 35% interconnecting voids and composed of 100% crushed material or can include an unbound aggregate base.
- *Thicker HMA layer:* A thicker HMA layer has been shown to slow the occurrence and progression of reflection cracks but can result in higher costs and thicker pavement structures, which could affect bridge clearances.
- *Saw and seal the HMA layer:* Sawing and sealing the HMA layer above the joints in the PCC base has been the most successful method for controlling reflection cracking in HMA/PCC pavements and has been used by many states for more than 40 years.

Although the occurrence of a reflection crack is the only aspect considered in most of these control techniques, the severity of the crack also is critical. Only the saw and seal method directly addresses this aspect. In addition, reflection cracks and deterioration of reflection cracks are primarily an issue only if the PCC is jointed and is not an issue if the PCC is a properly designed CRC with adequate steel reinforcement and PCC thickness.

Fatigue Cracking

Area fatigue cracking, which is typically observed in flexible pavements, does not usually initiate at the bottom of the HMA layer for HMA/PCC composite pavements because the HMA is almost always in compression, unless there is a loss of friction between the HMA and PCC layers. Fatigue cracks in HMA/PCC composite pavements normally initiate at the bottom (and top) of the PCC layer (bottom of the HMA layer only if HMA does not exhibit friction with the JPC) and propagate to the surface with continued traffic applications. The primary pavement response related to fatigue cracking is the maximum tensile stress at the top and bottom of the PCC layer.

HMA/CRC also can develop fatigue-related distress in the form of edge punchout. This distress initiates with repeated load erosion of support, the deterioration of closely spaced transverse cracks, and fatigue damage at the top of the slab to create a "ladder" longitudinal crack about 48 in. from the pavement's edge.

Because the PCC layer is the primary load-carrying component of the HMA/PCC composite pavement system, the material properties of the PCC layer (along with thickness and joint spacing) affect the structural capacity of the composite pavements. Key material properties include flexural strength, elastic modulus, coefficient of thermal expansion (CTE), permanent built-in temperature gradient, thermal conductivity, and heat capacity. In addition, the moisture content at the top of the slab beneath an HMA surface is near saturation, as is the bottom of the slab, thus eliminating a moisture gradient through the slab. One or more of these factors are affected by cement type, cementitious material content in the mix, water–cement ratio, aggregate type, ultimate shrinkage, and curing.

Rutting

Rutting is a materials-related issue and has been observed on a limited basis in HMA/PCC composite pavements. Rutting can be prevented through the mixture design and materials selection process. The "flexible" layers above the PCC layer usually consist of one or multiple layers of HMA. The most important property of the HMA layer is its stability of resistance to permanent or plastic deformation. The fatigue resistance of the HMA mixtures is less important because of the PCC layer that reduces the deflections and horizontal strains throughout the HMA layers. Thickness of the HMA layer will affect rutting potential. Rutting in the HMA layer (which is the only place where HMA/PCC can permanently deform) is related to the state of stress or strain in the HMA layers. When a heavy load is applied and repeated on a composite pavement, some permanent deformation develops in the HMA layer. Permanent deformation may, depending on the stress levels, develop in asphalt-bound or unbound layers beneath the PCC slab after the slab cracks into many pieces. Permanent surface deflection reflects the permanent deformation of the HMA layer only, whereas the total loaded deflection (elastic and plastic) reflects the permanent deformation of the HMA layer, as well as any permanent deformation in the layers beneath the PCC slab. The magnitude of the rutting in the unbound aggregate base layers and subgrade is nonexistent under the intact PCC layer because the vertical compressive strains in those unbound layers are small.

Debonding or Loss of Interlayer Friction

Another problem that has been observed on a few HMA/PCC composite pavements is the lack or loss of interface friction or bond between the HMA surface and PCC base. Inadequate bond will result in fatigue cracking, potholes, and slippage cracks.

A permanent and full adhesion and friction between the HMA and rigid layer is critical for the durability of the entire structure. Thus, a tack coat has to be applied. A tack coat is a light application of asphalt, normally asphalt emulsion (asphalt diluted with water). It is also beneficial to texture the PCC surface to enhance permanent bonding and friction between the HMA and PCC layer with no slippage. A detailed literature review on friction and debonding is included in Appendix O.

Low-Temperature Thermal Cracking

Low-temperature thermal cracking is a minor issue that is not very likely to occur in HMA/PCC composite pavements, assuming that adequate bond is retained between the different layers. Thermal cracking results when tensile stresses, caused by temperature variations or low temperatures, exceed the material's fracture strength. Joint reflection cracks relieve low-temperature stresses, but regular low-temperature cracks have not been observed in HMA/CRC pavements in cold areas.

Longitudinal Cracking

Longitudinal cracking is not a critical issue for HMA/PCC composite pavements and usually results from paving operation problems. Surface-initiated cracks for good quality composite pavements are small because the tensile strains at the surface of the HMA layer are small, if they occur at all.

Freeze–Thaw Degradation

The freeze–thaw durability of the underlying PCC layer is a key factor that affects the long-term performance of HMA/PCC composite pavements. Although the surface layer can be expected to be removed and replaced every 10 to 15 years, the underlying PCC layer is expected to be designed for more than 30 years. Freeze–thaw durability is particularly important if recycled concrete aggregate (RCA) is used in the underlying PCC layer.

Construction Defects

Construction defects that occur during placement can result in distresses on HMA/PCC composite pavements. Construction defects include segregation in the HMA (both longitudinal and truck-to-truck segregation), inadequate densities along longitudinal construction joints, centerline streak down the center of the paver, and so forth. These defects can be related to placement or to the materials used. Segregation is probably the most common defect that has been exhibited on many HMA layers. Segregation will result in raveling and cracking of the HMA layer. Construction defects can be reduced only with an adequate quality control (QC) and quality assurance (QA) and inspection program.

Use of HMA/PCC Composite Pavements

A key question that often is asked with regard to HMA/PCC composite pavements is "Where will composite pavements be used, and what will be the demand?" HMA/PCC composite pavements allow the pavement designer to design pavements using the best qualities of both HMA and PCC pavements to produce a more functional and economical structure that generally is more cost-effective in terms of service throughout its life. Specifically, HMA/PCC composite pavements are optimal solutions for the following situations:

- In some design situations, based on materials, climate, traffic, and support conditions, the life-cycle costs for HMA/PCC composite pavements can be lower than those for conventional HMA or PCC pavements. This is particularly true when the thickness of the PCC can be reduced because of the decrease in thermal and moisture gradients in the PCC relative to bare PCC pavement. Comparative designs included in this report show a significant reduction in PCC slab thickness.
- In urban areas with high costs of lane closures, rapid renewal is paramount. HMA/PCC pavements can be designed for the PCC to have a long life, structurally speaking (if durable materials are used). The HMA can be milled and replaced rapidly with minimal disruption to traffic.
- In some situations, agencies want to design and construct pavements with the structural capacity of PCC pavements but functional characteristics of HMA surfacing—premium pavement.
- Where high-quality aggregates for PCC are not available (or expensive because of long haul distances), local PCC aggregates may be susceptible to polishing and other durability-related distresses. In these situations, HMA surfaces can protect the structural integrity of the PCC and be milled and rapidly replaced as needed.
- Similarly, the HMA layer can be used as a sacrificial layer, rather than providing a thicker PCC layer (designed for future milling/grinding), where studded tires are an issue. The HMA layer can be milled and rapidly replaced as needed.
- Many urban areas and some rural areas exist with old PCC pavements that can be removed and processed and recycled directly back into lower layer PCC for use in HMA/PCC composite pavements. This provides excellent improved sustainability opportunities for pavements.
- In urban areas with large populations in close proximity to the pavements, low pavement noise is needed. HMA surfacings of PCC provide riding surfaces with low noise, good friction, and good ride quality. Arizona has built many miles of major freeways with porous rubberized asphalt surface over new JPC and CRC to minimize noise. Noise considerations also are a major reason HMA/PCC composite pavements are constructed in many European countries.
- Where transverse cracks and deterioration of transverse cracks are a problem, HMA/CRC is a good alternative to eliminate reflection of transverse cracks.
- HMA/PCC composite pavements may be used for widening existing PCC or HMA/PCC pavement such that the widened section is compatible structurally with the existing pavement. The new and existing lanes typically are covered with one or more lifts of HMA.

Differences Between HMA Overlay of Old Concrete and New HMA/PCC Composite Pavement

There are several key differences that should provide for superior performance of a new HMA/PCC composite pavement as compared with an HMA overlay of existing jointed plain concrete pavement (JPCP):

- The concrete slab is undamaged.
  - No fatigue damage or fatigue cracks exist in the concrete slabs; thus, with proper design, fewer fatigue cracks are expected to develop over the design life.
  - No durability-related distresses or spalling exist in the concrete slabs, thus minimizing the chances of localized failures of the HMA surface.
  - A new concrete slab is less likely to have localized areas that rock and cause reflection cracks through the HMA surface.
  - New transverse joints have much higher load transfer, leading to lower deterioration rates for the functional thin HMA surface. This is a major difference that reduces the deterioration of reflection cracks from transverse joints.
- The new PCC layer should be built to smoothness specifications, and this provides the opportunity to build a very smooth HMA surface on top.
- There is improved bond between the HMA surface and the concrete slab because of the tack coat and because it is cleaner and textured for a mechanical.

CHAPTER 2

HMA/PCC Test Sections

Introduction

The field composite pavement sections used in the structural modeling primarily included regularly constructed projects from the past 50 years but also a few special research sections.

1. Regularly constructed projects by states, local governments, and other countries:
   a. Arizona has built many new composite sections consisting of a thin ARFC layer over JPC. Two sections of ARFC over CRC also were included. Several heavily trafficked sections in the Phoenix and Tucson areas were included in the database, including one section on I-10 under very heavy traffic for 16 years that shows only a little surficial deterioration. One Arizona HMA/RCC section from the Long-Term Pavement Performance (LTPP) program also was included.
   b. Ontario has built several sections of HMA/JPC composite pavements, and several were included in the database.
   c. Washington state has built a few HMA/JPC composite pavements, including one built in 1966 that has gone through three cycles of HMA surface rehabilitation. However, no repair to the JPC has been needed. This pavement section was included in the database.
   d. Texas has constructed new HMA/CRC composite pavements and one of these—a remarkable 25 years old without any HMA overlays—was included.
   e. Oregon added a thin HMA overlay to an older CRC in excellent condition under very heavy traffic, and this section was included even though it does not meet the "new" definition. The existing pavement was not visibly damaged at time of the surfacing with HMA.
   f. Columbus, Ohio, has built many HMA/RCC composite pavements over the years. Several of these were included in the database as examples of lower truck volume pavements.
   g. The Illinois Tollway constructed several widening sections with new HMA/JPC in the Chicago area under very heavy traffic. They also constructed two sections (one on an on-ramp and one on an off-ramp) designed and planned by the SHRP 2 R21 research team on I-94 north of Chicago.
   h. The Netherlands has built more than a dozen porous HMA/CRC composite projects on major freeways since 1998. These projects include 2 to 4 in. of porous HMA over about 10 in. of CRC over an HMA base and other layers for a design life of 40 years (for the CRC). The main motivations are very low noise, no splash/spray, no reflection cracking, and very smooth pavements with surface that lasts more than a dozen years and has no noticeable structural damage. The oldest section was surveyed and included in the database.
   i. Germany constructed a section of composite SMA/JPC on a very heavily trucked freeway south of Munich that was surveyed and included in the database. This section is more than 13 years old and has carried 47 million trucks with only minor surface deterioration.
   j. Illinois and Virginia have constructed some new HMA/CRC composite pavement as widening sections in recent years. These were included in the database. No reflection cracking has developed over time.
   k. LTPP General Pavement Studies (GPS)-2 sections include a few with HMA over lean concrete, concrete-treated base (CTB), or RCC that could be labeled as composite pavements, and these were included in the database.
   l. The United Kingdom has built several major highways with a thin surface course system (TSCS) over CRC that have produced excellent performance and low noise.
2. Specially constructed research sections:
   a. MnROAD included two HMA/JPC composite sections on I-94 under heavy truck traffic and severe weather conditions:
      - Cell 70 was constructed in May 2010 under SHRP 2 R21. This section was 3-in. HMA over 6-in. JPC

(using RCA). The inner lane transverse joints included no dowels, and the outer lane included dowels. Special sawing and sealing of the transverse joints was performed. This section exhibited no distress after a full year of 1 million heavy trucks.

- Cell 106/206 was constructed in May 2009 under a pooled fund study (not officially part of R21). This section was 2-in. HMA over 5-in. nondoweled and doweled JPC. This section was designed to test the limits of composite pavement, and it performed as expected, developing major structural cracking after 2 years of heavy traffic (2 million trucks).

b. UCPRC Advanced Transportation Infrastructure Research Center (ATIRC) facility at the University of California at Davis constructed test sections for loading by the Heavy Vehicle Simulator (HVS). The composite HMA/JPC pavement has four lanes consisting of two HMA mixtures, with two HMA thicknesses, two JPC thicknesses, and JPC with and without dowels.
c. New York City has constructed many new composite pavements. A series of experimental sections was built in 2000 that evaluate joint reflection crack treatments that are included in the database.

Figure 2.1 shows the geographic locations of the HMA/JPC and RCC composite sections, and Figure 2.2 shows the locations of the HMA/CRC composite sections. The sections can be seen to offer a reasonable spread across different geographic and climatic conditions in the United States and Ontario, Canada. The sections in Germany and the Netherlands are also shown.

These composite pavement sections include different types of relatively thin surfacing, such as dense-graded HMA, porous HMA, ARFC, SMA, and warm mix asphalt (WMA). These sections also include different types of PCC slabs, such as nonjointed PCC, JPC with dowels, JPC without dowels, CRC, and RCC with joints (nondoweled).

These sections show a wide range of designs, including the following:

- The asphaltic surfaces range from conventional HMA to ARFC to WMA to porous HMA to SMA. The thicknesses range from 0.5 to 5 in.
- The PCC slabs range from no joints to short JPC to RCC with joints to CRC. The thickness ranges from 5 to 14 in. JPC sections include both doweled and nondoweled transverse joints. Shoulder types range from HMA to tied concrete.
- Age of the sections ranges from 1 to 45 years. Numbers of trucks range from 1 to 30 million in the heaviest trafficked lane (or, for interior widening, the widening lane).

Test Sections at MnROAD

Introduction

In May 2010, a full-scale HMA/PCC test section was constructed on I-94 at MnROAD to emulate best practices of constructing HMA/PCC composite pavements. A summary of the construction of the test section from initial site grading and aggregate base compaction to PCC and HMA placement and instrumentation installation is presented in this section. Details of each of these topics are included in Appendix F.

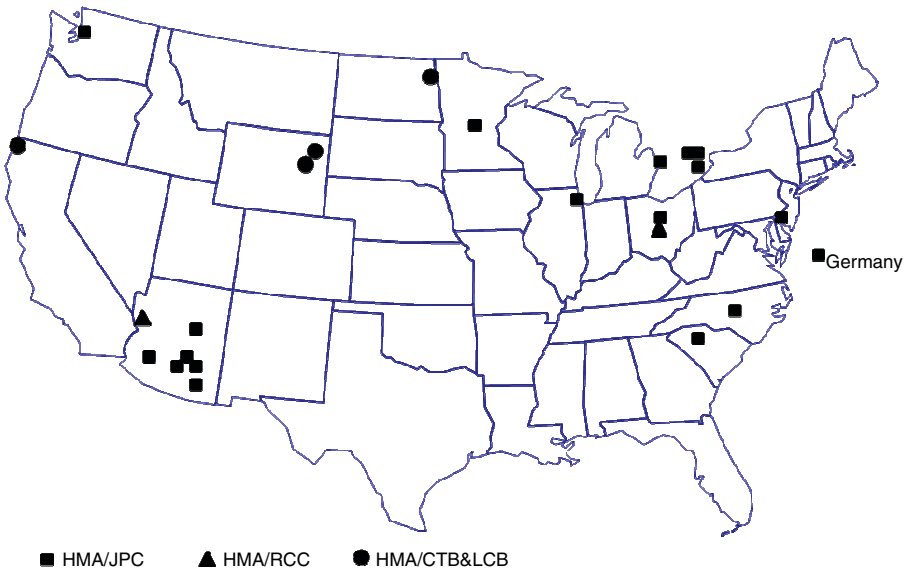

Figure 2.1. Map showing geographic dispersion of HMA/JPC, HMA/CTB and LCB, and HMA/RCC.

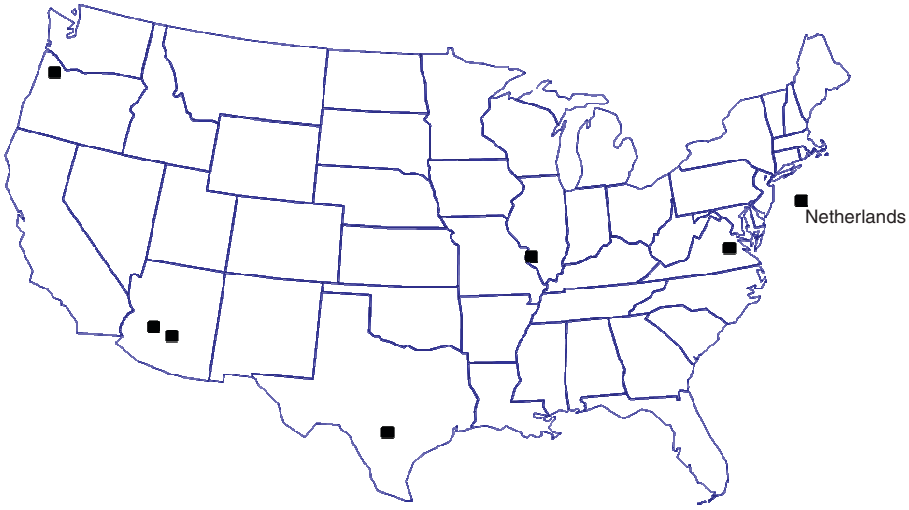

Figure 2.2. Map showing geographic dispersion of HMA/CRC composite pavements.

Figure 2.3 shows the location of the MnROAD test section relative to Minneapolis. An aerial view of a portion of the MnROAD facility is shown in Figure 2.4.

Design and Specifications

The project consisted of recycling an existing concrete pavement; the coarse aggregate (RCA) from the recycled pavement was used to construct the lower PCC layer. There were several candidate HMA materials that were considered, including porous HMA, rubber-asphalt porous friction course, Novachip, and SMA. The cost of placement of any specialized material on such a short roadway section prohibited the use of any of these surfaces. A typical Superpave HMA conforming to Minnesota Department of Transportation (MnDOT) specifications was specified. The relatively thin (3 in. [75 mm]),

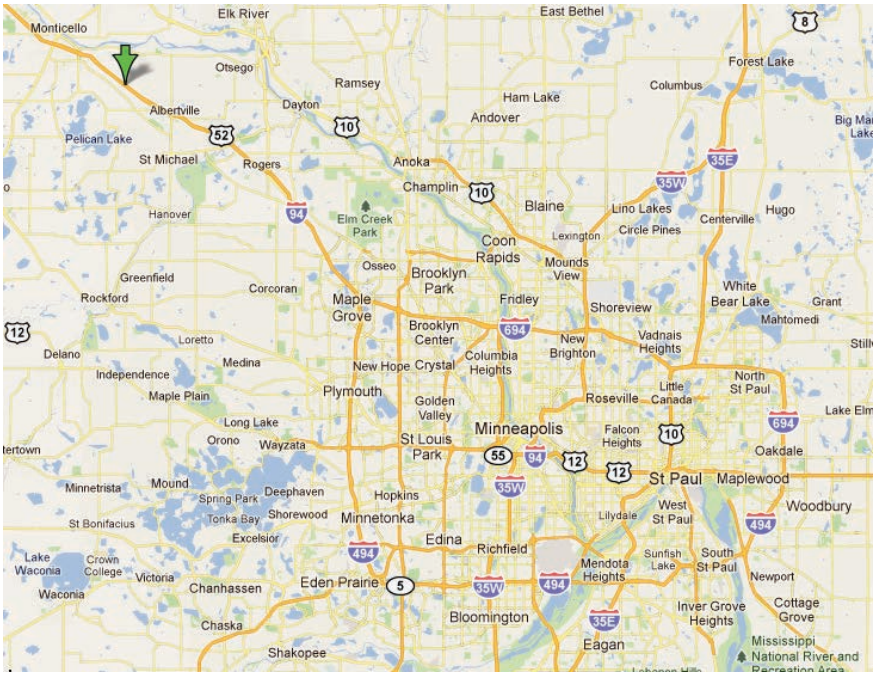

Source: © 2012 Google.

Figure 2.3. Location of the MnROAD HMA/PCC on I-94 near Albertville, approximately 40 miles northwest of Minneapolis.

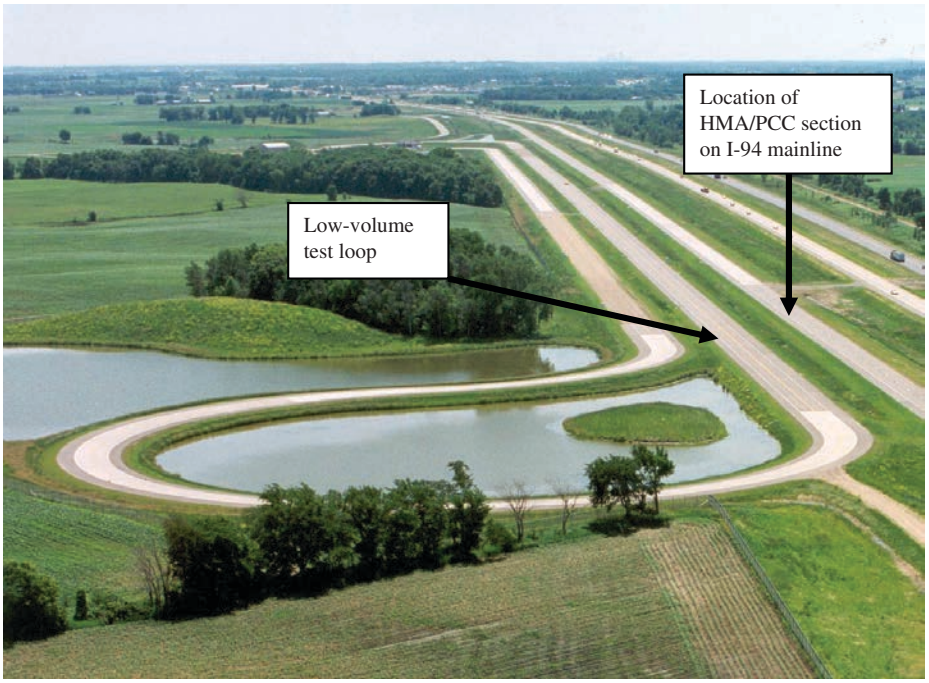

Figure 2.4. Aerial view of MnROAD facility and location of HMA/PCC test section. Note that the mainline I-94 traffic is diverted to the center lanes during construction and testing.

high-quality, dense-graded HMA layer was placed and bonded to the newly placed PCC layer after the PCC had hardened sufficiently.

The HMA/PCC section was designed to feature a 3-in. (75-mm) high-quality Superpave HMA layer over a 6-in. (150-mm) low-cost RCA PCC lower lift. The design is shown in Table 2.1.

Construction of the Test Section

The construction project was awarded to C. S. McCrossan of Maple Grove, Minnesota. WSB and Associates, Inc., was responsible for the administration of the construction contract and the inspections. Table 2.2 shows a timeline of the major steps involved in the construction process.

Table 2.1. HMA/PCC Design for MnROAD Section

Section		Cell 70 HMA/PCC (475 ft [145 m])
HMA	Thickness	3 in. (75 mm) placed in two lifts
	Binder	PG 64-34
	Mix	Superpave wearing course designated SPWEB440F with 0.5 in. (12.5 mm) nominal maximum aggregate size (SP 12.5)
PCC	Thickness	6 in. (150 mm)
	Mix	Low portland cement concrete (~360 lb/yd^3) plus 240 lb/yd^3 (40%) fly ash, Class C (FAC)
	Coarse	50% RCA, 50% Mn/DOT Class A
	Aggregate	Maximum aggregate size 1.25 in. (32 mm)
Base		8 in. (200 mm) Class 5 unbound
Subgrade		Clay
Joint spacing		15 ft (4.6 m)
Dowels		1.25 in. (32 mm) placed on baskets in driving lane at PCC middepth and nondoweled passing lane
Joints		Saw and seal HMA over PCC joints (except last six joints)

Table 2.2. Construction Timeline for Major Tasks

Major Task	Date
Salvage and recycling operations	April 12–16, 2010
Trimming and grading of subgrade	April 19–22, 2010
Aggregate base placement	April 23, 2010
Trimming base and prepping for PCC instrumentation placement	April 26–30, 2010
PCC placement and instrumentation	May 5, 2010
HMA placement and instrumentation	May 20, 2010
Saw and seal bituminous joints	May 22, 2010
Open to traffic	June 7, 2010

Because of the unique nature of this project, special provisions were used as part of the bid package to modify the DOT's existing specifications. The special provisions included:

1. Salvage concrete pavement: Specifications for the salvage operation to recycle and reuse coarse aggregate from existing on-site concrete pavement.
2. Structural concrete: Specifications for the concrete mix design and lower layer concrete design details.
3. Concrete curing and texturing: Specifications for the curing and texturing of the PCC surface to ensure adequate bond with the HMA layer.
4. Concrete pavement joints: Specifications covering details of saw cutting the joints in the PCC layer.
5. HMA joints: Specifications covering details of saw cutting and sealing of joints in the HMA layer.
6. HMA/PCC composite pavement operation: Sequence of paving activities for the construction of HMA/PCC composite pavements.

Recycling Operations

The recycling operations consisted of breaking, removing, transporting, crushing, washing, screening, and stockpiling the concrete pavement material from an existing MnROAD cell to be used as coarse aggregate in the recycled concrete mix. The concrete portions of the existing cells were broken with a guillotine crusher (Figure 2.5), removed (Figure 2.6), and transported to a crushing location.

The crushing method and system determines some of the qualities of the RCA, such as mortar content and the gradation. An increase in the number of crushing processes reduces the mortar content (Sanchez de Juan and Gutierrez 2009). As specified, all joint material, reinforcing members, and other inert materials (such as wood) were separated from the concrete sections before the existing concrete was crushed into coarse aggregate. For this project, the contractor used

Figure 2.5. Guillotine crusher breaking existing concrete for recycling into the PCC layer of the HMA/PCC composite pavement.

an industrial crushing operation that included a primary jaw crusher (Figure 2.7) operating at less than full capacity and a secondary cone crusher (Figure 2.8), then washed, screened, and stockpiled. The jaw crusher jaws were distanced to adjust the maximum aggregate size produced. The cone crusher was used as secondary crusher to further remove the mortar from the natural aggregates. A cone crusher squeezes material between an eccentrically gyrating spindle and a bowl below. As the pieces are broken, they fall to the lower, more closely spaced part of the crusher and are further crushed until small enough to fall through the bottom opening.

Laboratory tests on the recycled aggregate (American Association of State Highway and Transportation Officials [AASHTO] T84 and T85) revealed that the RCA absorption was 2.93%.

Subgrade Soil Grading and Compaction

A string line was set for trimming of the subgrade and the base. The subgrade was cut with a trimming machine (Figure 2.9)

Figure 2.6. Removal of existing concrete pavement for recycling.

Figure 2.7. The primary crusher was the jaw crusher operating at less than full capacity.

Figure 2.9. Trimming the subgrade using a string line and trimmer.

and compacted with a steel drum roller (Figure 2.10). Hand holes and conduits were set for the instrumentation cables (Figure 2.11). Testing was performed on the compacted subgrade using a dynamic cone penetrometer (DCP), light weight deflectometer (LWD), and falling weight deflectometer (FWD). The Class 5 aggregate base was constructed in two 4-in. lifts.

PCC Mix Design

Per the special provisions, the RCA comprised 50% of the total coarse aggregate in the PCC mix. In addition, aggregate fines less than 4.75 mm (No. 4) and coarse aggregates greater than 25.4 mm (1 in.) used in the PCC mix were specified to come from virgin aggregate sources. The special provisions also required the contractor to clean and wash the RCA. As much as 10% of the total recycled coarse aggregate could consist of bituminous particles per the special provisions. The cementitious fraction was specified to consist of as much as 60% supplementary cementitious materials, including but not limited to fly ash (actual fly ash substitution was 40%). Table 2.3 shows the mix design for the HMA/PCC pavement constructed at MnROAD. A comparison of the design gradation with the designated upper and lower limits specified in the special provisions is shown in Figure 2.12.

HMA Mix Design

The job mix formula (JMF) for the HMA mix proposed by the contractor and approved by the DOT included local granite and limestone sand and gravel. The target HMA amount was

Figure 2.8. A cone crusher was used as a secondary crusher to further remove the mortar from the natural aggregates.

Figure 2.10. Compacting the subbase using a steel drum roller.

Figure 2.11. Installing conduits to carry and protect the instrumentation cables.

5.4% with 4.0% air voids. Tests indicated a gyratory density of 2,386 kg/m^3 (149 lb/ft^3) at 90 design gyrations. One hundred percent of the aggregates pass the 19-mm (¾-in.) sieve, and 4.5% of the aggregates pass the No. 200 sieve.

Instrumentation Plan

To determine the overall response of the pavement to environmental loads, the physical response of the pavement and the climatic conditions within the structure were monitored. Environmental sensors were installed to document the temperature and moisture gradients that develop throughout the depth of the slab. Temperature sensors were located in each of the different pavement structures so that the seasonal, daily, and construction temperature profiles that developed could be documented. Moisture sensors were installed in the concrete to study the effects of the surface layers on the moisture distribution through the depth of the slab. Static strain gauges were used to monitor the effects of uniform moisture and temperature changes, as well as moisture and temperature gradients on the slab shape. Figure 2.13 shows the elevation and plan view of the instrumentation layout.

The response of the structures to applied vehicle loads was measured using dynamic strain sensors installed within the

Table 2.3. PCC Mix Design for HMA/PCC Construction at MnROAD

Materials	Weight per Cubic Yard (lb/yd^3)
Water	234
Cement	360
Fly ash	240
Sand	1,200
CA No. 1 (virgin aggregate)	825
CA No. 2 (recycled aggregate)	920
Water–Cement ratio	0.39
Maximum slump	3 in.
Entrained air content	7%

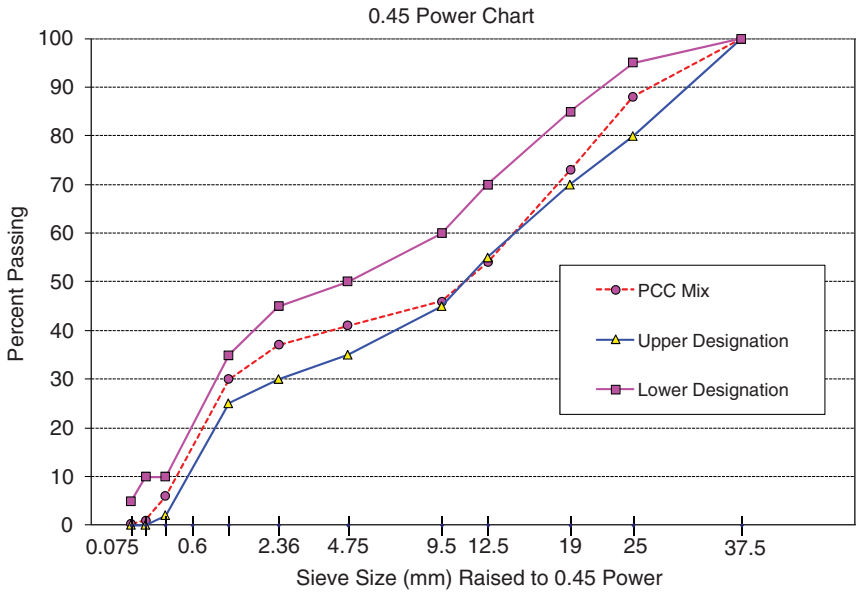

Figure 2.12. Design gradation for PCC mix using RCA and the specified limits.

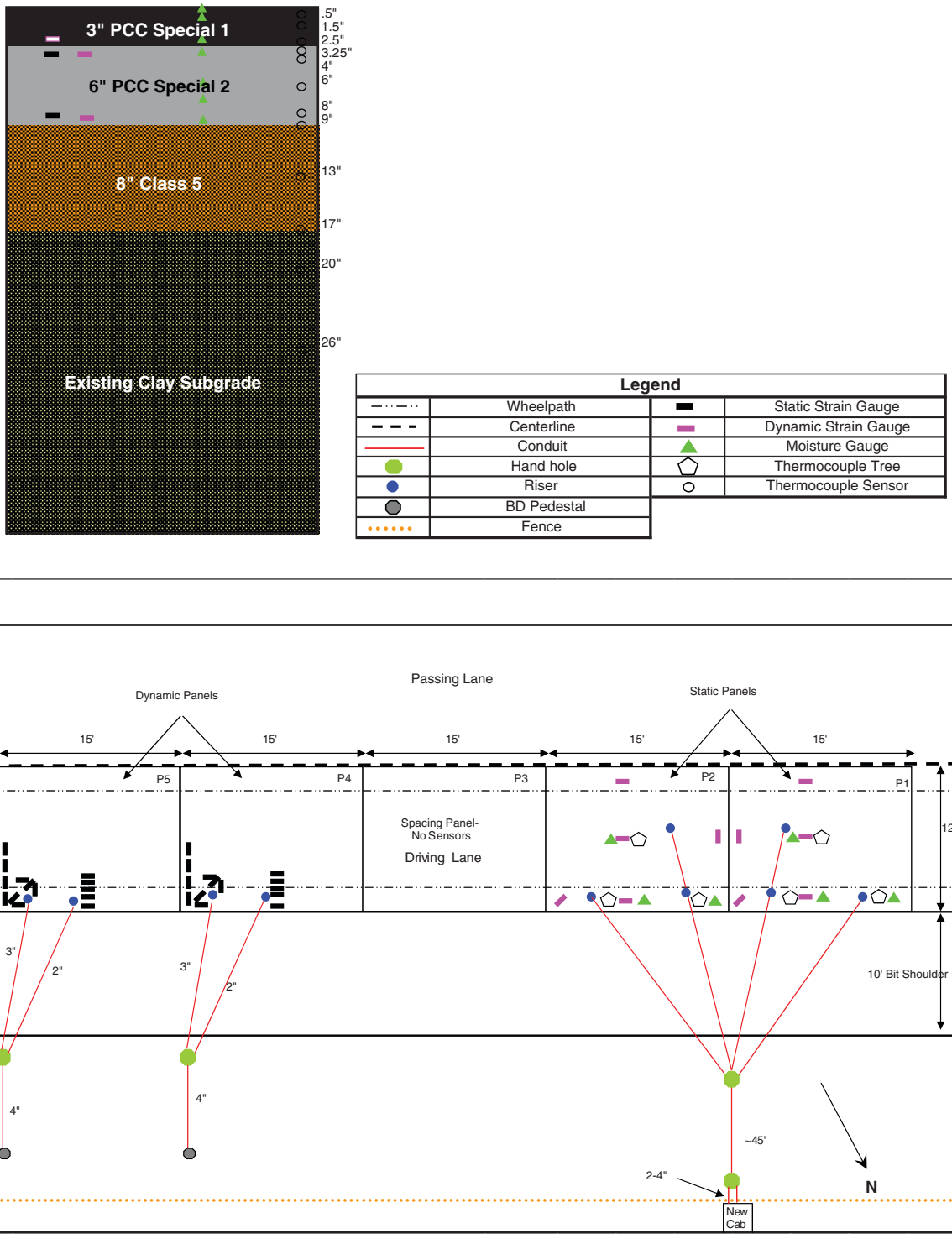

Figure 2.13. Elevation and plan view of instrumentation layout for HMA/PCC test section at MnROAD.

pavement structure. An on-site weather station recorded air temperature, relative humidity, and wind speed every 15 minutes. The various sensors installed at the MnROAD test section are described below:

- Temperature sensors: Thermocouples were used for measuring temperature throughout the pavement structure. Critical locations for monitoring temperature included the midslab, the slab corner, and midslab adjacent to the longitudinal joint.
- Concrete moisture: To measure moisture levels within the concrete, 24 Sensirion SHT75 relative humidity and temperature sensors were installed. The SHT75 sensor is a relatively small (approximately $0.75 \times 0.25 \times 0.125$ in.) and cost-effective means of measuring relative humidity in concrete.
- Static strain: The PCC response to static loads generated was measured with vibrating wire (VW) strain gauges. The VW gauges were used to provide several critical pieces of information related to the performance of the HMA layer, including
  - Degree of bonding between HMA layer and PCC slab;
  - Slab curvature; and
  - In-place drying shrinkage and thermal coefficient of expansion.

  Geokon Model 4200 vibrating wire concrete embedment strain gauges were used. The gauges operate on the VW principle. A steel cable is tensioned between two metal end blocks. When the gauge is embedded in concrete and concrete deformations occur, these end blocks move relative to one another. The movement of the end blocks influences the degree of tension in the steel cable. The tension in the cable is quantified by an electromagnetic coil, which measures the cable's resonant frequency of vibration upon being plucked. The sensor is also equipped with a thermistor so corrections for temperature can be made.
- Dynamic strain: Dynamic strain sensors were installed to measure the slab and HMA layer response to loads applied by truck traffic and the FWD. The dynamic sensors used in the concrete were Tokyo Sokki PML-60-2L strain gauges, which consist of a copper/nickel alloy resistance foil gauge attached to two lead wires. This foil is attached to an electrically insulated backing and, with the use of a special adhesive, is attached to one of two thin acrylic plates. The two plates are sealed together to protect the gauge from contamination when installed in the concrete. These acrylic plates are coated with a fine granular material to improve bonding to the surrounding concrete. The insulated backing expands and contracts with the concrete, causing the resistance in the foil gauge to change.
- Data acquisition: Automated static and dynamic data (or "online" data) were entered into the MnROAD database through the MEGADAC acquisition system. This system of dynamic cabinets, computers, fiber-optic cables, and copper-wire sensors automatically retrieved data from instruments at the MnROAD facility in Albertville and returned this information to the MnROAD database in Maplewood.

Instrumentation Installation

Figure 2.14 shows dynamic strain gauges, static strain gauges, humidity sensors, and thermocouples affixed to the aggregate base prior to PCC placement. The lead wires are buried in the sublayers and carry the signal from the gauges to the data acquisition unit. The gauges were packed in the concrete, and the concrete was vibrated with a hand vibrator to ensure consolidation of concrete around the gauges (Figure 2.15).

Paving Operations

The paving operations for the construction of HMA/PCC composite pavement at MnROAD are summarized here:

1. Place lower PCC layer. The lower PCC layer was paved on May 5, 2010 (Figure 2.16). The tie bars and dowel bars (with the use of dowel baskets) were placed in the lower layer of the concrete at the middepth (75 mm [3 in.]) of the PCC layer. Dowels were used only in the driving lane, whereas the passing lane was nondoweled as per plans. The pavement layers were instrumented with embedded thermocouples, moisture sensors, dynamic strain gauges, and vibrating wire strain gauges. There were some issues present with the air content of the mix, and four loads were rejected. The slump was generally close to 1.5 to 1.75 in. (the low slump concrete was chosen as a trial run for paving the PCC/PCC composite pavement the following day).
2. Finish smooth. The surface was finished smooth to remove surface irregularities (Figure 2.17).
3. Texture surface (longitudinal tined). The surface of the PCC layer was longitudinally tined to texture the surface and ensure a mechanical bond between the PCC and HMA layer (Figure 2.18). Texturing the surface of the concrete has been shown in previous studies to improve bond strength (Al-Qadi et al. 2008, Leng et al. 2008).
4. Spray on a curing compound. The surface of the PCC layer was sprayed with a curing compound to control the surface drying of the PCC and minimize early-age distresses (Figure 2.19). The PCC was specified to be cured for 7 days or until the flexural strength of the concrete samples reached 550 psi, before the HMA layer was to be placed. There was some concern that the curing compound would reduce the bond between the HMA and PCC. Bonding will be examined over time through coring and nondestructive testing.

Figure 2.14. Instrumentation installed prior to placement of the PCC to measure pavement responses to temperature and traffic loads (static strain gauge,* top left*; dynamic strain gauges,* bottom left*; humidity sensors,* top right*; temperature sensors (thermocouple tree),* bottom right*).

Figure 2.15. Overview of instrumentation packed in concrete before PCC paving.

Figure 2.16. Placement of PCC layer on the aggregate base.

Figure 2.18. Tining the PCC surface to provide texture for mechanical bonding between PCC and HMA layers.

5. Saw concrete joints. Unsealed single saw cuts for both transverse and longitudinal joints were cut in the PCC as soon as it gained adequate strength to perform the saw cutting operation without spalling the PCC. Both transverse and longitudinal joints were cut at depth of T/3, where T indicates the thickness of the PCC (50 mm [2 in.] for the 150-mm [6-in.] PCC).
6. Pave HMA surface. The HMA surface was specified to be paved after 7 days or a concrete flexural strength of 550 psi. The paving of the HMA layer was performed on May 20, 15 days after the construction of the PCC layer, at the discretion of the paving contractor, because of weather-related delays. A bituminous tack coat was sprayed on the concrete before the HMA paving to further help ensure adequate long-term bonding between the PCC and the HMA (Figure 2.20). Applying a tack coat to the PCC surface has been shown in previous laboratory and field studies to improve bond strength (Donovan et al. 2000, Al-Qadi et al. 2008, Leng et al. 2008).
7. Saw and seal HMA over the PCC transverse joints. Bituminous transverse joints were cut with a single saw cut of 12.5 mm (0.5 in.) wide by 16 mm (⅝ in.) deep for the HMA layer (Figure 2.20). The sawed bituminous joints were specified to be located within 12.5 mm (0.5 in.) of the concrete joints. The contractor ensured this by using stakes beyond the aggregate shoulders to mark the location of the joints in the PCC. Six joints were left unsealed for research purposes.

As-Constructed Properties

The FHWA Mobile Concrete Lab visited the R21 construction site and collected PCC cores and material samples. The results, which are the average of two tests, are summarized in Table 2.4.

Figure 2.17. Finishing the PCC surface to remove surface irregularities.

Figure 2.19. Applying curing compound to the surface of the PCC to control surface drying of the PCC and minimize early age distresses.

Figure 2.20. Tack coat applied to PCC surface* (top left) *prior to HMA paving* (top right)*. Sawing* (bottom left) *and sealing* (bottom right) *HMA layer; saw cuts in the HMA were matched to the saw cuts in the PCC below to within 12.5 mm (0.5 in.).

Table 2.4. As-constructed RCA PCC Properties

Property	Fresh Concrete	7 Day	14 Day	28 Day
Entrained air content	6.5%	na	na	na
Unit weight	146.4 lb/ft^3	na	na	na
Compressive strength	na	3,012 (psi)	4,168 (psi)	4,945 (psi)
Flexural strength	na	579 (psi)	629 (psi)	689 (psi)
Modulus of elasticity	na	4.55×10^6 (psi)	NA	5.04×10^6 (psi)
Poisson's ratio	na	NA	NA	0.25
Split tensile strength	na	NA	NA	368 (psi)
Coefficient of thermal expansion	na	NA	NA	10.4×10^{-6}/°C

Note: NA = not available; na = not applicable.

Table 2.5. As-constructed HMA Mix Properties

Property	Value
% Passing 12.5-mm (½-in.) sieve	93%
% Passing No. 200 sieve	4.4%
Asphalt binder percent by weight	5.5%
Voids in mineral aggregate	15.8%
Bulk specific gravity	2.435
Maximum specific gravity	2.511
Percent fine aggregate angularity	46%
Density	151.7 lb/ft^3

As-constructed material properties for the HMA mix are shown in Table 2.5.

Test Sections at UCPRC

The SHRP 2 R21 HVS test track was constructed at the UCPRC ATIRC facility at the University of California, Davis. A summary of the construction of the test track from initial site grading and aggregate base compaction to PCC and HMA placement and instrumentation installation is presented in this section. HVS test sections and test track joint load transfer efficiencies from deflection testing are also summarized. Details of each of these topics are included in Appendix G.

The test section pavements were designed to support the HVS experimental design and testing plan to evaluate rutting and cracking performance and provide data for validation of performance models. Figure 2.21 shows an aerial photograph of the ATIRC facility and the R21 test sections along the north-south test track. Finished total test track size is 48 × 135 ft (15 × 41 m).

Figure 2.22 shows the pavement plan design. The composite HMA/PCC pavement has four lanes (A through D) consisting of two HMA mixtures, with two HMA thicknesses, two PCC thicknesses, and PCC with and without dowels. The three sections (1, 2, 3) in each lane consist of three slabs, each 15 ft in length, totaling 45 ft in length, to ensure that the HVS is properly supported and that each test section trafficked by the HVS includes one complete slab and two PCC joints.

Construction of the Test Track

Table 2.6 shows a timeline of the major steps involved in the construction process.

Subgrade Soil Grading and Compaction

The native subgrade was graded and compacted before aggregate base placement. Typical grading plans are shown in Figure 2.23 for subgrade, aggregate base, and HMA with a total material area of 250 yd^2 (225 m^2). The transverse cross-slope built into the subgrade and maintained in the aggregate base and PCC layers was 1.5% to a drainage line on the east side of the track. Scarification was performed to 12 in. (300 mm) below natural subgrade before compaction. A Vibramax sheepsfoot roller was used to compact the subgrade in two 6-in. (150-mm) lifts to meet the Caltrans Standard Specifications Section 19 for earthwork (subgrade) relative compaction of 95%. Based on the Caltrans CTM 216 procedure, the subgrade maximum dry density is 118 lb/ft^3 (1.9 g/cm^3), at an optimum moisture content of 12%. For clay soils, the CTM 216 procedure tends to produce maximum dry densities and optimum water contents between those of Standard and Modified Proctor compaction. Field measurements at 6-in. (150-mm) depth and at subgrade surface level gave results of 95% to just more than 100% of Modified Proctor AASHTO T180 relative compaction. Laboratory tests determined Atterberg limits for the subgrade as Liquid Limit 40, Plastic Limit 24, and Plasticity Index 16. The soil is classified as CL based on the Unified Classification System.

Aggregate Base Placement and Compaction

Virgin aggregate base with a nominal thickness of 6 in. was placed using a Caterpillar G140 Motor Grader and rolled

Figure 2.21. Aerial photograph of ATIRC facility taken December 2009.

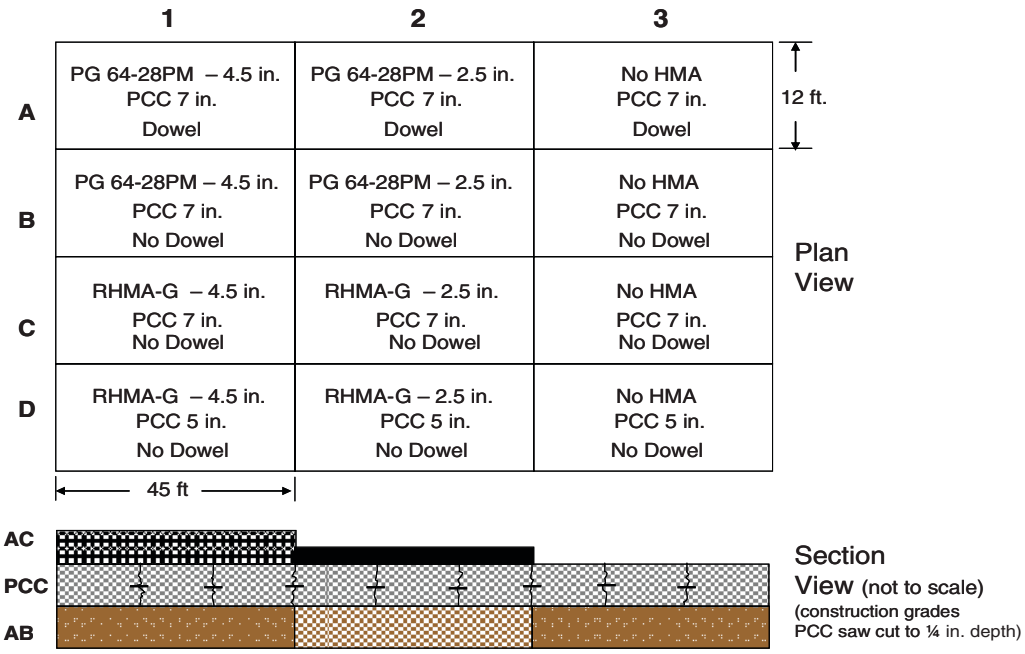

Figure 2.22. Plan view of R21 test track sections.

with a vibratory steel drum roller. Total material placed and compacted was approximately 435 tons (395 metric tons) of Caltrans ¾-in. (19 mm) Class 2 aggregate base. The Class 2 aggregate base has a minimum *R*-value of 78. The gradation specification is summarized in Table 2.7. The aggregate base was compacted to meet the Caltrans specification of 95% density relative to CTM 216, which tends to produce densities similar to those of the Modified Proctor method for granular materials. Maximum dry density of the aggregate base was measured at 140 lb/ft^3 at an optimum moisture content of 5.7%. Figure 2.24 shows grading and compaction of the aggregate base course.

Prime Coat Application

An SC-70 asphalt prime coat meeting Caltrans specifications section 93-1.01 was applied in December 2008 to the 250 yd^2 (225 m^2) aggregate base to minimize winter rain damage prior to PCC paving in 2009. The application rate was 0.20 g/yd^2 (0.90 l/m^2).

Table 2.6. Construction Timeline for Major Tasks

Major Task	Date
Excavation and grading of subgrade	November 2008
Aggregate base placement	December 2008
Prime coat application to protect base in winter	December 2008
Instrumentation purchase and assembly	January to August 2009
PCC instrumentation placement on base	July and August 2009
PCC placement	August 2009
HMA placement and instrumentation	October 2009

Instrumentation Preparation and Installation

Figure 2.25 shows a plan view of the layout for PCC instrumentation placed on top of the aggregate base. The letters in the figure correspond to the following: J is the joint deflection measurement device (JDMD), H is the horizontal joint deflection measurement device (HJDMD), T is the thermocouple, D is the dynamic strain gauge, S is the static strain gauge, and M is the moisture sensor. The numbers above each letter indicate the number of sensors placed at different heights above the aggregate base at each location. The sensor types are described below. Figure 2.26 shows, top to bottom, dynamic strain, static strain gauges, and thermocouples, affixed to the aggregate base prior to PCC placement.

- Joint deflection measurement device: JDMDs are devices designed to measure absolute vertical movement of PCC slab joints, from which the relative movement of the two slabs on each side of the joint can be measured.
- Horizontal joint deflection measurement device: HJDMDs are similar to vertical JDMDs except they are used to measure relative horizontal joint movement caused by the opening and closing of PCC slab joints. They typically are placed at joint corners where maximum movement occurs under load.

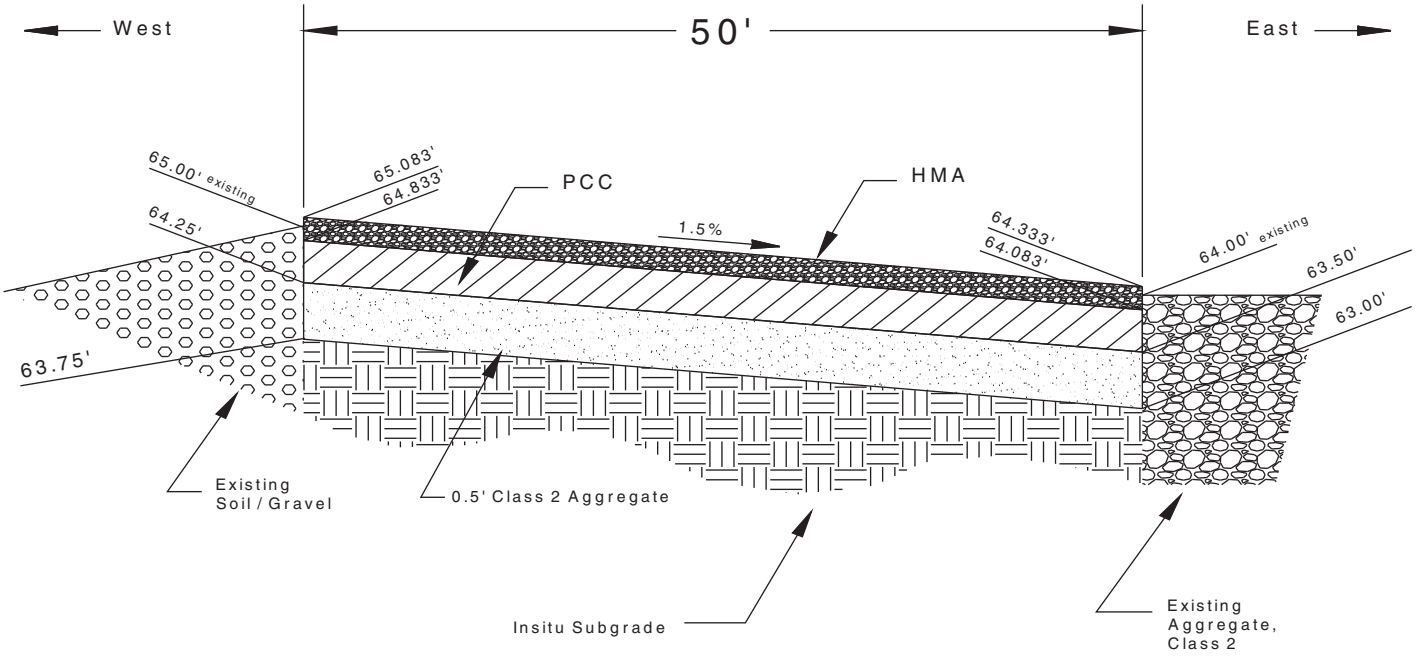

Figure 2.23. Typical transverse cross section of test track showing elevations and cross-slopes.

- Thermocouple: Thermocouples for measuring PCC temperature were placed in three locations in the PCC slabs, two slab corners, and center slab. At each of these three locations, the sensors were placed at five uniformly spaced depths within the PCC slabs. Thermocouple depths are approximately 0.5 in. from the top and bottom of the slabs, and the five thermocouples are spaced at 1.5 in. apart for 7-in. and 5-in. slabs, respectively.
- Dynamic strain gauge: Dynamic strain gauges were placed at slab corners and centers. Two gauges were placed for each location selected, nominally at 0.5 in. (13 mm) below and above the top and bottom of the slab, respectively, to measure strains occurring under the moving HVS wheel.
- Static strain gauges: Static strain gauges were installed to measure slowly changing PCC strains at the top and bottom of the slab caused by creep, shrinkage, warping, and curling. They were placed parallel to the direction of traffic loading and nominally 0.5 in. from the top and bottom of the PCC slab.
- Moisture sensors: Three moisture sensors were placed in the PCC. All sensors were placed parallel to direction of traffic and parallel to the slab 1.0 in. from bottom and top of the slab to provide relative measurement of top and bottom slab moisture.

Control and Data Acquisition

The data acquisition system consisted of an HVS-based system for JDMDs and dynamic strain gauges, and a data logger-based system for all other instrumentation.

Table 2.7. Class 2 Aggregate Base Gradation Specification

Sieve Size (mm)	Percent Passing	
	Operating Range (%)	Contract Compliance (%)
1 in. (25)	100	100
¾ in. (19)	90–100	87–100
No. 4 (4.25)	35–60	30–65
No. 30 (1.18)	10–30	5–35
No. 200 (0.075)	0–2	0–12

Figure 2.24. Compaction and grading of test track aggregate base.

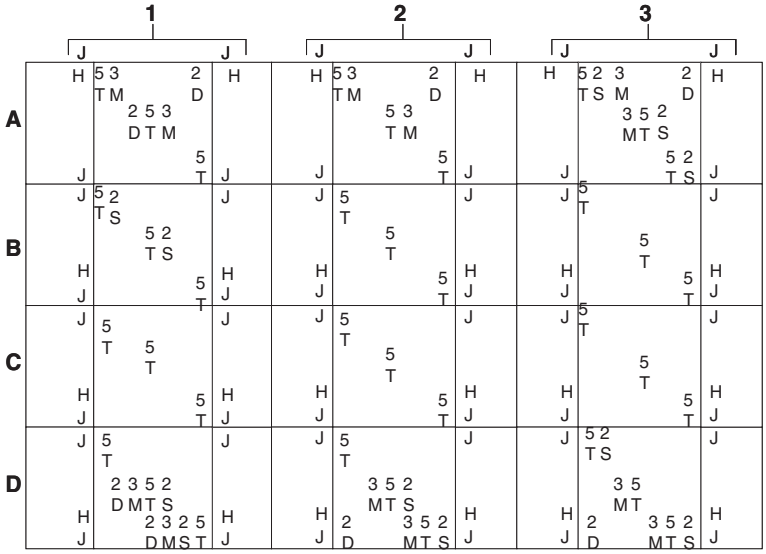

Figure 2.25. Test track plan view showing sensor placement.

- HVS data acquisition system (DAS): The JDMD data acquisition relies on the HVS DAS built by the Council for Scientific and Industrial Research, South Africa. This system consists of a 64-channel National Instruments data acquisition board mounted in a PC and an electronics equipment chassis box. The DAS is designed to collect data while the pavement is undergoing dynamic loading under the HVS test wheel. As the test wheel moves closer to an instrument, the clock triggers the first data point and the acquisition system continues to record data until the wheel stops moving.
- Data logger-based DAS: The data logger-based DAS is controlled by CR10X data loggers manufactured by Campbell Scientific. The online system consists of five CR10X data loggers, two AM16/32 analog multiplexers, 12 AM25 thermocouple multiplexers, and one AVW200 vibrating wire spectrum analyzer, all of which are enclosed in a plastic outdoor garden tool box.

Instrument Installation

Crews placed the harnesses and the instruments in their wire holders and fixed them to the prime coated base in preparation for PCC paving. The cabling was placed either parallel or perpendicular to the expected pavement joints and their locations documented so that cracking patterns could be compared with cable locations. The cables were then placed in their final positions and fastened with an asphaltic strip and nails. Figure 2.27 shows an overview of the test track with the fixed cables. A trench was dug at the west end of the track, and the cables were placed in a PVC pipe in the trench, which was later backfilled, to protect them during construction.

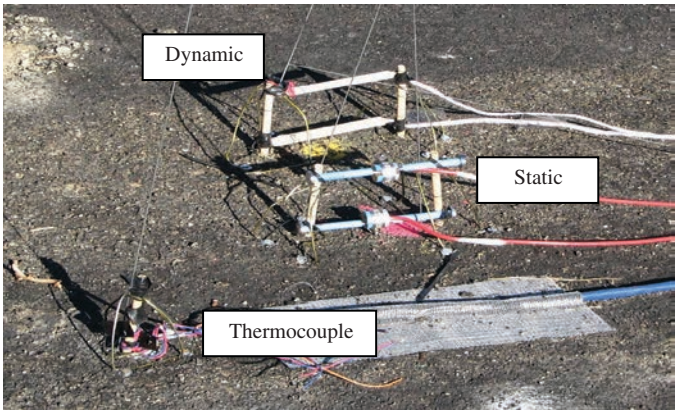

Figure 2.26. Dynamic strain gauges, static strain gauges, and thermocouples affixed to the aggregate base prior to PCC placement.

HVS Test Sections

The HVS test section layout, test setup, trafficking, and measurements followed standard testing protocols. Pavement cells

Figure 2.27. Track overview showing sensor wires fixed to track.

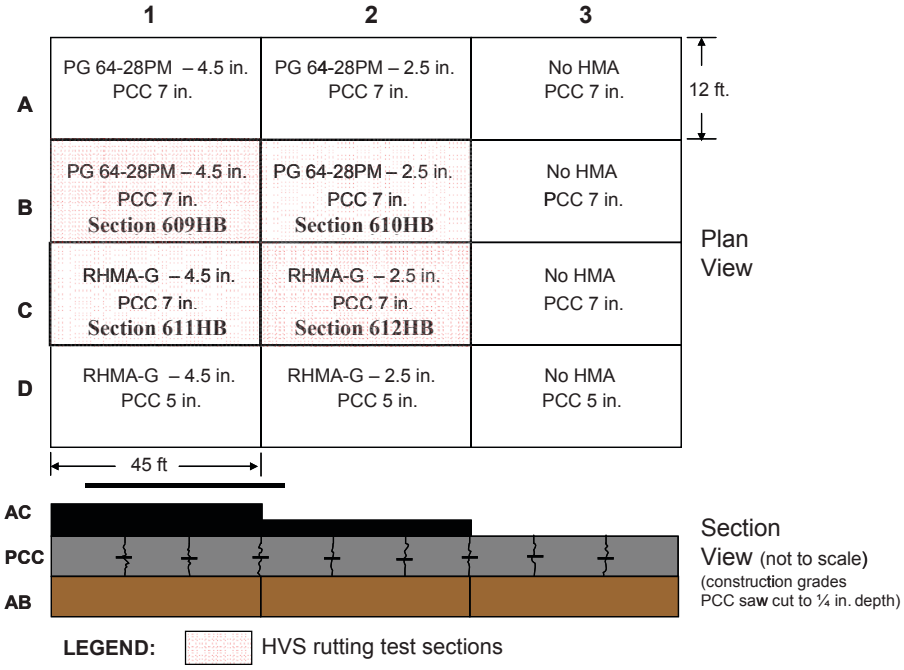

Figure 2.28. Test track with HVS rutting cells highlighted.

on which HVS rutting test sections were performed are shown in Figure 2.28. Cracking tests were performed on cells D1 and D2 under separate Caltrans funding. Additional cracking tests will be performed after completion of R21 using state funding.

Pavement Instrumentation and Monitoring

Instrumentation for the HVS rutting test sections is shown in Figure 2.29 and included the following types and collection intervals:

- Laser profilometer, a portable beam with a traveling laser collecting 260 points across its 8-ft (2.3-m) length, used to measure transverse surface profile across the wheelpath, with measurements taken at each 1.65-ft (0.5-m) station and at load repetition intervals selected to provide characterization of the rut development.
- Thermocouples, to measure ambient and pavement temperature, with measurements taken at Stations 4 and 12 and for ambient temperature at 1-hour intervals during HVS operation.
- HMA strain gauges at 50 mm depth in the HMA.

Surface and in-depth deflections were not measured during the HVS rutting tests. HMA strain gauges were used to collect pavement response in the HMA layers throughout the HVS tests. These strain gauges were located under the wheelpath and at the edge of the wheelpath to provide information about the response of the HMA layer to the shearing action of the tires. Results for the strain gauge measurements are presented in Appendix L.

Concrete Pavement Construction

Dowel Bars, Instrumentation, and Forms

Dowel bar assemblies (12 dowels) were placed at all eight joints in Lane A. The ones used were steel, 1-in. (25-mm) diameter, epoxy- and Tectyl-coated dowels that were soldered on one end to the basket assembly. Dowel bar spacing was 1 ft on center. The basket assemblies were attached to the aggregate base with the supplied fastening pins beaten into the base with sledgehammers to withstand the force of the pumped concrete.

All instrumentation (approximately 200 sensors) was verified for full functionality before PCC placement. The control and data acquisition box was completed, and cabling was attached and verified for correct placement. Each sensor was excited, and responses were measured at the box. Calibrations were performed to ensure that strain and temperature measurements were accurate.

PCC paving was performed by Teichert Construction of Sacramento, California. On August 5, Teichert Construction placed wooden forms on the test track according to the grid placed on the aggregate base, which were then checked for accuracy.

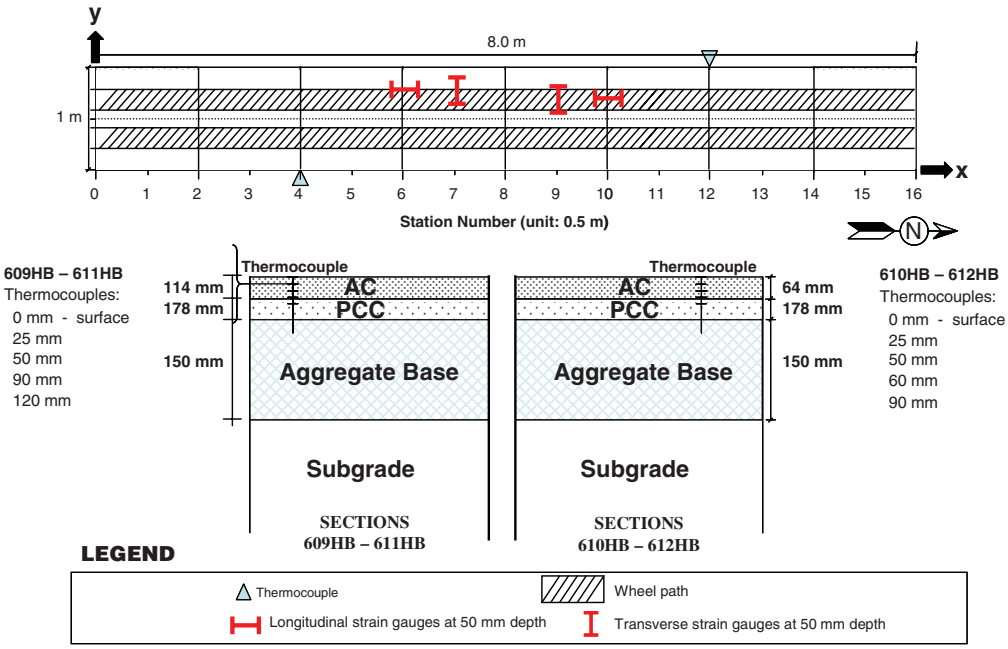

Figure 2.29. HVS rutting test section layout and location of thermocouples.

Concrete Mix

PCC was supplied that met the Caltrans Standard Specification Section 90: Portland Cement Concrete mix design. The concrete was classified as a Type 3, having a cementitious material content of 564 lb/yd^3, which includes 85 lb of fly ash. No chemical admixtures were used in the concrete. Concrete was batched at the ready mix plant and hauled approximately 20 miles to the test track site. Mix design details are presented in Appendix G.

Concrete Placement and Finishing

PCC construction began on August 7, 2009. Starting on the south end, concrete was placed on Lanes A and C by a 160-ft concrete boom pump. It was deemed necessary to pump the concrete because of difficulties in using slipform paving on the short sections with heavy instrumentation. Figure 2.30 shows the pumping process. Wet concrete was placed by hand around and over each instrument and carefully rodded and vibrated. The concrete was placed just ahead of the pumping for the rest of the slab to minimize differential curing between the concrete around the instrument and the rest of the slab. Light vibration was applied around the instruments without touching them using Minnich Manufacturing and Wacker Co. ¾-in. electric flex shaft vibrators ("stingers") as shown in Figure 2.31. Construction flags were placed to the wire holder at each instrument to indicate their position in the concrete to alert construction crew personnel. One sensor was lost when it was stepped on under the wet concrete. A motorized screed was used for surface vibration, strike-off, and initial finishing, as shown in Figure 2.32.

The surface was floated and textured by hand. Two layers of white curing compound were sprayed on the surface for a total spread rate of approximately 1 gallon/100 ft^2. Joints

Figure 2.30. View from east, concrete pump.

Figure 2.31. Hand packing concrete around instrumentation.

Figure 2.32. Motorized screed on Lane C, Day 1 PCC paving.

were cut to one-quarter slab thickness within 5 hours of concrete placement using an early entry saw. The cut joints were sprayed again with curing compound where the curing compound had been removed during the cutting process.

Both curing compound and tarps were used to minimize the risk of early-age slab cracking caused by the hot, dry weather. When the curing compound was sufficiently dry to walk on, Burlene tarps (proprietary product consisting of 10 oz/yd^2 burlap and 4 mil polyethylene sheeting sewn together) were soaked with water and placed on the concrete surface, burlap side down.

During both construction days, beams and cylinders were produced from most of the delivery trucks according to AASHTO T23-08. Specimens were rodded, and curing compound was sprayed on the surface of each specimen. Wet Burlene tarps were placed on all specimens. A set of beams and cylinders was randomly selected for strength monitoring.

Two beams and two cylinders were connected to maturity meters to monitor curing progression. The Burlene tarps were removed 3 weeks after concrete placement, following the manufacturer's recommendations. Details of curing, maturity, strength, and coefficient of thermal expansion on all beams and cylinders tested are presented in Appendix G.

HMA Construction

HMA Materials

Two types of HMA, both meeting their respective Caltrans specifications, were placed on the test track. On Lanes A and B, the mix placed was a ¾-in. (19-mm) maximum aggregate size, dense graded mix with polymer modified PG64-28 binder, referred to as PG64-28PM. On Lanes C and D, the mix placed was a ½-in. (12.5-mm) maximum aggregate size mix with gap graded aggregate and an asphalt rubber binder produced using the wet process, referred to as RHMA-G. The mix design information provided by the plant for both mixes is summarized in Table 2.8.

Construction Process

The first lift of each mix type was placed over 90 ft of the track (Sections 1 and 2), and the top lift was placed over the first

Table 2.8. Plant Mix Designs for RHMA-G and PG64-28PM Mixes

½-in. RHMA-G			¾-in. PG64-28PM		
Sieve Size	**Operating Range (%)**	**Target (%)**	**Sieve Size**	**Operating Range (%)**	**Target (%)**
1 in.	100	100	1 in.	100	100
¾ in.	100	100	¾ in.	95–100	99
½ in.	95–100	97	½ in.	na	87
⅜ in.	80–95	86	⅜ in.	65–80	74
No. 4	55–65	60	No. 4	45–55	59
No. 8	38–48	42	No. 8	31–41	36
No. 16	na	31	No. 16	na	27
No. 30	19–29	23	No. 30	15–25	21
No. 50	na	17	No. 50	na	16
No. 100	na	11	No. 100	na	10
No. 200	3–8	6.7	No. 200	3–8	6.2
Design binder content: 7.5% by dry weight of aggregate			Design binder content: 5.0% by dry weight of aggregate		
Theoretical maximum density (RICE): 2.55			Theoretical maximum density (RICE): 2.57		

Note: na = not applicable.

Figure 2.33. Start of PG64-28PM placement following application of tack coat.

Table 2.9. Nuclear Density Gauge Testing on HMA Lifts

Section	Description	Air Voids (%)
A1, A2, B1, B2 2.5 in. PG64-28PM	Bottom lift for 90 ft Lanes A and B	7.8
A1, B1 2.0 in. PG64-28PM	Top lift for 45 ft Lanes A and B	7.8
C1, C2, D1, D2 2.5 in. RHMA-G	Bottom lift for 90 ft Lanes C and D	8.0
C1, D1 2.0 in. RHMA-G	Top lift for 45 ft Lanes C and D	7.3

45 ft (Section 1) of the track. This was done to evaluate the effects of different HMA thickness on rutting and cracking performance for thin HMA layers on concrete slabs. HMA densities comparable to that typically found in the field were sought in the construction, with target values of approximately 7% air voids for the PG64-28PM mix and 10% for the RHMA-G. With such short test sections, overcompaction could easily occur, and approximate densities using the nuclear gauge after each roller pass were monitored. HMA construction began with the application of an anionic SS-1h emulsion tack coat over Sections 1 and 2 of all four lanes. The emulsion contained 61.5% solids by weight of emulsion. The asphalt in the emulsion had a penetration value of 51.

Once the tack coat had broken, 2.5 in. (65 mm) of the PG64-28PM was placed and compacted on Lanes A and B in Sections 1 and 2. The paver used was a Terex-Cedar Rapids CR552 with the 10-ft standard paving screed extended to 12 ft. The compactor used was a Caterpillar model CB-534D XW with 24,860-lb gross weight, 79-in. drum, operated at 2,520 cycles per minute at 0.01-in. vibration magnitude when in vibratory mode. Figure 2.33 shows this process, and Figure 2.34 shows the compaction and placement of the RHMA-G lifts.

Nuclear density testing was performed, and the testing results are shown in Table 2.9. Detailed density testing reports are presented in Appendix G. Air void contents were calculated from theoretical maximum density (TMD) tests (AASHTO T209) performed on loose mix collected during construction. The average field mix TMD for the PG64-28PM was 2.590, and for the RHMA-G it was 2.558. Laboratory-measured binder content for the PG64-28PM was 5.0%, and for the RHMA-G it was 7.55%.

Asphalt strain gauges were placed on the first lift in Lanes A and B of PG64-28PM while it was cooling prior to placement of the second lift (Figure 2.35). These strain gauges were located under and adjacent to the planned HVS wheelpath as part of a study of HMA movement under wheel load. Gauges were similarly placed on the first lift in Lanes C and D in the RHMA-G.

The same emulsified SS-1h tack coat was applied between lifts over all four lanes in Section 1 only. After tack coat placement and breaking, 2.0 in. (50 mm) of RHMA-G was placed and compacted on Lanes C and D. The paver was cleaned, and a 2.0-in.-thick lift of PG64-28PM was placed and compacted on Lanes C and D, Section 1 only. Figure 2.36 shows the completed test track with the second lift applied to the first 45 ft of the track.

Laboratory-compacted HMA specimens using rolling wheel compaction from the field mix in parallel with the placement and compaction of the test track were prepared. The

Figure 2.34. Compaction and placement of RHMA-G in Lanes C and D.

Figure 2.35. Measurement of the positions of strain gauges on first lift of PG64-28PM, before placement of second lift.

Figure 2.36. Completed test track showing two HMA lift thicknesses and PCC sections.

Figure 2.37. Compaction of ingots with rolling wheel compactor.

compacted "ingots" were later cut into 15 in. (380 mm) × 2.5 in. (62.5 mm) × 2.0 in. (50 mm) beams and 6 in. (150 mm) × 2 in. (50 mm) cores for flexural fatigue and repeated shear testing, respectively, to determine performance modeling parameters. Figure 2.37 shows the HMA in the mold frame. Additional details on test results for specimens produced from these ingots are presented in Chapter 3 and Appendix G.

Test Sections at the Illinois Tollway

Introduction

Two HMA/PCC segments were constructed by the Illinois Tollway on the ramps from I-94 to Milwaukee Avenue (off-ramp in the eastbound direction and on-ramp in the westbound direction) near Gurnee, approximately 40 miles north of Chicago and 5 miles from the Illinois-Wisconsin border. The ramps were constructed in October and November 2010 to emulate best practices of constructing HMA/PCC composite pavements using recycled aggregate. Figure 2.38 shows the location of the Tollway ramp sections.

Design and Specifications

The project consisted of using stockpiled recycled asphalt pavement (RAP) coarse aggregate in the PCC mix with a

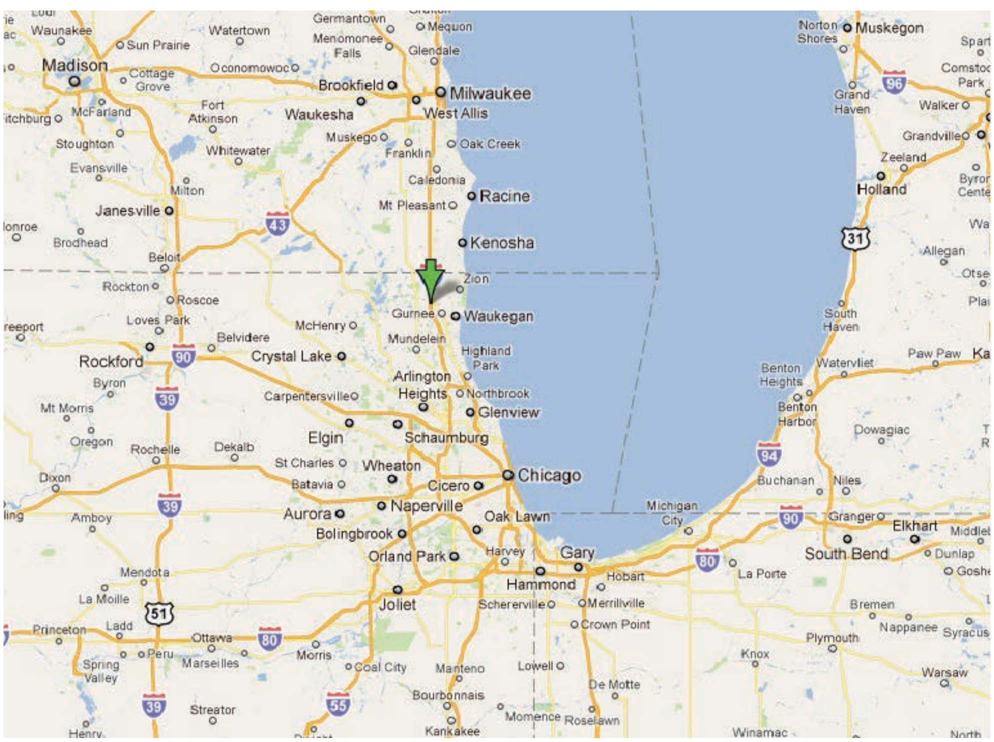

Source: © 2012 Google.

Figure 2.38. Location of the Illinois Tollway HMA/PCC on I-94 to Milwaukee Avenue.

Table 2.10. WMA/PCC Design for Illinois Tollway Section

Section		Illinois Tollway Milwaukee Avenue Ramp Reconstruction Tri-State Tollway (I-94) MP 9.9 to 10.1 WB On-Ramp 683 ft; EB Off-Ramp 981 ft
HMA	Thickness	2 in. (50 mm) placed in one lift
	Binder	PG 70-22 polymer modified
	Mix	WMA wearing course Illinois DOT designation 19536R with ⅜ in. (9.5 mm) nominal maximum aggregate size (N90F) and 0.5% Evotherm J1 additive
PCC	Thickness	9 in. (225 mm)
	Mix	Portland cement (~515 lb/yd^3 [310 kg/m^3]) Fly ash (~140 lb/yd^3 [85 kg/m^3])
	Coarse	30% RAP, 70% "A" quality
	Aggregate	Maximum aggregate size 1.5 in. (38 mm)
Base		4 in. (100 mm) unbound
Subgrade		Clay
Joint spacing		15 ft (4.6 m)
Dowels		1.25 in. (32 mm) placed on baskets in driving lane at PCC middepth and non-doweled passing lane
Joints		Saw and seal HMA over PCC joints

Note: EB = eastbound; WB = westbound; MP = milepost.

WMA surface layer. The relatively thin (2 in. [50 mm]), high-quality, dense-graded WMA layer was placed and bonded to the newly placed 9-in. (225-mm) low-cost PCC lower lift after the PCC had hardened sufficiently. The design is shown in Table 2.10.

Construction of the Test Section

This test section was designed and constructed to implement various sustainability features, including

- Recycled coarse aggregate from old asphalt pavements (RAP).
- Partial replacement of cement with fly ash (~20% to 25%). Fly ash is a by-product of coal-fired electric generating plants. The use of RAP and fly ash offers environmental advantages by diverting the material from the waste stream, reducing the energy investment in processing virgin materials, conserving virgin materials, and minimizing pollution.
- Use of WMA wherein the mix is heated to a lower temperature (~60°F to 90°F reduction compared with conventional HMA). Lower temperatures mean less fuel consumption, lower stack emissions, and less fume and odor generation at the plant and job site.

As in the case of the MnROAD sections, because of the unique nature of this project, special provisions were used as part of the bid package to modify the Tollway's existing specifications. The special provisions included

1. Structural concrete: Specifications for the concrete mix design and lower layer concrete design details.
2. Concrete curing and texturing: Specifications for the curing and texturing of the PCC surface to ensure adequate bond with the HMA layer.
3. Concrete pavement joints: Specifications covering details of saw cutting the joints in the PCC layer.
4. HMA joints: Specifications covering details of saw cutting and sealing the joints in the HMA layer.
5. HMA/PCC composite pavement operation: Sequence of paving activities for the construction of HMA/PCC composite pavements.

PCC Mix Design

Per the special provisions, the coarse aggregate fractionated from the RAP comprised 30% of the total coarse aggregate in the PCC mix (allowable range was 30% to 50%). In addition, aggregate fines less than 4.75 mm (No. 4) used in the PCC mix were specified to come from virgin aggregate sources. The special provisions also required the contractor to fractionate, clean, and wash the RAP (Figure 2.39). As much as 15% of the total recycled coarse aggregate could consist of agglomerated sand/asphalt particles per the special provisions. Table 2.11 shows the PCC mix design for the HMA/PCC pavement constructed at the Illinois Tollway.

HMA Mix Design

The JMF for the HMA mix proposed by the contractor and approved by the Tollway included 90% local aggregates and 10% RAP (with 5.2% asphalt binder content). The target HMA amount was 5.5% with 4.0% air voids. Tests indicated

Table 2.11. PCC Mix Design for HMA/PCC Construction at the Illinois Tollway

Materials	Weight per Cubic Yard (lb/yd^3)
Water	228
Cement	494
Class C fly ash	134
Sand	1,095
CA No. 1 (virgin aggregate)	1,334
CA No. 2 (recycled aggregate)	536
Water-Cement ratio	0.363

Figure 2.39. Fractionating, cleaning, and washing the RAP for use in the PCC mix.

a gyratory density of 150 lb/ft³ at 90 design gyrations. One hundred percent of the aggregates pass the 12.5-mm (½-in.) sieve, and 4.8% of the aggregates pass the No. 200 sieve.

Paving Operations

The paving operations for the construction of HMA/PCC composite pavement at the Illinois Tollway followed the same general sequence as at MnROAD, including placing the lower PCC layer, finishing the PCC layer, texturing (tining) the surface of the PCC layer, application of curing compound, sawing transverse joints in the PCC, marking the location of the sawed transverse joints, application of tack coat, paving the HMA surface, and sawing and sealing the HMA over the PCC transverse joints (see Figures 2.40 and 2.41).

Figure 2.40. Application of tack coat on PCC and marking the shoulder (to identify saw cut locations for sawing and sealing HMA).

Figure 2.41. Placement of HMA lift onto lower PCC layer.

As-Constructed Properties

As-constructed properties were collected as part of the QC/QA program on this construction. The results, which are the average of multiple tests, are summarized in Table 2.12 and Table 2.13.

Field Survey Sections

Introduction

In addition to the constructed test sites, additional field sites were identified to cover other types of HMA/PCC composite sections and to bring some long-term performance data into the analysis. An on-site condition survey was conducted, and detailed information regarding traffic, materials, and additional performance data was collected from the highway agencies and the LTPP database.

Table 2.14 provides a list of the HMA/PCC composite pavements that were included, along with images of LTPP composite sections that included an HMA surface over a lower strength concrete slab. These sections have all of the measured data needed, including FWD, cores and testing of the specimens, soil

Table 2.12. As-constructed RCA PCC Properties

Property		7 Day	14 Day	28 Day
Entrained air content	4.4%–7.1% (average 5.6%)	na	na	na
Unit weight	146.4 lb/ft³	na	na	na
Compressive strength	na	4,165 psi	4,430 psi	5,210 psi

Note: na = not applicable.

Table 2.13. As-constructed WMA Mix Properties

Property	Value
% Passing 12.5-mm (½-in.) sieve	100.0%
% Passing No. 200 sieve	4.9%
Asphalt binder percentage by weight	5.5%
Voids in mineral aggregate	15.0%
Bulk specific gravity	2.398
Max specific gravity	2.482
Average core density	143.8 lb/ft^3

borings, and long-term condition surveys with measurement of International Roughness Index (IRI), fatigue cracking, rutting, and joint faulting. Most of these sections were built in the 1980s and 1990s.

These tables show a range of characteristics and performance of these composite pavements:

- Asphaltic surfaces include 1.2-in. SMA over PCC and over HMA, 2- to 5-in. dense-graded HMA, 1-in. permeable HMA over dense HMA, porous friction course over HMA, 1-in. ARFC over PCC, and a 0.6-in. Novachip over HMA.
- The concrete layers show a wide range of thicknesses, from 5 to 14.5 in. JPC. The RCC ranges from 6 to 15 in.
- Joint spacing for JPC ranged from 15 to 30 ft typically. Joints were often not cut in RCC; however, some were cut at 15- to 45-ft intervals.
- Dowels were on some heavily trafficked sections but were not used on many. No dowels were used with RCC. Reflection cracks often dramatically showed the benefits of dowel bars to control joint load efficiency.
- Truck traffic ranged from low to very heavy. Typically, the following ranges existed in units of trucks per year in the heaviest travel lane:
  - Interstates and freeways: 1.4 million trucks/year (range, 0.5 to 3.6);
  - Highways: 0.2 million trucks/year (range, 0.1 to 0.3); and
  - Local streets: 0.05 million trucks/year (range, 0.004 to 0.08).
- The total trucks in the design lane ranged up to 47 million, and the age ranged up to 45 years.
- One section had a total life of 45 years, during which the asphaltic surface was replaced three times but the PCC did not require repair in any way. In fact, fatigue cracks developed only on the exceptionally thin PCC layers on some experimental sections. None of the typical thickness JPC developed any structural fatigue cracking of the slab.
- The composite pavements exist in all major climatic zones and over many types of subgrade soil.

Table 2.14. HMA/PCC Composite Pavement Field Sections

Composite Pavement Type	Location	Construction Year and Traffic	Comments
HMA/CRC Composite Pavements			
4-in. HMA over 12-in. CRC	San Antonio, Texas I-10 eastbound (southbound) MP 560–562 24 million trucks in 25 years in outer lane	1986 Outside lane widening of existing continuously reinforced concrete pavement (CRCP)	2011: No reflection transverse cracks. Some longitudinal cracks in both wheelpaths (~5%) and full length near shoulder (reflection from CRC/shoulder joint). Medium severity raveling. No other distresses. 0.4-in. rutting.
			

(continued on next page)

Table 2.14. HMA/PCC Composite Pavement Field Sections (continued)

Composite Pavement Type	Location	Construction Year and Traffic	Comments
2-in. SMA over 2.25-in. HMA binder over 8-in. CRC	O'Fallon/Fairview Heights, Illinois I-64 westbound MP 9-16 1.4 million trucks in 5 years in inner lane	2006 Inside lane widening of existing CRC pavement	2011: No transverse reflection cracking. Pavement is in excellent condition. Occasional minor midlane longitudinal cracking (could be PCC longitudinal joint reflection). No other distresses. ~0.0-in. rutting.
			
2-in. porous HMA over 9-in. CRC	Wilsonville/Oregon City, Oregon I-205 eastbound MP 3-8 5.2 million trucks in 4 years in outer lane	2007 porous HMA 1968 CRCP Outside lane widening of existing CRCP	2011: No reflection transverse cracks. Some longitudinal cracks in both wheelpaths (~5%) and full length near shoulder (reflection from CRC/shoulder joint). Medium severity raveling. No other distresses. 0.4-in. rutting.
			

(continued on next page)

Table 2.14. HMA/PCC Composite Pavement Field Sections (continued)

Composite Pavement Type	Location	Construction Year and Traffic	Comments
1.5-in. SMA over 3.0-in. HMA binder over 8-in. CRC	Henrico County/Richmond, Virginia I-64 westbound MP 184-185 1.7 million trucks in 5 years in outer lane	2006 Outside lane widening of existing CRCP	2011: Pavement is in excellent condition. No observable distresses. No transverse reflection cracks. Condition rating 97/100. 0.14-in. rutting.
			
2-in. porous HMA over 10-in. CRC	The Netherlands, West of Utrecht A12 19 million trucks in 10 years in outer lane	1998 construction Heavy truck traffic New HMA/CRC construction	2008: Excellent performance over 10 years. Minor rutting. No reflection cracking. Some raveling of porous asphalt surface. Raveling not excessive but likely will necessitate that the surface layer be replaced within about 5 years.
			

(continued on next page)

Table 2.14. HMA/PCC Composite Pavement Field Sections (continued)

Composite Pavement Type	Location	Construction Year and Traffic	Comments
2.8-in. porous HMA over 10-in. CRC	The Netherlands, Province of Limburg, between Venlo and Echt-Susteren A73 2 million trucks in 1 year in outer lane	2007 New HMA/CRC construction	2008: Excellent condition. No distresses. No reflection cracking or any other kind of cracking. Very low noise and extremely smooth ride. Delegation's hosts stated that the construction quality was excellent on this project.
		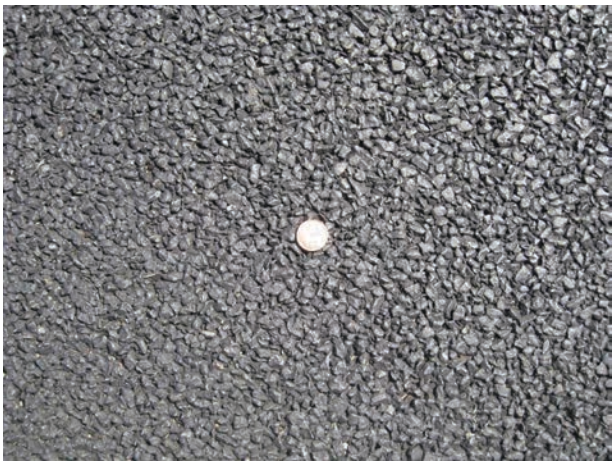	
0.5-in. Asphalt rubber friction course (ARFC) over 13-in. CRC	90 miles west of Phoenix, Arizona I-10 westbound MP 76 20 million trucks in 16 years in outer lane	1994 construction New ARFC/CRC construction outer lane	2011: Pavement in poor condition over 16 years and very heavy truck traffic. Minor rutting. Most transverse reflection cracks have come through due to thin surface. 20 punchouts per mile. Raveling of porous asphalt surface. Project needs rehabilitation.
			

(continued on next page)

Table 2.14. HMA/PCC Composite Pavement Field Sections (continued)

Composite Pavement Type	Location	Construction Year and Traffic	Comments
1.0-in. ARFC (2005) over 9-in. CRC (1989)	Phoenix, Arizona Loop 101, MP 7-14 2.6 million trucks over 5 years in outer lane	2010 ARFC (2005) over CRC (1989) construction	2011: Excellent condition. No distresses. Very low noise and extremely smooth ride.
			
HMA/RCC Composite Pavement			
3.0-in. HMA over 8-in. RCC	Grove City/Columbus, Ohio White Road, ~700 ft east of Buckeye Parkway 70,000 trucks over 7 years in outer lane	2003 New HMA/RCC construction	2010: Very good condition. Excellent ride. No RCC cracks or any other transverse cracking. RCC sawed at 45 ft spacing. HMA sealed immediately after reflection cracks came through. Very minor wheelpath raveling in parts. 0.04-in. rutting.
			

(continued on next page)

Table 2.14. HMA/PCC Composite Pavement Field Sections (continued)

Composite Pavement Type	Location	Construction Year and Traffic	Comments
1.5-in. HMA over 8-in. RCC	Columbus, Ohio Lane Avenue, approximate address is 350 West Lane Avenue 270,000 trucks over 9 years in outer lane	2003 New HMA/RCC construction	2010: Very good condition. Excellent ride. One unsealed reflection crack observed. Others were sealed after crack came through. RCC sawed at 30-ft spacing. Cracks at 90 ft spacing and some additional cracking suggest (40%) have reflected to date. 0.04-in. rutting.
			
HMA/JPC Composite Pavement			
3.5-in. HMA over 12.5-in. JPC 20-ft joint spacing Slab width 12.5 ft (milled original 3.5-in. HMA in 2001 and new 3.0-in. HMA placed)	Chicago, Illinois I-294 eastbound and westbound MP 17.7 to 36.4 30 million trucks over 19 years in outer lane	1992 and 2001 Outside lane widening of existing JPCP from three to four lanes Milled original 3.5-in. HMA in 2001 and new 3.0-in. HMA placed	2010: Four sections surveyed. Only reflection cracking from 20-ft spaced transverse joints, no midpanel cracks. Some roughness caused by minor raveling and reflection crack sealing and deterioration of reflection cracks. 0.2-in. rutting.
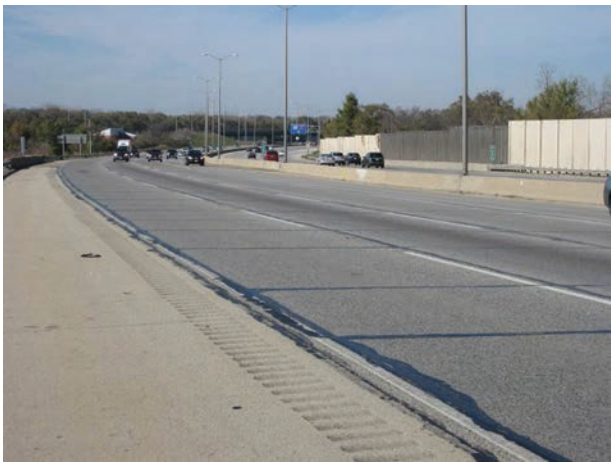			

(continued on next page)

Table 2.14. HMA/PCC Composite Pavement Field Sections (continued)

Composite Pavement Type	Location	Construction Year and Traffic	Comments
3.0-in. HMA over 8-in. JPC 20-ft joint spacing	Grove City/Columbus, Ohio Hoover Road, between Stringtown Road and Dartmoor Road 400,000 trucks over 8 years in outer lane	2003 New HMA/JPC construction	2010: Good condition. ~60% of the sawed joints in the JPC have reflected through. HMA sealed after reflection cracks came through. Only transverse cracks are reflection cracks. Some roughness attributable to crack sealant and utility cuts. 0.04-in. rutting.
			
3.0-in. HMA over 8-in. JPC 20-ft joint spacing	Grove City/Columbus, Ohio Buckeye Parkway, ~2,000 ft south of Holton Road 100,000 trucks over 10 years in outer lane	2003 New HMA/JPC construction	2010: Very good condition. ~90% of the sawed PCC joints have reflected through. HMA typically sealed after reflection cracks came through. Only transverse cracks are reflection cracks. Some minor polishing in wheelpath. No other distresses. 0.02-in. rutting.
			

(continued on next page)

Table 2.14. HMA/PCC Composite Pavement Field Sections (continued)

Composite Pavement Type	Location	Construction Year and Traffic	Comments
3.0-in. HMA over 7-in. JPC 18-ft joint spacing	Columbus, Ohio Approximate address is 3218 McCutcheon Crossing Drive, a residential subdivision street 42,000 trucks in 9 years in one lane	2003 New HMA/JPC construction	2010: Very good condition. ~90% of the sawed PCC joints have reflected through. Some HMA sealed after reflection cracks came through. Only transverse cracks are low-severity reflection cracks. 0.00-in. rutting.
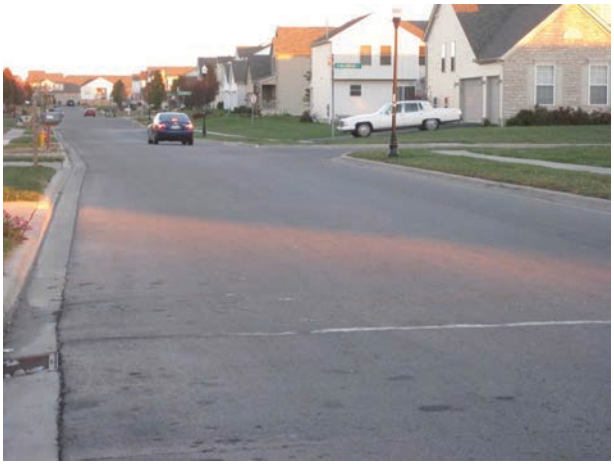			
1.2-in. SMA over 10.3-in. JPC (widened slab) 16.4-ft joint spacing	Germany, south of Munich A93 47 million trucks over 13 years in outer lane	1995 New SMA/JPC construction	2008: Excellent performance over 13 years. All transverse and longitudinal joints sawed and sealed. Minor rutting. No additional reflection cracking or midslab cracking. Some SMA patching at transverse joints for unknown reasons.
	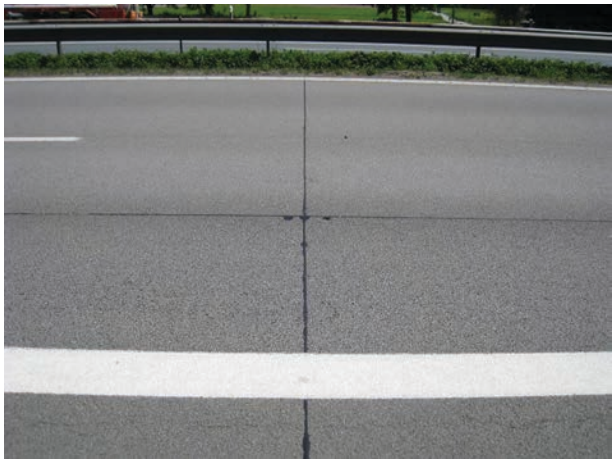		

(continued on next page)

Table 2.14. HMA/PCC Composite Pavement Field Sections (continued)

Composite Pavement Type	Location	Construction Year and Traffic	Comments
4-in. HMA over 6-in. JPC	Seattle, Washington I-5 northbound and southbound MP 178 to 198 30 million trucks over 45 years in outer lane	1966 (1.8-in. HMA overlays in 1979, 1995, and 2006) New HMA/PCC construction	2011: Pavement overlay in 2006 and existing pavement in excellent condition. Very few reflection cracks. No other distresses.
			
3-in. HMA 9-in. JPC 20-ft joint spacing 12 sections constructed to evaluate various reflection crack treatments	New York, New York Jamaica Avenue Between 127th Street and Van Wyck West Service Road 300,000 trucks in 7 years in outer lane	2000 New HMA/PCC construction	2007: Two 20-ft sections included in analysis: one with sawed and sealed joints and one with no reflection crack treatments (control). 0.05-in. rutting. Pavement in good condition with all control joints (80% total length) reflected through. Various reflection crack treatment options had varying performances by sawed and sealed joints best performing.
			

(continued on next page)

Table 2.14. HMA/PCC Composite Pavement Field Sections (continued)

Composite Pavement Type	Location	Construction Year and Traffic	Comments
3-in. HMA 9-in. JPC 15-ft joint spacing 12 sections constructed to evaluate various reflection crack treatments	New York, New York Jamaica Avenue between Van Wyck East Service Road and Sutphin Boulevard 300,000 trucks in 7 years in outer lane	2000 New HMA/PCC construction	2007: Two 15-ft sections included in analysis: one with sawed and sealed joints and one with no reflection crack treatments (control). 0.05-in. rutting. Pavement in good condition with all control joints (60% total length) reflected through. Various reflection crack treatment options had varying performances by sawed and sealed joints best performing treatment.
			
1-in. ARFC 14.5-in. JPCP doweled 13-, 15-, 17-ft joint spacing	Tucson, Arizona (01-86) I-10 urban freeway MP 255 20 million trucks in 9 years in outer lane	2002 construction of new ARFC/JPC	2011: Only transverse joint low severity reflection cracks, no transverse fatigue cracks. Very smooth, 0.12-in. rutting. Pavement in excellent condition.
		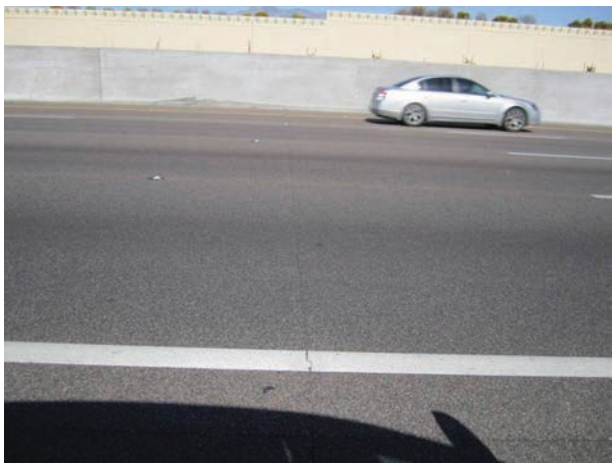	

(continued on next page)

Table 2.14. HMA/PCC Composite Pavement Field Sections (continued)

Composite Pavement Type	Location	Construction Year and Traffic	Comments
1-in. ARFC 13-in. JPCP, doweled Widened slab 13-, 15-, 17-ft joint spacing	California/Arizona state line, MP 8 (02-24) I-10 11 million trucks in 6 years in outer lane	2004 construction both ARFC and JPC	2011: Only transverse joint low severity reflection cracks, no transverse fatigue cracks. Very smooth, 0.08-in. rutting. Pavement in excellent condition.
			
1-in. ARFC 14-in. JPCP, doweled, widened slab 13 ft 13-, 15-, 17-ft joint spacing	100 miles west of Phoenix, Arizona I-10 (92-39) MP 60 EBL 20 million trucks in 17 years in outer lane	1994 New ARFC/JPC construction	2011: Only transverse joint low severity reflection cracks, no transverse fatigue cracks. Very smooth, 0.08-in. rutting. Pavement in good condition after 15 years.
			

(continued on next page)

Table 2.14. HMA/PCC Composite Pavement Field Sections (continued)

Composite Pavement Type	Location	Construction Year and Traffic	Comments
1-in. ARFC 11.5-in. JPCP, nondoweled 13-, 15-, 17-ft joint spacing	Phoenix, Arizona L-101 (98-159) Urban freeway 5 million trucks over 9 years in outer lane	2001 New ARFC/JPC construction	2011: Only transverse joint low severity reflection cracks, no transverse fatigue cracks. Very smooth, 0.06-in rutting. Pavement in excellent condition after 10 years.
		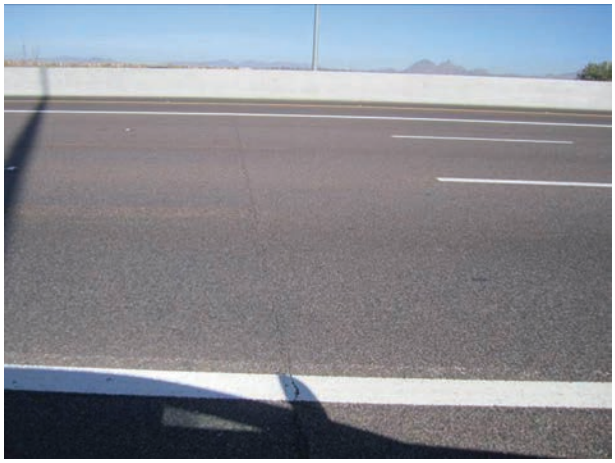	
1-in. ARFC 13-in. JPCP, nondoweled 13-, 15-, 17-ft joint spacing	Phoenix, Arizona L-202 (03-06) Urban freeway 600,000 trucks in 5 years in outer lane	2005 New ARFC/JPC construction	2011: Only transverse joint low severity reflection cracks, no transverse fatigue cracks. Very smooth, 0.07-in. rutting. Pavement in excellent condition after 6 years.
			

(continued on next page)

Table 2.14. HMA/PCC Composite Pavement Field Sections (continued)

Composite Pavement Type	Location	Construction Year and Traffic	Comments
1-in. ARFC 14-in. JPCP, doweled 13-, 15-, 17-ft joint spacing	Flagstaff, Arizona I-40 (04-68) 5 million trucks over 3 years in outer lane	2007 New ARFC/JPC construction Heavy truck loadings	2011: Only transverse joint low severity reflection cracks, no transverse fatigue cracks. Very smooth, 0.08-in. rutting. Pavement in excellent condition after 4 years.
			
3-in. HMA 6-in. JPCP, doweled and non-doweled, 15-ft joint spacing	R21 MnROAD site 40 miles west of Minneapolis, Minnesota I-94 WBL 600,000 trucks in 1 year in outer lane 70,000 trucks in 1 year in inner lane	2010 New HMA/JPC construction	2011: Transverse joints sawed and sealed in good condition, other low severity reflection cracks, no transverse mid-panel fatigue cracks. Very smooth, minor rutting. Pavement in excellent condition after 1 year.
	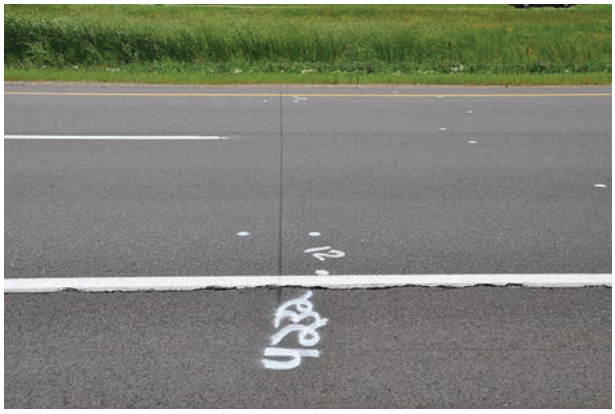		

(continued on next page)

Table 2.14. HMA/PCC Composite Pavement Field Sections (continued)

Composite Pavement Type	Location	Construction Year and Traffic	Comments
2-in. HMA 5-in. JPCP, doweled and non-doweled, 15-ft joint spacing	MnROAD site (pooled fund) 40 miles west of Minneapolis, Minnesota I-94 WBL 1,000,000 trucks in 2 years in outer lane 116,000 trucks in 2 years in inner lane	2009 New HMA/JPC construction (pooled fund project)	2011: Reflection transverse non-doweled joints high severity, doweled joints low-medium. About 50% slabs cracked outer lane and 10% cracked inner lane. Reconstruction after 2 years.
			
Additional HMA/JPC or HMA/RCC Composite Pavement			
⅝-in. Novachip 3-in. HMA 11-in. JPC doweled Random 18-,19-, 21-, and 27-ft joint spacing	Raleigh, North Carolina I-40 MP 270 to 279 4.4 million trucks over 5 years in inner lane	2005 Inside lane widening of existing JPC	2010: Rides very well, no reflection cracking or any other cracking. JPCP and Novachip in good condition. 0.2-in. rutting.
3-in. HMA 8-in. JPC 15-ft joint spacing	Franklin County, Ohio Route 161 MP 16.75 to 23.84 (from I-270 to East County Line) 2.4 million trucks over 11 years	1993 New HMA/JPC construction	2004: Condition rating 78/100. 0.1-in. rutting. Milled and overlaid in 2005/2006.
1-in. porous HMA 1.6-in. HMA 10-in. JPC, dowels 15-ft joint spacing	Scarborough/Pickering Ontario, Canada Hwy 401 1 km east of White Road to Brock Road 18 million trucks over 13 years in outer lane	1996 Outside lane widening of existing JPC	2009: Condition rating 84/100, IRI 70 in./mi, 0.15-in. rutting. Good condition. All PCC transverse joints have reflected through the HMA layers.
1-in. porous HMA 1.6-in. HMA 10-in. JPC 15-ft joint spacing	Scarborough/Pickering Ontario, Canada Hwy 401 Neilson Road to 1 km east of White Road 21 million trucks over 14 years in outer lane	1995 Outside lane widening of existing JPC	2009: Condition rating 84/100, IRI 81 in./mi, 0.16-in. rutting. Good condition. All PCC transverse joints have reflected through the HMA layers.
1.6-in. SMA 2.0-in. HMA 9-in. JPC 15-ft joint spacing	Toronto Ontario, Canada Hwy 401 Renforth Drive to Hwy 27 15 million trucks over 5 years in outer lane	2002 Outside lane widening of existing JPC	2009: Condition rating 90/100, IRI 70 in./mi, 0.21-in. rutting. Excellent condition. Majority PCC transverse joints have reflected through the HMA layers.

(continued on next page)

Table 2.14. HMA/PCC Composite Pavement Field Sections (continued)

Composite Pavement Type	Location	Construction Year and Traffic	Comments
3.2-in. HMA 10-in. JPC 15-ft joint spacing	Toronto Ontario, Canada Hwy QEW Stoney Creek to St. Catharines 27 million trucks over 16 years in outer lane	1993 Heavy truck traffic Outside lane widening of existing JPC	2009: Condition rating 67/100, IRI 95 in./mi, 0.20-in. rutting. Average condition. All PCC transverse joints have reflected through the HMA layers.
1.0-in. porous HMA 4.0-in. HMA 10-in. JPC, no dowels 15-ft joint spacing	Rock Hill, South Carolina South of Charlotte, North Carolina I-77 MP 84 to 90 2 million trucks over 10 years in outer lane	2000 Inside two lanes JPC widening of existing CRC	2009: Condition rating 4.05/5.0, IRI 53 in./mi, 0.15-in. rutting. Excellent condition. No observed reflection cracks. Still looks excellent.
3.2-in. HMA 7.4-in. JPC no dowels 15-ft joint spacing	LTPP Section 872811, London Ontario, Canada Route 402 Eastbound driving lane about 1 km west of Hwy 21 junction 5.4 million trucks over 23 years in outer lane	1977 New HMA/JPC construction	2010: IRI 95 in./mi, 0.24-in. rutting. Average condition. All PCC transverse joints have reflected through the HMA layers.
1-in. HMA 15-in. RCC No joints	LTPP Section part of SPS-1 US 93 Northwest Arizona 1.4 million trucks over 13 years	1993 New HMA/RCC construction	2006: Transverse reflection cracks moderate severity, 0.18-in. rutting, minimum alligator cracking.
HMA/CTB or LCB Sections from LTPP Database			
4.2-in. HMA 6.6-in. LCB	LTPP Section 062038 Del Norte County, California Route 101 MP 30; 1.7 mi north of Railroad Avenue overcrossing and 0.6 mi south of Grants Pass/ Route 199 exit 5.7 million trucks over 25 years	1972 New HMA/LCB construction	2007: IRI 82 in./mi, 0.16-in. rutting. Average condition. 1 transverse crack every 10 to 20 ft. Sealcoated in 2000.
2.4-in. HMA 6.3-in. LCB	LTPP Section 382001 West Grand Forks County, North Dakota Route 2 MP 340; 9.5 mi east of State Hwy 18, 16.5 mi west of I-29 1.1 million trucks over 11 years	1978 New HMA/LCB construction	1989: IRI 105 in./mi, 0.47-in. rutting. Fair condition. 1 transverse crack every 10 to 20 ft. Sealcoated in 1990.
2.4-in. HMA 11.2-in. CTB	LTPP Section 562017 Campbell County, Wyoming Route 387 MP 136.1. 4.3 miles east of Pine Tree Junction (State Hwy 50 and State Hwy 387) 1.7 million trucks over 16 years	1982 New HMA/CTB construction	1998: IRI 124 in./mi, 0.20-in. rutting. Poor condition. One transverse crack every 10 to 20 ft. Overlaid in 1999.
4.2-in. HMA 10.6-in. CTB	LTPP Section 562019 Campbell County, Wyoming Route 59 MP 103.3. 9.1 miles south of I-90 overpass 1.4 million trucks over 9 years	1985 New HMA/CTB construction	1994: IRI 105 in./mi, 0.20-in. rutting. Fair condition. One transverse crack every 20 ft. Overlaid in 1997.

Note: EBL = eastbound lane; WBL = westbound lane.

CHAPTER 3

HMA/PCC Analysis and Performance Modeling

Introduction

This chapter summarizes the results of the field testing for the constructed test sections, the details of which are included in the appendices. These results were used to refine and validate rutting and reflection cracking models, as well as to perform mechanistic-empirical (M-E) modeling of HMA/PCC composite pavements using the DARWin-ME models and compare the models with observed field performance.

Analysis of Field Data at MnROAD

As discussed in Chapter 2, a HMA/PCC field test section was constructed at the MnROAD facilities. The HMA/PCC section (with RCA in the PCC mix) constructed was labeled Cell 70. Two other test sections, Cell 71 and Cell 72, also were constructed at MnROAD. Both of those were PCC/PCC composite pavements constructed wet-on-wet. Cell 71 had the same lower lift PCC mix as Cell 70 with RCA in the PCC mix, whereas Cell 72 did not have RCA in PCC mix. Construction details for Cells 71 and 72 are included in Appendix F and discussed in Volume 2. For the sake of comparing HMA/PCC with PCC/PCC and understanding the effects of the HMA surface layer, some information from Cells 71 and 72 is included in this chapter.

PCC Slab Temperature Profiles

The simplest way to characterize the temperature distribution in the slab is by assuming a linear distribution for the temperature throughout the depth of the slab. The linear temperature gradient (LTG) is calculated as the temperature difference between the top and bottom of the slab taken over the distance between the two. However, several field studies have shown that the distribution of temperature throughout the slab depth is primarily nonlinear (Armaghani et al. 1987, Yu et al. 1998). To account for the nonlinearity of the temperature distribution in the slab, the equivalent temperature gradient concept was developed (Thomlinson 1940, Choubane and Tia 1992, Mohamed and Hansen 1997). The effective linear temperature gradient (ELTG) is a linear gradient that would produce the same curvature in the slab as the original nonlinear temperature gradient. The ELTG concept was later generalized for nonuniform, multilayered slabs (Khazanovich 1994, Ioannides and Khazanovich 1998). The latter method in which the ELTG is established for an effective slab, with a thickness and stiffness equivalent to that of a composite multilayer section, is employed in this study.

Effect of Location on Slab (Midslab versus Edge versus Corner)

Temperature distribution throughout the slabs for Cell 70 was compared at three different locations (midslab, edge, and corner) within both instrumented HMA/PCC slabs, as shown in Figure 3.1. The figure shows that the LTG for all locations throughout the majority of the day is consistent. The peak LTG for all locations is observed in the late afternoon, when the peak ambient temperature and solar radiation are seen. The highest LTG was observed at midslab, and the smallest occurred in the corner, although the variation is marginal.

The depths of the two thermocouples used at each location to establish the gradients affect the magnitude of the LTGs. The as-built depths for the thermocouples in Slabs 1 and 2 are given in Table 3.1. The table shows that the as-built depths for the thermocouples in Slab 1 are the same for all locations. For Slab 2, corner thermocouples are approximately 0.25 in. above the top thermocouples at the edge and midslab locations. Therefore, the depths of the thermocouples can be considered to be approximately the same for all locations. It

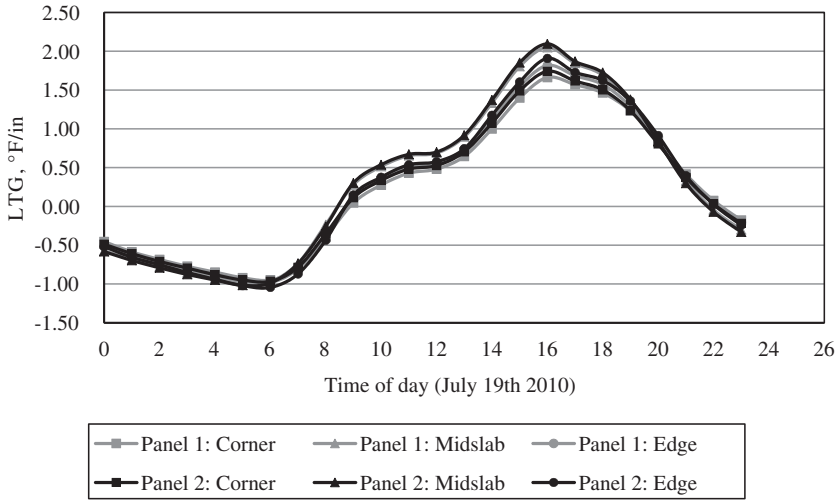

Figure 3.1. LTG in the PCC layer for various slab locations in Cell 70 on July 19, 2010.

should be noted that the depth of the sensors throughout the slab was established by subtracting the design depth from the surveyed position of the top sensor. The possible differences between the actual and estimated depths of the sensors most likely contributed to some variation in the magnitude of the LTGs.

Figure 3.1 shows that there is some variation in the LTG as a function of the location of the thermocouples within the slab. The magnitude of the gradient is slightly larger at midslab for both slabs. The LTGs at the edge are also slightly larger than the corner for both slabs.

Effect of HMA Layer

For comparison between the temperature gradients that develop in Cells 71 and 72 with respect to Cell 70, only the data for Cell 71 were used because the data for Cell 71 were complete, unlike those for Cell 72. In the case of Cell 70, the curling of the PCC layer covered with HMA is dictated by the temperature gradient in the PCC because of the relatively lower stiffness of the HMA. Therefore, the temperature gradient through just the PCC layer for Cell 70 is considered in the analysis. In Cell 71, the curling induced by a temperature gradient is caused by the temperature distribution throughout the entire slab. Therefore, the temperature gradient was established in Cell 71 based on the composite temperature distribution of both the upper PCC layer and the lower PCC layer.

Table 3.1. Depths at the Top and Bottom Thermocouples for the PCC Layer in Cell 70

	Corner (in.)	Midslab (in.)	Edge (in.)
Top	3.75	3.75	3.75
Bottom	9.25	9.25	9.25

Figure 3.2 and Figure 3.3 show the distribution of the LTGs in the PCC layer for Cell 70 and the entire slab for Cell 71, respectively. Table 3.2 summarizes a statistical comparison made between the distributions of LTGs. As shown in Table 3.2 and the histograms for the two pavement cells, the LTGs are lower for Cell 70 than for Cell 71. This suggests that for Cell 70, as expected, the nonlinearity of the temperature gradient decreases because of the HMA overlay. Additional details are provided in Appendix H.

Figure 3.4 provides a direct comparison between the average LTGs for both slabs in Cells 70 and 71. Cell 70 shows a higher frequency of occurrence of gradients near zero and a lower frequency of larger gradients, when compared with Cell 71. Again, the upper HMA layer in Cell 70 serves as an insulating layer.

The previous two analyses have shown that although the magnitude of the weighted average temperature (WAT) for Cell 70 was relatively large, the LTGs that developed were less. It is hypothesized that not only is the magnitude of the gradient lower in Cell 70 when compared with Cells 71 and 72, but the nonlinear component of the temperature gradient is also reduced. The upper HMA layer helps to buffer the lower PCC layer from more rapid temperature swings, thereby reducing the potential for highly nonlinear temperature distributions to develop in the upper portion of the PCC layer. Figure 3.5 and Figure 3.6 illustrate the temperature distributions in the slabs throughout a single summer day for Cells 70 and 71, respectively. As can be seen from these figures, the deviation of the temperature profiles from a linear gradient is more pronounced in Cell 71.

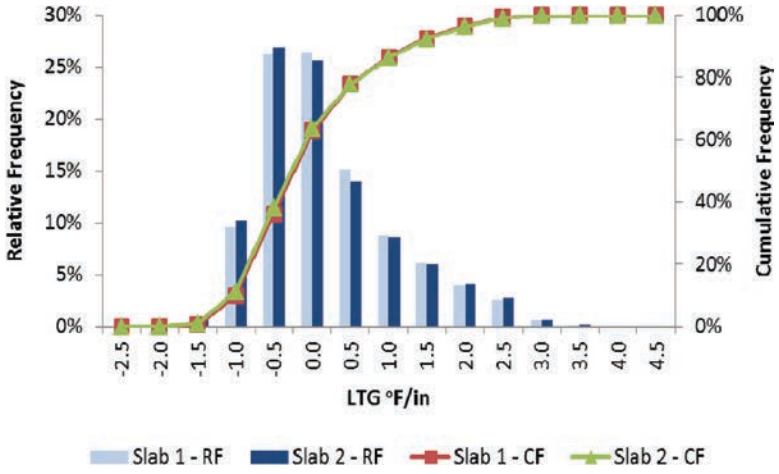

Figure 3.2. LTG distribution for Slabs 1 and 2 for Cell 70.

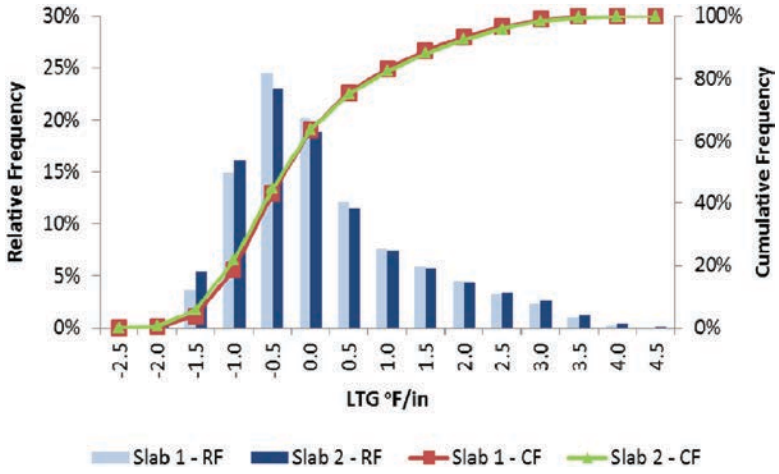

Figure 3.3. LTG distribution for Slabs 1 and 2 in Cell 71.

Based on this, it can be concluded that the LTG alone is not sufficient in characterizing the actual variation of the temperature throughout the depth. The nonlinearity of the temperature distribution also should be evaluated.

The ELTGs were estimated for Cells 70 and 71 using Equations 3.1 through 3.3.

Table 3.2. Comparison of Statistics of LTG Between Cells 70 and 71

	LTG, °F/in.			
	Cell 70		Cell 71	
	Slab 1	Slab 2	Slab 1	Slab 2
Average	–0.06	–0.08	–0.09	–0.10
Maximum	3.32	3.37	3.94	4.14
Minimum	–1.83	–1.97	–2.20	–2.26
Standard deviation	0.88	0.90	1.14	1.22
Median	–0.27	–0.30	–0.36	–0.38

$$\Delta T_{eff} = \frac{12}{h_{eff}^2} \times \left\{ \int_{-x}^{h_{top}-x} (T(z) - T_0) z dz + \frac{\alpha_{bot} \cdot E_{bot}}{\alpha_{top} \cdot E_{top}} \int_{h_{top}-x}^{h_{top}+h_{bot}-x} (T(z) - T_0) z dz \right\} \quad (3.1)$$

where

ΔT_{eff} = difference between temperatures at the top and bottom surfaces of the effective slab,
$T(z)$ = temperature distribution through the PCC concrete,
T_0 = zero-stress temperature,
z = vertical coordinate measured downward from the neutral axis of the composite pavement,
h_{top} = thickness of the upper layer,
h_{bot} = thickness of the lower layer,
E_{top} = elastic modulus of the upper layer,
E_{bot} = elastic modulus of the lower layer,
α_{top} = coefficient of thermal expansion of the upper layer,
α_{bot} = coefficient of thermal expansion of the lower layer, and

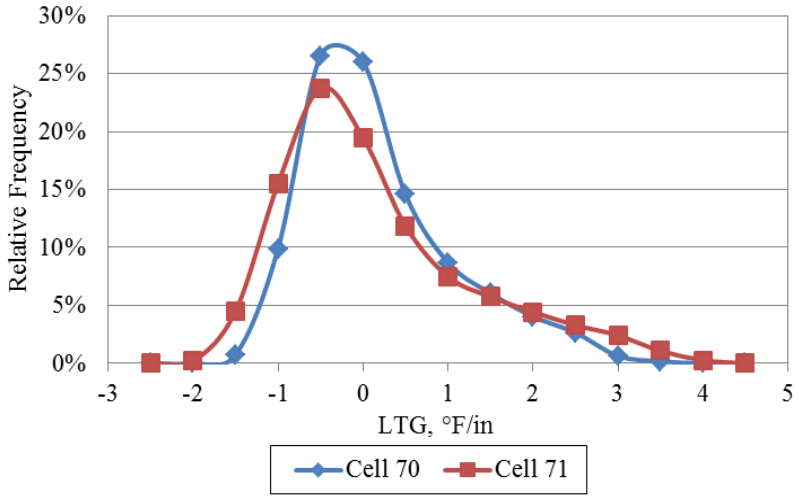

Figure 3.4. Comparison of relative frequencies for LTGs in Cells 70 and 71.

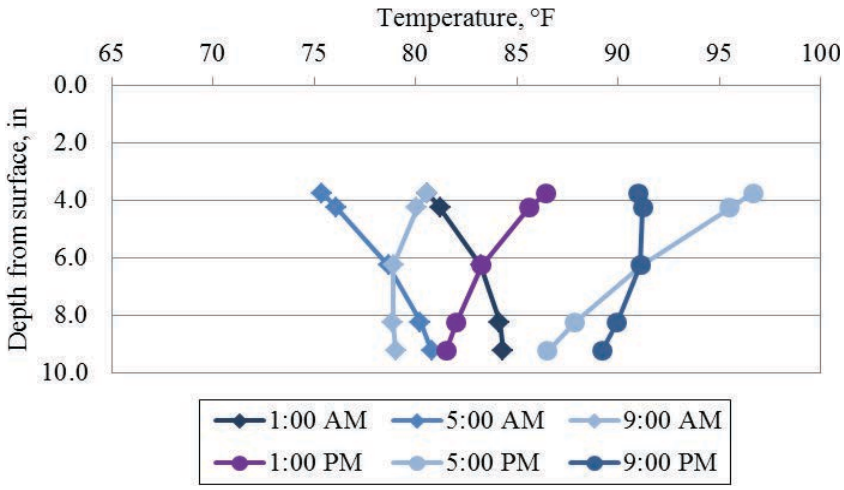

Figure 3.5. Temperature distributions in the PCC for Cell 70.

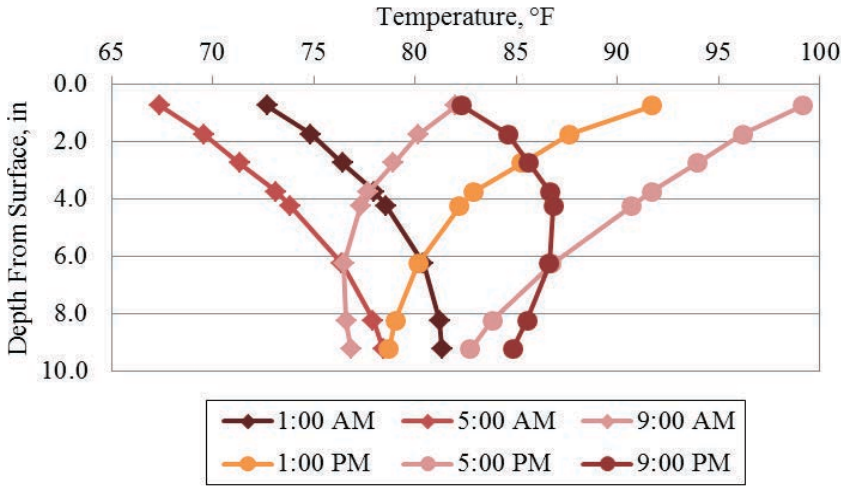

Figure 3.6. Temperature distributions in the composite section for Cell 71.

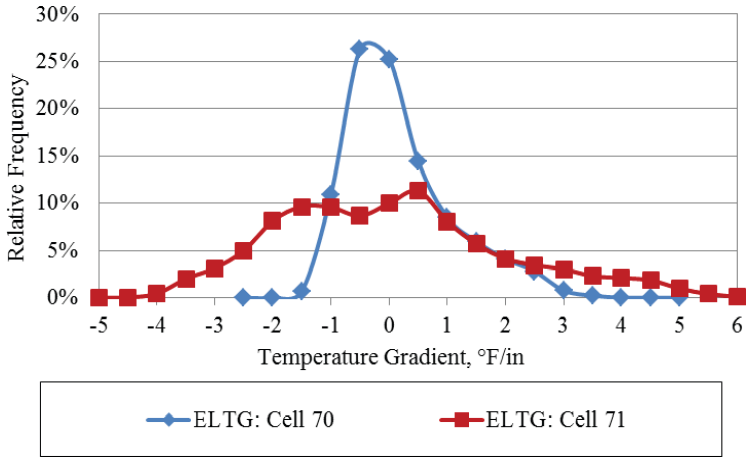

Figure 3.7. Comparison of relative frequencies for ELTGs in Cells 70 and 71.

h_{eff} = effective thickness of the pavement, which can be determined from Equation 3.2:

$$h_{eff} = \sqrt[3]{h_{top}^3 + \frac{E_{bot}}{E_{top}} h_{bot}^3 + 12\left(\begin{array}{l} h_{top}\left(x - \frac{h_{top}}{2} \right)^2 \\ + \frac{E_{bot}}{E_{top}} \left(h_{top} + \frac{h_{bot}}{2} - x \right)^2 h_{bot} \end{array} \right)} \quad (3.2)$$

x = distance between the neutral plane and the top surface of the upper layer, which can be determined from Equation 3.3.

$$x = \frac{\frac{h_{top}^2}{2} + \frac{E_{bot}}{E_{top}} h_{bot}\left(h_{top} + \frac{h_{bot}}{2} \right)}{h_{top} + \frac{E_{bot}}{E_{top}} h_{bot}} \quad (3.3)$$

Figure 3.7 shows the variation in the ELTGs between Cells 70 and 71. The summary statistics for the ELTGs that developed in both cells are presented in Table 3.3 and Table 3.4. As noted, Cell 70 shows a higher frequency of occurrence of ELTGs close to zero, when compared with Cell 71. As seen in Figure 3.7, the shape of the frequency distribution curve of LTGs and ELTGs for Cell 70 is quite similar, whereas a considerable variation is observed in Cell 71. Unlike the LTGs, the ELTGs for Cell 71 are more evenly distributed over a broader range. To investigate the significance of variation in LTGs and ELTGs within a cell and the variation of each of these gradients between the cells, paired *t*-tests for two sample means were performed. Results from the *t*-tests are given in Table 3.3 and Table 3.4. The variation between the LTGs and ELTGs for Cell 70 is not significant, whereas it is quite significant for Cell 71. This indicates that the gradients that develop in the HMA/PCC pavements tend to be more linear than those in the PCC/PCC pavements, as is supported by the temperature profiles provided in Figure 3.6.

The results of the paired *t*-test for the ELTGs between Cells 70 and 71 also conclude the difference in the ELTGs is significant at a 95% confidence level. The ELTGs in Cell 71 (PCC/PCC) are much higher over a larger period of time than are those for Cell 70 (HMA/PCC). Figure 3.7 shows clearly that the magnitude of the temperature gradients, as well as the frequency at which these higher gradients develop, is significantly greater for a PCC/PCC pavement than for an HMA/PCC pavement.

PCC Slab Moisture Profiles

Besides temperature variation within the slab, the moisture variation through the depth is important because the moisture variation through the depth of the slab produces an upward warping of the slab, which under the influence of

Table 3.3. Comparing the LTG and ELTG for Cells 70 and 71

	Cell 70		Cell 71	
	LTG	ELTG	LTG	ELTG
Average, °F/in.	–0.07	–0.07	–0.08	–0.20
Variance, °F/in.	0.79	0.829	1.29	3.85
Observations	28,649			
Hypothesized mean difference	0			
Degrees of freedom	28,648			
t-statistic	1.43		14.64	
p-value	0.15		0	
t-critical two-tail	1.96		1.96	

Table 3.4. Comparing the ELTG Statistics for Cells 70 and 71

	ELTG, °F/in.	
	Cell 70	**Cell 71**
Average	–0.070	–0.195
Maximum	3.540	5.951
Minimum	–1.864	–4.699
Standard deviation	0.911	1.961
Median	–0.292	–0.336
Paired *t*-test results		
Variance, °F/in.	0.829	3.845
Observations	28,649	
Hypothesized mean difference	0	
Degrees of freedom	28,648	
t-statistic	15.11	
p-value	0	
t-critical two-tail	1.96	

traffic load can result in additional stresses. To capture the variation in the moisture content through the depth of the concrete layers, relative humidity was measured at different depths and locations.

A total of 108 humidity sensors were installed in the three cells. Ambient relative humidity, temperature, and solar radiation were also measured with the weather station on-site. The variation in the daily average ambient relative humidity at the project location over the analysis period (May 2010 to March 2011) can be seen in Figure 3.8. The range of the average daily ambient relative humidity is between 50% and 100%.

To assess the seasonal trends in the ambient relative humidity, the average ambient relative humidity for each month of the analysis period was calculated as shown in Figure 3.9. It can be seen that the ambient relative humidity increases in the winter, with the highest values in November and December and the lowest value in September.

Figure 3.10 and Figure 3.11 present the variation in relative humidity with depth for the locations in Cell 70. For the first 2 to 3 weeks after paving, there is a significant drop in relative humidity. This may be attributed to hydration of the concrete. Figure 3.10 was produced using the relative humidity data from the edge of the slab in Cell 70. It shows a variation in the relative humidity in the concrete during the winter months, but the variation was less than that experienced at the corner location (Figure 3.11).

In late November, the variation in the relative humidity increased suddenly and continued throughout the winter and early spring. The increase in relative humidity during the winter months is the result of a decrease in the temperature and not a change in the moisture content. Unfortunately, the moisture content in the concrete cannot be measured directly and must be estimated based on the measured relative humidity. Therefore, when interpreting these data, it is important to remember that the relative humidity will increase when the temperature decreases even when the moisture content remains constant. For this reason, it is important to make comparisons between the concrete relative humidity measurements made at the same time of the year over a longer time period (5 or 6 years). It typically takes about 5 to 7 years before all of the irrecoverable drying shrinkage develops at the surface of the slab. Unfortunately, the complete interpretation of the moisture data is not possible because less than 1 year's worth of data were available at the time the analysis for this report was performed.

In Cell 70, the relative humidity near the surface of the lower PCC layer (4.8 in. from the HMA surface) experienced a

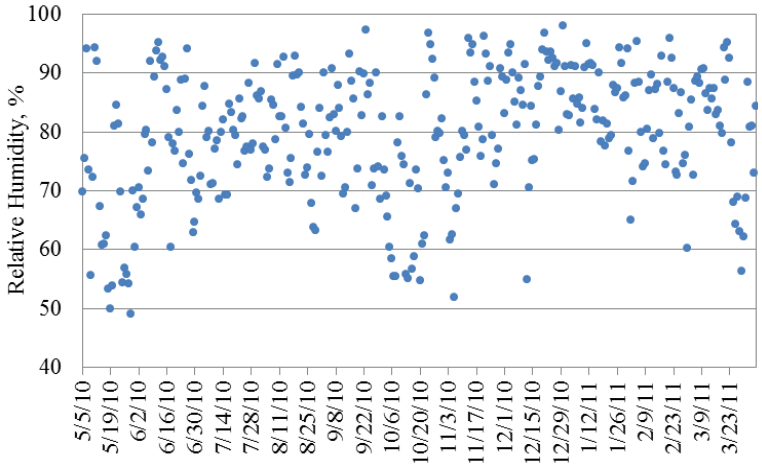

Figure 3.8. Daily average ambient relative humidity at MnROAD from May 2010 to March 2011.

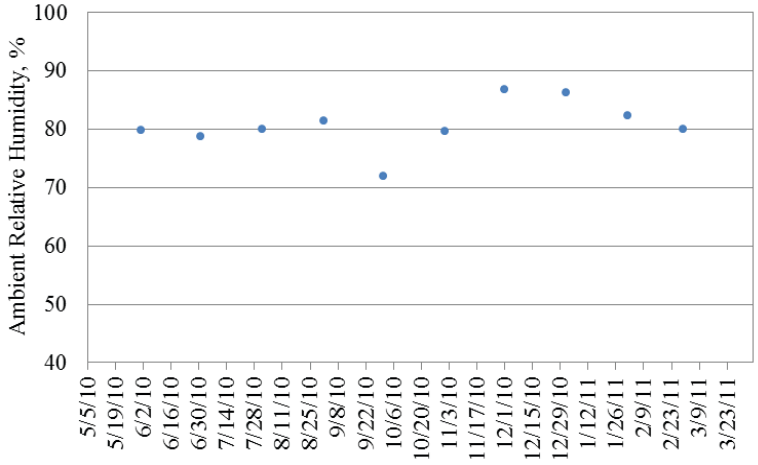

Figure 3.9. Monthly average ambient relative humidity at MnROAD from May 2010 to March 2011.

sudden drop in relative humidity in the third week of May. This time coincides with the time during which the HMA overlay was placed (May 20, 2010). To further investigate the reason for this sudden drop in relative humidity, the daily variation of the relative humidity and temperature in the concrete in Cell 70 can be found in Figure 3.12. The graph depicts approximately 4 days before and 3 days after the HMA overlay was placed.

The placement of the HMA overlay is indicated by a spike in the temperature of the sensor at a depth of 4.8 in. (from the overlay surface). The relative humidity drops at the time of the placement of the HMA layer because the high temperature of the asphalt mix accelerates the evaporation of moisture from the surface of the concrete layer. After the HMA layer cools, it acts as an insulation layer to the underlying PCC layer. This is reflected in the flat trend exhibited for the higher relative humidity measured near the surface of the PCC layer after May 20, 2010. The HMA layer increased the humidity of the underlying PCC surface. This effect is important because it reduces the upward curl of the slab from a much dryer surface and reduces the amount of top-of-slab fatigue damage and cracking.

Comparison with Bare PCC Pavement

The most reasonable measurements of the relative humidity in bare concrete were obtained from Cell 72. These measurements are shown in Figure 3.13 and Figure 3.14. The relative humidity measured at the top of Slabs 1 and 2 for this cell show the largest daily variations. This is expected because the sensors close to the surface are most heavily influenced by the ambient conditions. However, the two top sensors in the adjacent slab do not show the same behavior over the analysis period. The variation in the relative humidity between the lower sensors is small and remains constant over the year after initial drying of the concrete. It is possible that this variability is the result of variations in the sensor depth because the exact as-built depths are unknown.

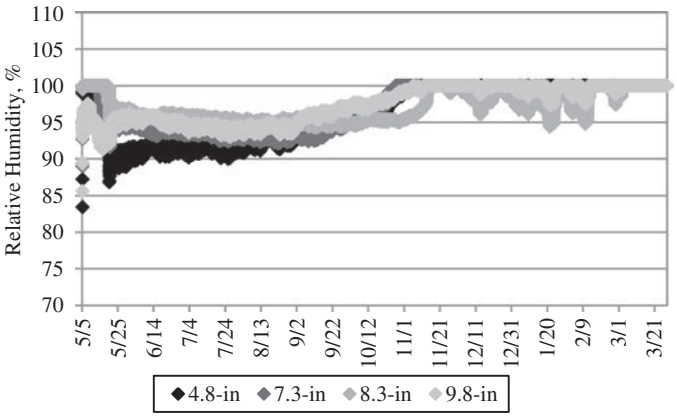

Figure 3.10. Relative humidity in the concrete at the edge of Slab 2 in Cell 70.

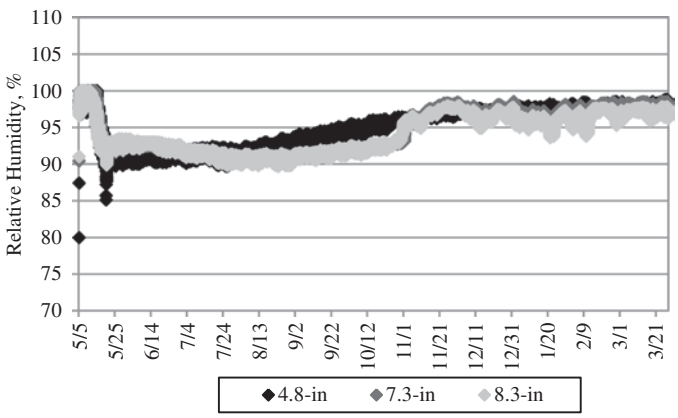

Figure 3.11. Relative humidity in the concrete at the corner of Slab 2 in Cell 70.

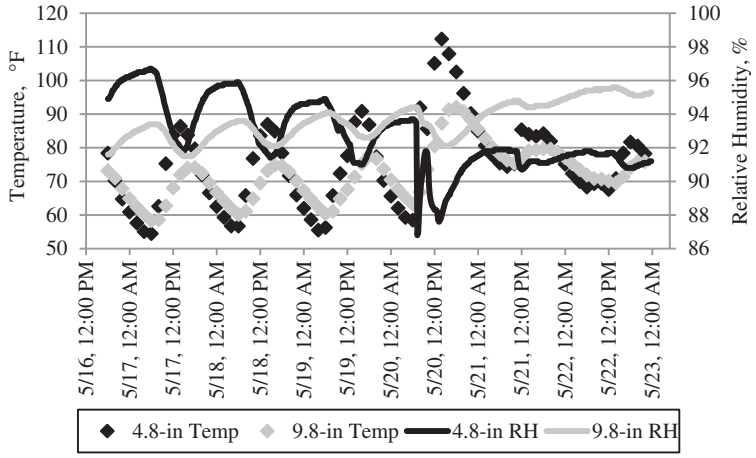

Figure 3.12. Daily variation in relative humidity and temperature in the PCC, 4 days before and 3 days after HMA overlay was placed in Cell 70.

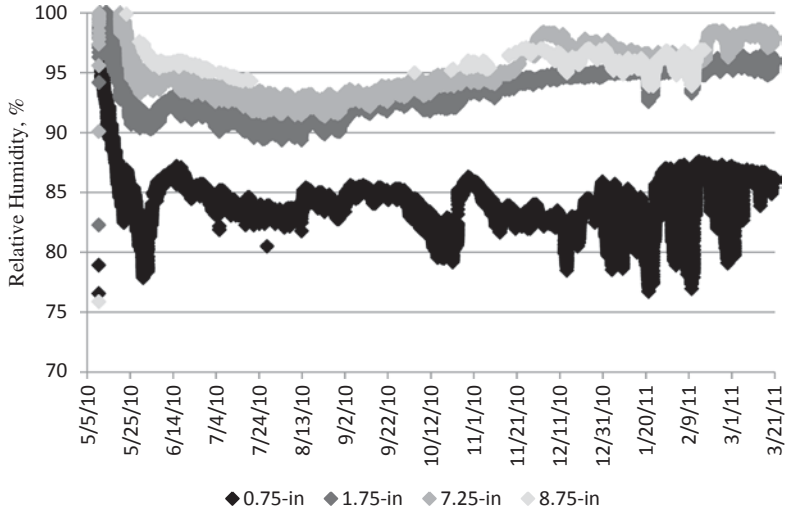

Figure 3.13. Relative humidity in the concrete at the edge of Slab 1 in Cell 72.

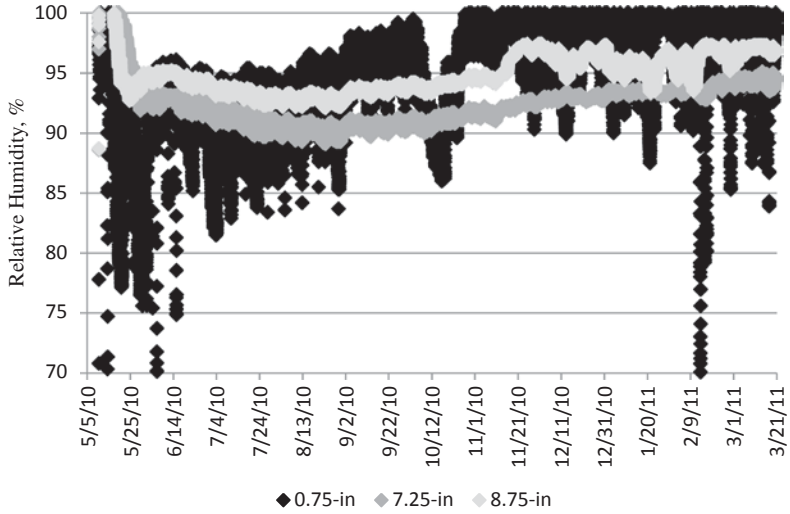

Figure 3.14. Relative humidity in the concrete at the edge of Slab 2 in Cell 72.

By comparing Cell 70 (HMA/PCC) and Cell 72 (PCC/PCC), one can conclude that for HMA/PCC pavements, although PCC top surface moisture content continues to decrease for a short while after the HMA layer is placed (thus increasing moisture gradient through the depth of the slab), eventually the PCC top surface moisture content starts to trend toward the relative humidity measured by the lower sensors (thus effectively having minimal moisture gradients through the depth of the slab). This was not the case for the PCC/PCC pavements, which showed variability in the surface moisture content depending on ambient conditions. This indicates that placement of the HMA layer controls both the variability and the magnitude of moisture gradients caused by ambient weather conditions (solar radiation, rainfall, wind, and so forth) through the PCC depth. Without the HMA layer, there is much greater variability and magnitude of moisture gradients through the PCC depth. These effects are significant for design and performance. The *MEPDG* does not model or change the moisture content in the PCC when an HMA surface is placed. This will need to be improved.

Effect of HMA Layer on PCC Slab Curvatures

The data obtained from the strain gauges embedded in the composite pavement slabs were used primarily to compare the curvature in the different cells. The data analysis consisted of two parts. The first part assessed the variability in the data within a given pavement cell, whereas the second part assessed the differences in between cells, as discussed in Appendix H. The curvatures for the two slabs in Cell 70 varied greatly but Cells 71 and 72 showed agreement between the two slabs at most locations. It is hypothesized that not all the joints cracked at the same time, and the different effective slab lengths resulted in inconsistent curvatures between slabs for Cell 70. Considering the large variation between the two slabs for Cell 70, the curvatures for both Slabs 1 and 2 for Cell 70 are compared with the average values of Cells 71 and 72, as shown in Figure 3.15. One should note that after the winter, Cell 72 has far more upward curvature than Cell 70 does.

Figure 3.15 shows no significant difference in curvature between Cells 71 and 72. However, a difference can be found between these two cells and Cell 70. For both slabs in Cell 70, a peak in curvature was reached in the middle of June, shortly after construction before HMA was placed. However, the difference between the two slabs is that Slab 1 presented a decreasing curvature since June, whereas Slab 2 regained some curvature between June and December. The initial peak in curvature likely is caused by the construction of the HMA layer. The high HMA temperatures at placement cause evaporation of the moisture in the upper portion of the lower PCC layer. However, the HMA layer has a higher permeability than a concrete layer of the same thickness, which makes it

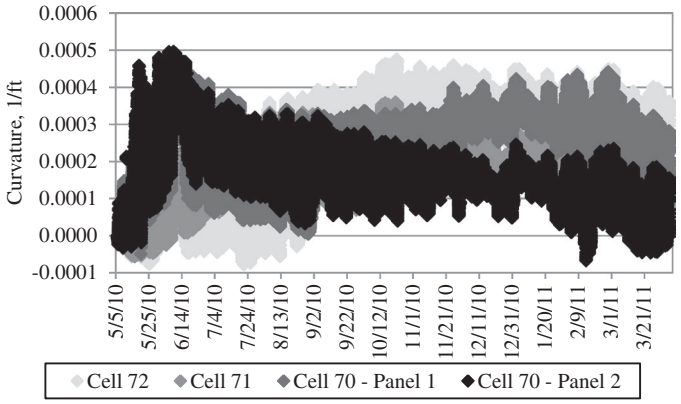

Figure 3.15. Comparison of average slab curvatures at the diagonal location.

possible for rewetting of the concrete to occur more readily. This is most likely why Slab 2 of Cell 70 is the only slab that presents a decreasing trend in curvature during the summer. Regarding Slab 1 of Cell 70, although an increasing curvature was observed between June and December, the magnitude of the increase is smaller ($0.0001 \times 1/\text{ft}$) than that for Cell 71 ($0.0002 \times 1/\text{ft}$) and Cell 72 ($0.00025 \times 1/\text{ft}$). This finding still implies the effect of the HMA overlay in diffusing moisture downward and therefore rewetting the top of the lower PCC layer. The effect of the HMA layer also can be verified with respect to the LTGs in the slab.

Figure 3.16 and Figure 3.17 present the variation in the LTG during the winter for Cells 70 and 71, respectively. The figures show that the positive temperature gradients in Cell 71 are much larger in magnitude than those in Cell 70. This results in larger daily fluctuations in the curvature, indicating the asphalt overlay has a significant insulating effect. Note the high upward curvature in March in Figure 3.17.

Based on the analysis of the strain gauge data, and consistent with the analysis of the temperature and moisture data,

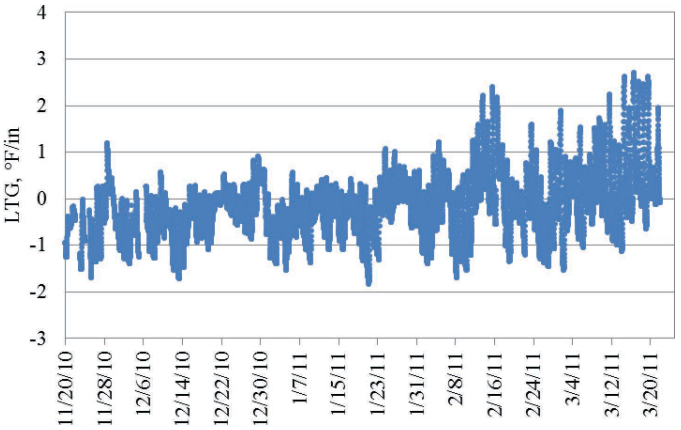

Figure 3.16. LTG over the winter at the midslab for Slab 1 in Cell 70.

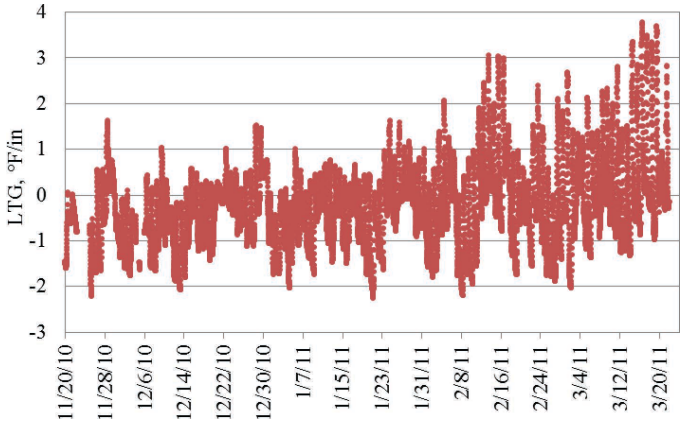

Figure 3.17. LTG over the winter at the midslab for Slab 1 in Cell 71.

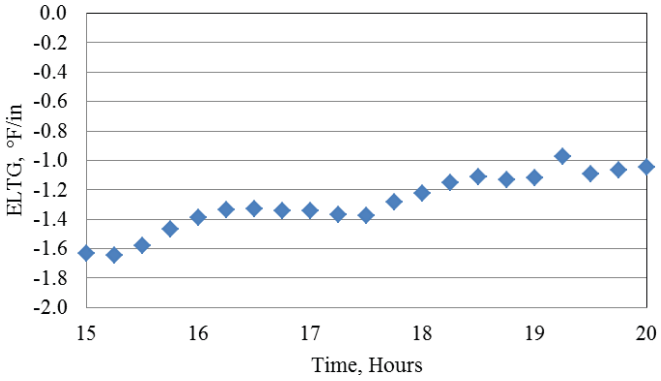

Figure 3.18. ELTG over the range of TZs for Slab 1 in Cell 70, using thermocouple data.

it is hypothesized that for Cell 70, the placement of HMA layer resulted in a sudden short-term increase in the curvature, which was attributed to the evaporation of moisture from the upper portion of the PCC layer. The HMA layer also had long-term effects on the behavior of the PCC layer. It acted as an insulation layer and reduced the temperature gradients that developed in the underlying PCC layer. Furthermore, the high permeability of the HMA layer resulted in additional rewetting of the PCC layer for Cell 70 in comparison with the other cells during the summer, resulting in reduced moisture gradients. The HMA layer also reduced the day-to-day variability of the temperature and moisture gradients in the PCC slab, thereby insulating the PCC slab from both temperature and moisture gradients. This has major implications regarding reduction of stresses at the top and bottom of the slab and resulting in reduced fatigue damage, especially at the top of the slab.

Establishing Built-in Gradients

The built-in gradient includes the temperature and moisture gradients that "lock" into the PCC slab at the zero-stress time (TZ). TZ occurs after final set and is the point in time when the slab has grown sufficient strength (essentially changing from semisolid to solid state) to respond to temperature changes. Although moisture gradients at TZ have been shown to be close to zero (Wells et al. 2006), temperature gradients at this point in time can have influential values. Built-in temperature gradients are important because, as a result of this gradient, the slab does not remain flat during its service life, even when temperature and moisture gradients are zero. Before TZ, the slab is flat regardless of the temperature gradient in the slab. The temperature gradient that is present in the slab at TZ is locked into the slab.

The TZ, WAT, and built-in temperature gradient were established for each instrumented cell at MnROAD. To establish TZ, two methodologies were employed, one methodology based on the variation seen in the measured strain with respect to temperature changes in the slab (Method 1) and the other methodology based on the initiation of curling in the slabs with respect to LTG (Method 2), as detailed in Appendix H. For Cell 70, neither Method 1 nor Method 2 could be used to compute TZ. Therefore, TZ was determined, based on the maturity concept, to be between 19 and 20 hours.

The slab WAT at TZ is another parameter that needs to be established. This parameter is significant because it defines the amount of uniform thermal expansion and contraction in the slab. The WAT between 19 and 20 hours after PCC paving is approximately 53°F.

The ELTG at TZ is the built-in temperature gradient that locks into the slab and influences its future shape. The ELTGs estimated using thermocouple data from Slab 1 between hours 15 and 20 after paving are shown in Figure 3.18. The data from the thermocouples in Slab 2 were not usable until day 5. The figure shows that the built-in temperature gradient for Cell 70 (using TZ of between 19 and 20 hours after PCC paving) is approximately −1.1°F/in., which corresponds to a built-in temperature difference of −6.6°F for a 6-in. PCC slab.

Reflection Cracking of the HMA Layer

Reflection cracking from the joints in the PCC layer into the HMA layer is an important performance indicator for HMA/PCC composite pavements. At MnROAD, to study reflection cracking, the HMA/PCC test section was constructed with the following subsections:

- 400-ft driving lane with 1.25-in. diameter dowels and sawed and sealed joints (78% trucks);
- 75-ft driving lane (~ 5 joints) with 1.25-in. diameter dowels and no sawed and sealed joints (78% trucks);

- 400-ft passing lane with no dowels and sawed and sealed joints (22% trucks); and
- 75-ft passing lane (~ 5 joints) with no dowels and no sawed and sealed joints (22% trucks).

The field survey of the HMA/PCC section after 1 full year of traffic (since construction) shows excellent performance of the sawed and sealed joints. Only three joints that were sawed and sealed exhibited some minor low-severity cracking (~ 6 in. in length) near the sealed joints. The joints that were not sawed and sealed all reflected through. This was true for both the doweled driving lane and the nondoweled passing lane. The effect of dowels is not clear because the two lanes are not directly comparable. Both lanes exhibited 100% low-severity reflection cracking at the transverse joints, but they are not comparable with respect to traffic level. In addition, the reflection cracks in one lane may have propagated transversely from one lane to another. Figure 3.19 shows side-by-side comparison of sawed and sealed joints with joints that were not sawed and sealed.

Analysis of Field Data at UCPRC

PCC Slab Temperature Profiles

Figure 3.20 illustrates the temperature changes within the bare PCC layer for a 5-day period measured using the thermocouples cast into the slabs. The figure shows that temperature measured by the thermocouple at the top of the PCC layer is immediately affected by the changes in air temperatures. On the other hand, the measurements indicate a time lag between the air temperature peak and peak temperature at the bottom of the PCC layer. This time lag creates the PCC temperature gradients between the top and bottom of the PCC layer, which cause thermal stresses at the top and bottom of the PCC.

To identify the effects of HMA and PCC layer thickness and HMA type on the variation of the PCC temperature gradients, one year-long set of temperature data (January 1, 2010, to December 31, 2010) from the thermocouples located on every section were analyzed. Figure 2.22 and Figure 2.25 show the lane configuration and instrumentation layout, respectively. Temperature data for Lane B are assumed to be similar to those

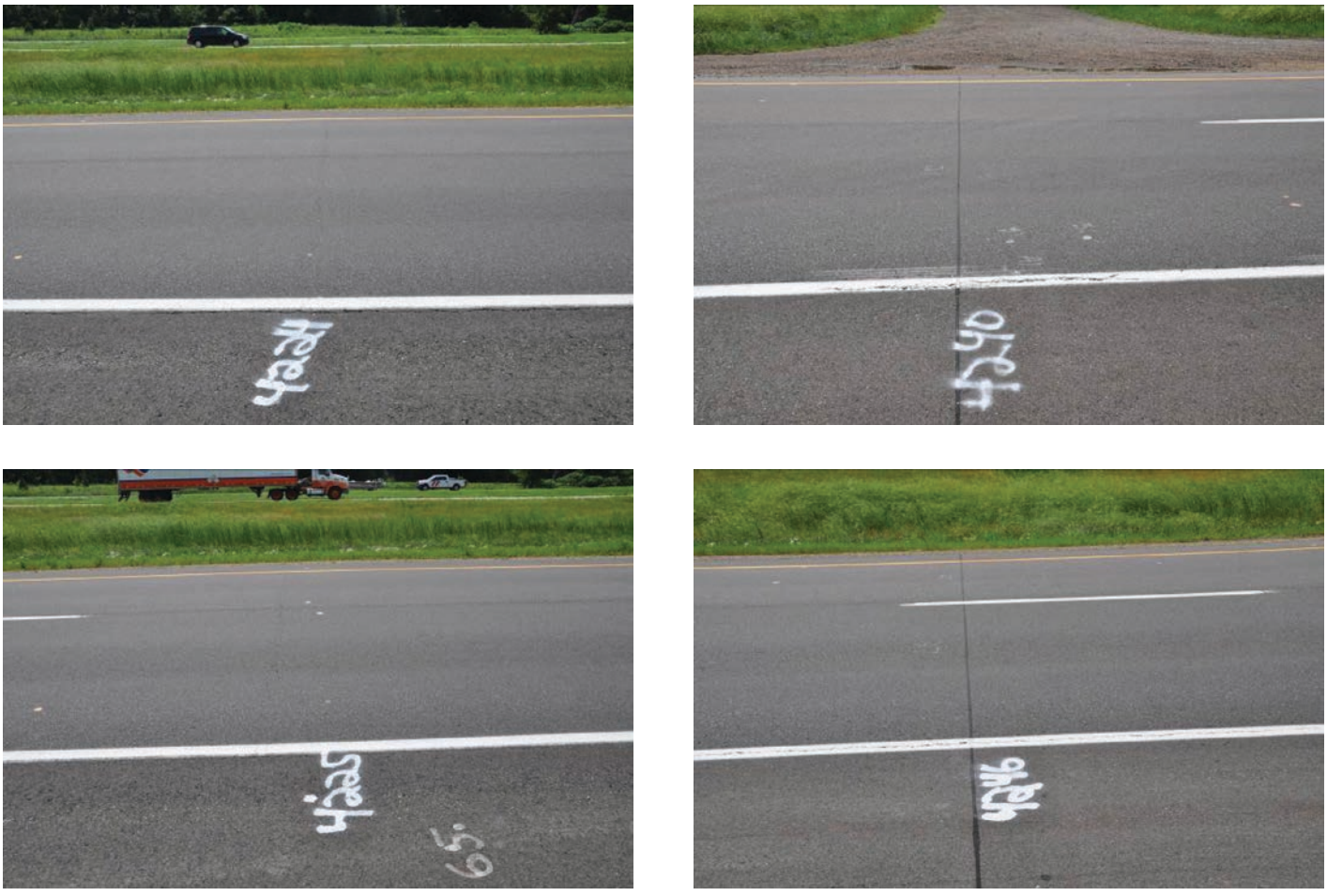

Figure 3.19. Side-by-side comparison of joints with no saw and seal (left) exhibiting reflection cracking and sawed and sealed joints (right) exhibiting no reflection cracking.

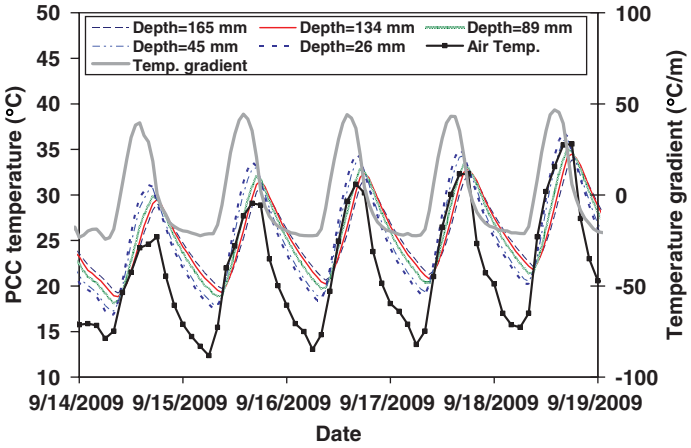

Note: Fahrenheit = Celsius × 9/5 + 32.

Figure 3.20. Changes in temperature within the PCC layer for a 5-day period.

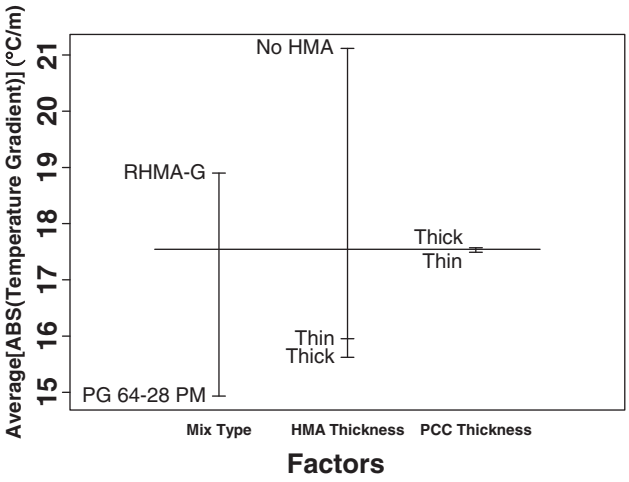

Note: Fahrenheit = Celsius × 9/5 + 32; 1 meter = 39.37 inches.

Figure 3.21. Design plot comparing the influence of variables HMA and PCC thickness and HMA type on the variation of the dependent variable PCC temperature gradient for 1 year of data.

for Lane A and not considered for the temperature analysis because the only difference between Lane A and Lane B is the dowel bars in Lane A. Lane C has the RHMA-G HMA layer with thick PCC layer (7 in. [178 mm]) underneath, whereas Lane D has the same mix with thin concrete (5 in. [127 mm]) underneath. Lane A has the PG64-28PM HMA layer with thick PCC layer (7 in. [178 mm]). HMA layer thicknesses also vary along the test sections.

PCC temperature gradient distributions were analyzed by using these distributions along with box plots, design, and interaction plots. Detailed information is given in Appendix J. In this section, only the design plot is used to evaluate the changes in temperature gradient between different test sections. Design and interaction plots generally are used to compare the influence of a factor on the variation of the dependent variable with respect to other factors. Absolute values of the PCC temperature gradients were used as dependent variables for the analysis because both negative and positive PCC temperature gradients will cause critical tensile stresses. PCC and HMA thickness and HMA mix type were used as the independent variables for the design and interaction plots. Figure 3.21 shows the design plot.

Key findings from the PCC temperature measurements were as follows:

- The HMA layer significantly reduces the PCC temperature gradients by acting as a thermal insulator.
- The thickness of the HMA layer (ranging from 2.5 to 4.5 in.) does not have a significant effect on the PCC temperature gradient.
- HMA type has an effect on the PCC temperature gradient. Significantly higher positive PCC temperature gradients were observed for the section with the RHMA-G HMA layer. This shows that the PG64-28PM HMA layer is reflecting more solar radiation (higher albedo) than the RHMA-G HMA layer. It can be concluded that the section with the RHMA-G layer will experience larger thermal stresses at the bottom of the PCC layer than the section with the PG64-28PM HMA layer as a result of the larger positive PCC temperature gradients.
- No significant effect of PCC layer thickness on the variation of PCC temperature gradients is observed.
- Although HMA aging significantly decreased the PCC temperature gradients in the underlying PCC layer investigated in this study (Appendix J), various cases should be analyzed by considering the measured solar radiation and albedo effects to produce more reliable conclusions.

HVS Rutting Tests

The purpose of the Heavy Vehicle Simulator (HVS) rutting tests was to evaluate the effects of HMA thickness on rutting performance for thin HMA layers on PCC slabs. For this reason, two HMA thicknesses were tested for each of the two mix types placed on the test sections at the UCPRC. Differences between the failure mechanisms of sections with PG64-28PM and RHMA-G mixes with two thicknesses also were investigated. The data collected from HVS tests will be used for model calibration.

HVS Test Criteria and Conditions

The failure criterion was defined as an average maximum rut of 12.5 mm (0.5 in.) over the full monitored section (Station 3 to Station 13). Note that the AASHTO *Manual of*

Table 3.5. Summary of HVS Loading Program

Section	Mix Type	As-built Thickness (mm)	Wheel Load[a] (kN)	Temperatures at 50 mm (2 in.)		Repetitions
				Average (°C)	SD[b] (°C)	
609HB	PG64-28PM	116	40	49.5	1.1	63,750
			60			136,250
610HB	PG64-28PM	72	40	49.8	1.0	64,000
			60			137,200
611HB	RHMA-G	118	40	48.7	1.1	18,503
612HB	RHMA-G	74	40	49.7	1.3	90,000
					Total	**509,703**

Note: 25.4 mm = 1 in., Fahrenheit = Celsius × 9/5 + 32.
[a] 40 kN = 9,000 lb; 60 kN = 13,500 lb.
[b] SD = Standard deviation.

Practice (*MOP*) recommends using maximum rutting threshold values at the end of design life of 0.40, 0.50, and 0.65 in. for interstate, primary, and other roadways, respectively. Testing was continued past a 12.5-mm average rut depth until the rutting accumulation rate stabilized. The pavement temperature at 50 mm (2.0 in.) deep was maintained at 50°C ± 4°C (122°F ± 7°F) to assess rutting potential under typical conditions.

The HVS loading program for each section is summarized in Table 3.5. All trafficking was carried out with a dual-wheel configuration with the centerlines of the two tires spaced 360 mm (14.2 in.) apart, using radial truck tires (Goodyear G159-11R22.5 steel belt radial) inflated to a pressure of 690 kPa (100 psi), in a channelized (no wander), unidirectional loading mode in which the wheel travels one direction loaded and is lifted off the pavement for the return pass. Channelized trafficking is used to simulate the tracking of radial tires in the wheelpath once a small rut forms and is more aggressive than field conditions in the initial stages of rutting before tires begin to track in the ruts. The results of the HVS rut tests are summarized here, and details are presented in Appendix L.

Figure 3.22 shows the average maximum rut, defined as the downward rut depth compared with the original pavement surface, averaged along the test sections. The wheel

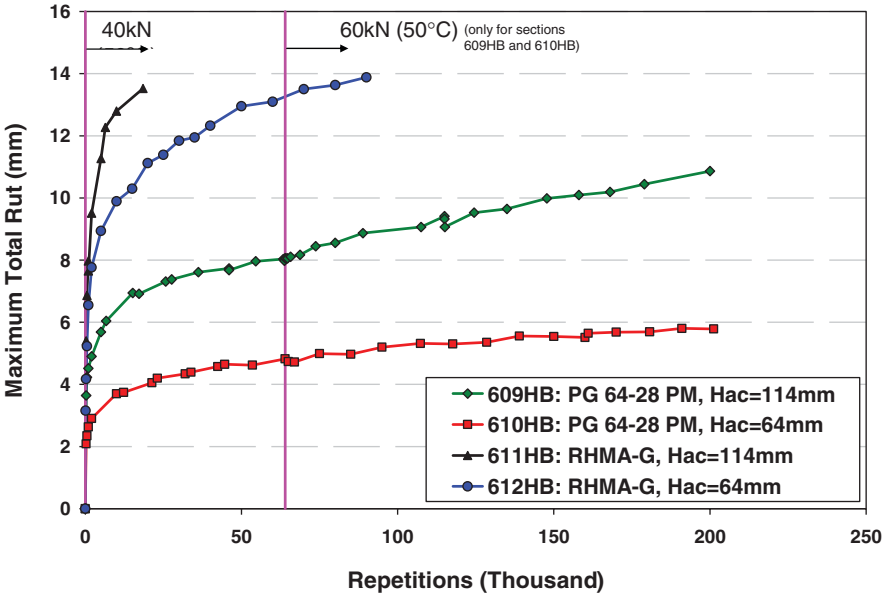

Note: 1 mm = 0.0394 in.; 40 kN = 9,000 lb; 60 kN = 13,500 lb.

Figure 3.22. Comparison of average maximum rut for different HMA thicknesses and asphalt grades.

load for the two sections with the PG64-28PM mix (609HB and 610HB) was increased from 40 kN to 60 kN at around 64,000 repetitions. However, increasing the load did not have any significant effect on the rutting accumulation rate. Early failure was observed for the thick RHMA-G section (611HB).

The average maximum rut depth (which considers both downward deformation and "humping" of material sheared to the sides of the wheelpath averaged along the test section) is approximately two times greater than the average rut depth (which considers only downward deformation) for both of the PG64-28PM sections. The average maximum rut depth is nearly three times greater for both of the RHMA-G sections. This indicates that shearing of material to the side of the wheelpath is as important a contributor or more important than just the downward rut.

To identify the effect of thickness on accumulated rutting, rutting measurements were converted to permanent shear strain (PSS), similar to the PSS determined in the laboratory repeated shear test, by dividing the measured average maximum rut by the HMA layer thickness of each section. Figure 3.23 shows the PSS curves for all sections and illustrates that the curves for the two thicknesses of the PG64-28PM mix (Sections 609HB and 610HB) are very close.

This result indicates that accumulated rutting for these two sections is approximately a linear function of thickness for the thickness range in this experiment in which the HMA thicknesses are less than 125 mm (5 in.). This result is compatible with results of viscoelastoplastic finite element simulations of rut depth for different HMA thicknesses on concrete pavement performed during the SHRP 1 A-003A project. The SHRP 1 A-003A simulations showed a typical increase in rut depth with increasing asphalt thickness at approximately a 1:1 ratio up to a thickness of approximately 200 mm (8 in.) for a given asphalt response to repeated wheel loading, and a diminishing effect of asphalt thickness at greater thicknesses, assuming uniform temperature and properties through the full depth of the asphalt and full bonding with the concrete. A less consistent result was observed for the RHMA-G sections (Section 611HB and Section 612HB), where the thinner section rutted at a faster rate relative to thickness than did the thicker section.

Key findings from the HVS rutting study were as follows:

- Maximum rut depths for same trafficking increased with thicker HMA layers for both mix types, with the PG64-28PM mix showing approximately a 1:1 relationship between rut depth development and thickness and a greater than 1:1 relationship, although less consistent, for the RHMA-G mix.
- The downward deformation in the wheelpath was approximately equal to the upward deformation of material at the sides of the wheelpath for the PG64-28PM mix. For the RHMA-G mix, the upward deformations at the sides of the wheelpath were greater than the downward wheelpath deformation.
- Increasing the wheel load for the PG64-28PM sections from 40 kN to 60 kN at around 64,000 repetitions did not appear to have any significant effect on rutting accumulation rate.

In general, all other things being equal, measured rutting is less for thinner HMA layers on PCC slabs than it is for thicker HMA layers.

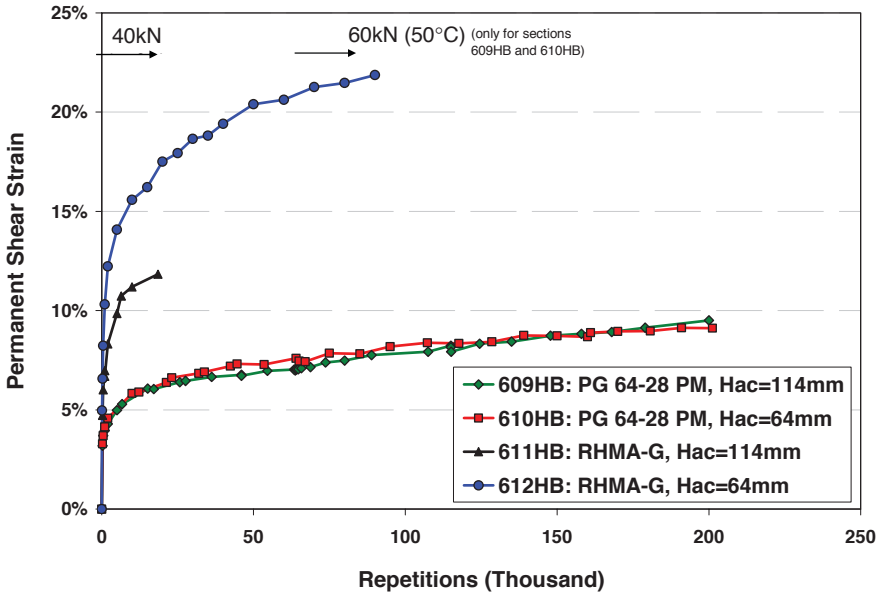

Figure 3.23. Comparison of PSS for all HVS rut test sections.

Table 3.6. Description of HVS Cracking Testing Program for Cell D2 (Section 613HB)

Stage	Substage	Beginning Repetition	Ending Repetition	Wheel Load (kip)	Target Pavement Temperature
1	1	0	7,200	6.7, 9, 13.5[a]	50°C/122°F
1	2	7,201	14,400	6.7, 9, 13.5[a]	Ambient[b]
2	1	14,401	100,000	9 (40 kN)	Ambient[b]
2	2	100,001	200,000	13.5 (60 kN)	Ambient[b]
2	3	200,001	300,000	18 (80 kN)	Ambient[b]

Note: Fahrenheit = Celsius × 9/5 + 32, 1 kN = 225 lb.

[a] Each wheel load level was maintained for 2,400 repetitions, with 100 repetitions applied at the beginning of each hour.

[b] Pavement temperature at 50-mm depth ranged from 8°C to 25°C during the test under ambient air.

HVS Cracking Tests

HVS cracking tests were used to investigate the failure mechanism of composite pavements and the effect of material, HMA thickness, and existence of dowels on pavement life. The first cracking test (Section 613HB) was conducted on Cell D2 of the UCPRC test track, with a 2.5-in. (64-mm) RHMA-G layer on 5-in. (120-mm) concrete without dowels. The second cracking test (Section 614HB) was conducted on Cell D1 of the UCPRC test track, with a 4.5-in. (114-mm) RHMA-G layer on 5-in. (120-mm) concrete without dowels. The testing began with a pavement response evaluation stage (Stage 1), followed by a crack-inducing stage (Stage 2). Each stage can be further divided into substages based on pavement temperature and wheel load level. Descriptions of the stages and substages are provided in Table 3.6 and Table 3.7.

All trafficking was carried out with a dual-wheel configuration with the centerlines of the two tires spaced 365 mm (14.4 in.) apart, using radial truck tires (Goodyear G159-11R22.5 steel belt radial) inflated to a pressure of 690 kPa (100 psi), in a channelized (no wander), bidirectional loading mode in which the wheel travels both directions loaded. The center of the test section (halfway between the two tires) was located approximately 28 in. (700 mm) from the edge of the slab, placing the outside tire edge and the slab edge 15.7 in. (400 mm) apart. Trafficking with the 27-kip (120-kN) load was carried out using a tubeless, single-wheel aircraft tire (BF Goodrich TSO C62C, 46 × 16) inflated to 1,380 kPa (200 psi).

Data collected during HVS testing included (a) pavement temperatures at various depths, (b) joint movements and surface deflections under the HVS wheel load, and (c) changes in transverse surface profile. For details of the instrumentation plan and measurement results, please refer to Appendix K.

Table 3.7. Description of HVS Cracking Testing Program for Cell D1 (Section 614HB)

Stage Code	Beginning Repetition	Ending Repetition	Ending ESALs (Million)	Wheel Load/ Half Axle Load (kip)	Target Pavement Temperature
ST_1.1	0	7,200	0.013	6.7, 9, 13.5[a]	50°C/122°F
ST_1.2	7,201	14,400	0.027	6.7, 9, 13.5[a]	Ambient[b]
ST_2.1	14,401	100,000	0.113	9 (40 kN)	Ambient[b]
ST_2.2	100,001	200,000	0.580	13.5 (60 kN)	Ambient[b]
ST_2.3	200,001	300,000	1.939	18 (80 kN)	Ambient[b]
ST_2.4	300,001	520,000	9.129	23.5 (100 kN)	Ambient[b]
ST_2.5	520,001	522,000	9.259	27 (120 kN) with single aircraft tire	Ambient[b]

Note: ESAL = equivalent single-axle load; Fahrenheit = Celsius × 9/5 + 32, 1 kN = 225 lb.

[a] Each wheel load level was maintained for 2,400 repetitions, with 100 repetitions applied at the beginning of each hour.

[b] Pavement temperature at 50-mm depth ranged from 8°C to 25°C during the test under ambient air.

Cell D2 (Section 613HB): Reflection cracking over both joints (Figure 3.24) was first observed after 140,000 load repetitions (0.30 million ESALs). Slab cracking was first observed reflected through the HMA layer after 260,000 load repetitions (1.38 million ESALs) but is believed to have occurred after 195,000 load repetitions (0.60 million ESALs) based on measured joint and slab deflection data. The cracks traced on the surface after HVS loading was stopped are shown in Figure 3.24. PCC slab cracking occurred at the corner and midslab edge of the slab after reflective cracking at the joints.

Cell D1 (Section 614HB): Cracks traced on the HMA surface at selected points in Cell D1 are shown in Figure 3.25. Reflection cracking from underlying joints was first observed after 298,400 load repetitions (2.5 million ESALs) over Joint J1. No additional surface cracking was observed after 520,000 load repetitions (12.8 million ESALs), at which point the dual wheel half-axle was replaced by single wheel aircraft tire and the wheel load was increased to 120 kN (27 kip) and 1.38 MPa (200 psi). Once the trafficking with the aircraft tire was begun, extensive surface cracking started to develop, and after only 2,000 additional load repetitions (0.13 million ESALs), the total length of the surface crack had increased from 0.8 m (2.5 ft) to 17.8 m (58.5 ft). Most of the surface cracks run longitudinally along the edge of the wheelpaths of the dual wheel. They were caused by the change of tire types (i.e., from dual wheel to single wheel) and thus were not a reflection of cracks in the underlying PCC slab. PCC slab cracking is believed to have occurred after 320,000 load repetitions (3.4 million ESALs) based on measured joint and slab deflection data.

Air Void Content Distribution in HMA Layers

Rectangular prism blocks were cut from Cells B1, B2, C1, and C2 for air void evaluation. Air voids were determined by the CoreLok (AASHTO T331) method. Air voids for the RHMA-G mix averaged 13.4%, and they averaged 10.2% for the PG64-28PM mix, both of which are higher than the average air void contents for these mixes (approximately 11% and

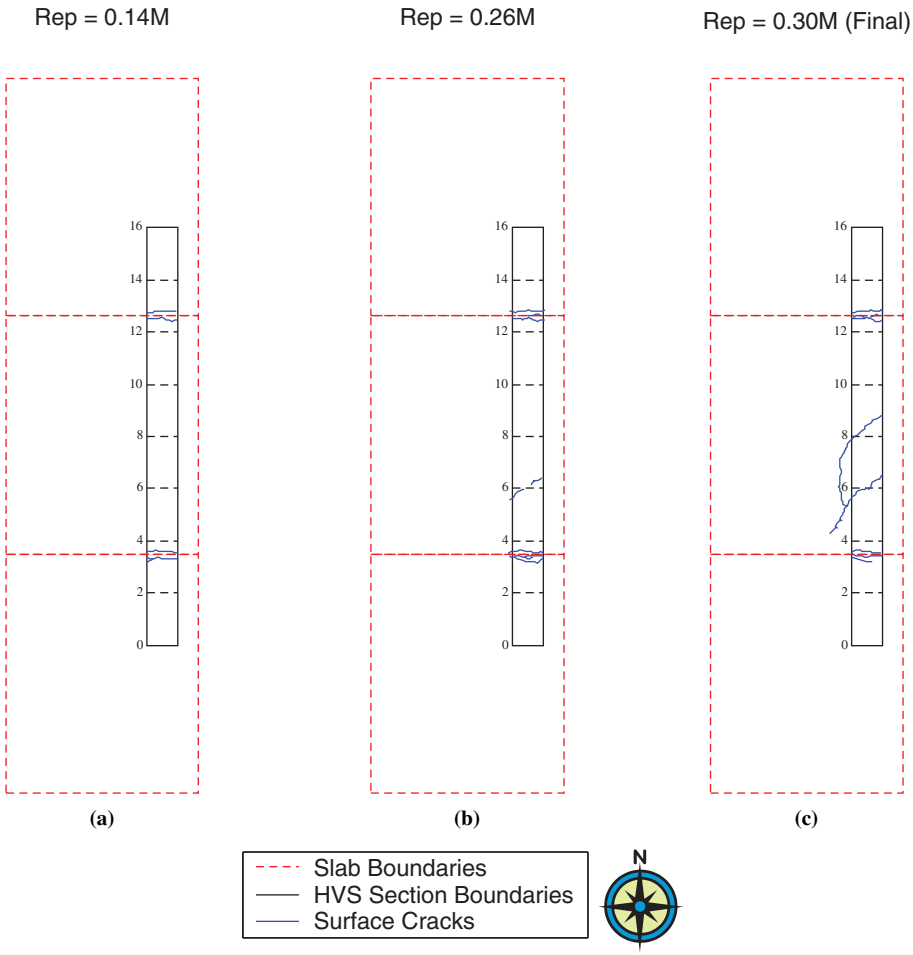

Figure 3.24. Surface cracks traced during the HVS cracking test for Cell D2 (Section 613HB) at UCPRC: (a) repetition = 0.14 million, crack length = 2.5 m (8.3 ft); (b) repetition = 0.26 million, crack length = 4.4 m (14 ft); and (c) repetition = 0.30 million, crack length = 6.4 m (21 ft).

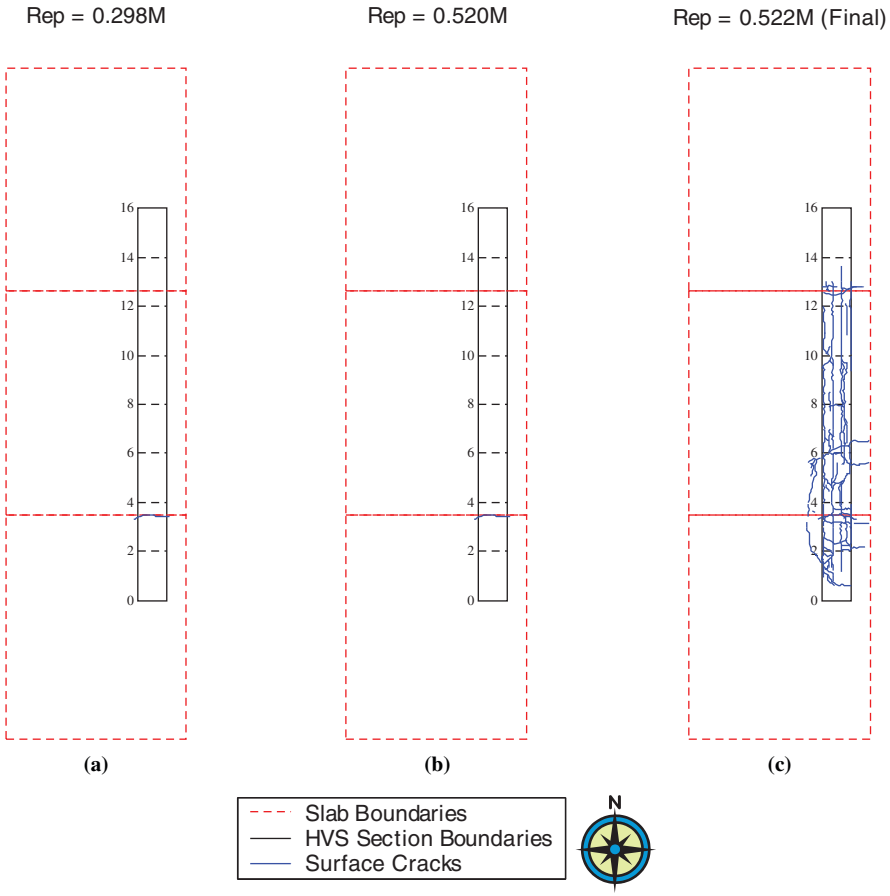

Figure 3.25. Surface cracks traced during the HVS cracking test for Cell D1 (Section 614HB) at UCPRC: (a) repetition = 0.298 million, crack length = 0.8 m (2.5 ft); (b) repetition = 0.520 million, crack length = 0.8 m (2.5 ft); and (c) repetition = 0.522 million, crack length = 17.8 m (58.5 ft).

7%, respectively) in practice on the highway network in California. Air void contents and distributions for the field blocks were also evaluated using computed tomography (CT) scanning performed at the University of California Davis Medical Center. Figure 3.26 shows the distribution of air voids for two rectangular samples sawed from HVS test sections. The image on the top left is for the PG64-28PM mix from test section 609HB (B1), and the image on the bottom left is for the RHMA-G mix from test section 611HB (C1). The plot on the right shows the air void content distribution for samples from test sections 609HB and 611HB (1 mm = 0.0394 in.). The figure shows that air void content in the middle depth of each lift is lower than the bottom and top of the lift, most likely the result of greater temperatures being retained longer in the middle of the lift. The figure also shows that the bottom lift is better compacted than the top lift. This is likely a result of the reheating and additional compaction of the bottom lift provided during the compaction of the top lift.

Changes in the distribution of air voids in HMA blocks also were evaluated by analyzing the CT images that were taken at the University of California Davis Medical Center, Radiology Department before and after the HVS tests. Four asphalt concrete specimens were sawed from each HVS rutting test section (16 specimens from four sections). The location of the CT blocks and the purpose of the study are described in Appendix L. Figure 3.27 illustrates the changes in air void distribution after HVS testing. The image on the left is the HMA block before HVS testing, and the image on the right is for the same HMA block after HVS testing.

Table 3.8 shows the changes in air void content of the HMA blocks after HVS loading. More densification is observed for the sections with PG64-28PM mix (609HB and 610HB).

Asphalt Strain Gauges

To quantify the effect of increasing load, temperature, and speed on elastic strain measurements at 50 mm depth, a

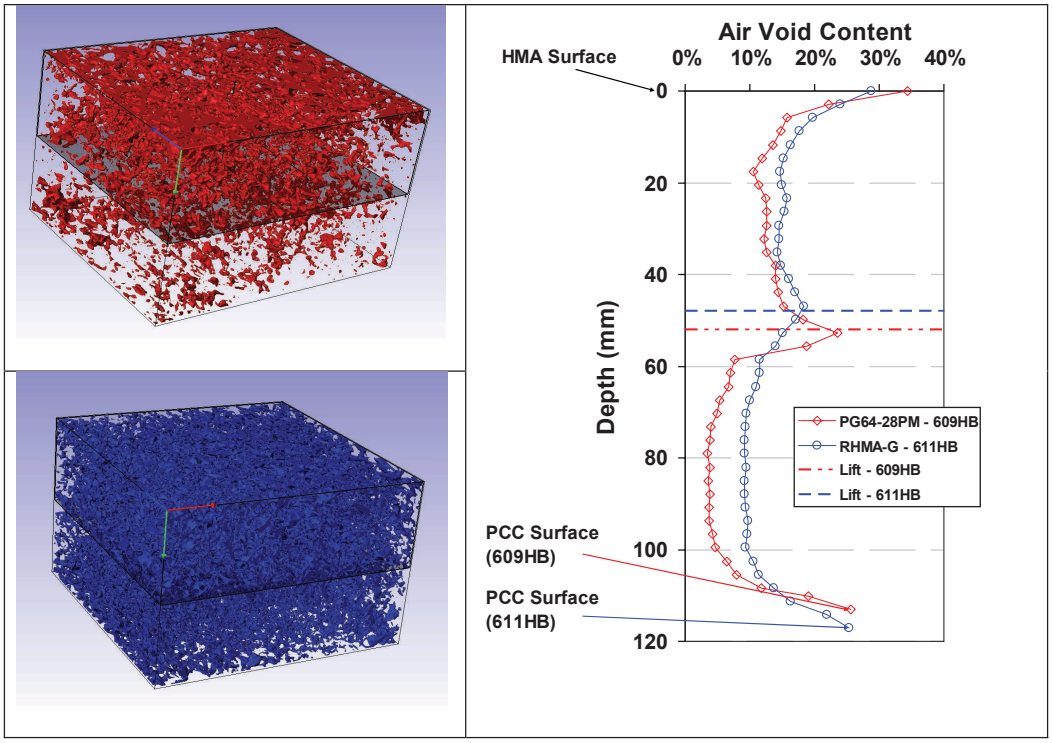

Figure 3.26. Air void distributions (colored volumes are air voids) from CT images.

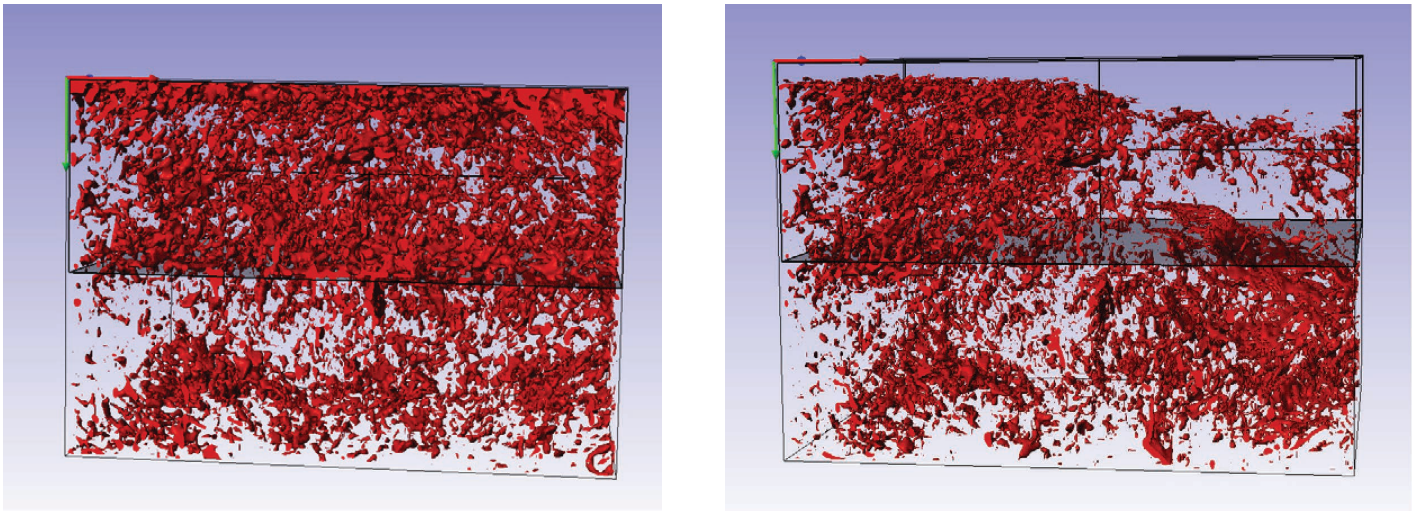

Figure 3.27. Distribution of air voids shown as colored volume.

Table 3.8. Average Distribution of Air Voids in the HVS Test Sections

Section	Mix Type	As-built Thickness (mm)	Before AV[a] (%)	After AV[b] (%)	Before AV Hump (%)	After AV Hump (%)	Before AV Rut (%)	After AV Rut (%)	AV Red. Rut (%)	AV Red. Total (%)
609HB	PG 64-28	116	9.8	8.1	10.5	10.0	9.1	6.0	33	17
610HB	PG 64-28	72	10.0	7.9	9.6	9.8	10.4	6.0	42	21
611HB	RHMA-G	118	13.8	11.4	14.5	13.2	13.1	9.3	29	17
612HB	RHMA-G	74	13.4	11.7	13.2	13.6	13.6	9.7	29	12

Note: AV = air void content; Red. = reduction, 1 mm = 0.0394 in.

[a] Before HVS testing.

[b] After HVS testing.

Table 3.9. Experimental Plan for Sensitivity Study

Sections	Load (kN)	Speed (km/h)	Temperature (°C)
609HB - PG64-28PM - 114 mm thick or 611HB - RHMA-G - 114 mm thick	40, 60, or 80	3.1, 5.9, or 8.7	20, 30, 40, or 50

sensitivity study was performed with strain gauges located in the HMA layer. The experimental plan for the sensitivity study is given in Table 3.9. A total of 72 tests were run. For each test, 100 repetitions were applied with the HVS (7,200 repetitions for the complete test).

Results for the sensitivity study for the thick RHMA-G section (611HB) are given in Figure 3.28 for the transverse strain gauge at the edge of the wheelpath at 50 mm depth. The figure shows that variability in measured strain for all tests is negligible. Temperature appeared to be the most significant parameter that affected the strain for both gauges. Strain levels increased drastically when temperature was increased from 40°C to 50°C for the gauge in transverse direction, the direction of flow to move material from out of the wheelpath to the sides of the wheelpath. Results of the analysis of variance (ANOVA) analysis (Appendix L) indicated that temperature is the most significant variable that affects the measured strain values, with *p*-values equal to zero for all strain gauge measurements. In addition, speed, for the narrow range of values considered in this sensitivity study, appears to be an important parameter affecting the measured strain values, with *p*-values smaller than 0.05 for all strain gauge measurements. On the other hand, load does not have a significant effect on measured strain for gauges located in the longitudinal direction, whereas changes in load significantly affect the transverse strain gauge measurements.

Joint Movement

Joint deflection measurement devices (JDMDs) were used to monitor horizontal opening and closing of the slab joints and vertical movements of the slab corners caused by daily temperature variation on a number of slab corners. Data were collected before and after HMA construction. The data were used to establish the effects of PCC layer thickness, existence of dowels, HMA thickness, and HMA material type on joint movements. Figure 3.29 shows an example of the measured data, in this case for a set of instruments measuring simultaneous horizontal opening and closing of joints on different sections. These results show less daily variation in joint opening for composite pavements compared with bare PCC pavement alone. Lower joint opening could mean fewer reflection cracks and less deterioration of these cracks because of improved joint load transfer.

The joint movement rate (JMR), defined as the amount of horizontal or vertical displacement caused by a unit increase in ambient air temperature, was calculated as the slope of the straight line fitted through the joint displacement versus air temperature data. The normalized horizontal and vertical joint movement rates are shown in Figure 3.30. In general, composite pavement HMA layers over PCC resulted in lower values of JMR compared with those of plain bare PCC pavement. The decrease in JMR tends to increase with HMA thickness, showing the beneficial insulation effects of HMA surfaces of PCC slabs

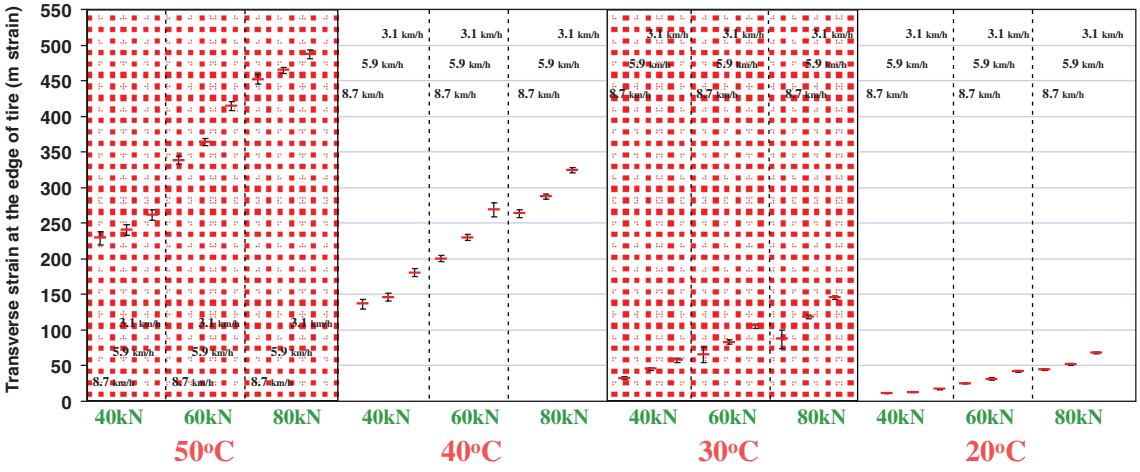

Note: Fahrenheit = Celsius × 9/5 + 32; 1 kN = 225 lb, 1 km/h = 0.62 mph.

Figure 3.28. Results for the sensitivity study for Section 611HB, transverse strain at the edge of tire.

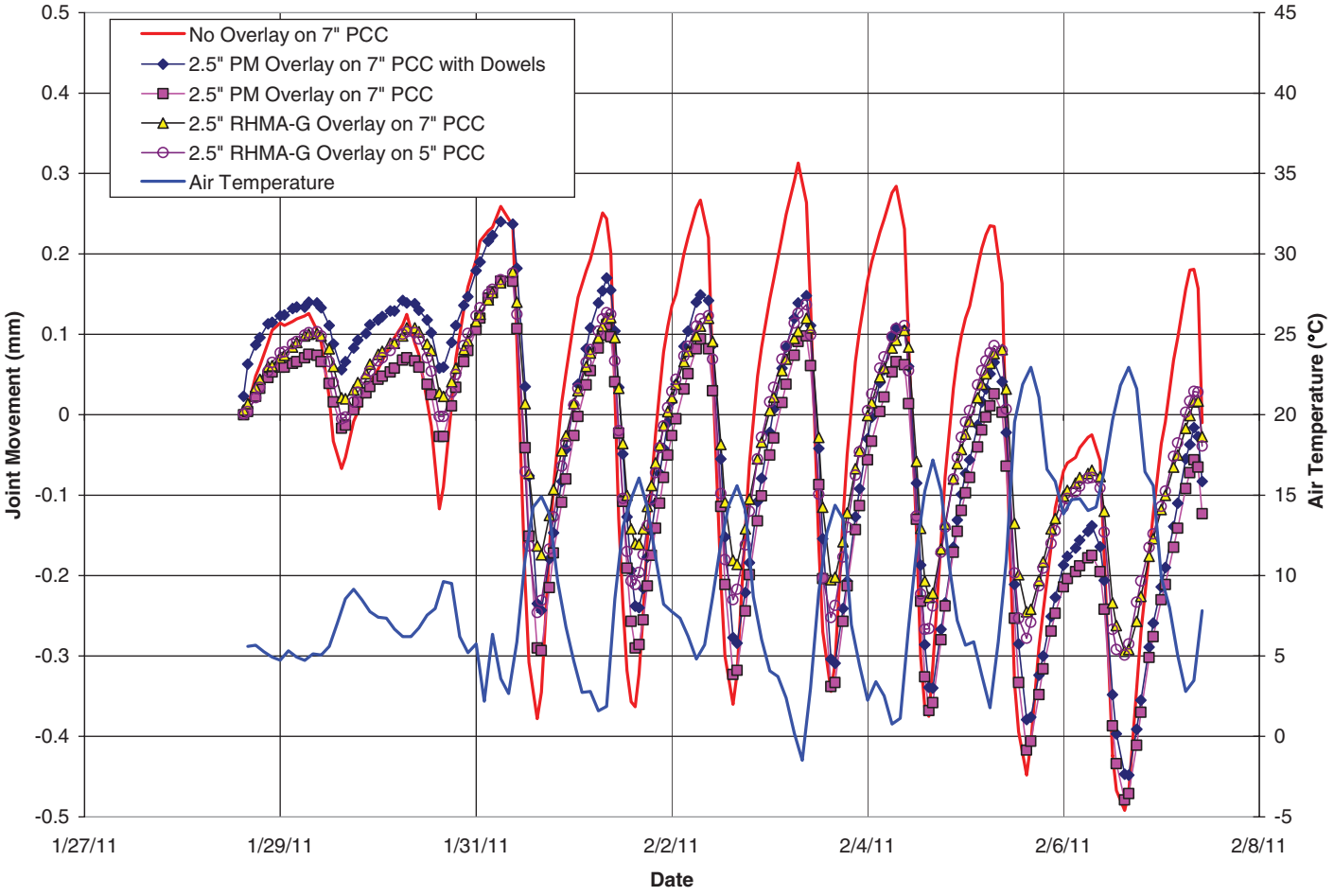

Note: 1 mm = 0.0394 in.

Figure 3.29. Comparison of horizontal joint movements for different structures, along with hourly air temperature recorded at the project site.

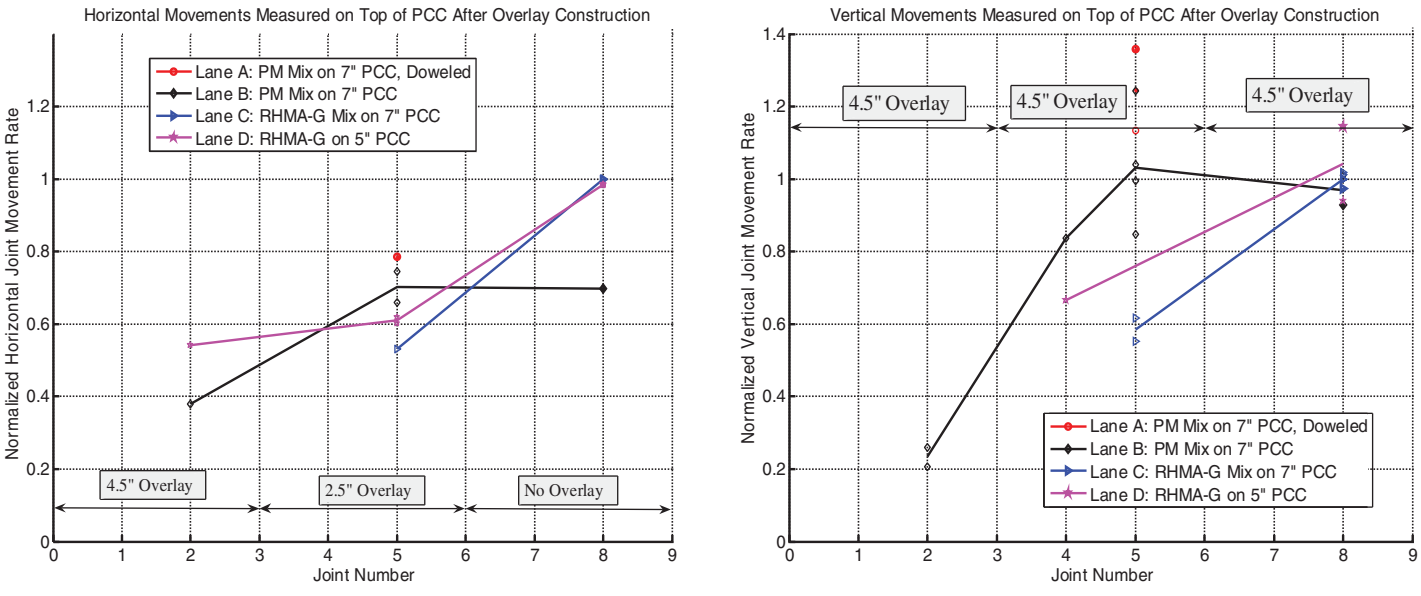

Figure 3.30. Normalized joint movement rates measured at different lanes and joints after HMA construction.

to reduce joint openings. This means improved joint load transfer at transverse joints.

HMA Fatigue Bottom-Up and Top-Down Cracking

Bottom-up area fatigue cracking and longitudinal top-down fatigue cracking in the wheelpath, typically observed in flexible pavements, are virtually nonexistent in HMA/PCC composite pavements because the HMA is almost always in compression, unless there is a loss of friction between the HMA and PCC layers. Thus, adequate and effective long-term bonding between the HMA and PCC is crucial for the long-term performance of HMA/PCC composite pavements. None of the field surveyed sections had any HMA fatigue cracking, even after more than 25 years and as many as 30 million trucks in the HMA/PCC lane. These pavements also exhibit improved long-term ride quality (IRI) and noise because wheelpath fatigue cracking is eliminated. These are key factors to be considered when evaluating the performance of HMA/PCC composite pavements.

Rutting Model

Multiple rut depth transfer functions have been developed over time. Most of these transfer functions were reviewed and summarized by Sousa et al. (1994) during the Future Strategic Highway Research Program (F-SHRP) work and by Von Quintus et al. (2011) in the conduct of National Cooperative Highway Research Program (NCHRP) Project 9-30. *MEPDG* software version 1.1 submitted to NCHRP as a product from NCHRP Project 1-37A included one rut depth transfer function, referred to as the Kaloush-Witczak equation (also referred to as the Kaloush equation). This transfer function was based on the use of repeated load uniaxial tests and was calibrated to rut depths measured on more than 100 test sections, most of which were included in the LTPP program. This transfer function also was used as the basis for developing the Asphalt Mixture Performance Test (AMPT) and in judging the acceptance of HMA mixtures under NCHRP Project 9-22. The rut depth prediction methodology included in the *MEPDG*, however, has received criticism for multiple reasons. Three of the more common reasons include the use of uniaxial or unconfined repeated load tests, the applicability of the depth function, and the resulting high standard error after the calibration-validation under NCHRP Project 1-40D. None of the pavement structures included in the initial calibration-validation process, however, included new HMA/PCC composite pavement structures.

The objective of NCHRP Project 9-30A was to recommend revisions to the HMA rut depth transfer function in the *MEPDG* software. The recommended revisions were based on the calibration and validation of multiple rut depth transfer functions with measured material properties and performance data from roadways and other full-scale pavement sections that incorporate modified or other specialty mixtures, as well as unmodified asphalt binders. This section summarizes the evaluation of the NCHRP 9-30A rutting models for HMA/PCC composite pavements, and details are provided in Appendix I.

MEPDG Version 9-30A for Predicting Rut Depths: Enhancements

Multiple revisions were made to the *MEPDG* under NCHRP Project 9-30A. The modified revision of the software is referred to as "*MEPDG* Version 9-30A." This section of the report identifies and discusses the more important revisions or enhancements for predicting rut depths for composite pavement structures, including (1) adding multiple rut depth transfer functions to the software, (2) adding layer-dependent plastic deformation parameters, and (3) revising the function used to consider the lateral distribution or wander of wheel loads.

Multiple Rut Depth Transfer Functions

Multiple rut depth transfer functions are included in *MEPDG* Version 9-30A. Three rut depth transfer functions were used for the calibration process to determine the applicability and accuracy of each for use in composite pavements: (1) the original version of the Kaloush rut depth transfer function, (2) a modified version of the Asphalt Institute vertical elastic strain and deviator stress transfer function, and (3) the WesTrack shear strain and shear stress transfer function.

MEPDG *Rut Depth Transfer Function*

The plastic strain relationship included in the *MEPDG* to predict rut depth in the HMA layer increments is shown as Equation 3.4 and represents the baseline condition for evaluating a mixture's susceptibility to distortion (NCHRP 2008).

$$\varepsilon_p = \varepsilon_r K_Z \beta_{r1} 10^{k_{r1}} (T)^{k_{r2}\beta_{r2}} (N)^{k_{r3}\beta_{r3}} \quad (3.4)$$

where

ε_p = incremental plastic strain at the middepth of a thickness increment;
ε_r = resilient strain calculated at the middepth of a thickness increment;
T = temperature at the middepth of a thickness increment, °F;
N = number of axle load applications of a specific axle type and load interval within a specific time period;
$\beta_{r1}, \beta_{r2}, \beta_{r3}$ = local calibration coefficients, which are all equal to 1.0 for the global calibration effort completed under NCHRP Project 1-40D;

k_{r1} = plastic deformation factor and equal to −3.35412 based on the global calibration effort;
k_{r2} = plastic deformation factor related to the effect of temperature and equal to 1.5606 based on the global calibration effort;
k_{r3} = plastic deformation factor related to the effect of wheel loads and equal to 0.4791 based on the global calibration effort; and
K_Z = depth function and equal to

$$K_Z = (C_1 + C_2 D)(0.328196)^D \quad (3.5)$$

$$C_1 = -0.1039 H_{HMA}^2 + 2.4868 H_{HMA} - 17.342 \quad (3.6)$$

$$C_2 = 0.0172 H_{HMA}^2 - 1.7331 H_{HMA} + 27.428 \quad (3.7)$$

where

D = depth to the middepth of the thickness increment, in., and
H_{HMA} = thickness of the HMA layers, in.

The rationale for the plastic to resilient strain ratio transfer functions is to consolidate the effects of stress level. Vertical stress affects the resilient elastic strain, as well as plastic strain. Normalizing the plastic strain to the elastic strain is hypothesized to capture the stress effect without including it in the regression equation or transfer function (Kaloush and Witczak 2000).

The regression coefficients or plastic deformation coefficients (k_{r1}, k_{r2}, k_{r3}) were determined from unconfined, uniaxial repeated load plastic deformation tests conducted in the laboratory and adjusted to field-measured values. The k_{r3} factor is the slope in the steady state or secondary range, whereas the k_{r1} is the intercept of the log-log relationship between the number of load applications and cumulative plastic strain. The k_{r2} factor is the effect of temperature on the intercept.

The *MEPDG* uses an incremental thickness and time approach in calculating total HMA rut depth. The depth function (refer to Equation 3.5) is included to consider the effect of confinement from the upper HMA thickness increments in calculating the incremental rut depths through all of the HMA layers. A time-hardening scheme is included to accumulate plastic deformation over multiple load levels and seasons (NCHRP 2008). There has been some industry criticism of the applicability of the depth function, whereas the time-hardening scheme has been used by others in calculating total HMA rutting with time.

Modified Leahy Rut Depth Transfer Function

A modified form of the Asphalt Institute or original Leahy equation was used in NCHRP Project 1-40B in an attempt to explain the large bias between the predicted and measured rut depths (Von Quintus 2005). This modified form is shown below but did not eliminate the bias or reduce the standard error using selected LTPP experiments Special Pavement Studies (SPS)-1 and SPS-5 test sections.

$$\text{Log}\left(\frac{\varepsilon_p}{\varepsilon_r}\right) = -0.505 + 0.25\text{Log}(N) + 0.110\text{Log}(\sigma_d) + 0.930\text{Log}(V_{beff}) + 0.501\text{Log}(V_a) \quad (3.8)$$

where

V_a = air voids, percent,
V_{beff} = effective asphalt content by volume, percent, and
σ_d = deviator stress, psi.

Temperature and viscosity terms were included in the original version of the Asphalt Institute transfer function but were removed because dynamic modulus is calculated on an incremental basis with HMA depth and time. It was hypothesized that the influences of temperature and viscosity on the intercept are adequately accounted for through dynamic modulus—smaller computed elastic vertical strains with increasing dynamic modulus values. The average intercept coefficient was determined at the equivalent temperature and calibrated to field-measured values. The effective asphalt content by volume and air void terms were left in the regression equation because of their significance (Von Quintus 2006). The other major difference between the original Asphalt Institute and the modified Leahy transfer function is that the modified Leahy equation was based on results from repeated load confined triaxial tests.

WesTrack Rut Depth Transfer Function

The WesTrack plastic shear strain transfer function was developed using data from the WesTrack field experiment (Epps et al. 2002). The mathematical formulation, shown in Equation 3.9, is M-E based for predicting HMA rutting using shear strain and shear stress. This formulation was developed to provide a more realistic simulation through laboratory testing of the horizontal plastic deformations that can occur in the field (Sousa et al. 1994).

$$\gamma_p = a e^{b\tau} \gamma_r N^c \quad (3.9)$$

where

γ_p = permanent shear strain at a depth of 2 in. beneath the tire edge,
τ = corresponding elastic shear stress,
γ_r = corresponding resilient shear strain,
N = number of axle load applications of a specific axle type and load interval within a specific time period, and
a, b, c = regression coefficients.

The resilient shear strain measured from the repeated load simple shear tests conducted at constant height was used in the calibration of the plastic deformation coefficients of the HMA mixture. The regression coefficients were determined at multiple temperatures, but temperature was excluded in the final regression equation. For conventional HMA mixtures, the recommended values for the transfer function are $a = 2.114$, $b = 0.04$, and $c = 0.124$. The form of the equation included in the *MEPDG* Version 9-30A software uses the intercept measured at the equivalent annual temperature.

The time-hardening principle included in the *MEPDG* is used to estimate the accumulation of plastic shear strains in the HMA under varying site conditions. To implement this transfer function in the *MEPDG* computational framework, the N_{virt} expression in the software was changed as follows:

$$\ln(N_{virt}) = [\ln(\gamma_p / \gamma_r) - \ln(a) - b\tau]/c \quad (3.10)$$

The incremental plastic shear strain is computed for a given stress state, load frequency, modulus, and N computed in accordance with Equation 3.9. The rutting that is estimated in the HMA layer attributable to the plastic deformation (PD) is determined from the following equation, where K equals a coefficient related to the thickness of the HMA layer, as shown in Table 3.10. As a result, the depth function included in the *MEPDG* is "turned off" when using the WesTrack transfer function.

$$PD = K\gamma_p \quad (3.11)$$

HMA Layer Specific Plastic Deformation Model Coefficients

In the *MEPDG* versions released through NCHRP, one set of plastic deformation coefficients is used for all HMA layers. The *MEPDG* computational methodology assumes that the differences in HMA dynamic modulus will correctly account for differences in rutting susceptibility between different mixtures. This assumption has been found to result in a bias and increases the standard error of the predicted rut depths (Von Quintus et al. 2005, Von Quintus 2005).

Under NCHRP Project 9-30A, the *MEPDG* software was revised to permit the user to enter layer-specific plastic deformation coefficients determined from laboratory repeated load tests. For composite pavements with one HMA layer, layer-specific plastic deformation parameters are not needed. However, some of the composite pavement sections do include two layers or lifts of HMA placed above the PCC slab layer.

Table 3.10. Values of K as a Function of HMA Layer Thickness for the WesTrack Transfer Function

HMA Thickness (in.)	*K*-Value
5–7	5.5
7–9	7.0
9–12	8.5
>12	10.0

Lateral Wander Effects

The standard deviation is used to define the practical limits of the width of the lateral distribution of wheel loads. A uniform distribution of wheel or axle loads is used between the limits defined by the standard deviation of wheel loads. A normal distribution is believed to provide a more realistic distribution of wheel loads for computing total rutting. Thus, under NCHRP Project 9-30A, the *MEPDG* was revised to include a normal distribution in the lateral location of the wheel loads for calculating the pavement responses in computing total rut depth.

Predicted Rut Depths: Transfer Function Coefficient Global Values

The three transfer functions and their global coefficients were used to predict the rut depths measured on the HVS test sections and on each of the composite field survey sections as described in Appendix I. The NCHRP Project 1-40B procedure (Local Calibration Guide) was followed in judging whether any of the transfer functions and their global coefficients is a reasonable simulation of the measured rut depths. Two parameters are used in determining whether the transfer function is adequate or needs to be recalibrated to the specific features under evaluation (composite pavement structures, in this case): the slope and intercept between the predicted and measured values. The following summarizes the comparisons.

- The Kaloush transfer function using the global coefficients provided a reasonable estimate of the rut depths of the HVS test sections for the PG64-28PM mixture but underpredicted the rut depths in the RHMA-G mixture. However, the Kaloush transfer function using the global coefficients generally overpredicted the rut depths measured along the R21 field survey sections.
- The modified Leahy transfer function using the global coefficients significantly underpredicted the rut depths measured along all HVS test sections and R21 field survey sections.

- The WesTrack transfer function using the global coefficients significantly under-predicted the rut depths measured along all HVS test sections and R21 field survey sections.

Rut depth time or loading series data are available for the HVS test sections, but only a few of R21 field survey sections include rut depths measured over time. Most of these include the rut depths measured at one point in time. The measured rut depths for the HVS test sections at varying loading cycles were compared with the rut depths predicted with each transfer function using the global values for the transfer functions as shown in Appendix I. The magnitudes of the predicted rut depths and relative change of predicted rut depths with number of load cycles deviate from the measured values.

In summary, the slope and intercept of the trend line between the predicted and measured rut depths deviate significantly from 1.0 (equality), and the trend line does not go through the origin for any of the transfer functions, except for the Kaloush transfer function in predicting the rut depths measured on the HVS PG64-28PM test sections. None of the rut depth transfer functions using their global coefficients are believed to provide an accurate simulation of the measured rut depths exhibited on the HVS test sections and R21 field survey sections. As such, all rut depth transfer functions need to be redefined for composite pavement structures.

Composite Pavement Calibration Parameters

The results from previous calibration studies were used in determining the coefficients for each of the three rut depth transfer functions, including NCHRP Projects 9-30, 1-40B, and 9-30A. The parameters that have been reported to reduce model bias and the standard error of the rut depth transfer functions include HMA thickness, stress term coefficient, and volumetric properties of the HMA layers (air voids, asphalt content, and gradation). A discussion of each of these parameters relative to HMA/PCC composite pavements is included in Appendix I. However, it should be understood that the in-place volumetric properties were adequately measured for the mixtures placed at the UCPRC HVS test sections, but the same properties were extracted from construction records for the R21 composite pavement field survey sections. The reliability of data extracted from construction records is undefined; as a minimum, these data include more error than the data for the UCPRC HVS test sections.

As discussed in Appendix I, NCHRP Project 9-30A concluded that, with the appropriate coefficients, all of the transfer functions can provide an accurate simulation of the measured rut depths (ranging from very low to high rut depths) over a diverse range of mixtures, conditions, and pavement structures. The other important observation was that the *N*-term exponent was found to be the same between all of the transfer functions.

UCPRC HVS Test Sections

The three transfer functions were used to predict the rut depths measured on the UCPRC HVS test sections and measured on each of R21 field survey sections. The difference between the field survey and HVS test sections is that repeated load constant height shear tests were performed on each of the HMA mixtures placed at UCPRC.

HVS-derived plastic deformation coefficients were determined for the thicker composite test sections that minimize the difference between the predicted and measured rut depths, as shown in Table 3.11. This analysis was completed to

Table 3.11. Summary of Field-derived Plastic Strain Coefficients from the 4.5-in. HMA Layer HVS Test Sections for the Three Transfer Functions

Mixture	Transfer Function	Transfer Function Coefficients		
		Intercept	Stress or Temperature Term Exponent	Slope; *N*-term Exponent
PG64-28PM	Kaloush	–2.761	1.5606	0.35
PG64-28PM	Modified Leahy	–2.163	1.0	0.35
PG64-28PM	WesTrack	3.619	0.01	0.35
RHMA-G	Kaloush	–2.20	1.5606	0.25
RHMA-G	Modified Leahy	–1.735	1.0	0.25
RHMA-G	WesTrack	13.30	0.01	0.25

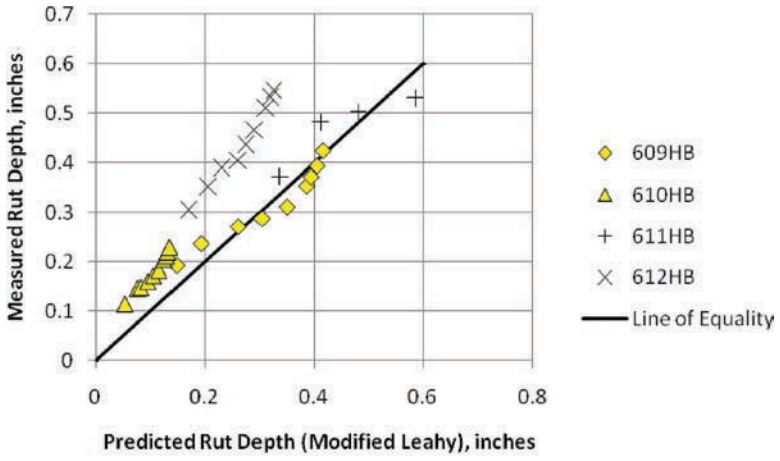

(a) Modified Leahy Transfer Function.

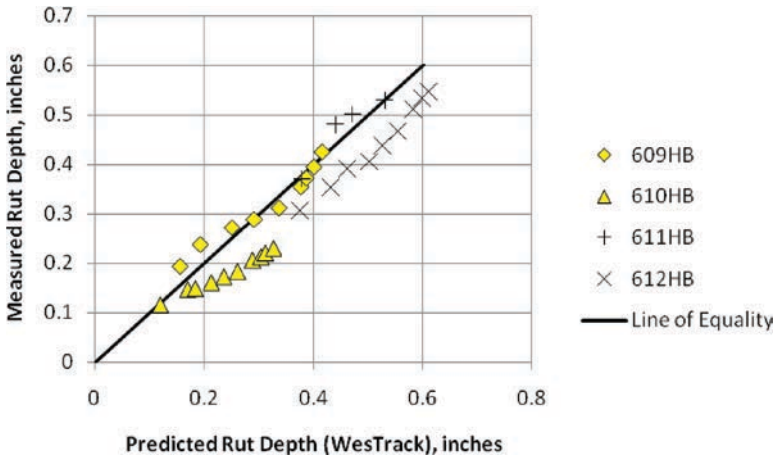

(b) WesTrack Transfer Function.

Figure 3.31. Measured and predicted rut depths using the Modified Leahy and WesTrack transfer functions for the HVS test sections.

determine the intercept coefficient for each transfer function that provides an accurate estimate of the rut depths measured over time. These HVS-derived coefficients were also used to determine the transfer functions that would or would not accurately predict the rutting evolution over a diverse range of mixtures.

Figure 3.31 compares the predicted and measured rut depths for each transfer function for the HVS test sections. As shown, all of the transfer functions can provide an accurate simulation of the measured rut depths (ranging from very low to high rut depths). The results also suggest, however, that thickness correction factors are needed for all transfer functions, even for the relatively thin HMA layers over PCC layers.

Thickness adjustment factors were estimated from these results to eliminate model bias caused by layer thickness. Table 3.12 summarizes the HMA thickness adjustment factors for each transfer function. Figure 3.32 provides a comparison between the predicted and measured rut depths after applying the thickness adjustment factor. In summary, all three transfer functions can provide an accurate simulation of the measured rut depths. Results from the HVS test sections were used to estimate the thickness correction factors for the R21 field survey sections.

Table 3.12. Thickness Correction or Adjustment Factors for HVS Test Sections

	HMA Layer Thickness	
Transfer Function	**2.5 in.**	**4.5 in.**
Kaloush	1.08	1.0
Modified Leahy	1.35	1.0
WesTrack	0.80	1.0

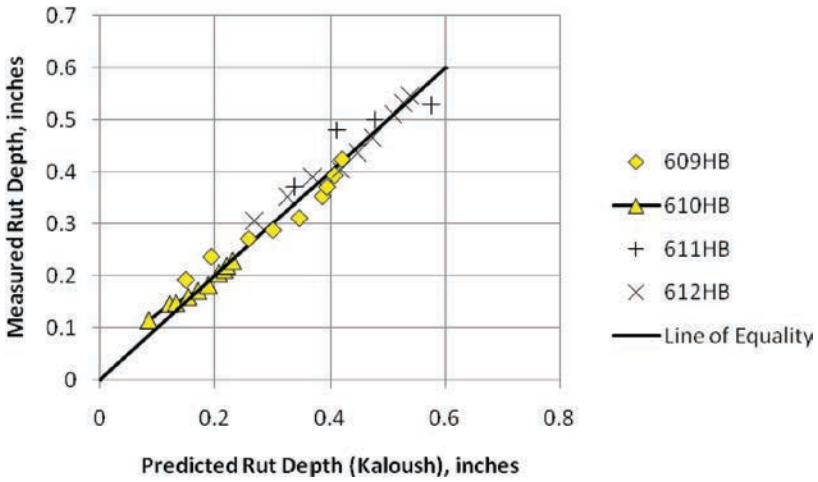

(a) Kaloush Transfer Function.

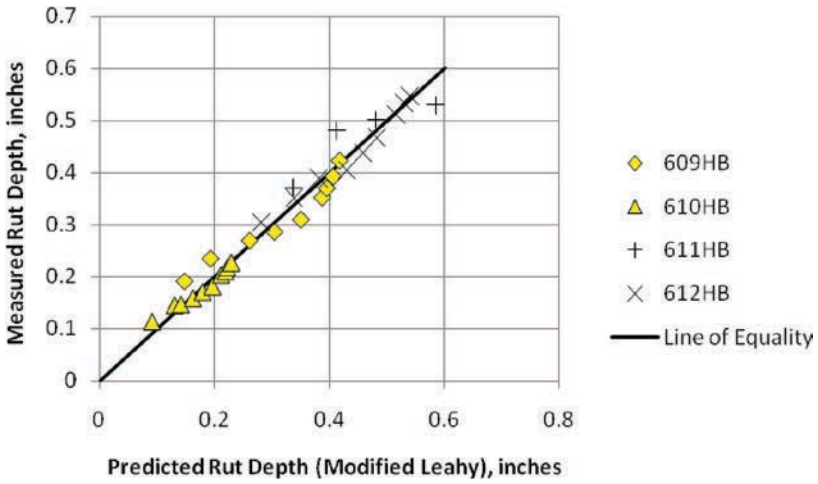

(b) Modified Leahy Transfer Function.

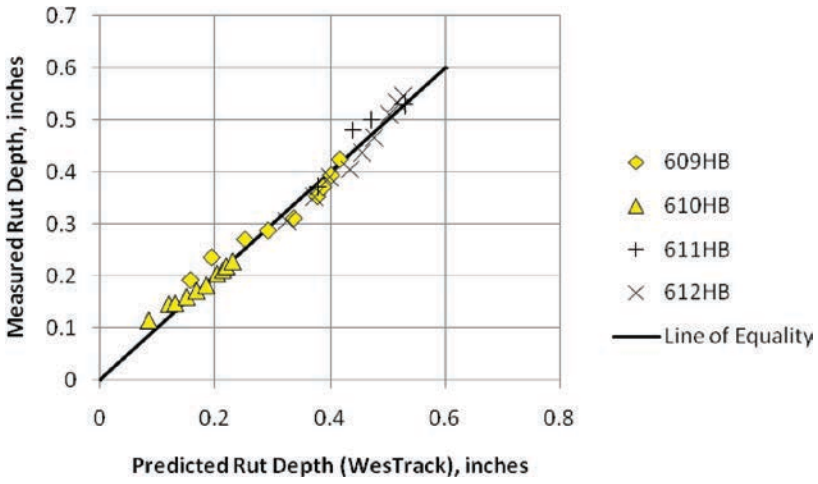

(c) WesTrack Transfer Function.

Figure 3.32. Measured and predicted rut depths for the HVS test sections.

R21 Field Survey Sections

The exponent for the number of load cycles for the three transfer functions was assumed for all R21 field survey sections because time series data were unavailable for most of these test sections. The rut depths measured on these sections are low and suggest well-designed mixtures that are resistant to deformation. Most of the measured rut depths are less than 0.30 in., with an average value from all sections of about 0.17 in. Some of these sections have heavy truck traffic. The slope value assumed for all projects was simply the average value determined for the test sections included in NCHRP Project 9-30A representing good quality mixtures—a value of 0.235. Plastic deformation coefficients were determined for the composite test sections in the same way as for NCHRP Project 9-30A.

Table 3.13 summarizes the transfer function intercepts or coefficients, which were found to be dependent on HMA layer thickness and air voids. Asphalt content was found to have little to no impact on reducing the model bias and standard error. However, asphalt content is an important parameter based on the results from NCHRP Projects 1-40B and 9-30A. It is believed that the values extracted from the project files include errors in determining the effective asphalt content by volume. This may account for the inconsistent results from other studies. Other important observations from these results for composite pavements are listed below:

- The magnitudes of the intercept for the three transfer functions are higher than reported for conventional and deep strength flexible pavement. Some of this difference probably is related to the stress term values and lower HMA thicknesses in comparison with other test sections used in the calibration process for flexible pavements.
- The effect of HMA thickness is inconsistent for all transfer functions. The coefficients do not consistently increase or decrease with increasing layer thickness. The higher intercept values occur in the range of 3 to 4 in.; thinner and thicker layers result in a decrease in the values for the intercept.
- Air voids in the typical range of construction specification have little impact on the measured and predicted rut depths. Air voids have an impact on the intercept when they exceed typical construction specifications. Higher air voids result in greater amounts of rutting.

Table 3.13. Transfer Function Coefficients Used to Predict the Rut Depths for the R21 Field Survey Sections

Transfer Function	HMA Layer Thickness (in.)	HMA Air Voids (%)		
		<6.0	6.1–9.0	>9.0
Kaloush; Equation 3.12, k_{r1}	<3	–2.30	–2.30	–2.05
	3–4	–2.15	–2.15	–2.05
	>4	–2.30	–2.30	–1.95
Modified Leahy; Equation 3.13, C_1	<3	–1.90	–1.90	–1.4
	3–4	–1.80	–1.80	–1.5
	>4	–2.00	–2.00	–1.3
WesTrack; Equation 3.14, a	<3	10.5	10.5	10.5
	3–4	14.0	16.0	20.0
	>4	10.5	10.5	16.0

The following transfer functions and their plastic deformation coefficients are used to predict the rut depths for all of the R21 field survey sections. It should be understood that the N-term exponent of 0.235 for all transfer functions represents well-designed mixtures resistant to plastic deformation.

$$\varepsilon_p = \varepsilon_r K_Z 10^{k_{r1}} (T)^{1.5606} (N)^{0.235} \tag{3.12}$$

$$\text{Log}\left(\frac{\varepsilon_p}{\varepsilon_r}\right) = C_1 + 0.235\text{Log}(N) + 1.0\text{Log}(\sigma_d) + 0.930\text{Log}(V_{\text{beff}}) + 0.501\text{Log}(V_a) \tag{3.13}$$

$$\gamma_p = ae^{0.01\tau}\gamma_r N^{0.235} \tag{3.14}$$

The k_{r1}, C_1, and a terms or intercept values are defined in accordance with Table 3.13.

Figure 3.33a provides a comparison of the predicted and measured rut depths for all R21 field survey sections using the Kaloush function, whereas Figure 3.33b provides a comparison of the residual errors and the predicted values. Figure 3.34 and Figure 3.35 provide a similar comparison for the other two transfer functions. As shown, all three transfer functions provide reasonable estimates of the measured values. Two of the composite pavement roadway sections, however, are considered outliers for all three transfer functions—Sections LTPP2 and TX1. All three transfer functions overpredict the rutting measured on Section TX1 and underpredict rutting for Section LTPP2. These sections are considered outliers.

Figures 3.33 through 3.35 (composite pavement plastic deformation coefficients) can be compared to the global plastic deformation coefficients (Appendix I) to illustrate the improvement in the model by considering layer thickness and air voids. All transfer functions are considered adequate for predicting the measured rutting. Although some of the model statistics are poor and indicative of a model that does not explain the variability in the measured values, trying to predict low rut depths is difficult at best, especially without project-specific or mixture-specific test data.

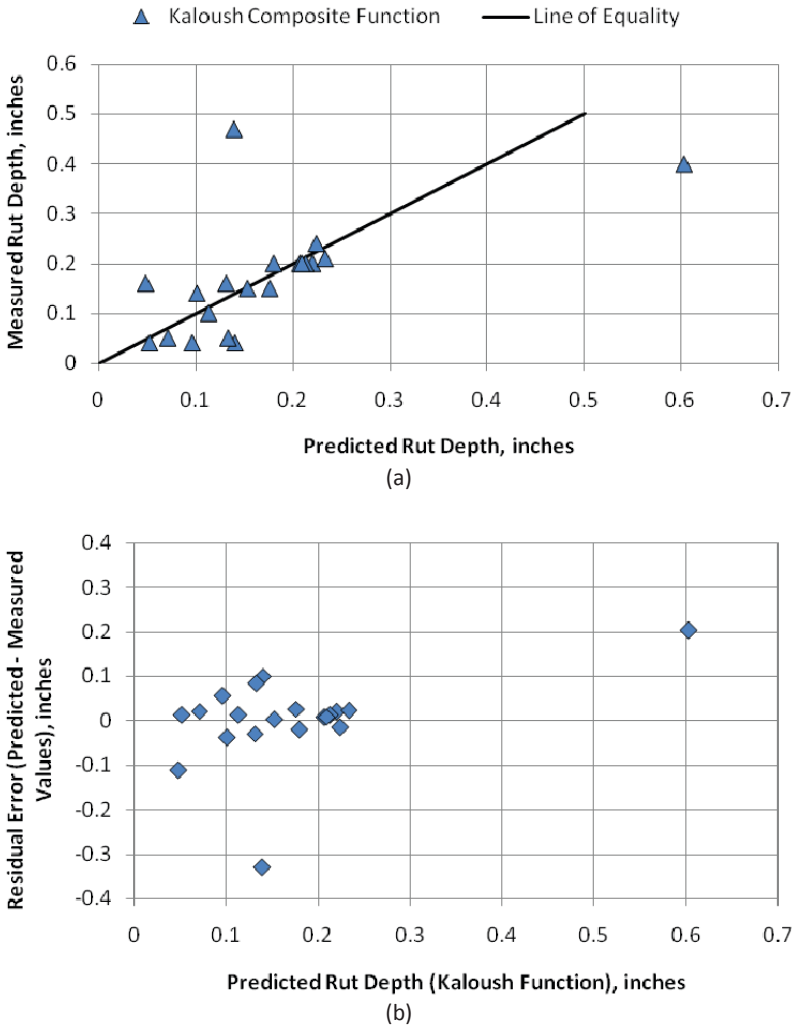

Figure 3.33. Measured and predicted rut depths using the Kaloush transfer function for the R21 field survey sections.

Summary

In summary, all three transfer functions did a fair job of predicting the measured rutting values using mixture properties and other pavement layer properties extracted from project files. Thus, the three rut depth transfer functions described and included in NCHRP Project 9-30A are believed to be reasonable for composite pavements.

Rutting Model and DARWin-ME

As described previously in this section, the *MEPDG* software version 1.1, submitted as a product of NCHRP Project 1-37A, included only one rut depth transfer function, the Kaloush transfer function with default coefficients of $k_{r1} = -3.35412$, $k_{r2} = 1.5606$, and $k_{r3} = 0.4791$. These coefficients were developed based on global calibration but can be changed by the user during execution of the software program. DARWin-ME was developed using the same models included in *MEPDG* software version 1.1, and as such includes the same global calibration coefficients and provides the functionality of allowing the user to change the coefficients.

The Kaloush coefficients described above ($k_{r1} = -1.95$ to -2.30, $k_{r2} = 1.5606$, and $k_{r3} = 0.235$), which were developed and refined as part of NCHRP Project 9-30A and SHRP 2 R21), cannot be used directly in DARWin-ME, although the model forms are identical. This is because of the difference in how the two versions account for lateral wander. *MEPDG* software version 1.1 (and the current version of DARWin-ME) uses a uniform distribution to account for lateral wander. *MEPDG* Version 9-30A and the R21 coefficients are based on a normal distribution model for lateral wander, which is believed to be more representative of field conditions. Until the lateral wander is changed from uniform to normal distribution in DARWin-ME, it is recommended that the global calibration

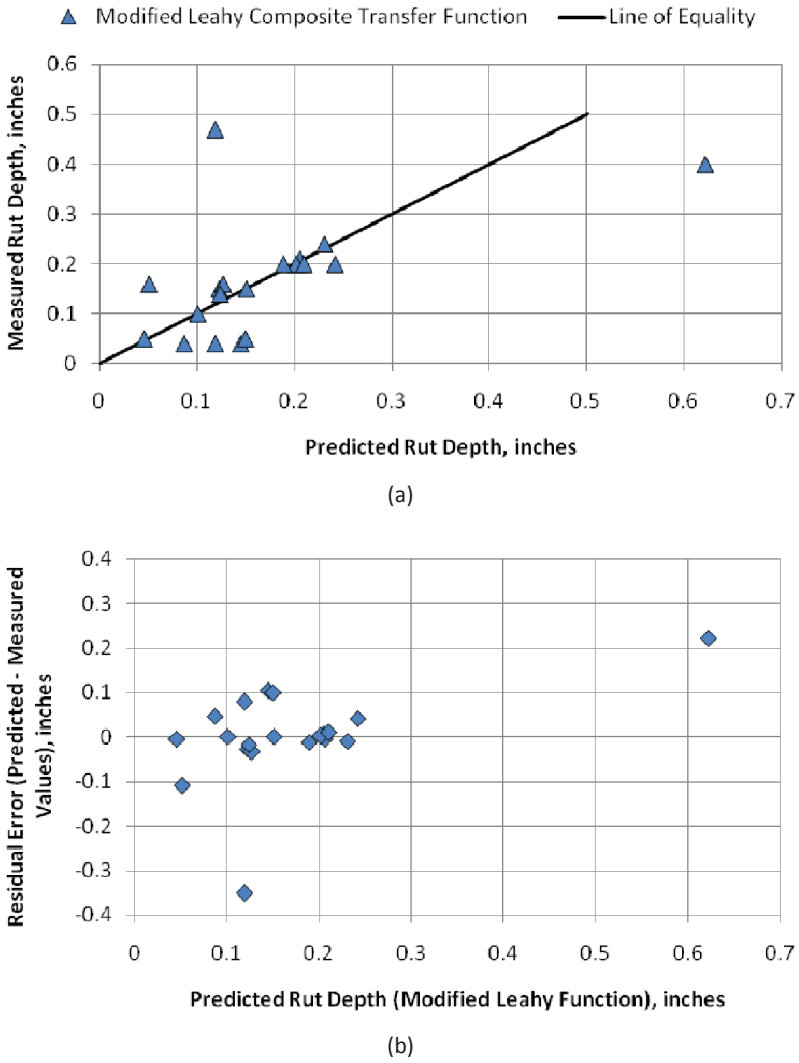

Figure 3.34. Measured and predicted rut depths using the Modified Leahy transfer function for R21 field survey sections.

default coefficients (k_{r1} = −3.35412, k_{r2} = 1.5606, and k_{r3} = 0.4791) be used to model rutting in HMA/PCC composite pavements when using DARWin-ME.

DARWin-ME and SHRP 2 R21 Field Survey Sections

The rutting history of R21 composite pavements field survey sections was very good, attributable in part to the relative thinness of the HMA layers but also owing to its high-quality materials. In addition, the stiffness of the PCC layer completely eliminates base, subbase, and subgrade rutting. Figure 3.36 shows the plot of rutting with age of the HMA surface. The trend line shows only 0.006 in./year increase in rutting over time.

The surface of HMA/PCC typically is less than about 4 in. The database includes surfaces from 0.5- to 5-in. asphaltic surfaces, including SMA, porous friction courses, asphalt rubber friction course (ARFC), permeable HMA, and dense HMA. The material was modeled in DARWin-ME as a distinct layer with the thickness, gradation, volumetric binder content and grade, and air voids. Rutting was predicted for each section using DARWin-ME, and the predicted value was compared with the measured value, where data were available. The predicted versus measured rutting is shown in Figure 3.37. Overall, rutting is very low except for one possible outlier. The one-to-one line shows that predicted rutting is reasonably close to measured rutting for these sections using DARWin-ME and the global calibration coefficients.

The Kaloush model using *MEPDG* Version 9-30A is a better fit than the Kaloush model using DARWin-ME (compare Figure 3.33 with Figure 3.37). Because normal distribution for lateral wander of the wheel load is believed to be a more accurate representation of field conditions

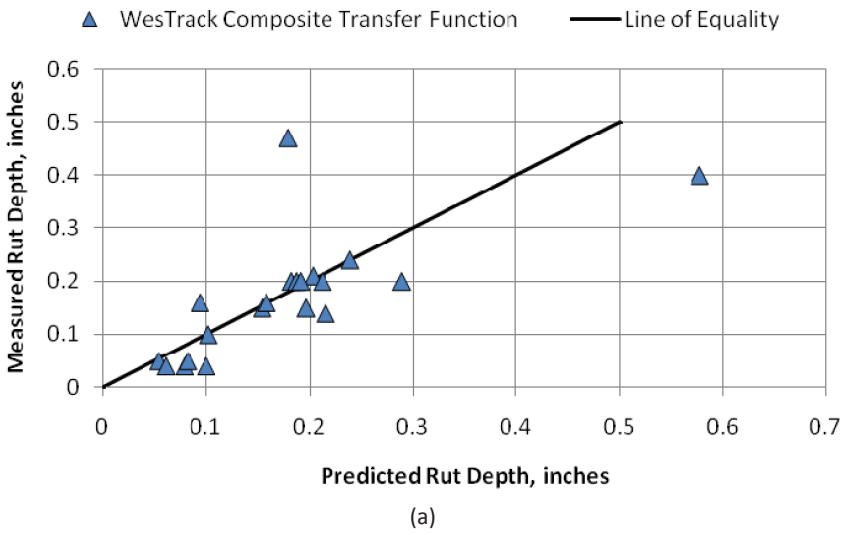

(a)

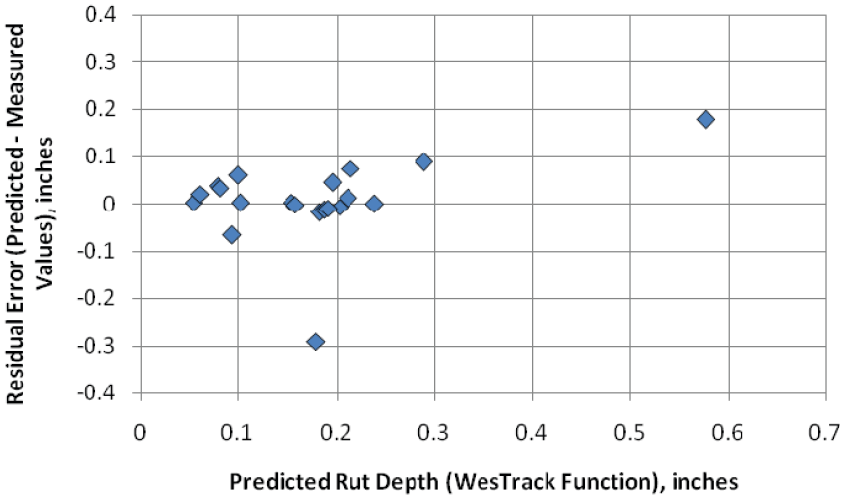

(b)

Figure 3.35. Measured and predicted rut depths using the WesTrack transfer function for the R21 field survey sections.

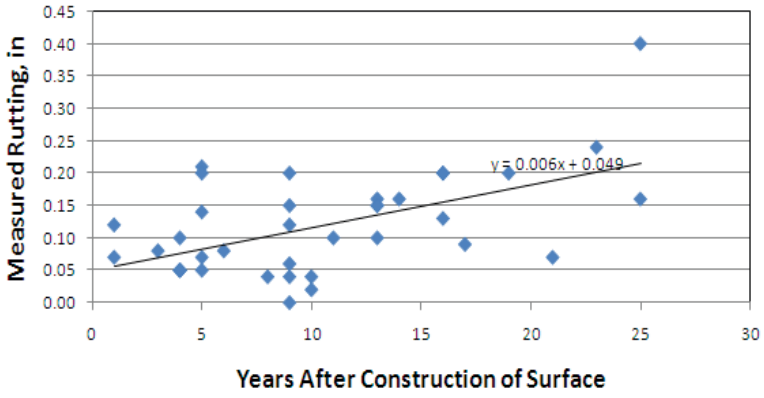

Figure 3.36. Rutting over time for SHRP 2 R21 field survey HMA/PCC composite pavement sections.

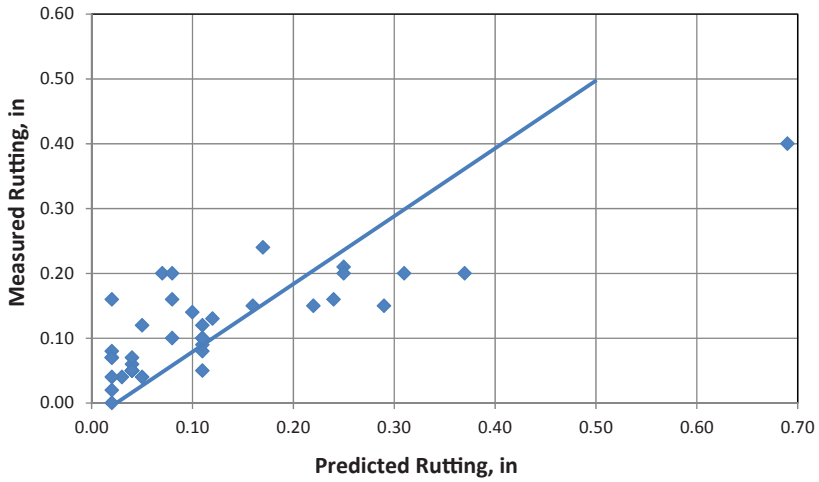

Figure 3.37. Predicted versus measured rutting for HMA surface courses for all R21 composite pavement sections using DARWin-ME and global calibration coefficients.

(as compared with uniform distribution), it is recommended that DARWin-ME be updated with the NCHRP 9-30A models. At this point the updated coefficients ($k_{r1} = -1.95$ to -2.30, $k_{r2} = 1.5606$, and $k_{r3} = 0.235$) can then be used to model rutting in HMA/PCC composite pavements.

Level 1 versus Level 3 Data

DARWin-ME and the *MEPDG* allow the user to enter HMA material properties at Level 1, Level 2, or Level 3. For Level 1 modeling, the laboratory-tested dynamic modulus properties of the asphalt concrete mixture and laboratory-tested asphalt binder properties are required. These were not available for the R21 field survey sections but were tested for the MnROAD HMA/PCC test section. For Level 3 modeling, the dynamic modulus properties are derived in DARWin-ME and *MEPDG*, using typical rheological properties of the asphalt binder grade and the aggregate gradation of the asphalt concrete mixture. Figure 3.38 and Figure 3.39 show comparisons between using Level 1 and

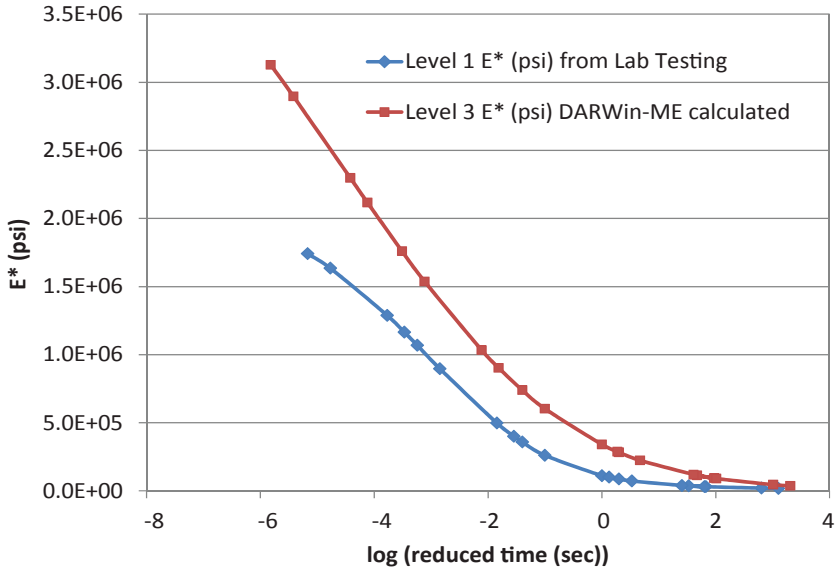

Figure 3.38. Level 1 (actual laboratory data) versus Level 3 (DARWin-ME estimated) dynamic modulus master curve for HMA mix used in the R21 HMA/PCC composite pavement section at MnROAD.

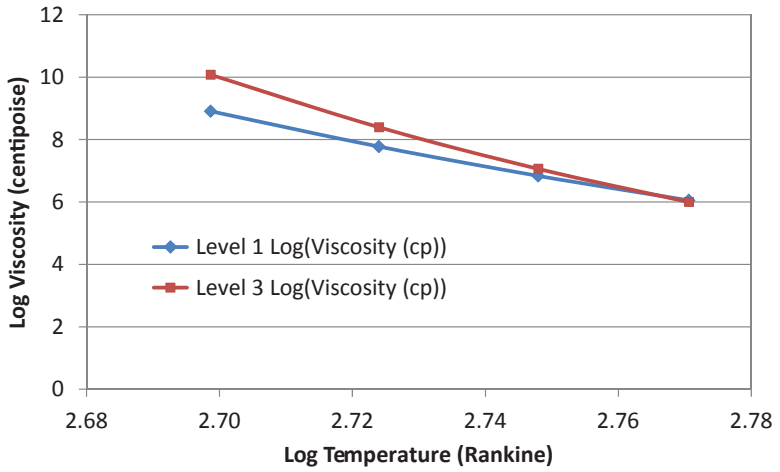

Figure 3.39. Level 1 versus Level 3 modeled viscosity (as a function of temperature) for PG64-34 binder used in the HMA mix for the R21 HMA/PCC composite pavement section at MnROAD (cp = centipoise).

Level 3 data for the HMA mix and HMA binder used at MnROAD.

The rutting performance of the MnROAD R21 HMA/PCC section (Cell 70) was modeled using both Level 1 and Level 3 data in DARWin-ME, then compared with field-measured average rut depths for the driving lane and the passing lane as shown in Figure 3.40 and Figure 3.41, respectively. The figures show an excellent match between field-measured rut depths and rutting modeled using Level 1 data in DARWin-ME. The figures also show that although Level 3 data are reasonable on average when considering a large number of sections (see Figure 3.37), for designing and modeling individual sections, Level 1 data provide the results that best match field performance.

Reflection Cracking Model

Reflection cracking is a major distress mode in new HMA/PCC composite pavements. The basic mechanism of reflection cracking is the propagation of cracks through the HMA layer

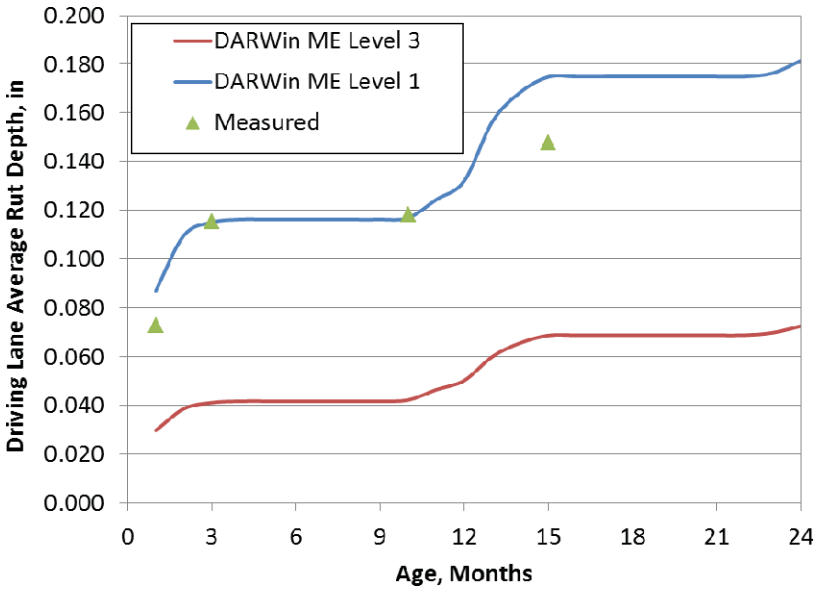

Figure 3.40. DARWin-ME–modeled rutting using Level 1 and Level 3 data versus field-measured average rut depths in the driving lane for the HMA/PCC test section at MnROAD.

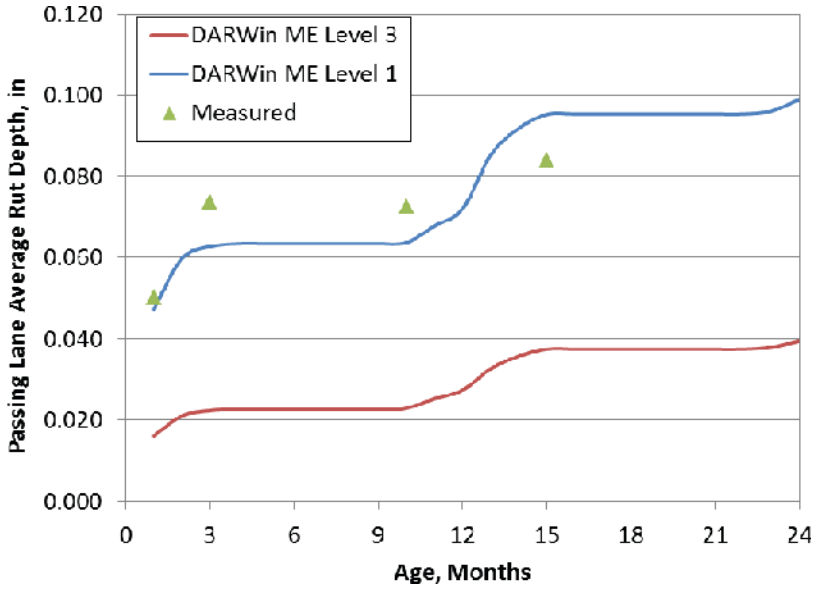

Figure 3.41. DARWin-ME–modeled rutting using Level 1 and Level 3 data versus field-measured average rut depths in the passing lane for the HMA/PCC test section at MnROAD.

caused by movements in the vicinity of cracks and joints in the PCC slab. This movement may be vertical due to loading, horizontal due to temperature changes, or a combination of both. Load-induced movements are influenced by the thickness of the HMA layer and the thickness, modulus, and load transfer in the PCC slab. Temperature-induced movements are influenced by daily and seasonal temperature variations, the coefficient of thermal expansion (CTE) of the HMA and PCC layers, and the spacing of cracks.

The complex combination of tensile and shear strains at the bottom of the HMA layer causes cracks to initiate at the bottom of the HMA layer. Over time, the cracks propagate upward through the HMA layer. As the process continues, multiple reflection cracks will form, and eventually portions of the HMA surface will spall and dislodge from the pavement surface. Even with routine maintenance, such as crack sealing or thin surface treatments, reflection cracks eventually lead to a reduction of pavement smoothness and shorten the life of the HMA layer.

Because of the thinness of the HMA layers in HMA/PCC composite pavements, a majority of the PCC joints can be expected to reflect through the HMA layer(s) within a few years after initial construction (depending on climatic conditions, HMA mix properties, load transfer at the joint, and traffic). The deterioration of these reflection cracks over time also depends on local climatic conditions, load transfer at the joint, maintenance activities (crack sealing, surface treatments, and so forth), and traffic.

Although reflection cracking modeling is presented in this section, sawing and sealing the HMA layer (at the location of the PCC joint), as discussed later in this section, is encouraged. Sawing and sealing creates a clean joint that lasts longer and deteriorates at a much slower rate than do joints that are not sawed and sealed. Note that reflection cracking was not observed to be an issue for the field-surveyed HMA/continuously reinforced concrete (CRC) composite pavements (with adequate steel reinforcement in the CRC). This is because the cracks in the CRC are held tight by the reinforcing steel and have relatively smaller differential vertical deflections and joint openings than do joints in jointed plain concrete (JPC).

During the development of the *MEPDG*, the state of M-E modeling of reflection cracking was limited. As a result, a simplified empirical model was included for reflection cracking analysis. The model predicts the percentage of cracks that propagate through the HMA layer as a function of time using a sigmoidal function. Equation 3.15 presents the general form of the sigmoidal model:

$$RC = \frac{100}{1 + e^{a+bt}} \tag{3.15}$$

where

RC = percent of cracks reflected (%),
t = time (years),
e = base for natural logarithm = 2.71828, and
a and b = fitting parameters.

The parameters of the model are a function of HMA thickness and the load transfer at joints and cracks. The regression fitting parameters, summarized in Table 3.14, are hard coded

***Table 3.14. Reflection Cracking Model Parameters in the* MEPDG**

Pavement Type	Parameters	
	a	*b*
Rigid, good load transfer	3.5 + 0.75 (h_{ac} – 1)	–0.688584 – 3.37302 (h_{ac} – 1)$^{-0.915469}$
Rigid, poor load transfer	3.5 + 0.75 (h_{ac} – 3)	–0.688584 – 3.37302 (h_{ac} – 3)$^{-0.915469}$

in the software. In other words, the designer cannot directly alter these parameters as inputs, but they can be changed in the software.

NCHRP Report 669

The most updated research on reflection cracking was performed as part of NCHRP Project 01-41 and published as NCHRP Report 669 (Lytton et al. 2011). Appendix R of NCHRP Report 669 includes a comprehensive review of available models for reflection cracking. The capabilities, advantages, and disadvantages of these models are also included. The three mechanisms of reflection cracking considered in this study were

1. Thermally induced fatigue caused by daily temperature change and corresponding opening and closing of the joints/cracks;
2. Crack growth caused by bending of the HMA layer above the joint as a result of traffic load; and
3. Crack growth caused by the shearing of the HMA layer above the joint as a result of traffic load.

Figure 3.42, originally printed in NCHRP Report 669, shows typical development of reflection cracking by various severity levels as a function of time or number of load applications. The cracking pattern follows a sigmoidal curve, so the functional form shown below was used to model reflection cracking for various severity levels.

$$D(N_i)(\%) = e^{-\left(\frac{\rho}{N_i}\right)^{\beta}} \tag{3.16}$$

where

$D(N_i)$ = percent of reflection crack length of maximum crack length at, N,
i = ith crack observation, and
N_i = number of days after overlay.

Note that ρ (the scale factor representing the width of the rising portion of the curve) is always equal to the total number of days to reach 36.8% (= 1/e) of the total amount of expected reflection cracking. The shape factor β represents the steepness of the rising portion of the curve (Figure 3.43).

The parameters ρ and β, the field-observed parameters that represent the scale and shape of the progression of reflection cracking, were calibrated for three different severity levels as a function of number of days for crack growth:

- ρ_H and β_H for high severity level;
- ρ_{MH} and β_{MH} for medium and high severity levels; and
- ρ_{LMH} and β_{LMH} for all severity levels.

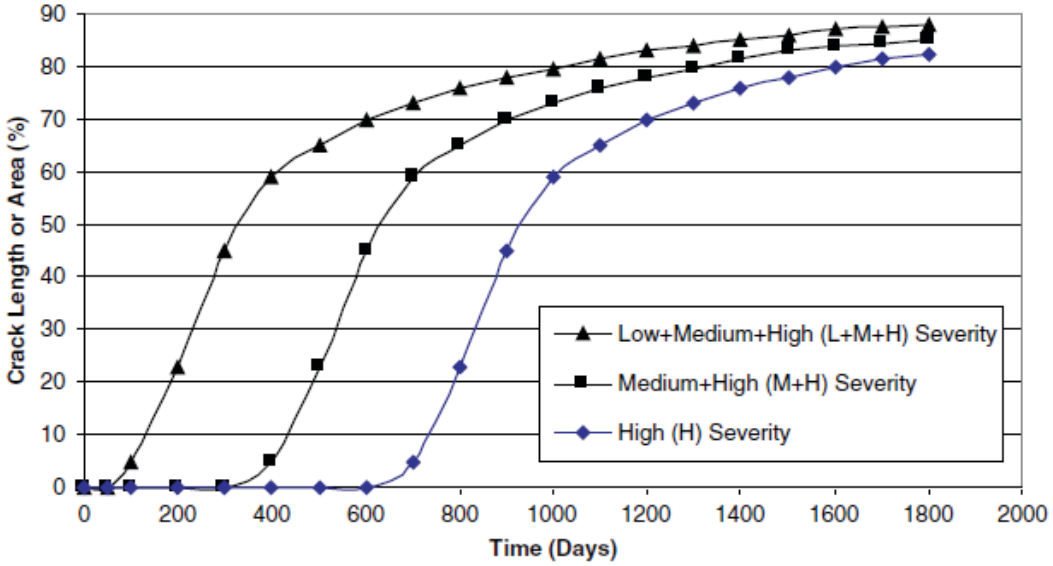

Courtesy of NCHRP (see Lytton et al. 2011).

Figure 3.42. Typical development of reflection crack by severity level.

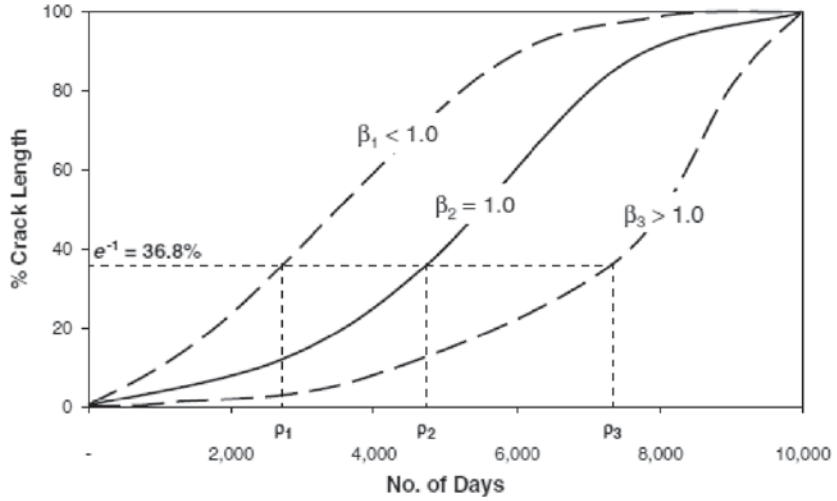

Courtesy of NCHRP (see Lytton et al. 2010).

Figure 3.43. Parameters in reflection cracking severity model.

Specifically,

$$\rho_{LMH} = N_{fB1}\left(\alpha_0 - \alpha_1\frac{N_{fB1}}{N_{fT1}} - \alpha_2\frac{N_{fB1}}{N_{fS1}}\right) + N_{fT2}\left(\alpha_3 - \alpha_4\frac{N_{fT2}}{N_{fS2}}\right) \quad (3.17)$$

$$\rho_{MH} = N_{fB1}\left(\alpha_5 - \alpha_6\frac{N_{fB1}}{N_{fT1}} - \alpha_7\frac{N_{fB1}}{N_{fS1}}\right) + N_{fT2}\left(\alpha_8 - \alpha_9\frac{N_{fT2}}{N_{fS2}}\right) \quad (3.18)$$

$$\rho_{H} = N_{fB1}\left(\alpha_{10} - \alpha_{11}\frac{N_{fB1}}{N_{fT1}} - \alpha_{12}\frac{N_{fB1}}{N_{fS1}}\right) + N_{fT2}\left(\alpha_{13} - \alpha_{14}\frac{N_{fT2}}{N_{fS2}}\right) \quad (3.19)$$

$$\beta_{LMH} = N_{fB1}\left(\beta_0 - \beta_1\frac{N_{fB1}}{N_{fT1}} - \beta_2\frac{N_{fB1}}{N_{fS1}}\right) + N_{fT2}\left(\beta_3 - \beta_4\frac{N_{fT2}}{N_{fS2}}\right) \quad (3.20)$$

$$\beta_{MH} = N_{fB1}\left(\beta_5 - \beta_6\frac{N_{fB1}}{N_{fT1}} - \beta_7\frac{N_{fB1}}{N_{fS1}}\right) + N_{fT2}\left(\beta_8 - \beta_9\frac{N_{fT2}}{N_{fS2}}\right) \quad (3.21)$$

$$\beta_{H} = N_{fB1}\left(\beta_{10} - \beta_{11}\frac{N_{fB1}}{N_{fT1}} - \beta_{12}\frac{N_{fB1}}{N_{fS1}}\right) + N_{fT2}\left(\beta_{13} - \beta_{14}\frac{N_{fT2}}{N_{fS2}}\right) \quad (3.22)$$

where

- α_0 through α_{14} are coefficients obtained through calibration, representing the scale factor ρ,
- β_0 through β_{14} are coefficients obtained through calibration, representing the shape factor β,
- N_{fB1} is the number of days for crack growth due to bending to reach Position I (see Figure 3.44),
- N_{fT1} is the number of days for thermal crack growth to reach Position I,
- N_{fS1} is the number of days for crack growth due to shearing stress to reach Position I,
- N_{fT2} is the number of days for thermal crack growth to go from Position I to Position II, and
- N_{fS2} is the number of days for crack growth due to shearing stress to go from Position I to Position II.

The number of days for crack growth is computed using fracture mechanics principles, particularly Paris and Erdogan's law for modeling crack propagation.

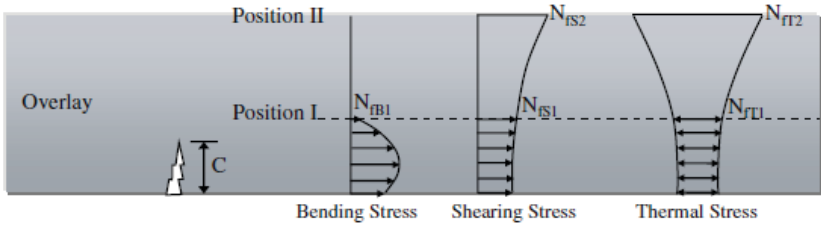

Courtesy of NCHRP (see Lytton et al. 2011).

Figure 3.44. Definition of number of days for crack growth.

$$N_f = \int_{c_0}^{h} \frac{dc}{A(\Delta K)^n} \quad (3.23)$$

where

c = crack length,
dc = incremental change in crack length
N_f = number of load cycles needed to propagate a crack of initial length c_0,
A and n = fracture properties of the asphalt mixture, and
ΔK = stress intensity factor (SIF) amplitude, which depends on the stress level, the geometry of the pavement structure, the fracture mode, and the crack length.

NCHRP Report 669 included the corresponding software that computes the various numbers of days for crack growth. The software uses artificial neural networks (ANN) to compute a finite element mechanistic-based SIF for thermal, bending, and shearing traffic stresses as a crack grows up through different thicknesses of HMA. Some key features of the SIF computed in the NCHRP study and the corresponding reflection cracking model include

- Use of a traffic load spectrum (similar to DARWin-ME) rather than total 18-kip equivalent single-axle loads (ESALs);
- Use of climatic data to calculate HMA temperature with depth below the surface (hourly air temperature, solar radiation, and surface reflectivity);
- Use of ANN to compute SIF;
- Stiffness, tensile strength, compliance, and fracture coefficients of the HMA mixture computed using the mixture properties, volumetric contents of the mixture components, aggregate gradation, and binder master curve characteristics;
- Healing shift factor that increases with the length of time between traffic loads;
- Computations of crack growth by each of the separate mechanisms (thermal, bending, and shearing) combined; and
- Calibration with field data.

NCHRP Report 669 includes software for design (used to predict/model reflection cracking) and also software for calibration (which computes the various number of days to crack growth that can be used to develop coefficients α_0 through α_{14} and β_0 through β_{14}, using Equations 3.17 through 3.22 and observed values of ρ_{LMH}, ρ_{MH}, ρ_H, β_{LMH}, β_{MH}, and β_H). The calibration software could not be used to calibrate HMA/PCC composite pavements because of insufficient time series reflection cracking data and a small number of sections. Use of the calibration software requires time series reflection cracking data to calculate ρ and β at various severity levels for each section and a sufficient number of sections per climatic zone (a minimum of 10, per NCHRP Report 669) to have a statistically valid model.

Because of the above limitation, the design software provided with NCHRP Report 669 was used to compare actual field performance with modeled performance. The design software was calibrated for HMA/JPC and HMA/CRC for only the wet freeze climatic zone using a relatively small number of sections (69 for HMA/JPC and 21 for HMA/CRC). A comparison of predicted versus measured reflection cracking for HMA surface courses for field survey R21 composite pavement sections is shown in Figure 3.45. In addition, the measured reflection cracking data are estimates based on field surveys (counts of number of joints that reflected through) and not precise measurements of actual lengths of reflection cracks.

The NCHRP Report 669 theory and models show promise for use in modeling reflection cracking in HMA/PCC composite pavements (Lytton et al. 2011). However, some caution is warranted for the following reasons:

- The models were calibrated for only a small number of sections in the wet freeze climatic zone.
- The research and models need to be vetted, verified, and validated for projects with various levels of traffic, with different materials, and in various locations (i.e., varying climatic and support conditions).
- There appear to be some bugs in the NCHRP Report 669 software, particularly with the use of appropriate calibration coefficients. The software should be incorporated into DARWin-ME and quality checks performed to ensure that the computations are being performed correctly.

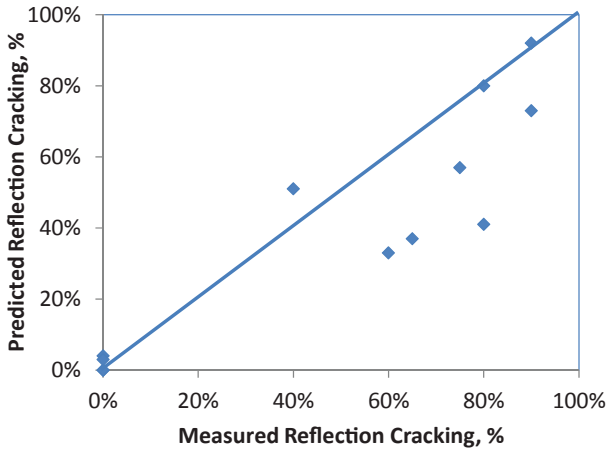

Source: Lytton et al. 2011.

Figure 3.45. Predicted versus measured reflection cracking for HMA surface courses for field survey R21 composite pavement sections in the wet freeze climatic zone using the NCHRP Report 669 software.

Reflection Cracking Control Strategies

Two strategies that are extremely effective in controlling the extent and severity of reflection cracking are (1) CRC (with adequate reinforcement) for the lower PCC and (2) sawing and sealing the HMA above the JPC joint.

Four other strategies that are less effective in controlling reflection cracking but that delay onset and minimize severity of reflection cracking include

1. Dowel bars (of sufficient diameter) at the JPC joints to provide adequate load transfer;
2. Additives (such as polymers) to the HMA;
3. Separator layers (such as asphalt rubber interlayers, fabrics and geotextiles, and geogrids) between the HMA and the JPC (particularly at the joint); and
4. Increased thickness of the HMA layer (not a particularly cost-effective option and one that is not recommended).

Use of CRC for the Lower PCC

Properly designed CRC layers (with adequate thickness and reinforcement to hold cracks tight) are very effective in controlling reflection cracking. The cracks in the CRC layer have high load transfer efficiencies and small differential deflections. In addition, because the cracks are spaced closely (typically less than 8 ft), the horizontal movements attributable to thermal movements also are minimal. All of this substantially reduces the strains in the asphalt layer, thus delaying and more often completely eliminating reflection cracking. This is also the experience of many states, such as Texas and Illinois, which have constructed continuously reinforced concrete pavements (CRCPs) and then overlaid them as part of maintenance and rehabilitation.

Field surveys of HMA/CRC composite pavements in Virginia, Illinois, Oregon, and Europe show no reflection transverse cracks. A special mention is the HMA/CRC composite pavement on I-10 in San Antonio, Texas, which had no reflection transverse cracking after 25 years of heavy traffic (see Chapter 2). The only section with reflection transverse cracking surveyed was the 0.5-in. ARFC over 13-in. CRC section on I-10, west of Phoenix, Arizona. However, this section had wide crack openings and major loss of load transfer efficiency because of low steel content and thus was not adequately designed (with respect to percent steel). The small amount of reflection cracking for HMA/CRC pavements is also predicted in the NCHRP Report 669 model, an example of which is shown in Figure 3.46. The figure shows less than

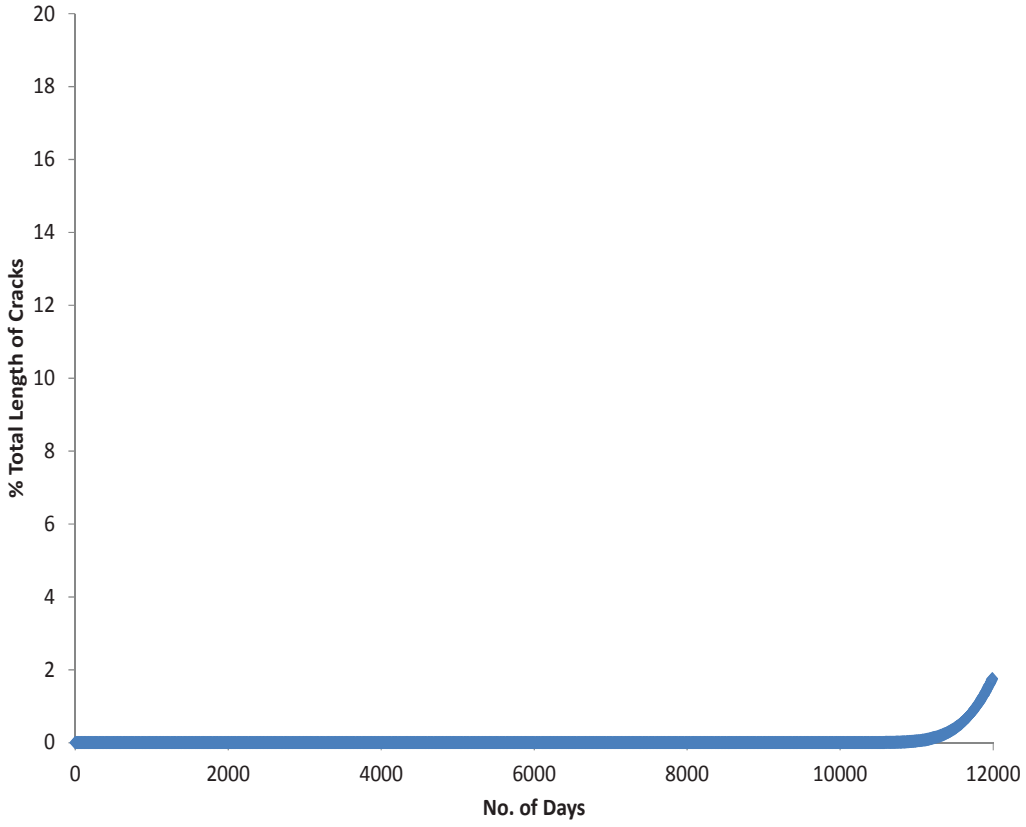

Source: Lytton et al. 2011.

Figure 3.46. NCHRP Report 669 software predicted cracking for HMA/CRC in Illinois.

2% reflection cracking length for a section in Illinois, even after 30 years.

Saw and Seal the HMA Above the JPC Joint

In 2007, Mallela and Von Quintus investigated several new HMA/JPC composite pavements as part of an experimental study to determine cost-effective materials and methods to minimize reflection cracks in the Queens borough of New York City. The as-constructed experimental plan includes the following variables:

- JPC joint spacing (two levels, 15 ft and 20 ft) saw and seal;
- Petrotac fabric (two levels differentiated by placement);
- Paveprep fabric;
- ISAC fabric; and
- Glasgrid (two levels).

Control sections without any treatments were also built for each of the two different joint spacings as baseline references. Evaluations, in the form of visual condition surveys and falling weight deflectometer (FWD) surveys, were conducted to monitor the performance of these sections. Performance was measured in terms of crack initiation, crack length, and crack severity, as well as load transfer deterioration across reflection cracks. The time history of reflection crack development as a percentage of total joint length is shown in Figure 3.47 and Figure 3.48 for the 20-ft sections and 15-ft sections, respectively. The figures show varying levels of performance for the various reflection crack treatments, all of which performed better than the control section. The sawed and sealed sections had far superior performance (both in terms of extent and severity) compared with all other sections, but particularly compared with the control sections. This was also observed during the R21 field survey of composite pavements. Sections in Columbus, Ohio, where the cracks are sealed (or are routed and sealed) immediately after they first come through, showed good performance. At MnROAD, the sawed and sealed joints on the R21 HMA/JPC section have performed well after 1 year of heavy traffic. Most of the control joints that were not sawed and sealed have reflected through and can be expected to deteriorate over time.

CalME Models for Rutting and Reflection Cracking

As an alternate to using the NCHRP 9-30A models for rutting and NCHRP 1-41 models for reflection cracking, as part of R21 research, the CalME models for rutting and reflection cracking were evaluated for HMA/PCC composite pavements. Details of this analysis are included in Appendix P.

Structural Modeling

The pavement sections described in Chapter 2 provide an extensive data set from which to perform structural modeling and compare model performance with field performance. For these sections, data were collected for each of the inputs to the DARWin-ME software. Inputs were measured or estimated at all levels (1, 2, and 3). Each HMA/JPC, HMA/RCC, and HMA/CRC was modeled in DARWin-ME, and the accumulated fatigue damage of the PCC slabs was computed over the service life of the pavement.

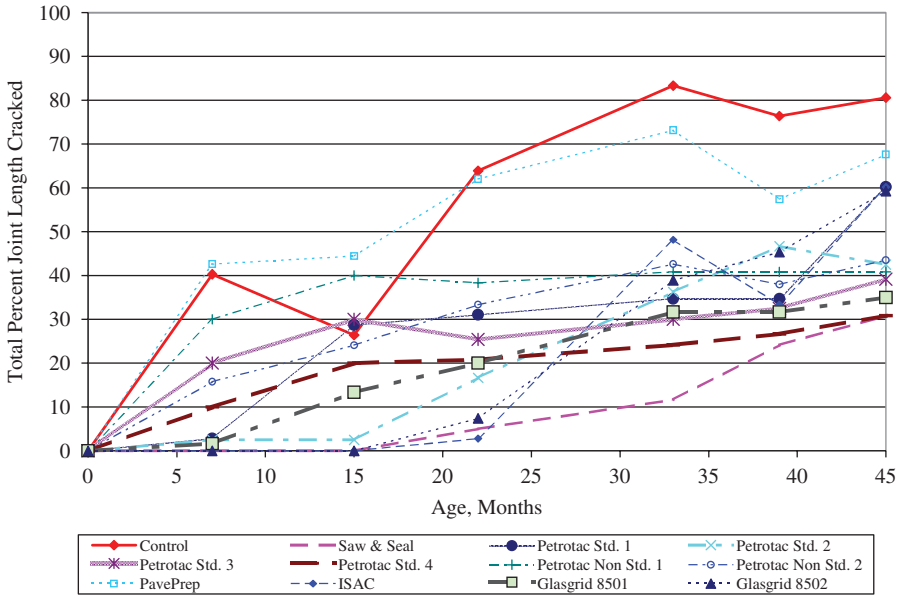

Figure 3.47. Time history of reflection crack development as a percentage of total joint length for the 20-ft sections (Joint Series 1 through 12).

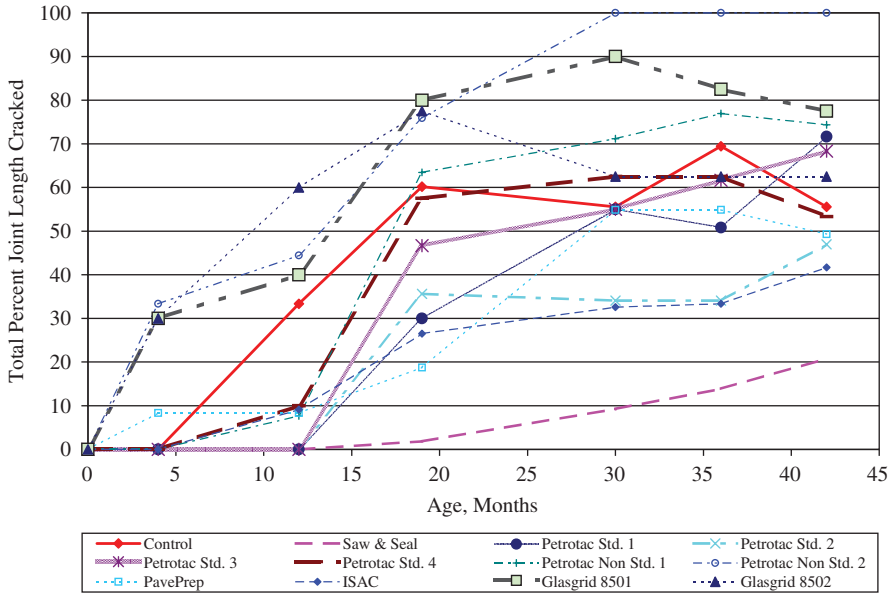

Figure 3.48. Time history of reflection crack development as a percentage of total joint length for the 15-ft sections (Joint Series 13 through 24).

HMA/JPC and HMA/RCC Sections

Tables 3.15 through 3.22 summarize the measured and predicted transverse fatigue cracking results for all HMA/JPC and HMA/RCC sections. The extent of transverse fatigue cracking was measured in units of percent slabs cracked transversely as reflected through the HMA surface course. Some observations of the results are as follows:

- Very few HMA/JPC or HMA/RCC composite pavements had any transverse fatigue cracking, even under very heavy traffic. Only a few experimental sections with a relatively thin slab (e.g., 5 in. to 6 in.) showed any fatigue cracking. Virtually no longitudinal cracking was observed.
- The fatigue damage is calculated on the top and bottom of the PCC slab. For these composite pavements, most of the damage occurred in the bottom of the slab. Very little top-down damage was computed. This is not the typical phenomenon that occurs in bare JPC pavements, where top-down cracking often dominates. This change is attributable to the reduced thermal gradients in the slab (thermal and moisture insulation of the slab) as modeled by DARWin-ME and validated through field measurements at UCPRC and MnROAD (described earlier in this chapter). The thicker the HMA surfacing, the lower the amount of top-down fatigue damage.
- A plot of accumulated fatigue damage versus measured transverse slab cracking is shown in Figure 3.49 for all of the HMA/JPC and RCC pavements. The figure also includes the current DARWin-ME bare JPCP calibration curve. The figure shows that the composite pavement damage curve follows the calibration curve of bare JPCP developed in 2007 using hundreds of sections under NCHRP Project 1-40. This is a validation of the JPCP fatigue cracking model and also suggests that the Enhanced Integrated Climatic Model (EICM) programmed into DARWin-ME automatically, correctly, and sufficiently accounts for the reduction in thermal gradients in the PCC attributable to the HMA layer.

The fact that the composite HMA/JPC fatigue cracking follows the bare JPCP damage calibration curve means that this same curve (and corresponding calibration coefficients) can be used for structural design of composite pavement. Note that this does not mean that a composite pavement will be the same thickness for the same reliability and cracking criteria. This will depend on the thickness of the HMA surface, among other factors. It only means that modified calibration factors are not required in DARWin-ME to use it for design of HMA/JPC or jointed RCC composite pavement.

HVS Testing Slab Cracking at UCPRC

Two test sections (613HB and 614HB) were loaded using the HVS until the PCC slab beneath the HMA layer failed structurally (cracked), as described in the analysis of field data at UCPRC section of this chapter. The structural failure was noted based on the slab and joint deflections and resulted in reflection cracking through the HMA layer soon after (see Figure 3.50 and Figure 3.51).

(text continues on page 102)

Table 3.15. Summary of the Arizona HMA/JPC Composite Pavement Sections Design, Traffic, Climate, and Measured/Predicted Structural Performance

Section, Location	Climate	No. of Trucks/Time on Composite Lane	HMA/JPC Year Construction, Joint Spacing, Dowels	Transverse Midpanel Fatigue Cracks	Comments
Arizona, I-10 AZ-3 (01-86) Tucson, Arizona	Dry Nonfreeze	20 million/9 years	1-in. ARFC/14.5-in. JPC, 2002, 13–17 ft, dowels	Predicted: 0% Measured: 0%	Transverse joint reflection cracks low severity, rutting minor
Arizona, I-10 AZ-4 (02-24) California/ Arizona state line	Dry Nonfreeze	11 million/6 years	1-in. ARFC/13-in. JPC, 2004, 13–17 ft, dowels	Predicted: 0% Measured: 0%	Transverse joint reflection cracks low severity, rutting minor
Arizona, I-10 AZ-5 (92-39) 100 miles west of Phoenix	Dry Nonfreeze	20 million/17 years	1-in. ARFC/14-in. JPC, widened slab, 1994, 13–17 ft, dowels	Predicted: 0% Measured: 0%	Transverse joint reflection cracks low severity, rutting minor
Arizona, L-101 AZ-6 (98-159) Phoenix	Dry Nonfreeze	5 million/9 years	1-in. ARFC/11.5-in. JPC, 2002, 13–17 ft, no dowels	Predicted: 0% Measured: 0%	Transverse joint reflection cracks low severity, rutting minor
Arizona, L-202 AZ-7 (03-06) Phoenix	Dry Nonfreeze	0.6 million/5 years	1-in. ARFC/13-in. JPC, 2005, 13–17 ft, no dowels	Predicted: 0% Measured: 0%	Transverse joint reflection cracks low severity, rutting minor
Arizona, I-40 AZ-8 (04-68) Flagstaff	Wet Freeze	5 million/3 years	1-in. ARFC/14-in. JPC, 2007, 13–17 ft, dowels	Predicted: 0% Measured: 0%	Transverse joint reflection cracks low severity, rutting minor
Arizona, US-93 AZ-9 LTPP Northwest Arizona	Dry Nonfreeze	3.4 million/13 years	1-in. HMA/15-in. RCC, 1993, no dowels	Predicted: 0% Measured: 0%	Transverse joint reflection cracks, low severity, rutting minor

Table 3.16. Summary of the Ontario HMA/JPC Composite Pavement Sections Design, Traffic, Climate, and Measured/Predicted Structural Performance

Section, Location	Climate	No. of Trucks/Time on Composite Lane	HMA/JPCP Year Construction, Joint Spacing, Dowels	Transverse Fatigue Cracks	Comments
Ontario, Hwy 401 ONT-1 Scarborough/ Pickering	Wet Freeze	18 million/13 years	Rehabilitation and widening, 1-in. Open-graded friction course (OGFC), 1.6-in. HMA, 10-in. JPC, 15 ft, dowels	Predicted: 0% Measured: 0%	All transverse joints reflected through
Ontario, Hwy 401 ONT-2 Scarborough/ Pickering	Wet Freeze	21 million/14 years	Rehabilitation and widening,1-in. OGFC, 1.6-in. HMA, 10-in. JPC, 15 ft, dowels	Predicted: 0% Measured: 0%	Predicted estimates measured well
Ontario, Hwy 401 ONT-3, Toronto	Wet Freeze	14 million/5 years	Rehabilitation and widening, 1.6-in. SMA, 2-in. HMA, 9-in. JPC, 15 ft, dowels	Predicted: 0% Measured: 0%	Predicted estimates measured well
Ontario, Hwy 401 ONT-3, Toronto	Wet Freeze	15 million/5 years	Widening, 1.6-in. SMA, 2-in. HMA, 9-in. JPC, 15 ft, dowels	Predicted: 0% Measured: 0%	Predicted estimates measured well
Ontario, Hwy QEW ONT-4, Toronto	Wet Freeze	27 million/16 years	Widening, 1.5-in. DFC, 1.5-in. HMA, 10-in. JPC, 15 ft, dowels	Predicted: 0% Measured: 0%	Predicted estimates measured well

Table 3.17. Summary of South Carolina, North Carolina, Illinois, Washington, and Germany HMA/JPC Composite Pavement Sections

Section, Location	Climate	No. of Trucks/ Time on Composite Lane	HMA/JPCP Year Construction, Joint Spacing, Dowels	Transverse Fatigue Cracks	Comments
South Carolina, I-77 SC-1, south of Charlotte	Wet Nonfreeze	2 million/ 10 years	Widening, 2 inner lanes, 1-in. Open graded. HMA, 4-in. HMA, 10-in. JPC, 15 ft joint spacing, no dowels	Predicted: 0% Measured: 0%	Predicted estimates measured well
Illinois, I-294 Illinois Tollway-1, Chicago	Wet Freeze	30 million/ 19 years	Widening outside lane (from 3 to 4 lanes), 3.5-in. HMA over 12.5-in. JPC, 20-ft joint spacing, HMA shoulder. Milled original HMA in 2001 and 3-in. new HMA placed	Predicted: 0% Measured: 0%	Predicted estimates measured well
Washington, I-5, Seattle	Wet Nonfreeze	Initial period: 5 million/ 13 years Full period: 30 million/ 45 years	Original composite pavement, 4-in. HMA and 6-in. JPC in 1966, assume 15-ft joint spacing, HMA shoulder. 1.8-in. HMA overlays in 1979, 1995, and 2006	Initial 13-year period predicted: 0% Full 40-year period predicted: 0% (1966–2006) Measured: 0% at either point	Predicted estimates measured well for initial period and over long term
North Carolina, I-40 Raleigh	Wet Nonfreeze	4.4 million/ 5 years	Widening, 0.625-in. Novachip, 3-in. HMA, 11-in. JPC, 18-, 19-, 21-, and 27-ft joint spacing	Predicted: 0% Measured: 0%	Predicted estimates measured well
Germany, A93, Munich	Wet Freeze	47 million/ 13 years	Original composite, 1.2-in. SMA, 10-in. JPC, 16.4-ft joint spacing, dowels	Predicted: 0% Measured: 0%	Reflection cracking of all joints, medium severity

Table 3.18. Summary of the Ohio HMA/JPC Composite Pavement Sections Design, Traffic, Climate, and Measured/Predicted Structural Performance

Section, Location	Climate	No. of Trucks/ Time on Composite Lane	HMA/JPCP Year Construction, Joint Spacing, Dowels	Transverse Fatigue Cracks	Comments
Ohio, White Road, Columbus COLOH01	Wet Freeze	70,000/7 years	3-in. HMA, 8-in. RCC, 45-ft joint spacing, no dowels	Predicted: 0.1% Measured: 0%	Predicted estimates measured well
Ohio, Hoover Road, Columbus COLOH02	Wet Freeze	400,000/8 years	3-in. HMA, 8-in. JPC, 20-ft joint spacing, no dowels	Predicted: 0.1% Measured: 0%	Predicted estimates measured well
Ohio, Lane Avenue, Columbus COLOH03	Wet Freeze	270,000/9 years	1.5-in. HMA, 8-in. RCC, 30-ft joint spacing, no dowels	Predicted: 13.7% Measured: 10%	Predicted estimates measured well
Ohio, Buckeye Parkway, Columbus COLOH04	Wet Freeze	100,000/10 years	3-in. HMA, 8-in. JPC, 20-ft joint spacing, no dowels	Predicted: 0% Measured: 0%	Predicted estimates measured well
Ohio, McCutcheon Crossing Drive, Columbus COLOH05	Wet Freeze	42,000/9 years	3-in. HMA, 7-in. JPC, 18-ft joint spacing, no dowels	Predicted: 0% Measured: 0%	Predicted estimates measured well
Ohio, Route 161 Franklin County OH01	Wet Freeze	2.4 million/ 11 years	3-in. HMA, 8-in. JPC, 15-ft joint spacing, dowels	Predicted: 0% Measured: 0%	Predicted estimates measured well

Table 3.19. Summary of New York HMA/JPC Composite Pavement Sections

Section, Location	Climate	No. of Trucks/ Years on Composite Lane	HMA/JPCP Year Construction, Joint Spacing, Dowels	Transverse Fatigue Cracks	Comments
New York, NY-1 Jamaica Avenue, New York City	Wet Freeze	0.3 million/4 years	3-in. HMA, 9-in. JPC, 20-ft joint spacing, no dowels, no reflection crack control	Predicted: 0% Measured: 0%	Predicted estimates measured well
New York, NY-2 Jamaica Avenue, New York City	Wet Freeze	0.3 million/4 years	3-in. HMA, 9-in. JPC, 20-ft joint spacing, saw and seal joints, no dowels	Predicted: 0% Measured: 0%	Predicted estimates measured well
New York, NY-3 Jamaica Avenue, New York City	Wet Freeze	0.3 million/4 years	3-in. HMA, 9-in. JPC, 15-ft joint spacing, no dowels, no reflection crack control	Predicted: 0% Measured: 0%	Predicted estimates measured well
New York, NY-4 Jamaica Avenue, New York City	Wet Freeze	0.3 million/4 years	3-in. HMA, 9-in. JPC, 15-ft joint spacing, saw and seal joints, no dowels	Predicted: 0% Measured: 0%	Predicted estimates measured well

Table 3.20. Summary of LTPP Sections in Wyoming, California, North Dakota, and Ontario, Canada, HMA/JPC Composite Pavement Sections

Section, Location	Climate	No. of Trucks/Time on Composite Lane	HMA/JPCP Year Construction, Joint Spacing, Dowels	Transverse Fatigue Cracks	Comments
California, CA-1, US 101, del Norte County	Wet Nonfreeze	5.7 million/25 years	4.2-in. HMA, 6-in. LCB, no joints (assume 15-ft spacing, which is mean transverse crack spacing), no dowels	Predicted: 1% Measured: 0%	Predicted estimates measured well
North Dakota, ND-1 (LTPP-2) US 2, Grand Forks County	Dry Freeze	1.1 million/11 years	2.4-in. HMA over 6.3-in. LCB (assume 15-ft spacing, which is mean transverse crack spacing)	Predicted: 39% Measured: 30%	Predicted estimates measured well
Wyoming, WY-1 (LTPP-3), Route 387, Campbell County	Dry Freeze	1.7 million/16 years	3.2-in. HMA over 11-in. JPC (assume 15-ft spacing, which is mean transverse crack spacing)	Predicted: 0% Measured: 0%	Predicted estimates measured well
Wyoming, WY-2 (LTPP-4), Route 59, Campbell County	Dry Freeze	1.4 million/9 years	4.2-in. HMA over 10.6-in, JPC (assume 20-ft spacing, which is mean transverse crack spacing)	Predicted: 0% Measured: 0%	Predicted estimates measured well
Ontario, ONT-5, (LTPP-5), HWY 402	Wet Freeze	5.4 million/23 years	3.2-in. SMA, 7.4-in, JPCP, 15-ft joint spacing, no dowels	Predicted: 0% Measured: 0%	Reflection cracking of all joints

Table 3.21. Summary of MnROAD HMA/JPC Composite Pavement Sections Design, Traffic, Climate, and Measured/Predicted Structural Performance

Section, Location	Climate	No. of Trucks/Time on Composite Lane	HMA/JPCP Year Construction, Joint Spacing, Dowels	Transverse Fatigue Cracks	Comments
Minnesota, I-94 MnROAD Site, R21 project site	Wet Freeze	Outer: 600,000/1 year Inner: 70,000/1 year	Original composite 2010 3-in. HMA, 6-in. JPC (RCA) (with and without dowels), 15-ft joint spacing, HMA shoulders	Predicted: 0% Measured: 0%	Transverse joints. reflection cracking: doweled: low non-doweled: medium
Minnesota, I-94 MnROAD site, pooled fund site	Wet Freeze	1.0 million/2 years	Original composite 2009 2-in. HMA, 5-in. JPC (with and without dowels), 15-ft joint spacing, HMA shoulders	Outer Predicted: 52% Measured: 45% Inner Predicted: 6% Measured: 10%	Section structurally failed in 2 years

Table 3.22. Summary of HMA/JPC and HMA/RCC Composite Pavement Fatigue Damage and Cracking

AC/JPC Section	Composite Type	Age (years)	Trucks (millions)	Accumulated Damage	Measured Transverse Crack (%)	Predicted Transverse Crack (%)
AZ-3	ARFC/JPC	9	20.0	6.00E-03	0.0	0.0
AZ-4	ARFC/JPC	6	11.0	1.46E-02	0.0	0.0
AZ-5	ARFC/JPC	17	20.0	6.40E-03	0.0	0.0
AZ-6	ARFC/JPC	9	5.0	5.70E-03	0.0	0.0
AZ-7	ARFC/JPC	5	0.6	1.30E-03	0.0	0.0
AZ-8	ARFC/JPC	3	5.0	1.54E-02	0.0	0.0
GER-1	SMA/JPC	13	47.0	1.38E-02	0.0	0.0
OH-1	AC/JPC	11	2.4	1.00E-04	0.0	0.0
ONT-1	AC/JPC	13	18.0	1.00E-06	0.0	0.0
ONT-2	AC/JPC	14	21.0	1.00E-06	0.0	0.0
ONT-3	AC/JPC	5	14.0	1.00E-06	0.0	0.0
ONT-4	AC/JPC	16	27.0	1.00E-06	0.0	0.0
SC-1	AC/JPC	9	1.6	1.00E-06	0.0	0.0
ILToll-1	AC/JPC	19	30.0	1.00E-06	0.0	0.0
WA-1	AC/JPC	13	5.3	1.00E-04	0.0	0.0
WA-1	AC/JPC	45	30.0	7.00E-04	0.0	0.0
NC-1	AC/JPC	5	4.4	1.00E-06	0.0	0.0
MN-1	AC/JPC[a]	1	0.2	4.60E-03	0.0	0.0
MN-2	AC/JPC[b]	1	0.6	9.90E-03	0.0	0.0
MN-3	AC/JPC[a]	3	0.3	2.48E-01	10.0	6.0
MN-4	AC/JPC[b]	3	1.0	1.05E+00	45.0	52.0
NYC-1	AC/JPC	4	0.3	3.00E-04	0.0	0.0
NYC-2	AC/JPC	4	0.3	3.00E-04	0.0	0.0
NYC-3	AC/JPC	4	0.3	1.00E-07	0.0	0.0
NYC-4	AC/JPC	4	0.3	1.00E-07	0.0	0.0
CA-1	AC/LCB	25	5.7	1.01E-01	0.0	1.0
ND-1	AC/LCB	11	1.1	7.92E-01	20.0	39.0
WY-1	AC/CTB	16	1.7	1.00E-05	0.0	0.0
WY-2	AC/CTB	9	1.4	1.10E-03	0.0	0.0
ONT-5	AC/JPC	23	5.4	7.20E-03	0.0	0.0
COLOH01	AC/RCC	10	0.1	3.30E-02	0.0	0.1
COLOH02	AC/RCC	8	0.4	2.22E-02	0.0	0.1
COLOH03	AC/RCC	9	0.3	4.00E-01	10.0	14.0
COLOH04	AC/RCC	10	0.1	9.40E-02	0.0	0.9
COLOH05	AC/RCC	9	0.0	1.40E-02	0.0	0.0
AZ-9	AC/RCC	13	3.4	1.00E-06	0.0	0.0

[a] Inside lane.

[b] Outside lane.

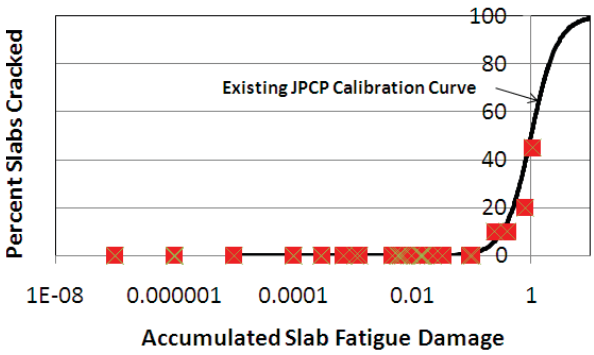

Figure 3.49. Fatigue damage versus measured transverse fatigue cracking (midslab) for all HMA/JPC or HMA/RCC composite pavements over their service life compared with existing JPCP calibration curve (derived in 2007 and used in the current version of DARWin-ME).

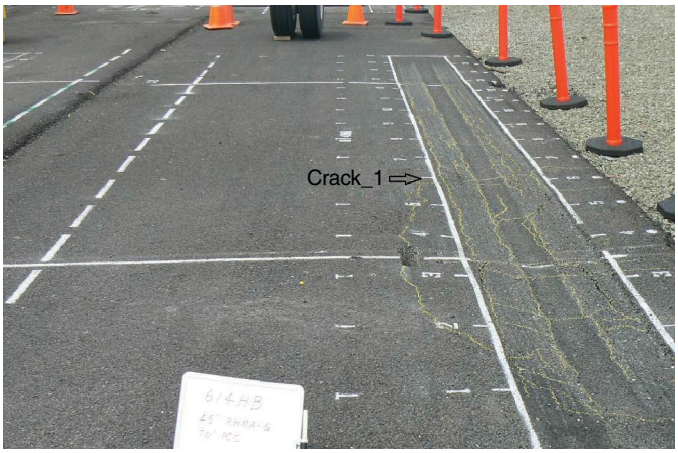

Figure 3.51. Structural failure of PCC slab beneath the HMA layer, followed by reflection cracking through the HMA layer, for Section 614HB at UCPRC.

(*continued from page 97*)

The two cells tested are identical in construction, except for the HMA thickness. Both cells are 5-in. (125-mm) nondoweled PCC with 15-ft joint spacing. Section 613HB has a 2.5-in. (64-mm) RHMA-G layer over the PCC slab, whereas Section 614HB has a 4.5-in. (114-mm) RHMA-G layer over the PCC slab. The loading sequences for the two sections are shown in Table 3.6 and Table 3.7, respectively. Based on data collected from the deflection sensors, the PCC in Section 613HB is believed to have structurally failed after approximately 195,000 load repetitions (14,400 repetitions of pavement response evaluation stage at 6,700, 9,000, and 13,500 lb, followed by 85,600 repetitions at 9,000 lb, and 95,000 repetitions at 13,500 lb). The PCC in Section 614HB is believed to have structurally failed after a total of approximately 320,000 load repetitions (14,400 repetitions of pavement response evaluation stage at 6,700, 9,000, and 13,500 lb, followed by 85,600 repetitions at 9,000 lb, 100,000 repetitions at 13,500 lb, 100,000 repetitions at 18,000 lb, and 20,000 repetitions at 23,500 lb). All loads were half-axle, dual-wheel loads, as described previously and detailed in Appendix K.

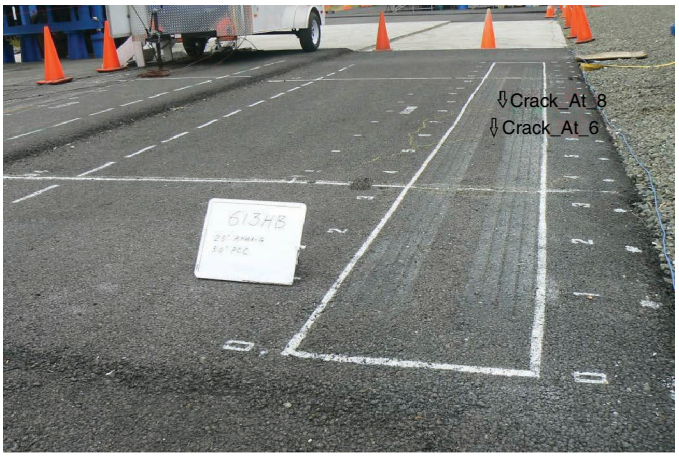

Figure 3.50. Structural failure of PCC slab beneath the HMA layer, followed by reflection cracking through the HMA layer, for Section 613HB at UCPRC.

Design files were created for DARWin-ME to match closely the climate, load, structure, and materials for the two HVS test sections. The results of the DARWin-ME runs for the two sections are shown in Figure 3.52 and Figure 3.53. Figure 3.52 shows DARWin-ME–predicted cumulative damage as 1.2 and 0.8 at observed failure for Sections 613HB and 614HB, respectively. The PCC slabs at the two test sections cracked after approximately 195,000 and 320,000 load repetitions, respectively. All fatigue damage and midpanel transverse cracking predicted by DARWin-ME is bottom-up, whereas the predicted top-down damage is close to zero. This is because the upward curling of the slab is substantially reduced due to the HMA layer above the PCC and because of the loading configuration used. Figure 3.53 shows DARWin-ME–predicted probability of slab cracking as 56% and 40% at observed failure for Sections 613HB and 614HB, respectively. The PCC slabs at the two test sections cracked after approximately 195,000 and 320,000 load repetitions, respectively. The two figures show excellent correspondence between DARWin-ME–predicted cumulative damage and probability of slab cracking versus actual field-observed slab cracking.

HMA/CRC Sections

There are seven HMA/CRC composite pavements in the R21 database. The design, performance, and prediction of these sections are summarized in Table 3.23. These sections were

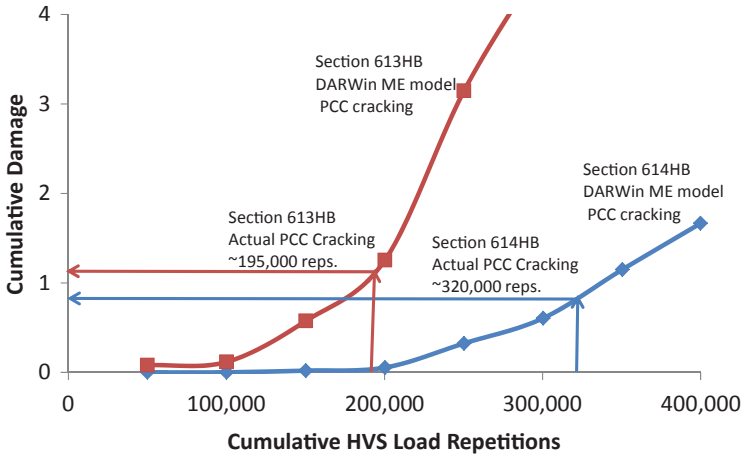

Figure 3.52. DARWin-ME–predicted cumulative damage for UCPRC test sections 613HB and 614HB versus cumulative load repetitions.

analyzed using DARWin-ME, and selected results are shown in Table 3.24. The results are summarized as follows:

- DARWin-ME cannot predict reflection cracks through the HMA surface, but it does predict the CRC crack width and load transfer efficiency over time. For six of these HMA/CRC sections, the cracks were predicted to be very tight (e.g., <0.020 in.) over the pavement life and to have very high load transfer efficiency (>90%). The field surveys revealed that none of these sections showed any reflection cracks over time periods ranging from 4 to 25 years (with an average of 10 years). The number of heavy trucks in the lane under consideration varied from 1 to 25 million, with an average of 11 million. The one section that showed considerable reflection cracking in the field was the 0.5-in. ARFC surface over CRC on I-10 in Arizona. DARWin-ME predicted excessively wide cracks and major loss of load transfer efficiency after 16 years because of low steel content and 20 million trucks.
- DARWin-ME predicts structural edge punchouts of CRC through a plot of measured punchouts/mile versus cumulated fatigue damage, as shown in Figure 3.54. A summary of the fatigue damage calculated for each section is shown in Table 3.24. This relationship initially was established in 2004 and revised in the 2007 update to the DARWin-ME. This curve represents data from several hundred CRC projects throughout the United States for the latest 2007 calibration. The seven HMA/CRC sections are also plotted on the graph to determine if the composite pavements generally follow the national calibration. The results show that these sections fit reasonably into the scatter of data from the national CRCP calibration, so it appears the

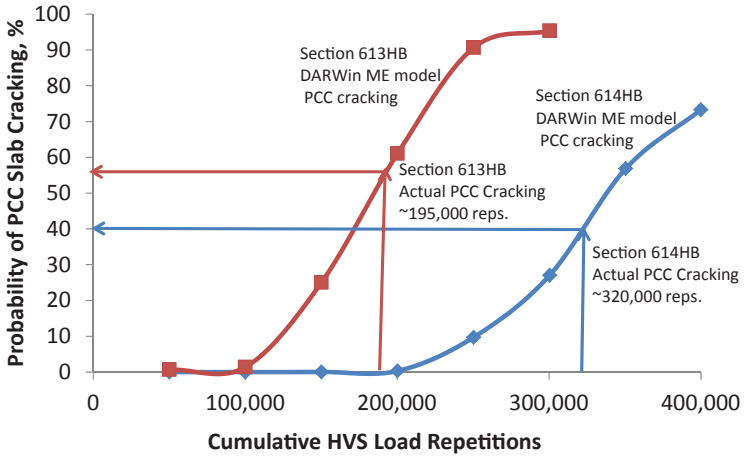

Figure 3.53. DARWin-ME–predicted probability of PCC slab cracking for UCPRC test sections 613HB and 614HB versus cumulative load repetitions.

Table 3.23. Summary of the HMA/CRC Composite Pavement Sections' Design, Traffic, Climate, and Measured/Predicted Performance

Section, Location	Climate	Trucks/Years on Composite Lane	HMA/CRCP, Year Construction	Transverse Shrinkage Cracks	Punchout and Fatigue Damage	Comments
AZ-1 (92-39) I-10 westbound, 90 miles west of Phoenix, Arizona	Dry Nonfreeze	20 million, 16 years	0.5-in. ARFC, 13-in. CRC, both 1994	Measured: 80% reflected Wide cracks, Poor LTE	Measured: 20/mile Predicted: 5/mile	Performance predicted well (crack width and LTE) but low for punchouts
AZ-2 (7079) Loop 101 Phoenix, Arizona	Dry Nonfreeze	2.6 million, 5 years for composite; 7 million, 21 years CRCP	1.0-in. ARFC (2005), 9-in. CRC (1989)	Measured: 0% reflected Tight cracks, 100% LTE	Measured: 0/mile Predicted: 0/mile	Performance predicted well
TX-1 Texas I-10 San Antonio, Texas	Wet Nonfreeze	24 million, 25 years	4-in. HMA, 12-in. CRC, both 1986 widening	Measured: 0% reflected tight cracks, 100% LTE	Measured: 0/mile Predicted: 0/mile	Performance predicted well
IL-2 Illinois I-64 north of St. Louis	Wet Freeze	1.4 million, 5 years	4.5-in. HMA, 8-in. CRC, both 2006 widening	Measured: 0% reflected tight cracks, 100% LTE	Measured: 0/mile Predicted: 0/mile	Performance predicted well
OR-1 Oregon I-205 Portland, Oregon	Wet, Nonfreeze	5.2 million, 4 years	2.0-in. porous HMA (2007), 8-in. CRC (1968)	Measured: 0% reflected Tight cracks, 100% LTE	Measured: 0/mile Predicted: 0/mile	AC overlay on older CRCP in good condition
VA-1 Virginia I-64 Richmond, Virginia	Wet, Freeze	1.7 million, 5 years	4.5-in. HMA, 8-in. CRC, both 2006 widening	Measured: 0% reflected Tight cracks, 100% LTE	Measured: 0/mile Predicted: 0/mile	Performance predicted well
The Netherlands A12, west of Utrecht	Wet, Freeze	19 million, 13 years	2.0-in. porous HMA, 10-in. CRC, both 1998	Measured: 0% reflected Tight cracks, 100% LTE	Measured: 0/mile Predicted: 0/mile	Excellent performance over 13 years

Note: LTE = load transfer efficiency.

Table 3.24. Summary of HMA/CRC Composite Pavement Fatigue Damage and Cracking

AC/CRC Section	Composite Type	Age (years)	Trucks (millions)	Accumulated Damage	Measured Punchouts (per mile)	Predicted Punchouts (per mile)
NL-A12	HMA/CRC	13	19.3	1.13E-06	0.0	0.0
AZ-1	ARFC/CRC	16	20.0	6.72E-01	20.0	5.0
AZ-2	ARFC/CRC	21	7.4	7.00E-05	0.0	0.0
TX-1	HMA/CRC	25	24.0	1.00E-07	0.0	0.0
IL-1	HMA/CRC	5	1.4	1.00E-07	0.0	0.0
VA-1	HMA/CRC	5	1.7	1.00E-07	0.0	0.0
OR-1	HMA/CRC	4	5.2	1.94E-04	0.0	0.0

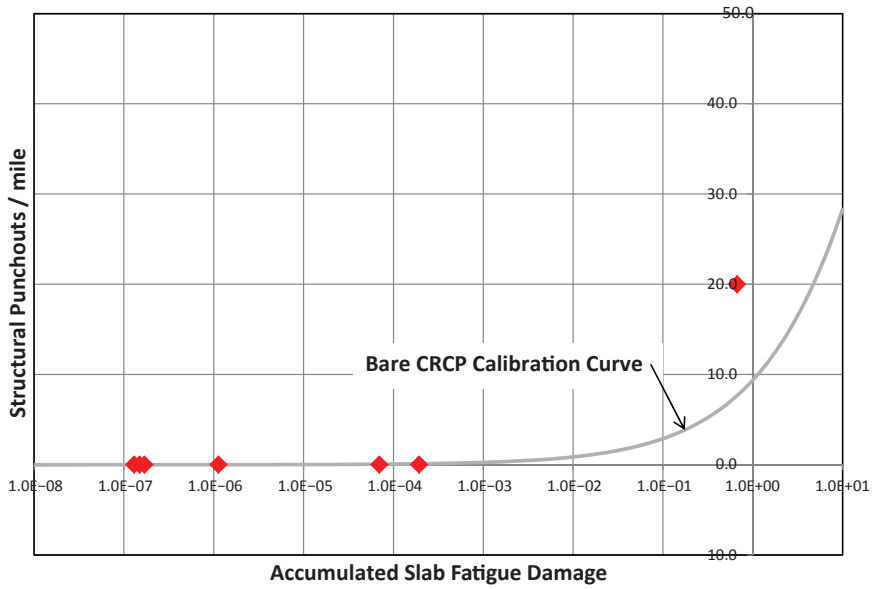

Note: The DARWin-ME bare CRCP (national) calibration curve is shown for comparison.

Figure 3.54. Plot of fatigue damage versus measured punchouts per mile for HMA/CRC projects in the R21 database.

national calibration of CRCP can be used for HMA/CRC composite pavement.

DARWin-ME predicted well the performance of transverse shrinkage cracks in the CRC for the composite HMA/CRC pavements in the database. Thus, the conventional criteria for CRCP design of crack width and load transfer efficiency should be used for new HMA/CRC composite pavements.

Functional Performance

Functional performance analysis of the database sections includes analysis of smoothness as measured using the International Roughness Index (IRI). Figure 3.55 shows the change in IRI over time for all sections included in the R21 database. The smoothness of these pavements over time is quite exceptional. The mean increase in IRI per year was 0.56 in./mi. Of course, if the surface deteriorates it can be replaced rapidly, and a very smooth surface can be obtained that typically would last for more than 10 years. DARWin-ME predicts IRI for composite pavements using empirical equations for both HMA/JPC and HMA/CRC. The predicted IRI is a function of the following for HMA/JPC composite pavements: initial IRI, transverse slab (midpanel) reflection cracking, transverse joint reflection cracking, and site factor that depends on age, subgrade percent fines, plasticity index (PI), and freezing index.

The predicted IRI is a function of the following for HMA/CRC composite pavements: initial IRI, punchout reflected through the asphaltic surface, and site factor that depends on age, subgrade percent fines, PI, and freezing index.

The IRI predicted using DARWin-ME is plotted versus the measured IRI for all of the composite pavement sections

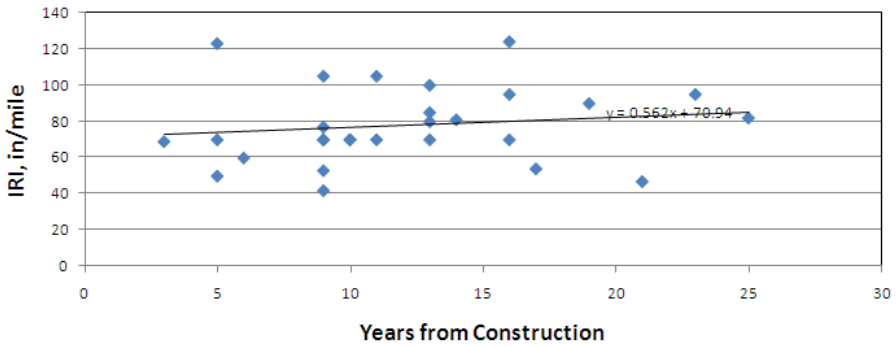

Figure 3.55. IRI over time for all composite pavements in the R21 database.

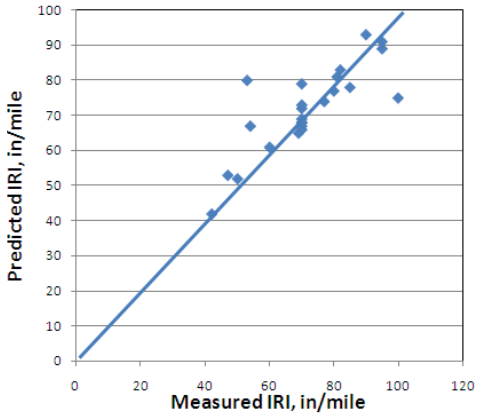

Figure 3.56. Plot of predicted versus measured IRI for HMA/JPC and HMA/CRC composite pavements.

where there were data available, as shown in Figure 3.56. The one-to-one line shows that predicted IRI is reasonably close to measured IRI for these sections; however, some overprediction is apparent. This likely will be remedied if the updated rutting and reflection cracking models described previously are incorporated into DARWin-ME.

Summary of Analysis and Performance Modeling

A detailed summary of information for HMA/JPC and RCC and HMA/CRC was prepared. A structural and functional analysis was conducted to show how these types of composite pavements have performed. Each section was modeled using the latest version of the DARWin-ME software and the results analyzed and plotted in many ways. Major findings are summarized below:

- Although HMA/JPC, HMA/RCC, or HMA/CRC composite pavements have not been constructed extensively, some states, Canadian provinces, and cities have built a variety of projects ranging from very heavily traveled interstate truck routes to low-volume collector types of streets. A large sample of these pavements was included in the R21 database, providing an excellent source of information for designers to become acquainted with this type of pavement.
- The structural performance of these composite pavements has been exceptional in terms of minimal structural fatigue damage. Many of these pavements are long-life pavements that likely will last more than 50 years and require only the replacement of the thin asphaltic surfacing over time.
- The functional performance of these composite pavements has been exceptional in terms of minimal rutting and ride quality over time. The rates of increase in rutting and IRI were very low, as averaged over all of the composite pavements.
- Bottom-up area fatigue cracking and longitudinal top-down fatigue cracking in the wheelpath, typically observed in flexible pavements, are virtually nonexistent in HMA/PCC composite pavements because the HMA is almost always in compression. These pavements also exhibit improved long-term ride quality and noise because of the elimination of contribution to IRI and tire-pavement noise from HMA wheelpath fatigue cracking.
- As the surface eventually deteriorates from raveling and/or reflection cracking, it can be removed and replaced rapidly using the latest technology for thin asphaltic or other surfaces over a structurally sound concrete slab. This will provide a very smooth surface with other desirable qualities, such as low noise and high friction, for many years to come.
- The HMA layer reduces temperature and moisture gradients (both magnitude and nonlinearity) in the PCC slab. The effect of this is a reduction in slab curvature and related load and thermal stresses. The reduction is substantial enough to dramatically increase structural capacity for the same PCC thickness. Alternatively, the PCC thickness can be reduced by 1 to 3 in., depending on factors such as traffic, climate, support conditions, material properties, and so forth, to have an equivalent structural capacity as compared with a bare PCC pavement.
- Although not modeled in DARWin-ME, the reduction in temperature gradients and slab curvature (particularly upward curling) is expected to reduce longitudinal cracking and corner breaks. None of the HMA/PCC sections surveyed exhibited any structural longitudinal cracking or corner breaking.
- Increasing thickness of the HMA layer increases structural capacity but not to the same extent as increasing PCC thickness. Increasing the thickness of the HMA layer also delays onset of reflection cracking. However, a consequence of increasing HMA thickness is an increase in the amount of rutting.
- The HMA mixture and asphalt binder properties have a large effect on the extent of rutting in the HMA layers. However, because of the presence of the stiff PCC layer, the rutting in the sublayers beneath the PCC (base, subbase, and subgrade) is eliminated (as compared with conventional flexible pavements). Thus, the total rutting in HMA/PCC pavements is lower than that in conventional flexible pavements of equivalent thickness.
- The HMA mixture and asphalt binder properties also have an effect on the extent and severity of reflection cracking. The onset of reflection cracking can be delayed and the severity of reflection cracking reduced through proper design of the HMA mix.

- The insulating effects of the HMA layer result in smaller thermal movements (opening/closing) at the PCC joints. Thus, load transfer efficiency at PCC joints of HMA/JPC composite pavements can be expected to be higher than bare PCC pavements, which is beneficial for faulting performance. However, it is still recommended that the JPC be designed with respect to dowel diameter and faulting performance assuming a bare PCC pavement. Note that dowels also delay the onset and minimize the severity of reflection cracks.
- Proper design of the CRC layer (thickness and reinforcement percent) is crucial for long-term performance of HMA/CRC composite pavements. With adequate reinforcement, punchouts and reflection cracking are virtually zero over the life of the pavement. Only the HMA surface needs to be replaced periodically to address functional and durability issues (raveling, friction, and so forth).
- DARWin-ME can model composite pavements reasonably well in terms of structural performance and functional performance although there are some limitations with respect to rutting, reflection cracking, and IRI, as follows:
  - **PCC transverse fatigue cracking:** The calibration model for transverse fatigue cracking of bare JPCP used in the current DARWin-ME software was validated for use with new HMA/JPC and new HMA/RCC composite pavements (see Figure 3.49 and Figure 3.53).
  - **PCC punchouts:** The calibration model for edge punchouts of bare CRCP used in the current version of DARWin-ME was validated for use with new HMA/CRC composite pavements (see Figure 3.54).
  - **Rutting:** The rutting model included in the current version of DARWin-ME with the global calibration coefficients can be used to obtain reasonable predictions of rutting in HMA/PCC composite pavements. However, the updated NCHRP 9-30A research results are recommended to be implemented in DARWin-ME, after which the updated calibrations coefficients are recommended for use (see Figure 3.33). Ideally, Level 1 data should be used in DARWin-ME to model HMA/PCC composite pavements to improve predictive capabilities.
  - **Reflection Cracking:** The empirical DARWin-ME transverse joint reflection model for HMA/JPC was not found to predict adequately. It is not recommended for usage. Instead, a fully calibrated model based on the results reported in NCHRP Report 669 is recommended to be implemented in DARWin-ME and used with caution (see Figure 3.45). In addition, alternatives such as sawing and sealing the HMA above the PCC joints (or use of CRC for the PCC layer) are strongly recommended.
  - **IRI:** The IRI model appeared to be reasonable for composite pavements. However, the updated rutting and transverse joint reflection cracking models described earlier in this chapter are recommended, which will have some effect on the IRI models (see Figure 3.55 and Figure 3.56).

CHAPTER 4

HMA/PCC Design Guidelines

Guidelines and Design Procedure Using DARWin-ME

Design recommendations for using DARWin-ME to design HMA/JPC, HMA/RCC, and HMA/CRC are provided below:

1. **General use of DARWin-ME for composite pavements.**
   a. Design Type: Select "AC Overlay". Although a new composite pavement is being designed and not an overlay, this is the proper Design Type to select until a Design Type specifically for new composite pavement is added by AASHTO.
   b. Pavement Type:
      - Select "AC/JPCP" for AC/JPC and AC/RCC composite pavements.
      - Select "AC/CRCP" for AC/CRC composite pavements.
   c. Design Life: Select desired life of structural design until major rehabilitation is needed. Composite pavements are very appropriate to a long structural life, exhibiting little structural deterioration over many years. DARWin-ME can design pavements for a design life as long as 100 years. To design a "long-life" pavement, select a longer life of more than 40 years. The HMA surface can be replaced as needed, but the PCC slab will remain over the long design life with little structural fatigue damage or joint load transfer efficiency loss.
2. **Trial design: Select all design inputs for a trial design.** The unique inputs for a HMA/PCC composite pavement are as follows:
   a. Design reliability and performance for composite pavements. Note that these are the only distress and IRI performance outputs worth considering in design.
      - Design reliability should be based on traffic level of the highway. Higher traffic levels warrant higher reliability levels.
        1. Interstates, freeways, divided highways: 95% to 99%;
        2. Other highways and urban collectors/arterials: 90% to 94%; and
        3. Local residential and farm-to-market roads: 75% to 89%.
      - Structural fatigue cracking and punchouts:
        1. JPCP: 10% slabs (range, 5% to 15%) transverse fatigue cracking; and
        2. CRCP: 10 punchouts per mile (range, 5% to 15%).
      - Smoothness, Terminal IRI should be based on traffic level of the highway. Higher traffic levels warrant lower terminal smoothness levels.
        1. Interstates, freeways, divided highways: 150 in./mile;
        2. Other highways and urban collectors/arterials: 160 in./mile; and
        3. Local residential and farm-to-market roads: 175 in./mile.
      - Permanent deformation (rutting of HMA only, which is total also): This should be 0.50-in. mean wheelpath.
      - Joint faulting for bare JPCP comparisons: This should be 0.15 to 0.20 in.
      - Initial IRI: The initial IRI for HMA/PCC composite pavements can be very low because of the multiple layering of the pavement. Initial IRI values as low as 35 in./mile have been achieved, with routine values from 40 to 50 in./mile.
      - Type and thickness of HMA surface layer. The type depends on the design objectives. If reducing noise levels to a minimum is required, some type of porous asphalt surface can be used. Thickness should be the minimum possible to provide durability and surface characteristics desired for a given truck traffic and climate. In warmer weather locations, a thinner surfacing is feasible, such as 1 in., but for colder weather and heavier traffic, as much as 3 in. total may be required.
   b. Type (JPCP or CRCP) and thickness of the PCC layer. This is the load carrying capacity layer for the composite pavement. The trial design should start with a typical thickness used for bare pavement. Depending

on the thickness of the HMA surface, the slab thickness may be reduced by 1 to 3 in. of concrete.

c. Joint design for JPCP. Joint design includes joint spacing and joint load transfer.
   - Joint spacing is considered directly in the DARWin-ME analysis and affects transverse fatigue cracking as well as joint faulting. A shorter slab has two distinct advantages:
     1. Thinner slab to control cracking; and
     2. Less joint reflection cracking and deterioration through the HMA surface. For nondoweled joints, the shorter the joint spacing, the higher the joint load transfer efficiency, reducing the deterioration of the reflection crack.
   - Joint load transfer requirement is similar to bare JPCP design in that dowels of sufficient size are required to prevent erosion and faulting for any significant level of truck traffic. The greater the dowel diameter, the higher the joint load transfer efficiency and the more truck loadings the pavement can carry to the terminal level of faulting.
     1. Simplified dowel design: The dowel diameter should be at least ⅛ the slab thickness. For example, a slab thickness of 12 in. requires a dowel diameter of at least 1⅛ = 1.5 in. For exceptionally heavy truck traffic highways, it may be necessary to add 0.25-in. diameter.
     2. Use of DARWin-ME: DARWin-ME can be run with all the same inputs but without the HMA surface to calculate joint faulting. In this case, joint faulting should be limited to no more than 0.15 to 0.20-in. at the design reliability level to ensure sufficient joint LTE.
     3. Low-volume roadways, where dowels would not normally be used for bare JPCP, do not require dowels for composite pavement. This is true for residential or farm-to-market streets, where JPC or RCC is used as the lower layer. When dowels are not used, it is highly recommended to reduce the joint spacing to 10 ft to reduce reflection cracking severity and increase joint load transfer efficiency.
   - Joints can be formed with a single saw cut or for RCC formed with a knife edge and do not require filling or sealing.

d. Joint design for RCC. Joints should always be provided for RCC at spacing even shorter than for JPCP for reasons described previously (e.g., 10 ft is recommended). These joints will not have dowels and can be formed in various ways other than sawing. Joints do not require sealing or filling.

e. Reinforcement design for CRC. The reinforcement content should be similar to bare CRCP. All of the same crack spacing, long-term width, and long-term load transfer efficiency are applicable. The reinforcement design is provided in the DARWin-ME. If these recommendations are followed, HMA/CRC composite pavements have shown no reflection cracking over many years and with very heavy traffic.

f. Concrete slab recommendations. The formed concrete or roller compacted concrete to be used for the lower layer of an AC/PCC composite pavement can vary widely, as described here:
   - Typical concrete used in bare JPCP or CRCP can be used with no changes. There are no special requirements different from those for bare pavement.
   - Lower cost concrete based on local aggregates or recycled concrete. The strength, modulus of elasticity, CTE, and drying shrinkage of the concrete can be varied because it is a direct input to the DARWin-ME software.
     1. The MnROAD experimental AC/JPC clearly showed that properly recycled concrete from a local roadway can be used for the lower layer.
     2. The MnROAD experiment AC/JPC also showed that a local aggregate source can be used successfully for the lower layer.
   - Both of these alternatives provide for substantial sustainability advantages and cost savings, yet show adequate durability. Certainly attention must be paid to good construction practices.

g. Base layer and other sublayers should be selected similar to bare JPCP or CRCP designs based on minimizing erosion, construction ease, and cost effectiveness. No attempts should be made to reduce the friction between the slab and the base because good friction is required to form joints in JPC/RCC and cracks in CRCP. Good friction also helps control erosion and pumping and reduces stress in the slab.

3. Design outputs interpretation

a. Run the trial design and examine the outputs. Note that although there are other DARWin-ME outputs, they should not be used for design at this time for HMA/PCC composite pavement.
   - JPCP and Jointed RCC: Transverse fatigue cracking, IRI, and HMA rutting must all meet the design reliability requirements for a trial design to be feasible.
   - CRCP: Edge punchouts, transverse crack width, transverse crack load transfer efficiency, IRI, and rutting must all meet the design reliability requirements for a trial design to be feasible.

b. If any of these do not "Pass" at the reliability level, a modification in the design is required. Some guidelines are as follows for making modifications:
   - Excess transverse cracking of JPC or jointed RCC slab: increase slab thickness, shorten joint spacing, add a

tied PCC shoulder or 1-ft widened slab, use a stabilized base course, increase PCC strength (with appropriate change in the modulus of elasticity), or use a different aggregate source (one with lower CTE).
- Excess punchouts for CRC: increase slab thickness, increase reinforcement content, use a tied PCC shoulder or 1-ft widened slab, use a stabilized base course, or use a different aggregate source (one with lower CTE).
- Excess rutting of HMA surface: modify binder grade; modify mixture parameters, such as as-built air voids and binder content; and reduce layer thickness. If these changes are not effective or acceptable, program a surface removal and replacement at the point of predicted rutting reaching the critical level.
- Excess IRI: reduce JPC or jointed RCC transverse cracking and HMA rutting, or require a smoother initial pavement. Composite pavements can be constructed with an exceptionally low initial IRI (e.g., 40 to 50 in./mile). Include incentive smoothness specifications with significant incentives so that the initial IRI is reduced. Smoothness incentives have been used with great success over several decades to improve initial IRI.

4. Other Joint Considerations

a. As described in Chapter 3, various options are available to design joints to control for reflection cracking in the HMA layer. In decreasing order of effectiveness, these include
   - Use CRC (with adequate reinforcement) for the PCC layer (instead of JPC). For JPC slabs, dowels can be used to provide load transfer at the joints and delay onset and minimize severity of reflection cracking.
   - Use sawed and sealed joints.
   - Use special additives (e.g., polymers) in the HMA mix to delay onset and minimize severity of reflection cracking.
   - Use reflection cracking treatment between PCC and HMA (such as asphalt rubber interlayers, fabrics and geotextiles, and geogrids).
   - Do nothing, which can be a viable option in certain climatic areas (e.g., dry nonfreeze) where historically reflection crack severity and deterioration are lower.

b. Bond breakers between the HMA and the PCC are not recommended because a good bond between the HMA and PCC is desirable to prevent other distresses.

c. Thicker HMA layer(s) to control or delay reflection cracking is not recommended because they typically do not justify the higher costs.

d. In all of these instances, it is desirable to route and seal or even just seal a reflection crack immediately after it reflects through the HMA to minimize and delay additional deterioration of the crack.

Illustrative Designs

Four different designs are provided below using the DARWin-ME procedure with recommended inputs and procedures for composite pavements:

1. HMA/JPC Composite Design for Interstate Highway—Tucson, Arizona.
2. HMA/JPC Composite Design for State Highway—Albertville, Minnesota.
3. HMA/RCC Composite Design for Local Street—Columbus, Ohio.
4. HMA/CRC Composite Design for Interstate Highway—San Antonio, Texas.

HMA/JPC Composite Design for Interstate Highway: Tucson, Arizona

a. Design reliability and performance requirements
   - Design life: 30 years.
   - $R = 95\%$.
   - Transverse slab cracking: 10% maximum.
   - Transverse joint faulting (bare JPCP): 0.20 in. Note that this requirement is specified to help control joint LTE to minimize reflection cracking severity. Start with minimum dowel diameter = slab thickness/8.
   - Rutting: 0.50 in.
   - IRI: 150 in./mile.

b. Materials
   - ARFC: Binder is rubber modified asphalt with equivalent grade of PG 70-22.
   - Concrete slab: Mean compressive strength is 5,000 psi; modulus of elasticity is 4.3 million psi.
   - Aggregate base course: Resilient modulus is 30,000 psi.

c. Site conditions
   - Traffic.
     1. Four lanes in each direction.
     2. Initial two-way average annual daily truck traffic (AADTT): 16,060 (directional distribution = 50%, lane distribution = 70%).
     3. Growth rate: 3% compound.
     4. Use Arizona specific DARWin-ME defaults for other traffic inputs.
   - Subgrade
     1. Subgrade soil survey revealed A-7-6 predominated.
     2. A subgrade "lab" resilient modulus is required at optimum moisture and density. To estimate this input, FWD testing was performed along the old existing pavement and the data used to backcalculate a modulus. An additional adjustment was made to convert from a field to a lab modulus and from in situ moisture to optimum moisture. The 1993 AASHTO

Design Guide, Part III Rehabilitation equation based on elastic layered analysis was used:

$$Es = 0.24\ P/(d \times S)$$

where

Es = elastic modulus of the subgrade (psi),
P = load on FWD (pounds),
d = deflection at spacing S from the loading plate (in.), and
S = spacing to outer sensor (in.), with a 60-in. sensor used.

The mean Es for this section is 29,702 psi. The subgrade elastic modulus, Es, is a field determined value at field moisture content and density. The Es must now be adjusted to the appropriate input resilient modulus for the DARWin-ME, which is a lab determined value at optimum moisture and density. This is accomplished by using a multiplier as follows that was obtained to adjust all of the backcalculated flexible pavement elastic modulus values in the national calibration.

Fine grained soil: 0.55; Coarse grained soil: 0.67.

Mean resilient modulus (M_R) was calculated as 29,702 × 0.55 = 16,336 psi. This is the appropriate input for the DARWin-ME. The value is not far from the default value for an A-7-6 soil of 13,000 psi given in the AASHTO *MOP*.

- Climate
  1. A virtual weather station was created for this site using the five closest stations.

d. Trial composite design
- Surface: Arizona uses 1 in. of ARFC surface for composite designs. This material is fairly porous.
- JPCP: A trial 10-in. slab will be evaluated first with a 15-ft joint spacing. Trial dowel diameter will be 10/8 = 1.25-in. for this thickness.
- Base: 4 in. of dense graded crushed stone will be used. This will be placed directly on the coarse grained prepared and compacted subgrade.

e. Output results for composite design:
- Total number of trucks in design lane in a period of 30 years: 97 million.
- Transverse cracking of JPCP: R > 95%: Pass.
- IRI: R > 95%: Pass.
- Rutting: R > 95%: Pass. Transverse joint faulting and load transfer efficiency check: DARWin-ME was run for a bare 10-in. JPCP with the same 1.25-in. dowels (and all other inputs the same). Results showed "Fail" (for a terminal level of 0.20 in., which is recommended for composite HMA/JPC design). The dowel diameter was increased to 1.5 in., and the result was Pass.

f. Final composite design: This design passes all of the requirements for slab fatigue transverse cracking, rutting, bare JPCP faulting (and thus, good joint load transfer efficiency), and IRI. All of the transverse joints are predicted to reflect through within 8 years. In addition, the thin ARFC surface likely will need to be removed and replaced after 10 to 20 years because of potential deterioration of the transverse reflection cracks and raveling of the material.
- Includes 1-in. ARFC.
- Includes 10-in. JPC with 1.5-in. diameter dowels.
- Includes 4-in. dense graded aggregate base.

g. Comparative bare JPCP design:
- Given the design obtained for the composite pavement, what would be an equivalent design for a bare JPCP at this location? DARWin-ME was run for the exact inputs as the composite design, and the design shown in Table 4.1 was required. These results show a substantial reduction in slab thickness (2 in.) and an untreated aggregate base, rather than an HMA base course.

Table 4.1. Equivalent HMA/JPC Composite Pavement and JPCP Designs Modeled Using DARWin-ME Designs for Interstate Highway: Tucson, Arizona

Design	ARFC/JPC Composite	JPCP
Surface	1-in. ARFC	None
JPC	H = 10 in. Dowels = 1.50 in.	H = 12 in. Dowels = 1.50 in.
Base	4-in. Untreated aggregate	4-in. HMA
Reliability	>95%	>95%

Note: H = PCC thickness.

HMA/JPC Composite Design for State Highway: Albertville, Minnesota

a. Design reliability and performance requirements
- Design life: 20 years.
- R = 95%.
- Transverse slab cracking: 10% maximum.
- Transverse joint faulting (bare JPCP): 0.20-in. Note that this requirement is specified to help control joint load transfer efficiency to minimize reflection cracking severity.
- Rutting: 0.50-in.
- IRI: 150 in./mile.

b. Materials
   - HMA: Binder is PG 64-34.
   - Concrete slab: Mean 28-day flexural strength is 677 psi and the modulus of elasticity is 4.9 million psi.
   - Aggregate base course: Resilient modulus is 18,000 psi.

c. Site conditions
   - Traffic.
     1. Two lanes in each direction.
     2. Initial two-way AADTT: 2,000 (directional distribution = 50%, lane distribution = 90%).
     3. Growth rate: 3% linear.
     4. Use site-specific DARWin-ME defaults for other traffic inputs.
   - Subgrade.
     1. Subgrade soil survey revealed A-6 predominated.
     2. A subgrade lab resilient modulus is required at optimum moisture and density. To estimate this input, FWD testing was performed along the old existing pavement and the data used to backcalculate a modulus. An additional adjustment was made to convert from a field to a lab modulus and from in situ moisture to optimum moisture. The 1993 AASHTO Design Guide, Part III Rehabilitation equation based on elastic layered analysis was used:

$$Es = 0.24\,P/(d \times S)$$

where

Es = elastic modulus of the subgrade (psi),
P = load on FWD (lb),
d = deflection at spacing S from the loading plate (in.), and
S = spacing to outer sensor (in.), with 60-in. sensor used.

The mean *Es* for this section is 13,660 psi. The subgrade elastic modulus, *Es,* is a field determined value at field moisture content and density. The *Es* must now be adjusted to the appropriate input resilient modulus for the DARWin-ME, which is a lab determined value at optimum moisture and density. This is accomplished by using a multiplier as follows that was obtained to adjust all of the backcalculated flexible pavement elastic modulus values in the national calibration.

Fine grained soil: 0.55; Coarse grained soil: 0.67.

Mean M_R was calculated as $13{,}660 \times 0.55 = 7{,}513$ psi. The mean dynamic *k*-value was 121 psi/in. This is the appropriate input for DARWin-ME. This value is about one-half of the default value for an A-6 soil of 14,000 psi given in the AASHTO *MOP.*

   - Climate.
     1. A virtual weather station was created for this site using the three closest stations.

d. Trial composite design
   - Surface: This composite design had a 3-in. HMA surface.
   - JPCP: A trial 6-in. slab will be evaluated first with a 15-ft joint spacing. Trial dowel diameter will be 1.25-in. minimum recommended.
   - Base: 8 in. of dense graded crushed stone will be used. This will be placed directly on the fine grained prepared and compacted subgrade.

e. Output results for composite design:
   - Total number of trucks in design lane in a period of 30 years: 8.4 million.
   - Transverse cracking of JPCP: $R > 95\%$: Pass.
   - IRI: $R > 95\%$: Pass.
   - Rutting: $R > 95\%$: Pass.
   - Transverse joint faulting and load transfer efficiency check: DARWin-ME was run for a bare 6-in. JPCP with the same 1.25-in. dowels (and all other inputs the same). Results showed Pass (for a terminal level of 0.20 in., which is recommended for composite HMA/JPC design).

f. Final composite design: This design passes all of the requirements for slab fatigue transverse cracking, rutting, bare JPCP faulting (and thus, good joint load transfer efficiency), and IRI. All of the transverse joints are to be sawed and sealed immediately after placement of the HMA surface. This will control reflection cracking severity along with high doweled joint load transfer efficiency. The HMA surface will likely need to be rehabilitated after 10 to 20 years because of various weathering problems that occur in this harsh climate.
   - 3-in. HMA. All transverse joints to be sawed and sealed after placement;
   - 6-in. JPC (recycled PCC from existing roadway) with 1.25-in. diameter dowels; and
   - 8-in. dense graded aggregate base.

g. Comparative bare JPCP design:
   - Given the design obtained for the composite pavement, what would be an equivalent design for a bare JPCP at this location? DARWin-ME was run for the exact inputs as the composite design, and the design shown in Table 4.2 was required. These results show a substantial increase in slab thickness (3 in.) and an increase in dowel diameter to 1.375 in.

HMA/RCC Composite Design for Local Street: Columbus, Ohio

The city of Columbus (and neighborhood suburbs such as Grove City) has constructed many residential, collector, and arterial composite pavements consisting of 2 to 3 in. of asphalt

Table 4.2. Equivalent HMA/JPC Composite Pavement and JPCP Designs Modeled Using DARWin-ME Designs for State Highway: Albertville, Minnesota

Design	HMA/JPC Composite	JPCP
Surface	3-in. HMA	None
JPC	H = 6 in. Dowels = 1.25 in.	H = 9 in. Dowels = 1.375 in.
Base	8-in. Untreated aggregate	8-in. Untreated aggregate
Reliability	>95%	>95%

Note: H = PCC thickness.

concrete over 6 to 8 in. of RCC. This design is for a typical collector street design.

a. Design reliability and performance requirements
   - Design life: 20 years.
   - $R = 85\%$.
   - Transverse slab cracking: 10% maximum.
   - Transverse joint faulting (bare JPCP): 0.2-in. Note that this requirement is specified to help control joint load transfer efficiency to minimize reflection cracking severity.
   - Rutting: 0.50 in.
   - IRI: 175 in./mile.

b. Materials
   - HMA: Binder is PG 64-34.
   - RCC slab: Test results were obtained from several RCC projects in the Columbus area, and the mean 28-day compressive strength was 5,000 psi. The RCC specified has concrete strength properties equal to or better than regular paving concrete.
   - Aggregate base course: Resilient modulus is 25,000 psi.

c. Site conditions
   - Traffic.
     1. Two lanes in each direction.
     2. Initial two-way AADTT: 150 (directional distribution = 50%, lane distribution = 90%).
     3. Growth rate: 3% linear.
     4. Use default DARWin-ME defaults for other traffic inputs.
   - Subgrade.
     1. Subgrade soil survey revealed A-7-6 predominated.
     2. A subgrade lab resilient modulus is required at optimum moisture and density. To estimate this input, FWD testing was performed along the old existing pavement and the data used to backcalculate a modulus. An additional adjustment was made to convert from a field to a lab modulus and from in situ moisture to optimum moisture.

        The 1993 AASHTO Design Guide, Part III Rehabilitation equation based on elastic layered analysis was used:

        $$Es = 0.24\,P/(d \times S)$$

        where
        - Es = elastic modulus of the subgrade (psi),
        - P = load on FWD (lb),
        - d = deflection at spacing S from the loading plate (in.), and
        - S = Spacing to outer sensor (in.), with 60-in. sensor used.

        The mean *Es* for this section is 15,152 psi. The subgrade elastic modulus, *Es,* is a field determined value at field moisture content and density. The *Es* must now be adjusted to the appropriate input resilient modulus for DARWin-ME, which is a lab determined value at optimum moisture and density. This is accomplished by using a multiplier as follows that was obtained to adjust all of the backcalculated flexible pavement elastic modulus values in the national calibration.

        Fine grained soil: 0.55; Coarse grained soil: 0.67.

        Mean M_R was calculated as $15{,}152 \times 0.55 = 8{,}334$ psi. The mean dynamic *k*-value was 317 psi/in. This is the appropriate input for the DARWin-ME. This value is about one-half of the default value for an A-7-6 soil of 13,000 psi given in the AASHTO *MOP.*
   - Climate.
     1. A virtual weather station was created for this site using the closest stations.

d. Trial composite design
   - Surface: Assume 2-in. HMA surface for this composite design. Every transverse joint will be sawed and sealed to control reflection cracking.
   - JPCP: A trial 6-in. slab will be evaluated first with a 15-ft joint spacing. The joints can be sawed or wet formed. No dowels will be used.
   - Base: 6 in. of dense graded crushed stone will be used. This will be placed directly on the fine grained prepared and compacted subgrade.

e. Output results for composite design:
   - Total number of trucks in design lane in a period of 30 years: 1.165 million.
   - Transverse cracking of JPCP: $R > 85\%$: Pass.
   - IRI: $R > 85\%$: Pass.
   - Rutting: $R > 85\%$: Pass.
   - Transverse joint faulting and LTE check: The DARWin-ME was run for a bare 6-in. JPCP with no dowels (and all other inputs the same). Results showed a reliability

Table 4.3. Equivalent HMA/RCC Composite Pavement and JPCP Designs Modeled Using DARWin-ME Designs for a Local Street: Columbus, Ohio

Design	ARFC/RCC Composite	JPCP
Surface	2-in. HMA	None
JPC	H = 6 in. No dowels	H = 9 in. No dowels
Base	6-in. Untreated aggregate	6-in. Untreated aggregate
Reliability	>85%	>85%

Note: H = PCC thickness.

level of 78%, which is a little less than the desired 85%. However, for this test, it is believed to be close enough for a low-volume design such as this.

f. Final composite design: This design passes all of the requirements for slab fatigue transverse cracking, rutting, bare JPCP faulting (and thus good joint LTE), and IRI. All of the transverse joints are to be sawed and sealed immediately after placement of the HMA surface. This will control reflection cracking severity. The HMA surface likely will need to be rehabilitated after 10 to 20 years because of various weathering problems that occur in this harsh climate
   - 2-in. HMA. All transverse joints to be sawed and sealed after placement;
   - 6-in. RCC (with formed joint spacing of 15 ft) and no dowels; and
   - 6-in. Dense graded aggregate base.

g. Comparative bare JPCP design:
   - Given the design obtained for the composite pavement, what would be an equivalent design for a bare JPCP at this location? The DARWin-ME was run for the exact inputs as the composite design and the design shown in Table 4.3 was required. These results show a substantial increase in slab thickness (3 in.), which must be balanced with the cost of a 2-in. HMA surface.

HMA/CRC Composite Design for Interstate Highway: San Antonio, Texas

a. Design reliability and performance requirements
   - Design life: 30 years.
   - $R = 95\%$.
   - Edge punchout: 10 per mile.
   - Transverse crack width: 0.020-in. maximum.
   - Transverse crack spacing: 3 to 6 ft.
   - Transverse crack load transfer efficiency: >85%.
   - IRI: 150 in./mile.

b. Materials
   - HMA surface course: binder PG 76-28.
   - HMA binder course: binder PG 76-28.
   - Concrete slab: mean flexural strength is 700 psi.
   - HMA base course: dense graded, binder PG 64-22.
   - Aggregate subbase course: resilient modulus is 30,000 psi.

c. Site conditions
   - Traffic.
     1. Four lanes in each direction.
     2. Initial two-way AADTT: 12,000 (directional distribution = 50%, lane distribution = 70%).
     3. Growth rate: 3% compound.
     4. Use DARWin-ME defaults for other traffic inputs.
   - Subgrade.
     1. Subgrade soil survey revealed that A-2-5 predominated.
     2. A subgrade lab resilient modulus is required at optimum moisture and density. No FWD deflection or lab testing was available, so the default mean resilient modulus provided in the AASHTO *MOP* was used. This value is 16,000 psi.
   - Climate.
     1. The San Antonio airport weather station was selected.

d. Trial composite design
   - Surface: 1.5 in. of HMA surface course and 1.5 in. of HMA binder course.
   - CRCP: A trial 11-in. slab will be evaluated first with a 0.70% steel for No. 6 rebars. Note that the crack LTE deteriorated toward the end of the design life, and thus 0.75% reinforcement was required.
   - Tied JPCP shoulders that will be placed and tied separately.
   - Base: 4 in. of dense graded HMA.
   - Subbase: 8 in. of crushed aggregate subbase, resilient modulus 30,000 psi.

e. Output results for composite design:
   - Total number of trucks in design lane in 30 years: 73 million.
   - Edge punchouts: $R > 95\%$: Pass.
   - Transverse crack spacing: 38 in.: Pass.
   - Transverse crack maximum width: 0.018 in.: Pass.
   - Transverse crack minimum LTE: >85%: Pass.
   - Rutting: $R < 95\%$: Not Pass. Rutting is predicted to exceed 0.50 in. at 18 years, at which time the HMA surface will need to be milled and replaced.
   - IRI: The IRI does not pass because of rutting. When the HMA surface is replaced because of rutting at 18 years, the IRI will begin anew.

f. Final composite design: This design passes all of the requirements for slab punchouts and transverse crack criteria for the 30-year design period. The HMA is predicted to exceed critical rutting at 18 years and will need to be replaced. This will renew the IRI at that time also.
   - 1.5-in. HMA surface course, 1.5-in. HMA binder course.
   - 11-in. CRCP with 0.75% longitudinal reinforcement.

Table 4.4. Equivalent HMA/CRC Composite Pavement and CRCP Designs Modeled Using DARWin-ME Designs for Interstate Highway: San Antonio, Texas

Design	ARFC/CRC Composite	Bare CRCP
Surface	1.5-in. HMA surface 1.5-in. HMA binder	None
CRC	H = 11 in. Reinforced = 0.75%, or Reinforced = 12 in.²/12 ft Tied JPCP shoulders	H = 13 in. Reinforced = 0.70%, or Reinforced = 13 in.²/12 ft Tied JPCP shoulders
Base	4-in. HMA	4-in. HMA
Subbase	8-in. Aggregate	8-in. Aggregate
Reliability	>95%	>95%
Future rehabilitation over 30 years	HMA surface replacement at 16 years	None

Note: H = PCC thickness.

- Tied JPCP shoulders that will be placed and tied separately.
- 4-in. dense graded HMA base.
- 8-in. dense graded aggregate subbase.

g. Comparative bare CRCP design:
Given the design obtained for the composite pavement, what would be an equivalent design for a bare CRCP at this location? DARWin-ME was run for the exact inputs and design as the composite design with two exceptions:
- The HMA surfacing was deleted.
- The percent by area reinforcement was reduced so that the reinforcement content of actual steel per 12 ft of lane cross section was held constant.

A bare CRCP thickness of 13 in. was required with 0.70% reinforcement to meet all the reliability and performance requirements, as shown in Table 4.4. This results in 2 in. of additional slab thickness and an increase in reinforcement quantity (an increase of approximately 10% in actual steel quantity), as shown above.

Summary of Illustrative Composite Pavement Designs

The following conclusions can be made regarding the results obtained for the composite designs and for comparative bare concrete pavement designs:

- The DARWin-ME design procedure, using the AC overlay of JPCP and CRCP, worked well with no problems to design a new composite pavement.
- The thickness of the composite slab layer is reduced from that required for a bare concrete pavement. For the CRC, the quantity of reinforcement across the lane is also reduced.
- These reductions may offset the increased cost of the various HMA surfaces. For the very heavily trafficked projects, the HMA surface will need to be replaced during the long design life.

Surfaces and slab thickness for comparable designs are summarized in Table 4.5.

Table 4.5. Summary of DARWin-ME Results for Illustrative Examples

Project	Traffic: Trucks in Design Lane, Analysis Period	HMA/PCC	Bare PCC
Interstate highway Tucson, Arizona	97,000,000, 30 years	1-in. ARFC/10-in. JPC (1.5-in. dowels)	12-in. JPCP (1.5-in. dowels)
State highway Albertville, Minnesota	8,400,000, 20 years	3-in. HMA/6-in. JPC (1.25-in. dowels)	9-in. JPCP (1.375-in. dowels)
Local street Columbus, Ohio	1,165,000, 20 years	2-in. HMA/6-in. RCC (no dowels)	9-in. JPCP (no dowels)
Interstate highway San Antonio, Texas	73,000,000, 30 years	3-in. HMA/11-in. CRC (0.75% reinforced) (reinforced = 12 in.²/12 ft)	13-in. CRCP (0.70% reinforced) (reinforced = 13 in.²/12 ft)

Table 4.6. Sensitivity Analysis (Showing Percentage Slabs Cracked) for Transverse Fatigue Cracking in HMA/JPC Composite Pavement in Minneapolis Climate

HMA Surface Thickness (in.)	JPC Slab Thickness (%)			
	5 in.	6 in.	7 in.	8 in.
1	100.0	92.0	32.5	0.0
2	98.7	26.0	0.2	0.0
3	84.9	0.2	0.0	0.0
4	15.5	0.0	0.0	0.0

Note: Design truck traffic over 20 years is 11 million.

Table 4.7. Sensitivity Analysis (Showing Percentage Slabs Cracked) for Transverse Fatigue Cracking in HMA/JPC Composite Pavement in Arizona Climate

HMA Surface Thickness (in.)	JPC Slab Thickness (%)			
	8 in.	9 in.	10 in.	11 in.
1	66.5	13.0	6.1	2.4
2	5.8	0.1	0.0	0.0
3	0.3	0.0	0.0	0.0
4	0.0	0.0	0.0	0.0

Note: Design truck traffic over 30 years is 97 million.

Sensitivity Analysis

Sensitivity analyses were conducted for composite HMA/JPC pavements and for a composite HMA/CRC pavement. The following key factors were varied and studied in the analysis:

- HMA surface thickness;
- JPC and CRC slab thickness;
- Number of heavy trucks; and
- Climate zones (Arizona, Minnesota, and Texas).

Minnesota. The Minnesota analysis was conducted using Example 2 detailed in the previous section. The climate is dry-freeze, and the truck traffic is about 0.5 million per year in the design lane. DARWin-ME was run over a factorial of HMA and JPC slab thicknesses. The key output evaluated is transverse fatigue cracking, which is the key structural load-carrying capacity distress. The results are summarized in Table 4.6 and shown in Figure 4.1.

Arizona. The Arizona analysis was conducted using Example 1 detailed in the previous section. The site is on I-10 in Tucson and is very heavily trafficked. The climate is dry-nonfreeze, and the truck traffic is about 3.2 million per year in the design lane. DARWin-ME was run over a factorial of HMA and JPC slab thicknesses. The key output evaluated is transverse fatigue cracking, which is the key structural load-carrying capacity distress. The results are summarized in Table 4.7 and Figure 4.2.

Texas. The Texas analysis was conducted using Example 4 in the previous section. The site is on I-35 in San Antonio and is heavily trafficked. The climate is generally wet-nonfreeze (but often is dry-nonfreeze), and the truck traffic is about 2.4 million per year in the design lane. DARWin-ME was run over a factorial of HMA and CRC slab thicknesses. The key output evaluated is edge punchouts, which is the key structural load-carrying capacity distress for CRC. The results are summarized in Table 4.8 and Figure 4.3.

The results of these sensitivity analyses show the following:

- Both HMA and PCC affect the load-carrying capacity of a composite pavement. The PCC layer is of course the primary structural layer and must be of sufficient thickness to prevent significant fatigue damage.

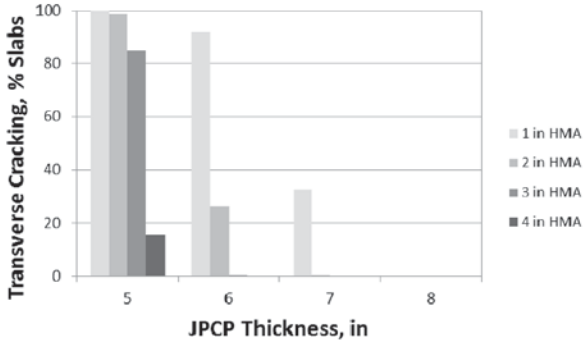

Figure 4.1. Sensitivity analysis showing effect of HMA surface and JPC slab thickness on transverse fatigue cracking for HMA/JPC composite pavement in Minnesota.

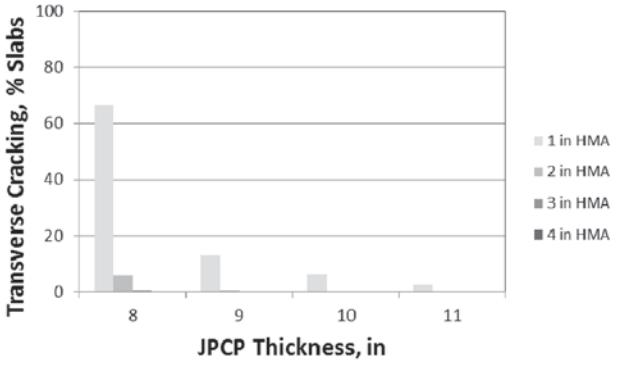

Figure 4.2. Sensitivity analysis showing effect of HMA surface and JPC slab thickness on transverse fatigue cracking for HMA/JPC composite pavement in Arizona.

Table 4.8. Sensitivity Analysis for Edge Punchouts (per Mile) in HMA/CRC Composite Pavement in San Antonio Climate

HMA Surface Thickness (in.)	CRC Slab Thickness (%)			
	8 in.	9 in.	10 in.	11 in.
1.5	27.6	7.3	2.2	0.0
3.0	4.3	1.4	0.5	0.0
4.5	1.0	0.5	0.1	0.0

Note: Design truck traffic over 30 years is 73 million.

- HMA surface thickness also has a significant effect on transverse fatigue cracking for thinner JPC and CRC slabs. Increasing HMA by 1 in. can sometimes have a very large effect on reducing fatigue damage. This impact is attributable to both the increased structure and the reduction in thermal and moisture gradients through the slab, resulting in reduced fatigue damage.
- JPC slab thickness has a very large effect on transverse fatigue cracking. Likewise, CRC slab thickness has a very large effect on punchouts. This layer must be designed with sufficient thickness to provide for long-term performance with minimal fatigue cracking.

Cost Analysis and Pavement Type Selection

New HMA/PCC composite pavements have not been constructed widely in the United States or in other countries. There are some exceptions, however, including the following applications:

- The most widely used application of HMA/PCC is widening of an existing PCC pavement or an existing HMA/PCC pavement, and it is desired to match layer types across the new traffic lanes. Many states have designed and built widening composite pavements, and these pavements have performed well.
- Arizona uses a thin, 1-in. ARFC over JPC and CRC to reduce tire-pavement noise levels in urban areas. The entire Phoenix freeway system was surfaced with ARFC beginning in 2003, and many of these were also new JPC segments. There are a number of ARFC/JPC sections on rural interstate highways that have been constructed since the early 1990s. This composite design has performed very well in Arizona.
- Ontario has built a number of new HMA/JPC composite pavements since the 1970s. However, none have been built in the past decade, with the exception of many widening projects of composite sections.
- Columbus, Ohio, New York, and several other cities have built HMA/RCC (jointed) or HMA/JPC composite pavements on urban residential, collector, and arterial streets.

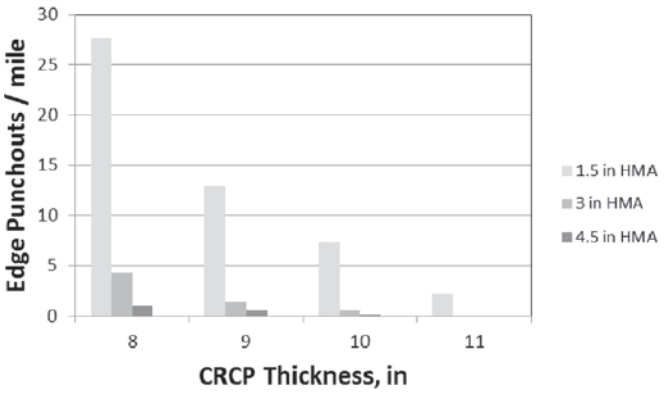

Figure 4.3. Illustration HMA surface and CRC thickness on edge punchouts for HMA/CRC composite pavement in Texas.

Although the performance of these pavements has been very good, few agencies consider them routinely in their pavement selection procedures. This may be due to the perception that they are more expensive to build than conventional HMA or PCC pavements. However, given the need to consider pavement alternatives that not only have long-term structural load carrying capacity but also excellent surface characteristics and that can be rapidly rehabilitated in the future, the interest in and use of HMA/PCC composite pavements may increase at both state and local highway agencies.

The information and technology assembled and developed under the SHRP 2 R21 project gives highway agencies much additional information related to HMA/PCC composite pavements:

- Performance of this type of composite pavement on interstates, other highways, and even lower-volume traffic urban streets;
- Validation of a rational M-E design procedure (DARWin-ME); and
- Construction guidelines and recommendations for building high-quality composite pavements.

This section of the report provides recommendations for pavement selection procedures and life-cycle cost analysis (LCCA) of HMA/PCC pavements. This information will help highway agencies to include composite pavements in their routine pavement selection process and to conduct the LCCA process properly. NCHRP Report 703 (Hallin et al. 2011) is recommended as a good process for addressing the selection process and the LCCA of composite pavements. Below is a

process that focuses on HMA/PCC composite pavements that follows closely the NCHRP report recommendations.

Step 1: Establish LCCA Framework

- **Analysis period.** The analysis period for HMA/PCC composite pavements should reflect the time over which the highway agency wants the pavement to perform without major structural damage at a high level of reliability. Well-designed SMA, HMA, porous HMA, WMA, Novachip, and ARFC surface courses last from 10 to 15 years or more before requiring replacement. Thus, over a long period of time there would be multiple renewings of these surfaces. However, the longer the HMA/PCC composite pavement is designed to exhibit low structural damage, the more cost-effective and sustainable it will be because small increases in structural design capacity result in long-term extension of fatigue damage. Of course, the design could be for only 20 years, but this would result in reduced cost competitiveness and sustainability benefits overall. Thus, a structural life of 40 years or even more is recommended. The HMA/PCC becomes essentially a long-life pavement with rapid surface renewal at intermediate times. One R21 section documented on I-5 in Washington State was constructed in 1966 and had received three surface rehabilitations (milling and overlay) in 45 years and still had several years of remaining life. This HMA/JPC composite pavement carried 30 million heavy trucks in the outer lane without a single slab replacement.
- **Discount rate.** Using the long-term real discount rate values provided in the latest edition of the Office of Management and Budget Circular A-94, Appendix C, is recommended.
- **Economic analysis technique.** The net present value (NPV) method using constant or real dollars and a real discount rate in computations is recommended.
- **LCCA computation approach.** There are two approaches to NPV analysis: deterministic and probabilistic. Either one could be used for HMA/PCC composite pavements. Estimation of the variabilities involved in the probabilistic approach is a major challenge. In either case, the service life must be estimated with sufficient accuracy, and for the probabilistic approach, the standard deviation and distribution also must be estimated. Recommendations for HMA/PCC composite pavement:
  1. **Service life (PCC layer structural life):** The R21 project analyzed HMA/JPC, HMA/RCC, and HMA/CRC composite pavements and found that they fit into the nationally calibrated DARWin-ME fatigue damage models for JPC or RCC and punchout models for CRC so that the prediction of structural life until the terminal level of cracking/punchouts is reached can be obtained from the DARWin-ME software output. The mean of 50% should be used as the estimate when it crosses the critical JPC cracking or CRC punchout limit. If this does not occur during the analysis period, the slab should be considered as having a long life and would have a significant remaining life at the end of the analysis period.
  2. **Service life (HMA layer functional life):** The R21 project showed examples of a number of HMA/PCC pavements that had performed from 9 to 25 years (typical life of 12 to 15 years), depending on climate and traffic. There are four main performance indicators that would result in terminal life for the thin HMA type of surface:
     - Reflection transverse cracking from joints: DARWin-ME cannot predict this because of a major deficiency in the model. However, the use of the saw and seal technique has been shown to perform far better than any other technique for mitigation of reflection cracks for thinner surfaces.
     - Rutting: The DARWin-ME models predicted rutting reasonably well for the thin surfaces. Rutting was rarely a problem for thin HMA surfaces.
     - IRI: The DARWin-ME models predicted IRI reasonably well for the thin surfaces as long as transverse reflection cracks did not deteriorate.
     - Raveling: This must be estimated by the local highway agency because it cannot be predicted. It is the main problem with permeable HMA or other types of mixtures.
  3. **Survival curves:** Often, the best way to estimate the mean service life of a pavement is to use survival analysis. This is particularly recommended for the thin HMA surface for use with HMA/PCC composite pavements. This requires a number of existing pavements in service that have performed for many years and thus may not be available for HMA/PCC composite pavements initially. The 50th percentile should be used as the mean life for the probabilistic approach.

Step 2: Estimate Initial and Future Costs

- *Initial construction costs.* This includes the cost of the pavement structure, including the HMA surface, PCC slab, and base and other embankment layers. Highway agencies routinely estimate these costs for construction. There are several special thin asphaltic surfaces that can be used for HMA/PCC composite pavements, including SMA, Novachip, porous HMA, dense HMA, and ARFC. These typically are built in different regions where highway agencies have specific goals, such as low noise, low splash

and spray, high friction, and very smooth surfaces. These all can be achieved routinely with thin surfaces.

- *Future rehabilitation and maintenance costs.* Future costs include the rehabilitation of the asphalt surface course through rapid removal and replacement, patching, or sealing with a special material.
- *Salvage costs.* Estimated cost of the pavement at the end of the design analysis period.
- *Initial and future highway (extra) user costs.* There are several components of extra highway user costs. The word "extra" is used to indicate that these are in excess of those obtained for smooth pavements because of increased roughness, accidents, and lane closures for maintenance and rehabilitation. The FHWA RealCost program includes estimates of most of these extra costs and reasonable procedures to estimate them. The timing of the thin asphaltic surface rehabilitation and its duration must be estimated.
- *Develop expenditure stream diagrams.* Basically, for HMA/PCC composite pavements, there will be the initial construction, future routine maintenance, and future rehabilitation of the surface layer (typically with removal and replacement with a better product at the time). An example is shown in Table 4.9, where the design analysis period is 40 years, and given the climate and traffic, the thin surfacing is expected to last 10 years. Some user delay and other user costs are expected every time lane closures are programmed, even if they are done during off-peak traffic hours.

Step 3: Compute Life-Cycle Costs

The FHWA RealCost program is convenient and efficient software for entering relevant life-cycle costs and computing NPV for a composite pavement. RealCost also computes highway user costs for project conditions. RealCost can use deterministic and probabilistic approaches for computing LCCA.

Step 4: Select Preferred Pavement Alternative

A composite pavement can be evaluated directly with conventional HMA or PCC pavement alternatives in terms of costs (NPV) and noneconomic selection factors. Although the NPV can be computed from all of the associated direct and indirect costs, it can be evaluated separately as follows:

- Initial construction cost;
- Highway user costs during initial construction;
- Future direct cost to highway agency for lane closures:
  - Maintenance;
  - Rehabilitation; and
  - Salvage.
- Future highway user costs during maintenance and rehabilitation lane closure activities; and
- Total costs NPV.

The noneconomic factors are important and include the following, as documented in NCHRP Report 703. In some cases, a composite pavement has advantages over conventional asphalt or concrete.

- Roadway/lane geometrics. HMA/PCC composite pavement may give the designer more options and flexibility when dealing with lane widths, shoulders, turning movements, and so forth, where the HMA surface can be striped differently than JPCP or CRCP.
- Continuity of adjacent pavements. If this is desired, then wherever the adjacent pavement is HMA or HMA/PCC, a HMA/PCC composite would be appropriate because the user would see the same type of surface.
- Continuity of adjacent lanes. When widening is being designed, it is usually good design practice to continue the widening with similar materials. When the existing pavement is old PCC or old HMA/PCC, then an HMA/PCC composite for the additional lanes has distinct advantages. The main advantage is ease to the driver in maintaining consistency across all lanes. There is also an advantage in connecting the existing and new traffic lanes together so that they will not separate and in providing a similar type of surface without the longitudinal joint failing from reflection cracking.
- Availability of local materials and experience. An HMA/PCC pavement can be built using recycled PCC from the

Table 4.9. Example of Expenditure Stream Table for Performing LCCA

Time, Years	0	5	10	15	20	25	30	35	40
User (U) $ Delay, etc.	0	$ U	$ U	$ U	$ U	$ U	$ U	$ U	0
Maintenance (M) $ Routine	0	$ M	$ M	$ M	$ M	$ M	$ M	$ M	0
Rehabilitation (R) $ Surface Layer	0	0	$ R	0	$ R	0	$ R	0	0
Initial (I) $ Salvage (SAL) $	$ I	0	0	0	0	0	0	0	$ SAL

existing or nearby old highway, or from a local pit with some types of substandard aggregates (such as softer aggregates susceptible to polishing). The SMA or HMA surfacing will take care of a smooth and durable surface for traffic.

- Conservation of materials/energy. HMA/PCC offers significant advantage in conservation of materials and energy.
- Local preference. As occurred in the Phoenix metropolitan area, the local preference called for a low noise surface, which led to an ARFC with low noise and a high degree of smoothness over the existing JPC (or in the case of newly constructed HMA/JPC).
- Stimulation of competition. An HMA/PCC composite pavement stimulates both the asphalt and concrete industries and is thus an excellent choice for this topic.
- Noise issues. HMA/PCC can be designed with porous HMA or ARFC that will provide very low noise levels for many years.
- Safety considerations. The thin HMA surfaces used for composite pavements can be designed to provide high friction and, by being somewhat porous, reduce the potential for hydroplaning.
- Experimental features. Building an HMA/PCC composite pavement with distinct experimental features may be a good way to get one built in a state or local highway agency. Special asphalt surfacing or base slab designs (e.g., CRC) are examples.
- Future needs. An HMA/PCC can be designed to have a very long structural life with only the removal and replacement of the thin surface every 10 to 20 years.
- Maintenance capability. It is relatively easy and rapid to remove and replace the thin surface over time as needed.
- Sustainability. HMA/PCC has several advantages over conventional pavements in terms of key sustainability issues:
  - The lower PCC layer can be designed for a very long fatigue damage life, such as 40 to 100 years with minimal fatigue cracking repair. This results in a concrete slab that will remain structurally sound over decades while requiring only that the thin asphaltic surface be removed and replaced every 10 to 20 years. Thus, there will be minimal if any full-depth slab replacements, which are very costly and require full days to perform.
  - The thin asphaltic surface can be replaced rapidly at off-peak hours every 10 to 20 years as needed due mainly to durability issues. The saw and seal technique for transverse JPC joints or the use of CRC with zero crack reflection is expected to extend the service life of these surfaces.
  - This renewal of the surface will provide excellent surface characteristics, including smoothness, low noise, good friction, and lower splash and spray for permeable surfaces.
  - This composite pavement design will thus reduce the number of lane closures over the long design life of the pavement. Reducing the number of lane closures has a major sustainability impact because of the reduction in emissions caused by the extra congestion caused by lane closures for maintenance and rehabilitation.
  - Reduction of the use of natural resources is another key for improved sustainability, as was done with recycled concrete in the lower PCC slab in the MnROAD R21 section. The existing concrete from I-94 was recycled as 50% of the coarse aggregate. There may be many projects for which such recycling of existing old PCC and old HMA/PCC pavements into the new composite pavement would result in a major reduction of the haul distances involved, which would result in lower energy use and costs. Of course, use of recycled concrete results in a savings of natural aggregates.
  - Increased use of fly ash in achieving a substantial reduction in portland cement content in the lower PCC slab. The lower layer of the I-94 composite section contained 60% fly ash replacement. This reduces the carbon dioxide emissions and improves the sustainability of construction.
  - There exist highways in certain states for which studded tire wear is the major cause of deterioration. A thin but durable wearing surface such as SMA could be used for an SMA/JPC or CRC composite pavement. The SMA could be replaced as it wears down from the studded tires, but the existing PCC would always be there, providing the load-carrying capacity.

Various methods are available for weighting economic and noneconomic factors. These include an alternative-preference screening matrix, as described in NCHRP Report 703.

Example Cost Comparison Project

A real-life project was prepared by the contractor on the MnROAD project for PCC/PCC composite pavement. No direct comparison was made for HMA/JPC. However, the resulting conclusions are believed to be the same regardless of the thin surface used. Both HMA/PCC and PCC/PCC top layers would have a higher cost, but the lower layer PCC was the same. A summary and conclusions are as follows for the PCC/PCC design.

The initial construction cost comparison between a 3-in. PCC over a 6-in. JPC composite pavement and a

one-layer 9-in. JPCP indicated approximately the same cost. The composite was actually 0.7% lower than the one-layer conventional.

The PCC/PCC example showed that, in the areas of the state in which Class A aggregates are not readily available or are very expensive, PCC/PCC composite paving is a viable alternative to conventional paving. The heavier the truck traffic, the thicker the lower layer of lower cost concrete would become and the greater the difference in cost between the conventional and the composite PCC/PCC pavement. Although this example was a case of having no readily available Class A concrete aggregates, it shows that it is possible for an alternative technique, such as composite paving, to compete essentially equally with the costs of a conventional paving process. The *MEPDG* performance prediction of both sections illustrates the ability of PCC/PCC to equal its single-layer JPCP structural equivalent in performance and service life.

The primary difference between the PCC/PCC and an HMA/JPC is that the life of the HMA surfacing is less than the high-quality PCC surface layer. This difference can be considered directly through life-cycle costing.

CHAPTER 5

HMA/PCC Construction Guidelines

Introduction

The construction of HMA/PCC composite pavements does not require any new technologies or equipment that is not already available in the United States. The key steps in the construction include

- Prepare the sublayers (including subgrade, subbase, and base courses);
- Place the PCC layer and tied shoulders (if specified):
  - For HMA/CRC construction, the steel reinforcement needs to be securely placed on chairs on top of the base course before the PCC layer is paved. The reinforcement depth for CRC should be at middepth of the PCC slab or higher as specified.
  - For HMA/JPC, dowels may be placed in dowel baskets that are securely attached to the base course before the PCC layer is paved. Alternatively, dowel bar inserters (DBIs) may be used. The dowels should be located at middepth of the PCC slab.
- Texture the PCC layer to provide a mechanical interlock with the HMA surface;
- Apply curing compound to the PCC layer;
- Saw cut joints in the PCC layer (for HMA/JPC composite pavements);
- Apply sufficient tack coat to the surface of the PCC layer (after PCC layer has hardened and gained sufficient strength to allow traffic on the PCC layer);
- Place the HMA layers;
- Place the shoulders. PCC shoulder must be tied to the traffic lanes, regardless of when they are placed; and
- Saw and seal the HMA at the location of the transverse and longitudinal PCC joints (for HMA/JPC composite pavements).

Guidelines for each of these steps are provided below. Sample specifications are included in Appendix W for PCC construction, HMA construction, texturing, curing, saw cutting, and sealing.

Construction Details

Prepare the Sublayers

The uniformity of the support conditions beneath an HMA/PCC pavement is critical for the long-term performance of the pavement, just as is in the case of bare PCC pavements. For the purposes of preparing the sublayers, there is no difference between an HMA/PCC composite pavement and conventional PCC pavements. Figure 5.1 shows an example of grading and compacting the subgrade and base in preparation for PCC placement. The same procedures and specifications that have been used to prepare the sublayers for PCC construction should be used and specified for the construction of HMA/PCC composite pavements. An agency may choose to incorporate one or more of the following to prepare the sublayers:

- Cement- or lime-treated subgrade soils;
- Asphalt- or cement-treated base course;
- Permeable base courses with drainage features (such as edge drains); and
- Recycled pavement materials (such as RCA or RAP) that are not used in the PCC mix.

Reinforcing steel (for HMA/CRC composite pavements) and dowel baskets (if used for HMA/JPC composite pavements) can be placed directly on the base course following normal agency practices. Dowels should be placed middepth of the PCC thickness (and not middepth of the combined HMA/PCC thickness). They need to be securely fastened to the base course to ensure that they are not pushed by the paver.

Place the PCC Layer

The PCC layer can be paved following the same procedures and guidelines as for conventional PCC pavements (Figure 5.2). The PCC layer is the key structural component

Figure 5.1. Grading and compacting the subgrade and base in preparation for PCC placement.

of an HMA/PCC composite pavement and as such should meet structural and durability criteria (such as compressive strength, flexural strength, air content, consolidation around dowel bars, and steel reinforcement). Measuring the locations of random dowels across transverse joints using a probe just after paving is recommended to ensure the dowels are being placed in the proper location. The same goes for depth of CRC reinforcement; having the proper depth is even more critical. Agency QC/QA practices for testing materials and monitoring construction activities for JPCP and CRCP should be followed for the PCC placement of HMA/PCC composite pavements. These practices include testing for slump, mix temperature, entrained air, and so forth (Figure 5.3).

One key difference is that an initial smooth ride quality for the PCC surface is not required. A smooth PCC surface is desirable to provide a smooth HMA riding surface because long and even medium wavelength roughness in the PCC surface may translate to higher initial roughness of the HMA/PCC composite pavement. However, short wavelength roughness in the PCC surface is not expected to translate to a rougher HMA/PCC ride because the placement of the HMA layer will smooth out the entire surface.

Another difference is that the durability of the surface texture of the PCC is not crucial. The HMA wearing course is the functional layer in an HMA/PCC composite pavement and is designed to be replaced after its useful life. The HMA wearing course protects the PCC surface from wear, so lower cost soft, durable aggregates that may be susceptible to polishing may be used in the PCC mix of HMA/PCC composite pavements, but they may not be appropriate

Figure 5.2. Paving the PCC layer.

Figure 5.3. QA testing of the PCC layer for entrained air and slump.

in conventional JPC or CRC. In addition, durable coarse aggregates, obtained by recycling RCA or RAP, can be incorporated in the PCC mix without significant deleterious effects.

Texture the PCC Layer

Texturing of the PCC surface (when still plastic) is necessary to obtain a good mechanical bond between the HMA and PCC layers (Figure 5.4). The simplest and most cost-effective way to obtain this texture is through the use of longitudinal (or transverse) tining. Typical agency guidelines for texturing the PCC surface through tining can be followed, and no additional modifications specific to HMA/PCC composite pavements are necessary. Alternate forms of texturing (such as heavy Astroturf drag) are acceptable provided sufficient PCC surface texture is obtained to ensure good mechanical bond between the HMA and PCC. It is not necessary (nor is it cost-effective) to texture the PCC surface by diamond grinding or grooving.

Apply Curing Compound to the PCC Layer

Although the PCC surface will be covered with HMA after the PCC hardens, it is still necessary to control rapid moisture loss from the surface of the wet PCC to prevent rapid surface drying and early-age cracking. Agency guidelines and specifications for controlling moisture loss, such as application of curing compound (or other practices such as wet burlap), should be specified (see Figure 5.4).

Figure 5.4. Longitudinal tining texture and curing compound applied to the wet PCC surface to ensure mechanical bond between the HMA layer and the PCC layer and control surface moisture loss.

Figure 5.5. This figure demonstrates marking location of sawed joints in PCC at a location that will not be covered by the HMA so the HMA can be sawed and sealed at the same location.

Saw Cut Joints in the PCC Layer

For HMA/JPC composite pavements, transverse contraction joints in the PCC should be saw cut at the location of the dowel bars following normal agency practices and specifications for JPCP. Longitudinal joints in the PCC (for multiple lane construction) should be saw cut at the location of the longitudinal tie bars following normal agency practices and specifications for JPCP and CRCP. A single saw cut to a depth of $h/3$ (where h = PCC thickness) is adequate to create the joint openings. No sealant reservoir is needed.

For HMA/JPC composite pavements, the transverse location of the saw cuts in the PCC should be precisely marked at a location away from the pavement (that will not be covered with the HMA lift), so that the HMA can be sawed and sealed at the same location (Figure 5.5).

Apply Tack Coat to the PCC Surface

After the PCC has gained sufficient strength to allow traffic (as specified by agency requirements for opening traffic on JPCP or CRCP), the HMA layer can be placed above the PCC. A tack coat (as specified by agency requirements for asphalt overlays of concrete pavements) should be applied to the surface of the PCC to ensure adequate mechanical and chemical bonding between the PCC and the HMA layer (Figure 5.6). For HMA/JPC composite pavements, if reflection crack treatments such as stress-absorbing membranes, geogrids, or geofabrics are desired, they can be applied at this point. However, they are not necessary if the joints are sawed and sealed. The rate of application of the tack coat should be sufficient to cover a large majority of the surface, which may require increasing the normal agency quantity per square yard. Tack coat application rate, coarse (tined) surface texture, and fine HMA mixtures (as is typical of a surface HMA mix) are key to good bond between the HMA and the PCC layers. As such, the curing compound on the surface of the PCC does not need to be removed or shotblasted before the application of the tack coat. Wet PCC surface significantly decreases interface bond, and the tack coat should be applied only to a dry PCC surface.

Place the HMA Surface (and Shoulders)

The HMA layer can be paved following the same procedures and guidelines used for conventional asphalt overlays of existing/rehabilitated concrete pavements (Figure 5.7). The HMA layer is the key functional component of an HMA/PCC

Figure 5.6. Tack coat applied to the PCC surface to ensure bond between HMA and PCC layers.

Figure 5.7. Placing and compacting HMA layer for HMA/PCC composite pavements.

composite pavement and as such should meet HMA JMF criteria (such as asphalt content, aggregate gradation, density, voids in mineral aggregate (VMA), and so forth). Agency QC/QA practices for testing materials and monitoring construction activities for HMA overlays should be followed for the HMA placement of HMA/PCC composite pavements. These include testing for mix temperature, density, smoothness (profile index or IRI), and so forth. Major efforts should be made to ensure a very smooth surface is obtained because the smoother the pavement immediately after construction, the smoother it will remain for many years to come, all other things being equal.

Saw and Seal the HMA

For HMA/JPC composite pavements, if desired, the new HMA surface should be saw cut, cleaned, dried, and sealed at the location of the marked transverse joints of the underneath PCC. This can be accomplished through a single saw cut to a depth of at least $t/3$ (where t = thickness of the HMA layer) and sufficient reservoir width (typically 0.5 in.) to pour the sealant. For relatively thin layers, a saw depth that extends as deep as the material may be more effective. The sawed asphalt joints should be specified to be located within 0.5 in. of the transverse PCC joints. To get the proper location, it is common to place secure steel plugs several feet from the slab edge on both sides (beyond the HMA edge) and then snap a chalk line between the plugs to establish exactly where to saw cut a transverse joint. The saw cut can be extended partially into the shoulder or completely into the shoulder if desired, as shown in Figure 5.8. If a tied jointed concrete shoulder exists, the saw cut should extend across the shoulder.

Figure 5.8. Saw cut and sealing of the HMA surface can be extended partially or completely into the HMA shoulder.

CHAPTER 6

HMA/PCC Conclusions and Recommendations for Future Research

Conclusions

The SHRP 2 R21 project involved extensive in-depth research on two types of composite pavements: (1) high-quality relatively thin HMA surfacing over a new PCC structural layer and (2) high-quality relatively thin PCC surfacing atop a thicker structural PCC layer.

Composite pavements have proved in Europe and in the United States to provide long lives with excellent surface characteristics (low noise, smoothness, and high friction), structural capacity, rapid renewal when needed, and to use recycled and lower cost materials in the lower PCC layer. Composite pavements also reflect the current direction of many highway agencies to build economical, sustainable pavement structures that use recycled materials and locally available materials.

Both types of composite pavements have strong technical, economical, and sustainability merits in fulfilling the key goals of the SHRP 2 program, including long-lived pavements, rapid renewal, and sustainable pavements. The objectives of this research were to investigate the design and construction of new composite pavement systems for all levels of highways and streets. As part of this research, the R21 research team

1. Determined the behavior, material properties, and performance of HMA/PCC composite pavements under many climatic and traffic conditions. Experimental composite pavements were constructed at major research sites (MnROAD and UCPRC) and were instrumented and monitored under climate and heavy traffic loadings. An HMA/JPC composite pavement was also constructed by the Illinois Tollway north of Chicago. Extensive field surveys were performed in the United States, Canada, and Europe of 43 sections of HMA/PCC composite pavements. The results of these performance studies show that HMA/PCC composite pavements have clear advantages over conventional HMA and PCC pavements in terms of life-cycle costs, sustainability, and long structural lives coupled with rapid renewal of the surface.
2. Evaluated, improved, and further validated the various structural, climatic, material, performance prediction models, and design algorithms that are included in the AASHTO *MEPDG* and DARWin-ME, CalME rutting, NCHRP 1-41 reflection cracking, and NCHRP 9-30A rutting models. The current DARWin-ME overlay design procedure for HMA overlay of JPCP and CRCP can be used for new HMA/PCC composite pavements. Summaries of the key analysis and performance findings were included in Chapter 3 and are not repeated here.
3. Provided detailed recommendations for inputs and modifications to the DARWin-ME software for composite pavements. Recommended revisions for the AASHTO *MOP* are also provided.
4. Developed practical recommendations for construction specifications and techniques, life-cycle costing, and training materials for adoption by the transportation community.

The products developed as part of the SHRP 2 R21 research project will result in improved design and life-cycle cost procedures for composite pavements. The guidelines, techniques, and specifications developed will greatly advance the state of the practice of constructing composite pavements. Composite pavements are compatible with the SHRP 2 renewal philosophy because they are designed to be long-lasting pavements that can be renewed rapidly. For highway engineers, designers, and agency decision makers, composite pavements provide another tool in the designers' arsenal and can be a cost-effective alternative to conventional concrete and asphalt pavements over the life cycle of the pavement. Together, the SHRP 2 R21 reports, software, and guidelines provide information for adoption by

the transportation community and for these technologies to become more widely adopted.

Based on the comprehensive results achieved from this study, the key characteristics of HMA/PCC composite pavement were determined as follows:

- Excellent surface characteristics from the high-quality thin HMA top layer. These include low noise (especially for permeable mixtures), high friction, very good initial and long-term smoothness, minimal rutting, and durability over at least a 10- to 15-year period.
- Ability to rapidly renew a thin surface course as it wears under traffic and weather (e.g., removal and replacement of HMA materials with the latest materials).
- Long life structural design of the lower PCC layer (e.g., designed for minimal fatigue damage over more than 40 years).
- Avoidance of certain distress types that occur regularly in conventional pavements but are rare or nonexistent in composite pavements. Table 6.1 shows the direct comparison for conventional HMA and HMA/PCC composite pavement.
- Improved life-cycle costs over a long life span due to overall lower construction costs (e.g., increased recycling, local aggregates, cement substitution amounts, lower PCC thickness), future maintenance costs (e.g., sawing and sealing of HMA joints will reduce impact and maintenance of reflection cracks), and future rehabilitation costs (e.g., no full-depth repairs of PCC slab due to reduction in fatigue damage, no HMA fatigue cracking and less rutting).
- Improved sustainability practices through structural and materials design of the lower PCC layer. Increased use of recycled materials (RCA, RAP), increased use of more local and less expensive aggregates, and higher substitution rates for cementitious materials (higher content of fly ash and other supplemental cementitious materials).

Table 6.1. Comparison of Conventional HMA and PCC Pavement with Composite HMA/PCC Pavement for Several Key Distress Types

Distress Type	Conventional HMA Pavement	Conventional PCC Pavement	Composite HMA/JPC and HMA/CRC
Bottom-up fatigue cracking	Yes, this is a major design concern.	Yes, this is a major design concern.	Fatigue cracking does not occur in HMA layer because the HMA is almost always in compression. Bottom-up and top-down fatigue cracking in JPC and CRC (for punchouts) are reduced because of insulating effects of HMA.
Low temperature or shrinkage transverse cracking in HMA	Yes, this is a major problem in many areas.	na	No, this was not observed on any HMA/JPC or HMA/CRC composite projects surveyed. The bonded HMA layer does not move independently of the PCC layer.
Top-down fatigue cracking in wheelpath	Yes, this has occurred on some projects.	Yes, longitudinal cracking has occurred on some projects.	Top-down fatigue cracking does not occur in HMA layer because the HMA is almost always in compression. PCC longitudinal cracking in wheelpath of HMA/JPC may be reduced or eliminated by the insulating effects of HMA.
Permanent deformation	Yes, rutting is a major design concern.	na; however, wear from studded tires may occur.	Rutting is minor on most HMA/PCC composite pavements because of high quality materials and thin layer. In addition, the stiff PCC layer completely eliminates base/subbase/subgrade rutting.
Transverse joint reflection cracks	No, this does not occur.	na	Yes, this occurs for HMA/JPC. Control through saw and seal technique. No, this does not occur with HMA/CRC.
Joint faulting	na	Yes, this is a major design concern.	Yes, this can occur, but little faulting comes through the HMA surface. Faulting must be considered in design of HMA/JPC.

Note: na = not applicable.

Intended Audience, Usage, Value Added to State of the Practice and State of the Art, Potential Benefits of Acceptance and Implementation

The key products of the SHRP 2 R21 project on Composite Pavements include examples of the performance of composite pavements, design procedures, construction guidelines, pavement selection type guidelines, and training materials.

The key intended audiences for these products are as follows:

- State highway agency managers, engineers, and consultants. Composite pavements need to be added to the routine pavement type selection procedures of state and local highway agencies. The performance examples, design tools, pavement selection type guidelines, construction guidelines and specifications, and training materials will all provide significant value-added technology to these engineers and managers regarding composite pavements. If DARWin-ME is upgraded to include composite pavements as a new pavement type along with the conventional types, this will be a major advancement in the consideration of composite pavements in the industry.
- FHWA management and engineers. FHWA managers and engineers need to be made more aware of the past performance and benefits of composite pavements so they can discuss the possibility of adding them to their regular pavement selection process. The R21 products provide the needed information.
- Researchers from academia, federal and state governments, and industry. There are lots of additional opportunities to improve on the design and construction of composite pavements, which open up the future of additional research. Making faculty more aware of the advantages of composite pavements and getting this instruction into the classroom are keys to educating students about the benefits of composite pavements. The training materials and various documents from the R21 project will be valuable for universities for future course development.

The key benefits of state and local highway agencies incorporating HMA/PCC composite pavements into their routine pavement type selection process include the following:

- Incorporation provides more flexibility in the highway agency pavement management strategy for new and especially for future rehabilitation and is another tool in the designers' toolbox. The design of composite pavement to achieve lower life cycle costs, increased sustainability, and longer life will require additional efforts in design, materials, and construction specifications by the highway agency to achieve these goals because new technology is involved.
- An HMA/PCC composite pavement can be designed cost-effectively to last comparably to a conventional HMA or PCC pavement. It can also be designed to be a long-life pavement with minimal structural fatigue damage over many years but with a surface that can be rapidly replaced every 10 to 20 years with no deep structural problems that require additional lane closures to repair and cure. The long-term LCCA should show favorable results for this type of design strategy.
- Excellent surface characteristics can be provided. This includes
  - Very smooth surfaces (e.g., initial IRI of 30 to 55 in./mile have been achieved for HMA/PCC composite pavements);
  - Low noise surfaces (e.g., porous HMA, ARFC, RHMA, SMA);
  - Reduction in splash and spray in heavy rain storms for porous surfaces; and
  - High friction and low potential for hydroplaning when porous surface used. In addition, minimal aggregate polishing for various high quality asphaltic surfaces such as SMA.
- Rapid removal and replacement of the thin surface. The relatively thin (<3 in.) HMA surfaces can be easily and rapidly milled and replaced during off-peak traffic hours. This would reduce traffic congestion over many years.
- Improved sustainability can be provided for composite pavements in several ways:
  - Increased composite pavement longevity is a key to improved sustainability.
    - The HMA/PCC type of composite pavement can be designed for a very long fatigue damage life, such as 40 to 100 years, using the DARWin-ME at a high level of reliability. Slab thicknesses required are significantly less than for bare JPCP or CRCP. Thus, there will be minimal if any slab fatigue cracking over the design period.
    - The thin HMA surface can be rapidly replaced at off-peak traffic hours every 10 to 20 years as needed due mainly to durability issues. The saw and seal technique for transverse JPC joints or the use of CRC is expected to extend the service life of these surfaces.
    - The renewal of the surface will provide excellent surface characteristics, including smoothness, low noise, good friction, and lower splash and spray for permeable surfaces, over the life of the pavement.

- This composite pavement design thus will reduce the amount of lane closures over the long design life of the pavement. This has a major sustainability impact because of the reduction in emissions caused by the extra congestion due to lane closures for maintenance and rehabilitation.

- Reduction of the use of natural resources is another key for improved sustainability. Successful use of RCA in the lower PCC slab was done successfully in the MnROAD R21 section. The existing concrete from Minnesota I-94 was recycled as 50% of the coarse aggregate. The HMA/PCC composite pavement constructed at the Illinois Tollway had recycled coarse aggregate from old asphalt pavements (RAP) compose 30% of the total coarse aggregate in the PCC mix. There may be many projects for which such recycling of existing old PCC and old HMA/PCC pavements into the new composite pavement would result in a major reduction of the haul distances involved, which would result in lower energy use and costs. Of course, use of recycled concrete results in a savings of natural aggregates.
- Increased use of fly ash in achieving a substantial reduction in portland cement content in the lower PCC slab is also key. The lower layer of the I-94 composite section contained 40% fly ash replacement. The HMA/PCC composite pavement constructed at the Illinois Tollway contained 20% to 25% fly ash replacement. Fly ash is a by-product of coal-fired electric generating plants. The use of RAP and fly ash offers environmental advantages by diverting the material from the waste stream, reducing the energy investment in processing virgin materials, conserving virgin materials, reducing carbon dioxide emissions, and minimizing pollution.
- In certain states, studded tire wear is the major cause of deterioration and needed rehabilitation for some highways. A thin but durable wearing surface such as SMA could be used for an SMA/JPCP or CRCP composite pavement. The SMA could be replaced as it wears down from the studded tires, but the existing PCC would always be there providing the load-carrying capacity. The EAC would provide a more durable surface that would resist wear of studded tires because of the very high quality aggregates used in the surface.
- HMA/PCC composite pavements are amenable to use of materials such as WMA, wherein the mix is heated to a lower temperature (~60°F to 90°F reduction) compared with conventional HMA. Lower temperatures mean less fuel consumption, lower stack emissions, and less fume and odor generation at the plant and job site. The HMA/PCC composite pavement constructed at the Illinois Tollway had a WMA surface on a JPC lower layer and shows excellent performance.
- Increased use of lower cost local aggregates in the lower PCC layer because the PCC is no longer the wearing course (e.g., aggregates susceptible to polishing) and the HMA surface provides some protection from freeze-thaw damage and wet-dry cycling. Use of local aggregates improves sustainability by reducing resources spent in hauling aggregates over long distances.

Recommendations for Additional Development or Refinement of the Products

Each of the R21 products is listed in Table 6.2, along with recommendations on required future development and refinement needed for full implementation.

Table 6.2. SHRP 2 R21 Project Recommendations for Additional Development of HMA/PCC Products

SHRP 2 R21 Product	Implementation Status	Additional Development Required	Comment
MEPDG R21 version software	R21 improvements to "Bonded PCC/PCC" to simulate new PCC/PCC and address limitations of existing structural and environmental models for PCC/PCC. Can be used for design of PCC/JPC, PCC/CRC, HMA/JPC, and HMA/CRC.	Reduction of moisture gradient for HMA/PCC because top of slab has high humidity with HMA.	*MEPDG* R21 version is available from SHRP 2 and AASHTO. Use "Overlay" design procedures for new composite pavements, with appropriate inputs.
AASHTO DARWin-ME software	"Overlay" design can be used to design new HMA/JPC and HMA/CRC composite pavement.	Modifications for PCC/PCC that were made in the R21 version need to be made to DARWin-ME software. User interface requires revision to show PCC/PCC and HMA/PCC composite pavements as new pavement alternatives.	Improvements should be made as soon as possible for highway agencies to design new composite pavement.

(continued on next page)

Table 6.2. SHRP 2 R21 Project Recommendations for Additional Development of HMA/PCC Products (continued)

SHRP 2 R21 Product	Implementation Status	Additional Development Required	Comment
AASHTO *MOP*	Detailed recommendations were prepared to include new composite pavements.	None.	Revision can be made in tandem with modifications to the DARWin-ME software.
MnROAD HMA/JPC test section	One HMA/JPC composite section constructed, instrumented, and being monitored under heavy interstate traffic for 1 full year. Construction and first year's performance measured.	Monitoring of the section over time would produce valuable longer term information to convince highway agencies to build composite pavements.	These sections should be monitored at least twice a year. Full performance will not be known for more than 10 years. Many major findings will be discovered over time for structural design, texture, and sustainability. These data can be used to update calibration coefficients and further verify long-term *MEPDG* structural responses to traffic and thermal loading and refine models (e.g., IRI and reflection cracking as appropriate).
UCPRC HMA/JPC test section	HMA/JPC composite sections constructed, instrumented, HVS loaded, and monitored.	R21 work is complete. Additional HVS loading may be done under other funding.	HMA/JPC composite sections are available for additional testing and analysis.
ISTHA HMA/JPC Section	Two HMA/JPC sections constructed with major sustainability advantages. Sections under traffic for off-ramps and on-ramps to I-94.	Monitoring of their performance would be valuable to determine how highly sustainable composite pavements perform in harsh climate.	Sections are in place, and monitoring can be easily performed on the ramps.
2008 Survey of European Composite Pavements	Report completed and published and available at www.trb.org/Main/Blurbs/163693.aspx.	None.	Already available to the public. There has been a great deal of interest.
Database of Composite Pavements	Data collected for 43 HMA/PCC composite sections are available in an Excel spreadsheet and *MEPDG* and DARWin-ME input files.	None.	These data may be of interest to agencies wishing to develop designs for new composite pavements.
Calibration constants for CalME	Constants for rutting and reflection cracking derived from UCPRC and MnROAD are available.	None.	These constants will be of interest to those using CalME for analysis of composite pavements.
NCHRP 9-30A	Constants for rutting derived from LTPP, UCPRC test sections, and field data are available.	None.	These constants will be of interest to those using the 9-30A version of the *MEPDG*.
JPCP fatigue cracking models in *MEPDG*	The JPCP model was validated for both HMA/JPC and PCC/JPC composite pavement data.	None. The global coefficients are sufficient.	JPC fatigue damage in composite pavements is critical to their structural design.
CRCP punchout model in *MEPDG*	The CRCP model was validated for HMA/CRC composite pavement data.	None. The global coefficients are sufficient.	CRCP punchout damage in composite pavements is critical to their structural design.
HMA rutting model in *MEPDG*	The model showed reasonable predictions for thin HMA, SMA, and porous friction course layers.	Although the global coefficients reasonably predicted low rutting, there are model deficiencies.	Rutting for thin HMA/PCC was low on nearly all sections.
Life-cycle cost guidelines	Recommendations using the FHWA RealCost spreadsheet for composite pavements were developed.	None.	The *MEPDG* predictions can provide pavement life estimation for use in LCC.

(continued on next page)

Table 6.2. SHRP 2 R21 Project Recommendations for Additional Development of HMA/PCC Products (continued)

SHRP 2 R21 Product	Implementation Status	Additional Development Required	Comment
Instrument data	Extensive instrumentation data exist for MnROAD and UCPRC and are included in the SHRP 2 R21 database.	The full analysis of these data was not possible under R21, and much additional analyses can be accomplished.	Some valuable data on temperature, moisture, strains from climatic change, and dynamic strains from loadings.
Examples of HMA/PCC composite designs	There exists a range of examples of composite pavement design and performance that were used in R21.	Further research into additional aspects of composite pavements can be accomplished with these data.	The performance of most composite pavements was very good. These sections can be used to demonstrate this to highway agencies.
Construction specifications for HMA/JPC	The MnROAD specifications are available that cover a wide variety of aspects of HMA and JPC. The specifications from UCPRC test sections are also available.	None.	Key aspects are HMA/PCC bonding, PCC lower layer mixture RCA characteristics, cement replacement, curing/retarding, and saw and seal of HMA joints.
RILEM CIF Concrete Freeze-Thaw Standard	Equipment was checked out and many PCC samples tested. Very useful results were obtained.	Additional testing on all quality levels of aggregate is recommended. This equipment should be more fully evaluated for U.S. applications.	An excellent field simulation for freeze-thaw damage of a given PCC.
Training products	Presentations on design, construction, materials, performance, and examples of both types of composite pavements.	None.	A variety of promotional and training presentations are available for use.
Advantages of composite pavements	R21 has brought to light the many advantages of HMA/PCC pavements.	Development of design and cost comparisons for conventional design versus composite designs at specific sites.	Direct comparison of designs and costs make a strong convincing case for HMA/PCC composite pavements.

Note: ISTHA = Illinois State Toll Highway Authority.

References

Al-Qadi, I. L. et al. *FHWA-ICT-08-023: Tack Coat Optimization for HMA Overlays: Laboratory Testing.* Illinois Center for Transportation, University of Illinois, September 2008.

Armaghani, J. M., T. J. Larsen, and L. L. Smith. Temperature Response of Concrete Pavement. In *Transportation Research Record, 1121,* TRB, National Research Council, Washington, D.C., 1987, pp. 23–33.

Baker, R. F. New Jersey Composite Pavement Project. In *Highway Research Record, 434,* HRB, National Research Council, Washington, D.C., 1973, pp. 16–23.

Choubane, B., and M. Tia. Nonlinear Temperature Gradient Effect on Maximum Warping Stresses in Rigid Pavements. In *Transportation Research Record 1370,* TRB, National Research Council, Washington, D.C., 1992, pp. 11–19.

Darter, M. I., and E. J. Barenberg. *Zero-Maintenance Pavement: Results of Field Studies on the Performance Requirements and Capabilities of Conventional Pavement Systems,* Report FHWA-RD-76-105. FHWA, U.S. Department of Transportation, 1976.

Donovan, E. P., I. L. Al-Qadi, and A. Loulizi. Optimization of Tack Coat Application Rate for Geocomposite Membrane on Bridge Decks. In *Transportation Research Record: Journal of the Transportation Research Board, No. 1740,* Transportation Research Board, National Research Council, Washington, D.C., 2000, pp. 143–150.

Epps, J. A., A. Hand, S. Seeds, T. Schulz, S. Alavi, C. Ashmore, C. L. Monismith, J. A. Deacon, J. T. Harvey, and R. Leahy. *NCHRP Report 455: Recommended Performance-Related Specification for Hot-Mix Asphalt Construction: Results of the WesTrack Project. Part II: Performance-Related Specification.* Transportation Research Board of the National Academies, Washington, D.C., 2002.

Hallin, J., S. Sadasivam, J. Mallela, D. Hein, M. Darter, and H. Von Quintus. *NCHRP Report 703: Guide for Pavement-Type Selection.* Transportation Research Board of the National Academies, Washington, D.C., 2011.

Hassan, K. E., J. C. Nicholls, H. M. Harding, and M. E. Nunn. Durability of Continuously Reinforced Concrete Surfaced with Asphalt. In *Transport Research Laboratory Report* TRL666, United Kingdom, 2008.

Ioannides, A. M., and L. Khazanovich. Nonlinear Temperature Effects in Multilayered Concrete Pavements. *ASCE Journal of Transportation Engineering,* Vol. 124, No. 2, 1998, pp. 128–136.

Jofre, C., J. Vaquero, and R. Alvarez-Loranca. 15 Years of Precracking in Spain: An Evaluation. *Proc., 4th International RILEM Conference,* Ottawa, Ontario, Canada, 2000, pp. 379–389.

Jofre, C., J. Vaquero, and C. Kraemer. Performance of precracked cement treated layers in Spain. *Proc., 3rd International RILEM Conference,* Maastricht, The Netherlands, 1996, pp. 72–81.

Kaloush, K. E., and M. W. Witczak. *Development of a Permanent to Elastic Strain Ratio Model for Asphalt Mixtures,* Development of the 2002 Guide for the Design of New and Rehabilitated Pavement Structures, NCHRP 1-37A, Inter-Team Technical Report, 2000.

Khazanovich, L. *Structural Analysis of Multi-Layered Concrete Pavement Systems.* PhD dissertation. University of Illinois, Urbana, 1994.

Leng, Z. et al. Interface Bonding between HMA and Various PCC Surfaces: Laboratory Assessment. Presented at Annual Meeting of the Transportation Research Board of the National Academies, Washington, D.C., 2008.

Lytton, R. L., F. L. Tsai, S. Lee, R. Luo, S. Hu, and F. Zhou. *NCHRP Report 669: Models for Predicting Reflection Cracking for Hot-Mix Asphalt Overlays.* Transportation Research Board of the National Academies, Washington, D.C., 2011.

Mohamed, A. R., and W. Hansen. Effect of Nonlinear Temperature Gradient on Curling Stresses in Concrete Pavements. In *Transportation Research Record 1568,* TRB, National Research Council, Washington, D.C., 1997, pp. 65–71.

NCHRP. 2003a. *NCHRP Results Digest Number 283: Jackknife Testing—An Experimental Approach to Refine Model Calibration and Validation.* National Cooperative Highway Research Program, Transportation Research Board of the National Academies, Washington, D.C.

NCHRP. 2003b. *NCHRP Results Digest Number 284: Refining the Calibration and Validation of Hot Mix Asphalt Performance Models: An Experimental Plan and Database,* National Cooperative Highway Research Program, Transportation Research Board of the National Academies, Washington, D.C.

NCHRP. 2008. *Recommended Practice for Local Calibration of the M-E Pavement Design Guide,* NCHRP Project 1-40B, Final Practice Submitted to NCHRP.

Ryell, J., and J. T. Corkill. Long Term Performance of an Experimental Composite Pavement. In *Highway Research Record, 434,* HRB, National Research Council, Washington, D.C., 1973, pp. 1–15.

Sanchez de Juan, M., and P. A. Gutierrez. Study on the influence of attached mortar content on the properties of recycled concrete aggregate. *Construction and Building Materials,* Vol. 23, No. 2, 2009, pp. 872–877.

Smith, P. Past Performance of Composite Pavements. In *Highway Research Record 37,* HRB, National Research Council, Washington, D.C., 1963, pp. 14–30.

Sousa, J. B., J. A. Deacon, S. Weissman, J. T. Harvey, C. L. Monismith, R. B. Leahy, G. Paulsen, and J. S. Coplantz. *SHRP Report SHRPA-415: Permanent Deformation Response of Asphalt-Aggregate Mixes.* TRB, National Research Council, Washington, D.C., 1994.

Thomlinson, J. Temperature Variations and Consequent Stresses Produced by Daily and Seasonal Temperature Cycles in Concrete Slabs. *Concrete Constructional Engineering,* Vol. 36, No. 6, 1940, pp. 298–307 and Vol. 36, No. 7, 1940, pp. 352–360.

Tompkins, D., L. Khazanovich, and M. I. Darter. *2008 Survey of European Composite Pavements. SHRP 2 Report S2-R21-RW-1,* Transportation Research Board of the National Academies, Washington, D.C., 2010.

Van Breemen, W. Discussion of Possible Designs of Composite Pavements. In *Highway Research Record, 37,* HRB, National Research Council, Washington, D.C., 1963, pp. 5–10.

Von Quintus, H. *Local Calibration Adjustments for the HMA Distress Prediction Models,* Preliminary Draft Final Report, NCHRP 1-40B, National Cooperative Highway Research Program, Transportation Research Board, Washington, D.C., 2005.

Von Quintus, H. *History and Hypothesis Behind the HMA Mixture Adjustment Factors for Rutting and Area Fatigue Cracking Predictions,* White Paper prepared for NCHRP Project 1-40B, "Local Calibration Guidance for the Recommended Guide for Mechanistic-Empirical Design of New and Rehabilitated Pavement Structures," 2006.

Von Quintus, H., F. Finn, R. Hudson, and F. Roberts. *Flexible and Composite Structures for Premium Pavements.* Reports RD-81-154 and 155. Federal Highway Administration, Washington, D.C., 1980.

Von Quintus, H., J. Mallela, R. Bonaquist, C. Schwartz, and R. Carvalho. Calibration of Rutting Models for HMA Structural and Mix Design. Draft Final Report. NCHRP 9-30A, 2011.

Wells, S. A., B. M. Phillips, and J. M. Vandenbossche. Quantifying Built-in Construction Gradients and Early-Age Slab Deformation Caused by Environmental Loads in a Jointed Plain Concrete Pavement. *International Journal of Pavement Engineering,* Vol. 7, No. 4, 2006, pp. 275–289.

Yu, H. T., K. D. Smith, M. I. Darter, J. Jiang, and L. Khazanovich. *Performance of Concrete Pavements Volume III: Improving Concrete Pavement Performance, Final Report.* Report FHWA-RD-95-111. FHWA, U.S. Department of Transportation, 1998.

Appendices A–V

Appendices A through V are available online: www.trb.org/Main/Blurbs/168145.aspx. The appendices are as follows:

Appendix A: History and Background of HMA/PCC Composite Pavements
Appendix B: History and Background of PCC/PCC Composite Pavements
Appendix C: Highway Agency Survey
Appendix D: Distress Mechanisms of HMA/PCC Composite Pavements
Appendix E: Distress Mechanisms of PCC/PCC Composite Pavements
Appendix F: Construction of Test Sections at MnROAD
Appendix G: Construction of Test Sections at UCPRC
Appendix H: Instrumentation and Analysis of Instrumented Data at MnROAD
Appendix I: HMA/PCC Rutting Model
Appendix J: Measurement and Analysis of PCC Slab Temperature Profiles at UCPRC
Appendix K: HVS Cracking Tests at UCPRC
Appendix L: HVS Rutting Tests at UCPRC
Appendix M: Joint Movement Monitoring at UCPRC
Appendix N: Laboratory Testing of HMA Mixes at UCPRC
Appendix O: HMA/PCC Bonding and Friction Literature
Appendix P: CalME Model
Appendix Q: Laboratory Testing of PCC Mixes
Appendix R: *MEPDG* Modifications for PCC/PCC Pavements
Appendix S: Lattice 3D Model Background
Appendix T: Recycled Concrete Aggregates in PCC
Appendix U: Freeze-Thaw Durability Testing of PCC Mixes
Appendix V: Brushing and Exposed Aggregate Concrete

Related SHRP 2 Research

Geotechnical Solutions for Soil Improvement, Rapid Embankment Construction, and Stabilization of the Pavement Working Platform (R02)

Modular Pavement Technology (R05)

Real-Time Smoothness Measurements on Portland Cement Concrete Pavements During Construction (R06E)

Using Existing Pavement In Place and Achieving Long Life (R23)